NASA CR-175128
N84-27980

F83-02

AUTONOMOUS OMNIDIRECTIONAL SPACECRAFT ANTENNA SYSTEM

THIS ANTENNA SYSTEM PROVIDES ROUGHLY 8 dB GAIN THROUGHOUT A SPHERICAL COVERAGE REGION

FINAL REPORT FOR PERIOD JULY 1980 - JANUARY 1983

TALIAFERRO H. TAYLOR, JR.

BALL AEROSPACE SYSTEMS DIVISION
P. O. BOX 1062
BOULDER, COLORADO 80306

JAN 1984 RECEIVED NASA STI FACILITY ACCESS DEPT.

MAY 1984 RECEIVED NASA STI FACILITY ACCESS DEPT.

FEB 1984 RECEIVED NASA STI FACILITY ACCESS DEPT.

FEBRUARY 1983

PREPARED FOR

GODDARD SPACE FLIGHT CENTER
RF TECHNOLOGY BRANCH
GREENBELT, MARYLAND 20771

ROBERT JACKSON, TECHNICAL OFFICER

Ball Aerospace Systems Division

BOULDER, COLORADO 80306



AUTONOMOUS OMNIDIRECTIONAL SPACECRAFT ANTENNA SYSTEM

Final Report for period July 1980 - January 1983

Contract No. NAS5-26240

January 1983

Prepared For:

Goddard Space Flight Center
RF Technology Branch
Greenbelt, Maryland 20771

Prepared by:

Robert T. Johnk

R. T. Johnk
Antenna Engineer

Approved by:

T. H. Taylor

T. H. Taylor
Program Manager

CLASSIFICATION

BR 278

TECHNICAL REPORT STANDARD TITLE PAGE

1. Report No.	2. Government Accession No.	3. Recipient's Catalog No.
F83-02		

4. Title and Subtitle	5. Report Date
Autonomous Omnidirectional Spacecraft Antenna System	February 1983
	6. Performing Organization Code
7. Author(s)	8. Performing Organization Report No.
Taliaferro H. Taylor	F83-02
9. Performing Organization Name and Address	10. Work Unit No.
Ball Aerospace Systems Division P.O. Box 1062 Boulder, CO 80306	11. Contract or Grant No. NAS5-26240
	13. Type of Report and Period Covered
12. Sponsoring Agency Name and Address	Final July 1980 - Dec. 1982
Goodard Space Flight Center Greenbelt, MD 20771 Technical Monitor: Robert Jackson	14. Sponsoring Agency Code

15. Supplementary Notes

16. Abstract

This report describes the development of a low gain Electronically Switchable Spherical Array Antenna. This antenna provides roughly 7 dBic gain for receive/transmit operation between user satellites and TDRSS. When used as a pair, the antenna provides spherical coverage. The antenna has been tested in its primary operating modes:

- Directed Beam
- Retrodirective
- Omnidirectional

This report concentrates on the tested performance of the antenna.

17. Key Words (Selected by Author(s))	18. Distribution Statement
Electronic Switching Spherical Array, TDRSS User Antenna	

19. Security Classif. (of this report)	20. Security Classif. (of this page)	21. No. of Pages	22. Price*
Unclassified	Unclassified	~ 200	unknown

*For sale by the Clearinghouse for Federal Scientific and Technical Information, Springfield, Virginia 22151.

PREFACE

The Autonomous Omnidirectional Spacecraft Antenna System (Auto Omni) has been developed as a low gain (7 dBic) antenna for receive and transmit communication between user spacecraft and TDRS. When configured as a set of antennas, one on each side of the spacecraft, Auto Omni provides uniform gain throughout a spherical coverage region. The Auto Omni provides four operating modes which are discussed in this report. These operating modes are:

- Omnidirectional
- Directed Beams
- Program Track
- Retrodirective (Automatic Direction Finding)

This final report provides the performance of the Auto Omni's final hardware configuration. Details about the evolution of this hardware have been reduced to a minimum so that a more complete performance description could be included.

Chapter 1 describes the interface to the Auto Omni in detail so that someone who is relatively unfamiliar with the antenna may operate it.

Chapters 2 through 9 describe key areas of Auto Omni's development and testing. These areas include:

Chapter 2 - Switching Power Divider Description
Chapter 3 - Microstrip Switching Power Divider Performance
Chapter 4 - Gain and Phase Performance Compared to Phase 1
Chapter 5 - Range Interfaced Gain Measurements
Chapter 6 - Modification of Element Selection Algorithm
Chapter 7 - Omnidirectional Gain Coverage
Chapter 8 - Phase Data - Omnidirectional Mode and Range Interface Mode
Chapter 9 - Retrodirective Mode Testing

The primary emphasis of each of these sections is the measured performance of the Auto Omni.

Additional testing is needed to verify conclusions regarding anomalous operation at several coverage angles. This additional testing includes:

- Verification that gain at the pole region is increased when SPD outputs 1 and 2 (higher loss outputs) are not used in element clusters.
- Verification that the gain is increased when elements 22, 23, and 35 are operating properly.
- Verify that the element selection algorithm should be modified to choose 5 element clusters when the desired pointing direction nearly coincides with an element's location.

Additional testing and development should be performed on the Switching Power Divider to define construction methods: die attachment, hermetic feed throughs etc., and to verify why the insertion loss on outputs 1, 2, 35 and 36 is excessive.

The Auto Omni has been tested in its primary operating modes. It has demonstrated a gain of 7 dB or higher over a significant portion of the hemisphere. Its performance is expected to be fully acceptable when the results of the recommended testing are employed.

TABLE OF CONTENTS

Chapter	Title	Page
	Preface	i
	Table of Contents	iii
1	OPERATING INSTRUCTIONS AND SOFTWARE DISCUSSION	1
	1.1 Introduction	1
	1.1.1 Initialization	1
	1.2 *Autonomous Omni Subprograms*	3
	1.2.1 Program for Steering the Beam from a Manually Entered Set of Phi and Theta Direction Inputs (Chip Set A or B)	4
	1.2.2 Program for Entering Active Elements (Chip Set A or B)	4
	1.2.3 Program for Entering the Omni Beam Mode (Chip Set A or B)	5
	1.2.4 Program Track Mode (Chip Set A only)	6
	1.2.4.1 Entering the Data for the Programmed Track Subprogram	6
	1.2.4.2 User Satellite Orbit Attitude Model	7
	1.2.5 Program for Steering the Beam to Align with the Antenna Range Positioner (Chip Sets A & B)	10
	1.2.6 Program to Automatically Determine the Direction to the Signal Source Retrodirective Mode (Chip Set B only)	11
	1.2.6.1 Phase 0 Acquisition	12
	1.2.6.2 Phase 1 Acquisition	12
	1.2.6.3 Phase 2 Acquisition	13
	1.3 Chip Sets A and B Replacement	17
2	SWITCHING POWER DIVIDER DESCRIPTION	18
	2.1 Overview	19
	2.2 Description	19
	2.3 Outer Teflon PWB with Connectors and Bias Network	20
	2.4 Hybrid	20
	2.4.1 Feedthroughs	21
	2.4.2 Epsilam Interconnect Ring	21
	2.4.3 Substrate	21

TABLE OF CONTENTS (Continued)

Chapter	Title	Page
3	MICROSTRIP SWITCHING POWER DIVIDER PERFORMANCE	23
	3.1 Introduction	24
	3.2 Case 1	24
	3.3 Case 2	25
	3.4 Case 3	25
	3.5 Conclusion	26
4	GAIN AND PHASE PERFORMANCE COMPARED TO PHASE ONE DATA	115
	4.1 Introduction	116
	4.2 Phase One Performance	116
	4.3 Phase Two Performance	116
	4.4 Phase Two Compared to Phase One	117
5	RANGE INTERFACED GAIN MEASUREMENTS	151
	5.1 Introduction	152
	5.2 Test Results	152
	5.3 Test Conclusions	152
	5.3.1 Category 1 - Area Near Pole, Coordinates (0°, 0°)	152
	5.3.2 Category 2; Area $50^o < \theta < 90^o$; $-180^o < \phi < -90^o$	153
	5.3.3 Category 3 - Area Near to Elements	154
6	MODIFICATION OF ELEMENT SELECTION ALGORITHM	161
	6.1 Introduction	162
	6.2 Modification to Include More Than Four Elements in a Cluster	162
	6.3 Modification to Provide Symmetrical Clusters	163
7	OMNIDIRECTIONAL GAIN COVERAGE	172
	7.1 Introduction	173
	7.2 Test Results	173
8	OMNIDIRECTIONAL MODE AND RANGE INTERFACE MODE	176
	8.1 Introduction	177
	8.2 Test Data - Range Interfaced Operating Mode	177

TABLE OF CONTENTS (Continued)

Chapter	Title	Page
	8.3 Test Data - Omnidirectional Mode	177
9	RETRODIRECTIVE MODE TESTING (with NASA Standard Transponder)	182
	9.1 Introduction	183
	9.2 Phase 1 Gain Calibration	183
	9.3 Phase 2 - Retrodirective Mode Tests - "Weak"	184
	9.4 Phase 3 - Retrodirective Mode Tests -- "Strong" Signal Level ~ -100 dBm Incident	185
APPENDIX A	ESSA/ERBS TDRS Tracking Program	A-1
APPENDIX B	MOTOROLA REPORT: SLE Module/TDRSS Engineering Model Transponder Integration and Test with the Autonomous Omni Antenna/Microprocessor	B-1

LIST OF FIGURES

Figure	Title	Page
1.1	Auto Omni Equipment Interconnection Diagram	2
1.2		8
1.3	Phase 2 Acquisition Beam Locations	15
2.1	Switching Power Divider	22
3.1 thru 3.27	Case 1 (Raw Data) SPD Insertion Loss Data with Resistive Loads	32 thru 58
3.29 thru 3.41	Case 2 (Raw Data) SPD Insertion Loss Data with Resistive Loads (A Repeat of Selected Group I Clusters to Verify Test Validity)	60 thru 72
3.42 thru 3.54	Case 3 (Raw Data) SPD Insertion Loss Data with Elements as Loads	74 thru 86
3.55 thru 3.67	Case 2 (Raw Data) SPD Insertion Phase Data with Resistive Loads	88 thru 100

LIST OF FIGURES (Continued)

Figure	Title	Page
3.68 thru 3.80	Case 3 (Raw Data) SPD Insertion Phase Data with Elements as Loads	102 thru 114
4.1 thru 4.13	Raw Data Autonomous Omni Phase II Gain (with SPD)	124 thru 136
4.14 thru 4.26	Raw Data Autonomous Omni Phase II Gain (with SPD)	138 thru 150
5.1	Range Interfaced Mode Gain at 2106 MHz	156
5.2	Range Interfaced Mode Gain Greater than 7 dB at 2106 MHz	157
5.3	Range Interfaced Mode Gain at 2287 MHz	158
5.4	Range Interfaced Mode Gain Greater than 7 dB at 2287 MHz	159
5.5	Element Clusters Shape Changes with Pointing Angles	160
6.1 thru 6.6	Raw Data Sector RDP's	166 thru 171
7.1	Omni Mode Gain at 2106 MHz	174
7.2	Omni Mode Gain at 2287 MHz	175
8.1	Range Interfaced Mode Composite Face at 2106 MHz	178
8.2	Range Interfaced Mode Composite Face at 2287 MHz	179
8.3	Omni Mode Phase at 2106 MHz	180
8.4	Omni Mode Phase at 2287 MHz	181
9.1	Gain Calibration Setup	186
9.2	Transponder AGC TLM vs. Test Signal Generator Level with Standard Antenna	187
9.3	Autonomous Omni Range Test Setup	188

LIST OF TABLES

Table	Title	Page
1.1	Phase 1 Acquisition Beams	14
3.1	SPD Insertion Loss Characteristics with Purely Resistive Loads (50Ω)	27
3.2	SPD Insertion Loss Characteristics with Purely Resistive Loads (50Ω)	28
3.3	The Maximum Insertion Phase Difference Between Channels for Selected Groups Purely Resistive Loads (50Ω)	28
3.4	SPD Insertion Loss Characteristics with the Circularly Polarized Elements as Loads	29
3.5	The Maximum Insertion Phase Difference Between Channels for Selected Groups. Circularly Polarized Element Loads	29
4.1	Selected Element Groups for RDP Measurements	118
4.2	Peak Gain (dBic) and Beam Peak Locations Measured with a Fixed 4-way Power Divider	119
4.3	Peak Gain and Beam Peak Locations	120 and 121
4.4	Differences in Peak Gain and Beam Pointing Angle Produced by the SPD. A Fixed 4-way Power Divider is Used as the Reference.	122
6.1	Gain Changes with Different Number of Elements in a Cluster	164
9.1	Phase 1 - Retrodirective Mode Testing with "Weak" Signal ~ -115 dBm Incident	189
9.2	Retrodirective Mode Performance Strong Signal Case (-100 dBm)	190

Chapter 1
OPERATING INSTRUCTIONS AND SOFTWARE DISCUSSION

Abstract

This chapter describes the software interface to the Auto Omni microprocessor so that someone unfamiliar with the hardware can execute each of the Auto Omni operating modes.

1.1 INTRODUCTION

The software programs developed for the Autonomous Omni were developed to:

- aid in the functional engineering tests of the antenna
- to demonstrate the operational modes of the antenna

All of these programs have been written in assembly code for the Texas Instruments 9900 microcomputer and are contained in four 1K byte eproms and 400K RAM. The first pair of eproms contain the programs and all of the special purpose subroutines. These programs are located at hexidecimal address >0000 - >FFF. This eprom set contains a test monitor, the I/O routines, and all general purpose subroutines such as the trigonometric and coordinate transformation subroutines. The Auto Omni programs also require the use of >400 hexidecimal bytes of volatile memory (RAM) located at memory addresses >FC00 - >FFFF.

1.1.1 Initialization

After interconnecting the hardware as shown in Figure 1.1 and turning on the AC power the Auto Omni microcomputer may be initialized through the following routine.

To initiate the program, the operator must depress the reset interrupt switch on the console and type the character "A". This input is used by the computer to establish the terminal baud rate. The operator must then type the character

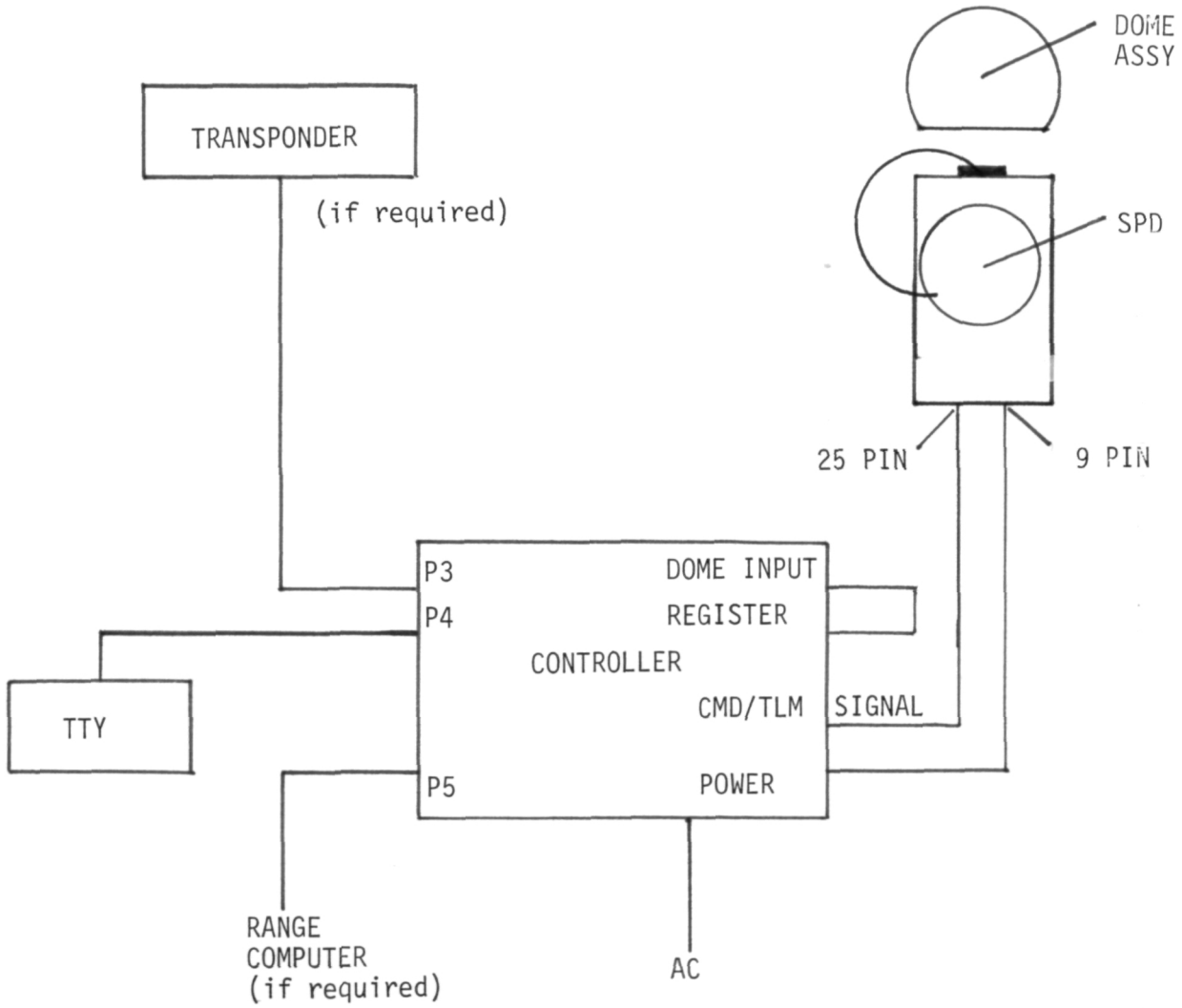


Figure 1.1 Auto Omni Interconnection Diagram

"R". The computer responds by typing the character "W" and the current address of the work space printer. The contents of the work space are unimportant since the program sets the work space upon execution. The operator should depress the space bar to display the contents of the Program Counter register. The operator must alter the contents of the program by typing 1000 <Carriage Return>. The operator then types the character "E" to start the program execution at location >1000.

Having initialized the microcomputer, a main program prompt routine will be executed. This prompt routine provides the following series of prompts (depending on the eprom chip set installed).

Chip Set "A"	Chip Set "B"
ENTER Y OR N TO THE FOLLOWING:	ENTER Y OR N TO THE FOLLOWING:
STEER TO PHI & THETA ?	STEER TO PHI & THETA ?
ENTER ELEMENTS ?	ENTER ELEMENTS ?
	OMNI MODE ?
OMNI MODE ?	RANGE TESTS ?
PROGRAM TRACK MODE ?	AUTO ACQ ?
RANGE TESTS ?	
AUTO ACQ. ? (do not use)	

Entering the letter Y to any of the above queries causes the program to branch to a separate subprogram that provides a unique test mode or demonstrates the inherent capability of the antenna. These seven unique programs are discussed in the sections that follow.

1.2 AUTONOMOUS OMNI SUBPROGRAMS

There are seven subprograms in the Autonomous Omni program modules. All seven programs share the major subroutines "Fire" and "Beams" and the I/O routines. These will be described in a separate section.

1.2.1 Program for Steering the Beam from a Manually Entered Set of Phi and Theta Direction Inputs (Chip Set A or B)

This program is accessed by typing the character "Y" to the query "STEER TO PHI AND THETA". The program then responds with a second query "ENTER THE1, THE2, DELTA-THE". The test engineer can either type in a single value for theta or three values defining a set of theta values. Suppose for a moment that only one value is entered, such as the number 30 followed by a carriage return. The porgram then prompts the test engineer with the query "ENTER PHI1, PHI2, DELTA-PHI'. Suppose that the test engineer types in the value 90 followed by a carriage return. The program would form the beam in the direction theta=30 degrees, phi=90 degrees. Now suppose that the test engineer had typed the set of numbers 0, 90, 30 <CR> for the second prompt. The program would then create a sequence of four beams at a constant theta value of 30 degrees and at phi angles of 0, 30, 60, and 90 degrees. Similarly, if three values such as 10, 60, 10 were typed in for the theta entry, followed by 0, 90, 30 for the phi entry, the program would form a set of four beams at phi of 0, 30, 60, 90 at a theta of 10 degrees, followed by another set at a theta of 20 degrees, followed by another set at a theta of 30 degrees, then another set of four at theta of 40 degrees until theta equals 60 degrees. Thus when entering a set, the first value equals the starting angle, the second value is the ending value, and the third entry is the increment. If there is no second entry, the program assumes a single value steering position. (Please note, all directions in this mode must be integer values.)

1.2.2 Program for Entering Active Elements (Chip Set A or B)

This program is accessed by typing the character "Y" to the query "ENTER ELEMENTS?". The program then responds with the prompt "ENTER ACTIVE ELEMENTS". The test engineer can then type in a set of one to 12 elements, each separated by commas with the set followed by a carriage return. The program will activate a beam with just those elements active. The operator is then prompted with the query "AGAIN?". Typing the letter "Y" will cause a program jump to the section that accepts another set of active elements. Typing anything but a "Y" will cause a branch back to the main program prompt routine.

1.2.3 Program for Entering the Omni Beam Mode (Chip Set A or B)

This program is accessed by typing the character "Y" to the query "OMNI MODE?". The program responds by turning on the four elements that create the standard omni beam pattern and then returns to the main program prompt section. The 10 elements that are activated to create the standard omni beam are elements 7 through 16.

1.2.4 Program Track Mode (Chip Set A only)

1.2.4.1 Entering the Data for the Programmed Track Subprogram

This program is activated by typing the character "Y" to the query "PROGRAM TRACK MODE?". However, prior to entering this program, one must enter an appropriate set of orbit tracking parameters in the volatile memory locations labeled "UM" (>FCDO), "UMTW" (>FCD2), "UMTE" (>FCD4), "RHOW" (>FCD6) "RHOE" (>FCD8), "RORATE" (>FCEO), "AITW" (>FCE2) and "AITE" in (>FCE4). These parameters define a simple circular orbit for the user satellite and two arbitrary TDRS satellites as a function of microcomputer time. The microcomputer uses these command input data to determine the orbital relationships between the satellites to compute the pointing direction to the TDRS system. (Refer to BASD TN82-06, included as Appendix A, for a physical description of these parameters.) Refer to Appendix B for a description of how to format the data for entry to the program.

To enter these data in the microprocessor memory, depress the main reset interrupt to force the microcomputer to vector back into the utility monitor (TI-BUG) program. The operator then types the letter "A" to provide an input for the program to re-establish the baud rate. The operator then answers the question mark prompt with the Modify/Examine memory command "M". If one wished to enter the hexadecimal value >708 in the memory cable location for "UM", the operator would respond to the ? prompt by typing M FCDO<CR>. The microprocessor would then output the current contents of the location >FCDO. If the operator types a line feed or a carriage return, the contents of the location >FCDO will remain unchanged. If, however, the operator typed the value 708 after the microprocessor typed out the current value, the processor will replace the contents with the new value >708. The decimal equivalent of >708 is 1800. Since a one decimal place significance is implied for all orbit input data, the result of the above action is to set the initial user satellite orbit plane angle (UM) to 180.0 degrees. Assume that the initial value in "UM" had been 7FC3. The keyboard printout would be as follows:

M_FCDO_7FC3 0708

The underlined characters and blanks are output from the processor while the non-underlined values are input from the operator.

1.2.4.2 User Satellite Orbit Attitude Model

The User Satellite orbit attitude model selected for the Autonomous Omni antenna system demonstration has the user satellite in a near circular orbit with the Z-axis of the two antennas normal to the orbit plane. Consider the geometric relationship shown in Figure 1.2. We begin with a coordinate system which has the X-axis on a TDRS geocentric position vector. The initial Z-axis is normal to the TDRS orbit. In this frame of reference, the X component of the geocentric vector to a TDRS is equal to the distance from the geocenter to TDRS while the Y and Z components are 0. This vector can be resolved into the antenna frame of reference by performing the following coordinate rotations and coordinate transformations for the general case:

A. Rotate the coordinate system around the Z-axis through the negative angle μMT. (This brings the new X-axis into the equatorial plane.)

B. Rotate the coordinate system around the new X-axis through the negative angle AIt. (This brings the new Y-axis into the equatorial plane.)

C. Rotate the coordinate system around the new Z-axis through the angle RHO. (This brings the new X-axis onto the ascending node of the user satellite orbit.)

D. Rotate the coordinate system around the new X-axis through the angle AIe. (This brings the new Y-axis into the orbit plane of the user satellite along with the new X-axis.)

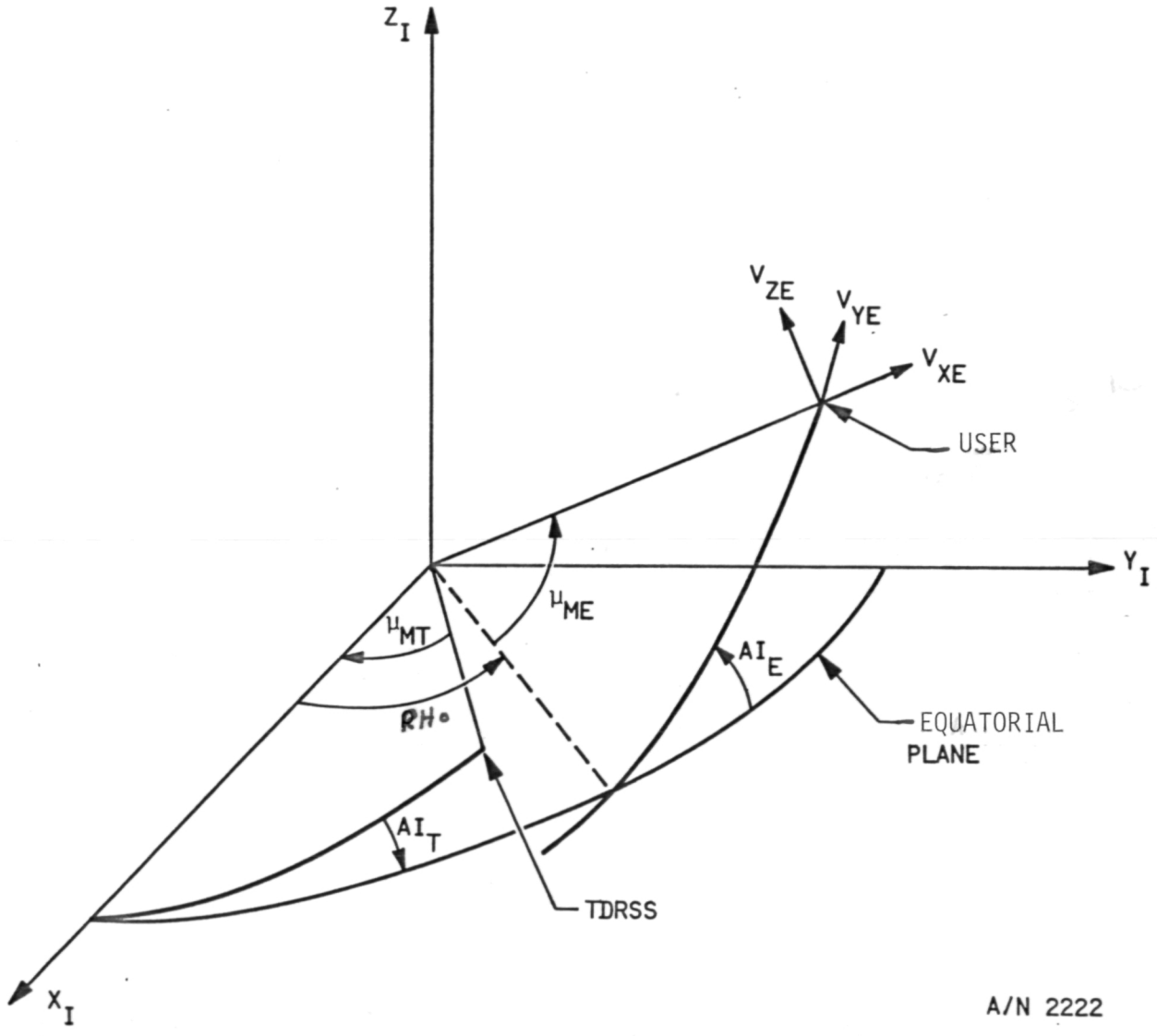

Z_I
V_{ZE}
V_{YE}
V_{XE}
USER
Y_I
μ_{ME}
μ_{MT}
AI_E
RHO
EQUATORIAL
PLANE
AI_T
TDRSS
X_I
A/N 2222

Figure 1.2

E. Rotate the coordinate system around the new Z-axis through the angle uME. (This makes the new X-axis parallel and concentric with the user satellite position vector.)

F. Translate the coordinate system from the center of the earth to the center of the user satellite system. [This can be done by subtracting the radius of the user satellite (assumed to be 600 nautical miles) from the new X component of the geocentric TDRS position vector.]

G. Rotate the coordinate around the Z-axis back through the angle uME. This provides an X-axis reference that remains parallel to the line of the orbit ascending node which is a stable inertial reference.

Once the vector from the user satellite to the TDRS satellite has been resolved in antenna coordinates, it is simple to solve for the beam pointing parameters PHI and THETA. THETA is the angle from the pole of the antenna down to the vector pointing to the TDRS satellite. In our new coordinate system THETA is:

$$\text{THETA} = \text{ARC COS}\left(Z / \sqrt{(X^2 + Y^2 + Z^2)}\right)$$

where X, Y, Z are projections onto the new coordinate system.

PHI is the angle from the X-axis to the TDRS position vector's projection into the X-Y plane of the antenna. The angle is positive in the counter-clockwise direction.

$$\text{PHI} = \text{ARC TAN}(Y/X)$$

1.2.5 Program for Steering the Beam to Align with the Antenna Range Positioner (Chip Sets A and B)

This program is accessed by typing the character "Y" to the query "RANGE TESTS?". The first function of the program is to prompt the operator to enter a PHI and a THETA offset. It should be possible to align the antenna on the test fixture so that a zero step readout corresponds to a zero elevation angle and a zero scan angle corresponds to a zero phi angle. If an exact alignment is not possible, then the fixed offsets entered above will be added to the range computer outputs for the step and scan angles to provide the Autonomous Omni computer the information it needs to maintain a directional beam always pointing at the RF source while the positioner is stepping and rotating the antenna.

The range computer and the Autonomous controller microprocessor function together in a closed loop fashion to control the beam steering for the automatic RDP test. First the range computer tells the antenna controller where the antenna positioner will be when the next measurement will be made. This information is received serially via an RS-232 port. If the input message appears to be correct, the antenna controller positions the beam at that location and answers with an "ACK". If the message does not appear correct, the antenna controller answers with a "NAK" and does nothing with the beam. If the range computer receives an "ACK",it moves the positioner to the prescribed location and takes the measurement. If the range computer receives a "NAK" from the controller, it repeats the message until an "ACK" is received.

1.2.6 Program to Automatically Determine the Direction to the Signal Source Retrodirective Mode (Chip Set B only)

This program is accessed by typing the character "Y" to the query "AUTO ACQ.?". This query is followed by the query "SIMULATOR ?". If the operator responds by typing "Y", the program will set the simulator flag in volatile memory active (SIML=0) and output a second prompt:

```
THETA PHI
        TARGET?
```

The operator would then respond by typing in PHI and THETA for the imaginary target. If, for example, the operator wished to locate a theoretical target at a THETA = 30 and a PHI = 90 degrees, he would answer the above prompt with the following entry:

```
THETA PHI
  30  90  TARGET?
```

(The program will create the blank fields in the test message and position the input print under the lables shown above.)

During subsequent execution, the program will branch into the subroutine "BAGC" whenever it needs a signal estimate. The first step in this subroutine is to examine the simulator flag. If this flag is not set, the routine branches to a section that reads the signal estimate from the A/D. If the flag is set, the routine drops into a section that computes a simulated signal estimate as a function of the square of the angular separation between the currently active beam and the theoretical target.

1.2.6.1 Phase 0 Acquisition

The first operational step in the acquisition sequence is a Phase 0 PN-CODE and CARRIER LOCK detect. The program forms the standard Omni Beam and cycles in a loop that tests the CRU input connected to a TTL point in the Motorola Transponder that registers the PN CODE LOOP LOCK. The program continues to the next step when this signal goes high. The next step is a similar loop to test the CARRIER DETECT TTL point in the Motorola Transponder. It continues on when this test point goes high. Both of the above wait loops are bypassed if the simulator flag has been set active.

1.2.6.2 Phase 1 Acquisition

Phase 1 is the next step in the acquisition sequence. Thirteen separate directional beams (Table 1.2) are output alternately with the omni beam. The signal estimate from each beam is saved in a table. At the termination of the search the beam with the strongest signal estimate is selected for the starting reference for the next phase. Toggling back to the omni beam after each directional search beam provides a sufficient integrated signal which enables the transponder to retain PN CODE LOOP LOCK and CARRIER LOCK for the sampling periods where the directional beams are directed away from the target. The duty cycle between the omni and the directional beams is 50 milliseconds.

1.2.6.3 Phase 2 Acquisition

Phase 2 converges on the target through successive search operations. It first sets up a four-beam target sampling and averaging operation. It then employs a differential correction algorithm to compute a new center for the four-beam sampling pattern and moves the center of the subsequent sampling pattern in the direction of the target. Figure 1.3 shows the four-beam sampling pattern. Beam 1 is centered on the starting reference, beam 2 is directly north of beam 1, beam 3 is southeast on an azimuth bearing 120 degrees from north and beam 4 is southwest of beam 1 on an azimuth bearing of 240 degrees from north. Initially, beams 2 through 4 are located on an arc radius of 24 degrees from the beam 1 starting reference. As the search progresses the distance between the center beam and outlying triangulation beams is gradually reduced. The search operation is terminated when n cycles are completed or when the processor detects a null condition from the relative signal estimates from the three outlying search beams.

The initial center reference for the Phase 2 acquisition sequence is the Phase 1 beam with the strongest signal estimate. The first step in Phase 2 is to position a beam on this reference and allow the Motorola Transponder AGC circuit to go active by dropping the TTL control line at the interface between the Autonomous Omni and the transponder. This insures that the transponder's signal estimate does not saturate the dynamic range of the analog signal estimate voltage as the Phase 2 search moves to successively stronger beam signals. (The current software allows the AGC circuit to stay active for 10 sample periods. Then the AGC circuit is inhibited by raising the TTL AGC control line at the processor/transponder interface.) After "locking" the transponder AGC, the microprocessor determines three test beams located around the reference position. These test beams are determined by the trigonometric identity subroutines "FGSC" and "FGSS".

The processor now activates each of the beams sequentially and sums the signal estimates for each through four repeat cycles. This operation is done using a look ahead procedure. The look ahead feature has the processor computing the active beam elements for the next beam while the transponder is

Table 1.1

PHASE 1 ACQUISITION BEAMS

Beam	Pointing Angle	
	THETA	PHI
1	64	0
2	64	36
3	64	72
4	64	108
5	64	144
6	64	180
7	64	216
8	64	252
9	64	288
10	64	324
11	22.5	0
12	22.5	120
13	22.5	240

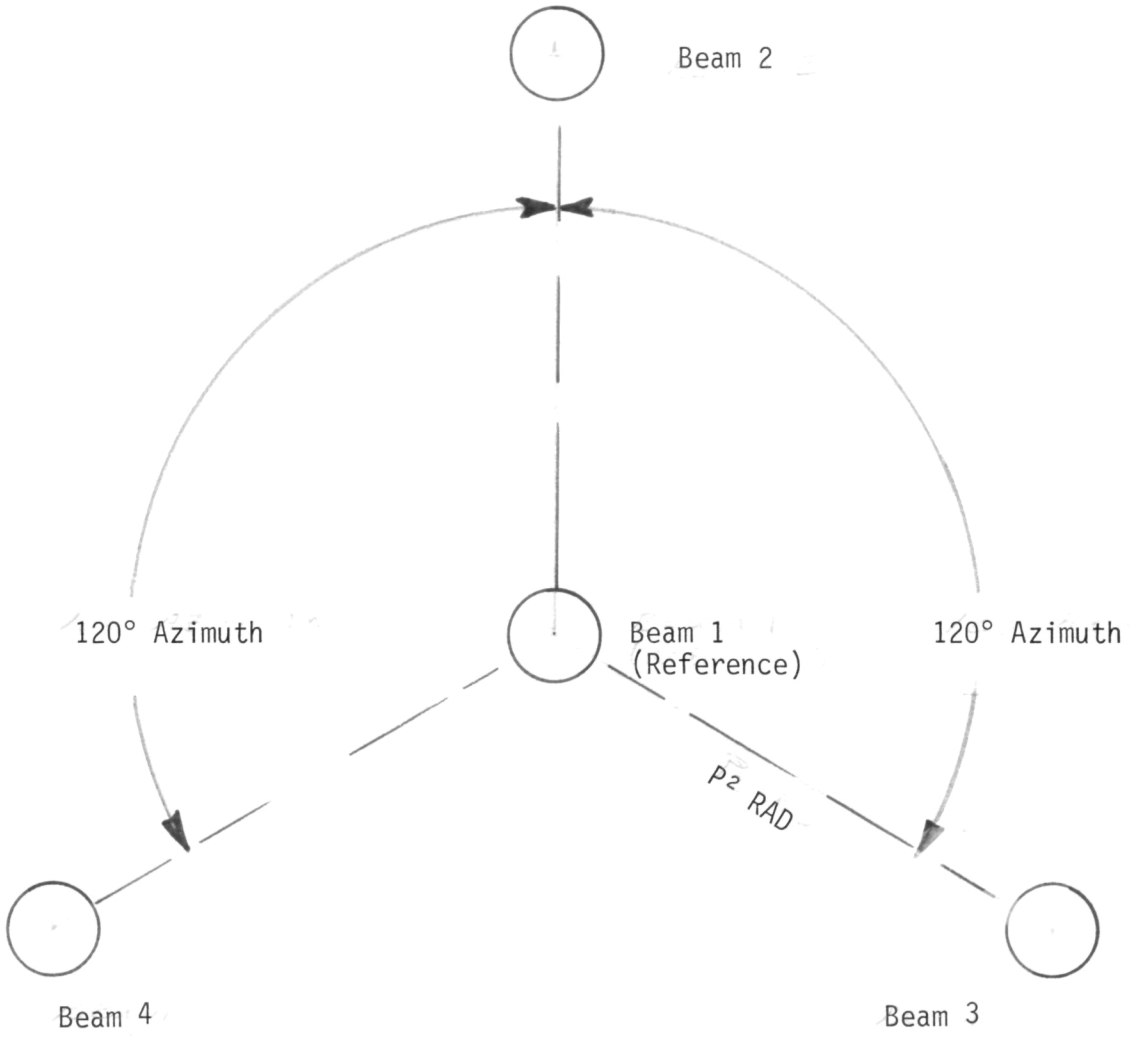


Figure 1.3 Phase 2 Acquisition Beam Locations

integrating the signal from the current beam. After the look ahead beam is computed, the processor waits in a loop until the "SAMPLE VALID" signal goes high. It then samples the "SIGNAL ESTIMATE" voltage from the transponder and immediately calls the beam activation routine "FIRE" to activate the "Look-ahead" beam before calling "BEAMS" to compute the active elements for the next "Look-ahead" beam.

The next step is to analyze the accumulated "SIGNAL ESTIMATES" to determine the direction and magnitude of the center shift. First we divide each accumulated "SIGNAL ESTIMATE" count by four to obtain an average count. Next we subtract the smallest of the search beam averages from each of the four averages. This will leave one triangulation beam signal count equal to zero. The magnitude of the shift in the triangulation beam is determined by the following equation:

$$\Delta R = P2RAD/2 - (P2RAD/2) \times (S(1)-S(N))/|SM|$$

where

P2RAD = search beam separation from the center reference. Initially P2RAD is set to 24 degrees and it is reduced by three degrees on each iteration.

S(N) = the signal estimate from one of the corner search beams

S(1) = the signal estimate from the center beam

|SM| = the larger of the two signal estimates S(N) or S(1).

The search beam with a zero value after normalizing is not weighed. It appears that one would want to move the center reference away from the beam showing the weakest signal strength. If the beam being weighed is the north search beam S(N=2), the value ΔR is subtracted from the center reference. If the beam being weighed is the southeast search beam, (S(N=3)), 1/2 of R is added to theta and 0.866 of R is added to phi. Similarly, if the beam being weighed is the southwest beam (S(N-4)) 1/2 of R is added to theta and 0.866 of R is subtracted from phi. Let us demonstrate the center shift equation with some theoretical signal estimates. Suppose the following average signal estimates are obtained from a measurement:

S(1) = 2450 CTS (CENTER REFERENCE BEAM)
S(2) = 3200 CTS (NORTHERN SEARCH BEAM)
S(3) = 2050 CTS (SOUTHEASTERN SEARCH BEAM)
S(4) = 1880 CTS (SOUTHWESTERN SEARCH BEAM)

After normalizing the number set is:

S(1) = 570
S(2) = 1320
S(3) = 170
S(4) = 0

Δ_{R_1} for the northern search beam is 24/2-24/2x ((570-1320)/1320)
= 12-12x(-.568) = 18.8 degrees

Δ_{R_2} for the southeastern beam is 24/2-24/2 x ((570-170)/570)
= 12-12x(.7) = 3.5 degrees

Having calculated a new center reference beam, the Phase 2 sequence is reentered. The search radius is decreased by two degrees and the procedure is repeated. The Phase 2 sequence is then reentered four more times to converge to a final beam location. A count relating to signal magnitude is also saved for each of the six Phase 2 beam centers. The beam center with the largest signal magnitude is then used as the final beam pointing direction. This final check is used to reduce the probability of a less than optimum beams being chosen.

1.3 CHIP SETS A AND B REPLACEMENT

Chip sets A and B may be installed into the microcomputer by removing the computer's front panel and removing the memory printed wiring board. The two integrated circuits (chip set) are marked even and odd. Replacing the chip set into the proper sockets allows the use of that chip set.

NOTE: The reinsertion of the PWB and the cables may be tedious. For normal operation, chip set B should be left installed.

Chapter 2
SWITCHING POWER DIVIDER DESCRIPTION

Abstract

This chapter describes the microstrip switching power divider. A microstrip implementation was used to avoid the problem of asymmetrical loading which is associated with the cavity type switching power divider.

2.1 OVERVIEW

Autonomous Omni was originally planned to use a cavity type switching power divider (SPD) similar to that developed by the 30 inch diameter ESSA engineering model. Early in the Auto Omni program, however, it became clear that there was not an interconnection method which would have acceptable symmetry for all beams. Realizing that a microstrip implementation would have better performance with asymmetrical output connections, the program shifted from the cavity to the microstrip approach. In a microstrip switching power divider, the principle of operation is that the paralleled impedance of the "ON" output ports be the same as the input port at the common node. The first microstrip SPD used packaged PIN diodes located at the end of quarter wavelength 70 ohm transmission lines radiating from a central node. The input line was impedance transformed through a quarter wavelength of 35 ohm line to provide an acceptable match. Unfortunately, the bandwidth of the SPD was severely limited by this approach. This limitation was the result of the fact that 32 quarter wavelength 70 ohm lines in parallel provided only a narrow band open circuit to the central node. By moving the diodes to the center node (as shown in the present SPD Figure 2.1) the SPD bandwidth was increased substantially.

2.2 DESCRIPTION

Figure 2.1 shows the switching power divider used in the present Auto Omni configuration. This SPD consists of two key assemblies:

- outer Teflon PWB with connectors and bias network
- hybrid

which are described in the following paragraphs.

2.3 OUTER TEFLON PWB WITH CONNECTORS AND BIAS NETWORK

The switching power divider used by the Auto Omni was developed with SMA type RF connectors on the input and output leads. The usage of these connectors greatly simplified the testing and fabrication of the hardware, however it increased the size and loss of the SPD. The SPD's size was determined by allowing roughly 0.5 inch spacing between each of the 36 output connectors and one inch from the closest output connectors to the input connectors. As a result, the diameter of the SPD was required to be at least 6.2 inches. If a connectorless interconnection method was used, the output radius could be reduced to 4.2 inches. As a result, two inches of 50 ohm microstrip transmission line could be deleted from the SPD. This would reduce the SPD loss by 0.1 dB.

The outer Teflon PWB consists of 37 50 ohm transmission lines. These transmission lines interconnect the diode hybrid and the RF connectors. Also located on this PWB are 100 ohm quarter wavelength bias inductors. These inductors are grounded through a bias capacitor which serves as a DC terminal.

2.4 HYBRID

The hybrid is presently a circular brass puck which mounts into the outer Teflon PWB assembly. Ground contact between the hybrid and this assembly is through a compression fit between ground planes. The hybrid consists of three key elements:

- feedthroughs
- epsilam interconnect ring
- substrate

2.4.1 Feedthroughs

The engineering model hybrid's feedthroughs consist of short sections of the inner conductor and dielectric of 0.085 inch semi-rigid cable which were epoxied into the hybrid case. For future hybrids, the feedthroughs will consist of low capacity glass to metal seal feedthroughs which will be soldered into place.

2.4.2 Epsilam Interconnect Ring

An annular ring of epsilam-10 was used as an interconnecting printed wiring board between the feedthroughs and substrate. This PWB allows the feedthroughs to be inserted on top of the interconnect ring and the package checked for hermeticity. After insuring that the package is acceptable, the substrate may then be installed and wirebonded to the interconnect ring.

2.4.3 Substrate

The substrate is the functional "heart" of the SPD. This circuit contains the impedance transformers for both the inputs and outputs along with the PIN diodes for switching.

Contact between the interconnect ring and the substrate is achieved by five mil wide gold ribbon that is welded to the end of the lines on the substrate. An inspection of Figure 2.1 reveals that the SPD has one input/output port and 36 output/input ports. The PIN diodes that bridge the gap between the substrate's central node and the 36 output/input lines can be selectively turned "on" by the application of current via the bias inductors located on the outer Teflon PWB. Back biasing the "off" diodes effectively removes them from the circuit. As previously noted, the substrates impedance transformers are optimized for the combination of four "on" diodes at a time.

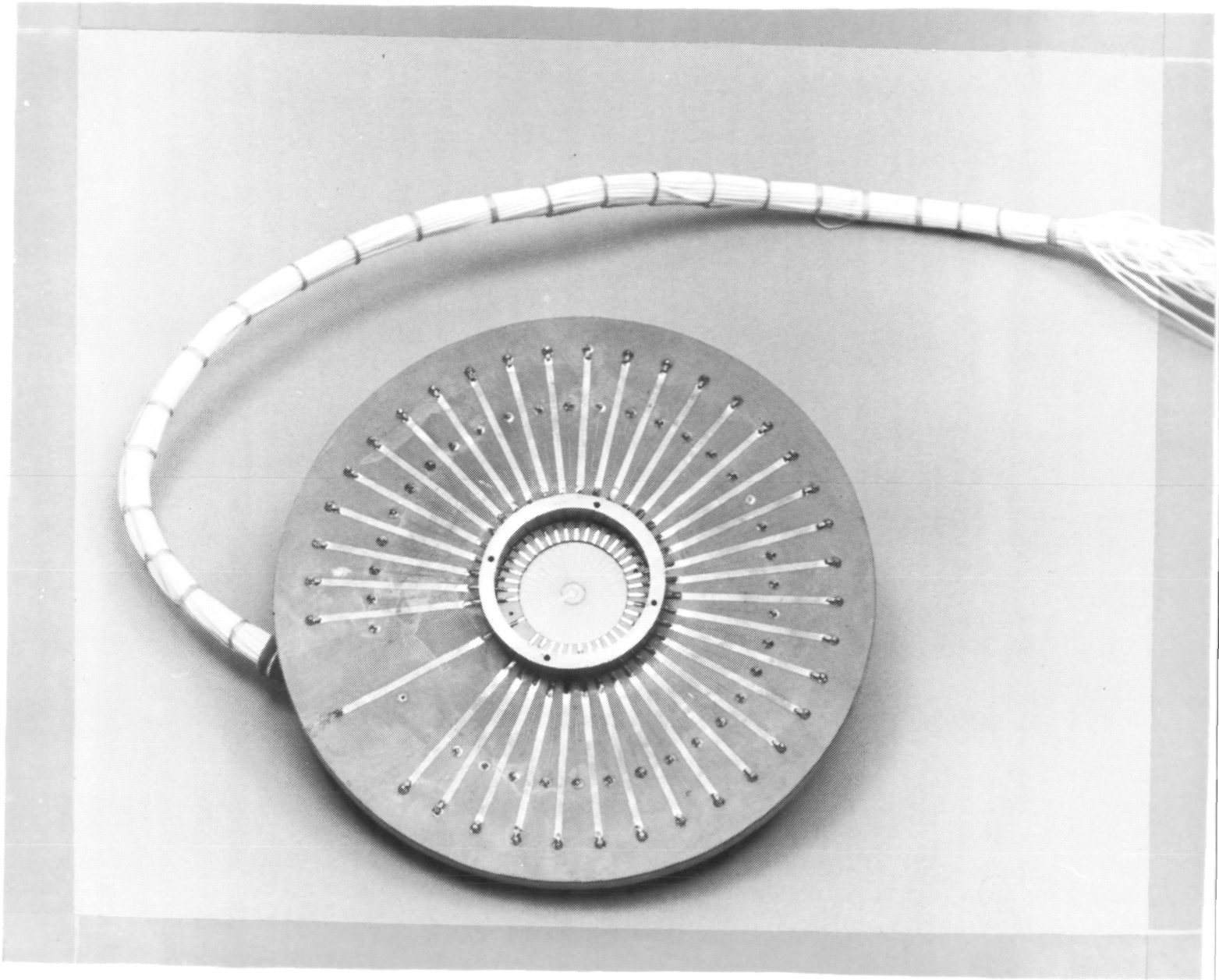


Figure 2.1 Switching Power Divider

Chapter 3
MICROSTRIP SWITCHING POWER DIVIDER PERFORMANCE

Abstract

In this chapter the SPD's performance is discussed. Average insertion losses of 6.95 dB (2106 MHz) and 7.87 dB (2287 MHz) are demonstrated for a set of typical output combinations.

3.1 INTRODUCTION

In order to verify the performance of the switching power divider, a large number of insertion loss and insertion phase measurements were taken. The raw data for these measurements is shown in Figures 3.1 through 3.78. This data was taken for three different connections:

- Case 1 - Resistive loads
- Case 2 - Repeat of Case 1 to verify validity
- Case 3 - Elements used as loads

In all cases, the data was taken for randomly selected sets of four outputs. The test data taken is believed to be representative of the symmetrical and asymmetrical output loading combinations.

3.2 CASE 1

In the Case 1 measurements, the insertion loss was measured for 27 different four-output combinations. For these tests, the outputs were all terminated by 50 ohm resistive loads. The raw data for this case is shown in Figures 3.1 through 3.27. Table 3.1 summarizes the data. This summary shows that the average insertion loss is 7.53 dB (2106 MHz) and 7.85 dB (2287 MHz) when four higher insertion loss outputs are excluded. These outputs 1, 2, 35, and 36 are symmetrically located about the 35 ohm input/output line. The cause for this higher insertion loss could be coupling, low quality feedthroughs or bad PIN diodes. Two diodes were replaced with no change in performance, therefore the loss is believed to result from either coupling or low quality feedthroughs. Additional investigation is needed to resolve this insertion loss anomaly. Also, output 32 was found to have a broken PIN diode wire bond which was later repaired.

Table 3.1 also shows that the average difference in insertion loss is 0.71 dB (2106 MHz) and 0.92 dB (2287 MHz) when the higher insertion loss outputs are disregarded.

3.3 CASE 2

To verify the validity of the Case 1 data, the tests were re-run. During this Case 2 test; however, both insertion loss and phase were recorded. Raw data for the insertion loss is shown in Figures 3.29 through 3.41. Insertion phase data is shown by Figures 3.55 through 3.67. Tables 3.2 and 3.3 summarize this data. A comparison of Tables 3.1 and 3.2 shows a difference in average insertion loss of only 0.17 dB which is close to the test repeatability.

From this, the average insertion losses of 7.87 dB (2106 MHz) and 8.00 dB (2287 MHz) shown in Table 3.2 are believed to be valid. Also shown in Table 3.2 is an average power split between outputs of 0.78 dB (2106 MHz) and 0.94 dB (2287 MHz).

Table 3.3 is a summary of the insertion phase difference between channels. The average difference is 14.5 degrees (2106 MHz) and 16.2 degrees (2287 MHz) with a worst case difference of 24 degrees (2287 MHz).

The power split and phase differences shown by the data in Tables 3.2 and 3.3 are expected to have only a small effect on the Auto Omni performance.

3.4 CASE 3

The impact of realistic VSWR loads on the insertion loss and insertion phase was determined by measuring these parameters with all elements except for the one under test connected to the Auto Omni elements. Raw data for this test is shown by Figures 3.42 through 3.54 and Figures 3.68 through 3.80. Tables 3.4 and 3.5 are summaries of this raw data.

When configured in this way, the average insertion loss was reduced to 6.95 dB (2106 MHz) and 7.87 dB (2287 MHz). The power split average difference was measured to be 0.75 dB (2106 MHz) and 1.24 dB (2287 MHz). This performance is acceptable for use with the Auto Omni.

Average insertion phase differences measured in this test are 13.1 degrees (2106 MHz) and 15.6 degrees (2287 MHz). A maximum phase difference of 25 degrees (2287 MHz) was measured.

3.5 CONCLUSION

The insertion loss and phase differences from the switching power divider may be improved by further refining the switching power divider. Even so, the net change in the Auto Omni performance is expected to be no more than 0.2 dB except for beams associated with elements 1, 2, 35 or 36.

Table 3.1 SPD INSERTION LOSS CHARACTERISTICS WITH PURELY RESISTIVE LOADS (50Ω)

Selected Channels	Average Insertion Loss in dB f = 2106 MHz	Average Insertion Loss in dB f = 2287 MHz	Maximum Difference in Power Split in dB f = 2106 MHz	Maximum Difference in Power Split in dB f = 2287 MHz
17, 18, 19, 20	7.56	7.58	0.52	0.70
9, 10, 11, 12	7.58	7.63	0.35	0.60
13, 14, 15, 16	7.70	7.60	0.75	1.00
21, 22, 23, 24	7.71	7.67	0.60	0.55
25, 26, 27, 28	7.53	7.60	1.00	1.00
29, 30, 31, 32	← #32 is bad →			
33, 34, 35, 36	7.80	8.55	3.40	4.30
1, 3, 5, 7	7.49	8.48	2.40	3.60
9, 11, 13, 15	7.40	7.75	0.40	0.80
17, 19, 21, 23	7.55	7.76	0.42	0.50
25, 27, 29, 31	7.83	8.15	1.30	1.70
1, 12, 24, 36	7.46	8.38	3.00	3.60
24, 28, 36, 32	← #32 is bad →			
1, 5, 9, 13	7.38	8.15	2.50	2.90
18, 23, 28, 32	← #32 is bad →			
7, 13, 19, 25	7.24	8.03	0.90	0.95
1, 2, 3, 6	7.84	9.00	3.80	5.55
1, 2, 37	7.90	8.93	4.10	5.40
2, 3, 7, 12	7.50	8.50	3.00	4.00
2, 7, 11, 12	7.33	8.08	1.10	1.60
2, 7, 12, 17	7.28	7.93	1.60	1.90
7, 12, 17, 18	7.40	7.83	0.40	0.60
7, 12, 17, 26	7.33	8.05	1.05	1.20
7, 17, 18, 27	7.60	8.28	0.20	0.50
1, 7, 30, 36	7.65	9.03	2.70	3.50
3, 7, 13, 18	7.40	8.15	1.35	1.80
2, 3, 17, 18	7.38	8.23	3.30	2.80
Average Values Excluding High Insertion Loss	7.53	7.85	0.71	0.92
Total Average for all Combinations	7.54	8.14	1.63	2.13

Table 3.2 SPD INSERTION LOSS CHARACTERISTICS WITH PURELY RESISTIVE LOADS (50Ω)

Selected Channels	Average Insertion Loss in dB f = 2106 MHz	Average Insertion Loss in dB f = 2287 MHz	Maximum Difference in Power Split in dB f = 2106 MHz	Maximum Difference in Power Split in dB f = 2287 MHz
6, 15, 19, 20	7.28	8.08	1.00	1.30
7, 15, 19, 20	7.16	7.98	1.15	1.35
7, 12, 15, 20	7.25	8.06	0.80	1.00
7, 11, 12, 20	7.23	8.01	0.95	1.00
7, 12, 17, 20	7.25	8.04	0.62	0.60
7, 12, 17, 18	7.34	7.84	0.45	0.53
7, 12, 17, 26	7.25	8.08	0.95	1.20
7, 17, 18, 27	7.50	8.24	0.18	0.40
12, 16, 17, 26	7.25	7.85	1.00	1.45
16, 17, 26, 27	7.62	8.11	0.70	1.05
16, 17, 18, 27	7.67	8.10	0.90	0.90
7, 13, 15, 18	7.56	7.88	0.80	0.70
15, 17, 18, 20	7.39	7.79	0.65	0.70
Average Results for all Combinations	7.37	8.00	0.78	0.94

Table 3.3 THE MAXIMUM INSERTION PHASE DIFFERENCE BETWEEN CHANNELS FOR SELECTED GROUPS PURELY RESISTIVE LOADS (50Ω)

Selected Channels	Maximum Phase Difference f = 2106 MHz	Maximum Phase Difference f = 2287 MHz
6, 15, 19, 20	23.5°	24.0°
15, 17, 18, 20	12.9°	14.5°
7, 13, 15, 18	15.6°	16.9°
16, 17, 18, 27	18.8°	20.4°
16, 17, 26, 27	7.0°	8.5°
12, 16, 17, 26	19.5°	21.4°
7, 17, 18, 27	19.0°	22.5°
7, 12, 17, 26	8.5°	9.0°
7, 12, 17, 18	18.0°	20.0°
7, 12, 17, 20	11.1°	13.0°
7, 11, 12, 20	13.5°	17.5°
7, 12, 15, 20	10.0°	12.3°
7, 15, 19, 20	10.5°	10.5°
Average Values	14.5°	16.2°

Table 3.4 SPD INSERTION LOSS CHARACTERISTICS WITH THE CIRCULARLY POLARIZED ELEMENTS AS LOADS

Selected Channels	Average Insertion Loss in dB f = 2106 MHz	Average Insertion Loss in dB f = 2287 MHz	Maximum Difference in Power Split in dB f = 2106 MHz	Maximum Difference in Power Split in dB f = 2287 MHz
15, 17, 18, 20	6.76	7.71	0.30	0.85
7, 13, 15, 18	7.18	7.71	1.05	0.97
16, 17, 18, 27	7.05	7.76	0.33	1.10
16, 17, 26, 27	6.96	7.88	0.85	1.30
12, 16, 17, 26	6.59	7.94	0.65	2.05
7, 17, 18, 27	7.29	8.09	0.50	0.65
7, 12, 17, 18	6.94	7.65	0.70	0.65
7, 12, 17, 20	6.73	8.11	0.75	0.90
7, 11, 12, 20	6.93	8.09	0.65	1.60
7, 12, 15, 20	6.84	8.05	1.00	0.90
6, 15, 19, 20	7.10	7.69	1.00	2.10
7, 15, 19, 20	7.05	7.76	1.20	1.80
Average Values	6.95	7.87	0.75	1.24

Table 3.5 THE MAXIMUM INSERTION PHASE DIFFERENCE BETWEEN CHANNELS FOR SELECTED GROUPS. CIRCULARLY POLARIZED ELEMENT LOADS.

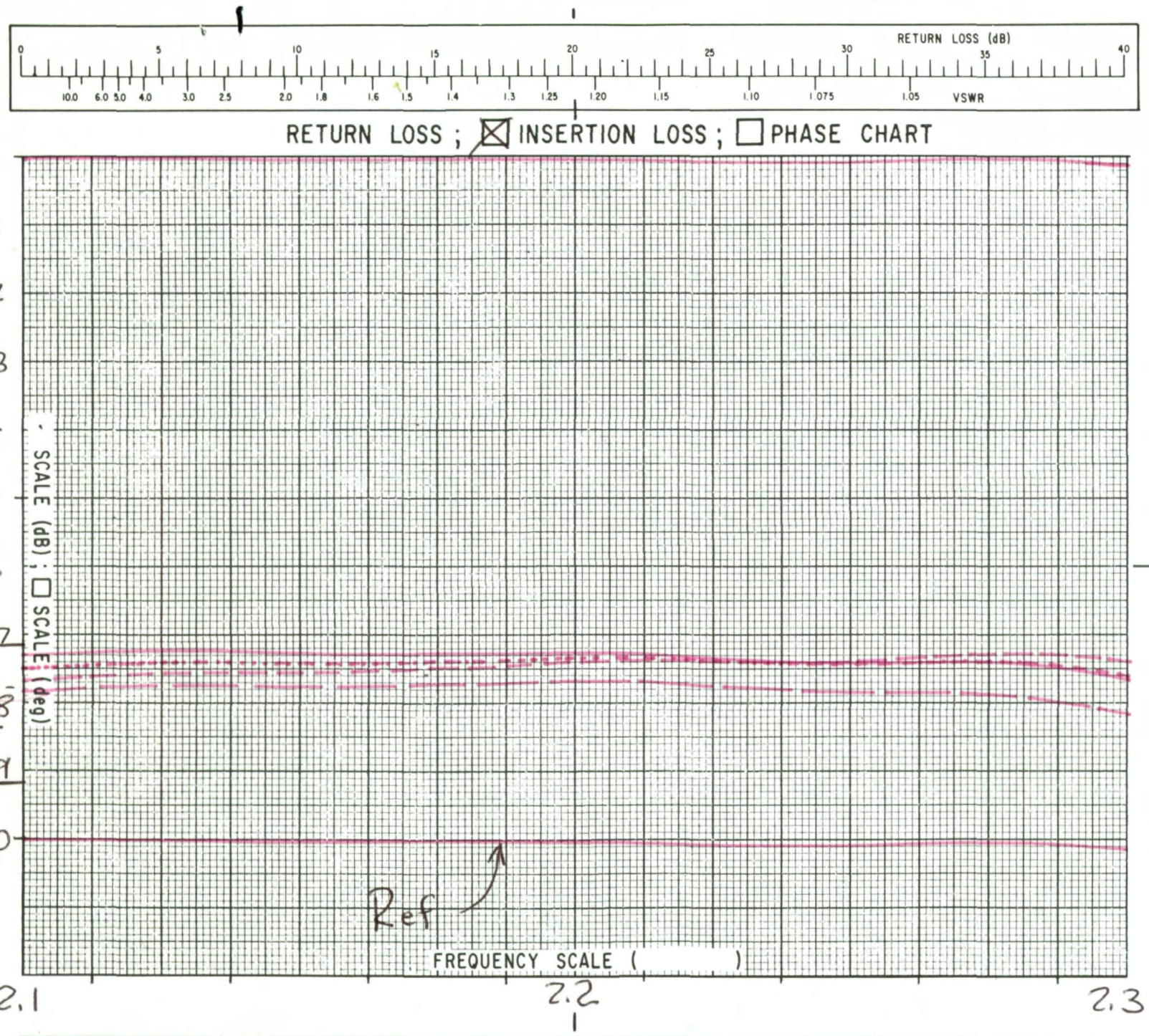
Selected Channels	Maximum Phase Difference f = 2106 MHz	Maximum Phase Difference f = 2287 MHz
15, 17, 19, 20	11.0°	13.0°
7, 13, 15, 18	13.5°	15.0°
16, 17, 18, 27	15.0°	21.0°
16, 17, 26, 27	5.5°	11.0°
12, 16, 17, 26	19.5°	18.5°
7, 17, 18, 27	16.0°	19.0°
7, 12, 17, 26	11.5°	11.0°
7, 12, 17, 18	17.0°	16.5°
7, 12, 17, 20	10.0°	11.0°
7, 11, 12, 20	10.5°	19.0°
7, 12, 15, 20	6.5°	13.5°
7, 15, 19, 20	11.5°	9.0°
6, 15, 19, 20	23.0°	25.0°
Average Values	13.1°	15.6°

Case 1 (Raw Data)

SPD INSERTION LOSS DATA WITH RESISTIVE LOADS

Figure	Outputs			
3.1	17	18	19	20
3.2	9	10	11	12
3.3	13	14	15	16
3.4	21	22	23	24
3.5	25	26	27	28
3.6	29	30	31	32
3.7	33	34	35	36
3.8	1	3	5	7
3.9	9	11	13	15
3.10	17	19	21	23
3.11	25	27	29	31
3.12	1	12	24	36
3.13	24	28	36	32
3.14	1	5	9	13
3.15	18	23	28	32
3.16	7	13	19	25
3.17	1	2	3	6
3.18	1	2	3	7
3.19	2	3	7	12
3.20	2	7	11	12
3.21	2	7	12	17
3.22	7	12	17	18

Figure	Outputs
3.23	7 12 17 26
3.24	7 17 18 27
3.25	1 7 30 36
3.26	3 7 13 18
3.27	2 3 17 18
3.28	Deleted



ANTENNAS

PROJECT NO. 2314-001 PROGRAM Auto Omni

PART NO. _____ MODEL NO. _____ SERIAL NO. _____

TEST TYPE: ☒ DEVELOPMENT ☐ PRE ☐ FINAL

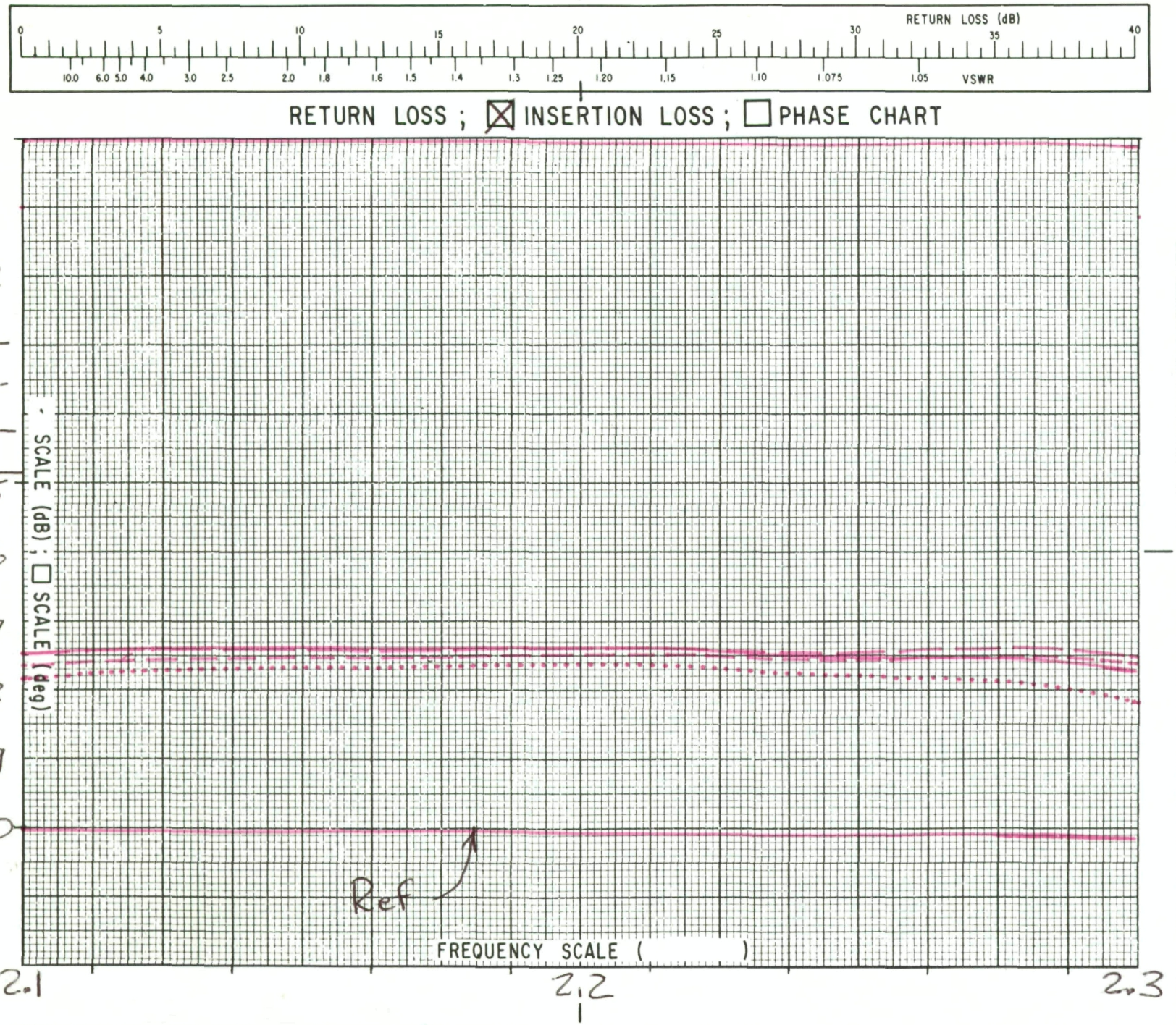
FREQUENCY RANGE 2.1 - 2.3 GHz SHEET ____ OF ____

BALL AEROSPACE SYSTEMS DIVISION

REMARKS SPD Insertion Loss

OPER. RJ WITNESSED _____ DATE 7-1-82

Figure 3.1



PROJECT NO. 2314-001 PROGRAM Auto Omni

PART NO. _____ MODEL NO. _____ SERIAL NO. _____

TEST TYPE: ☒ DEVELOPMENT ☐ PRE ☐ FINAL

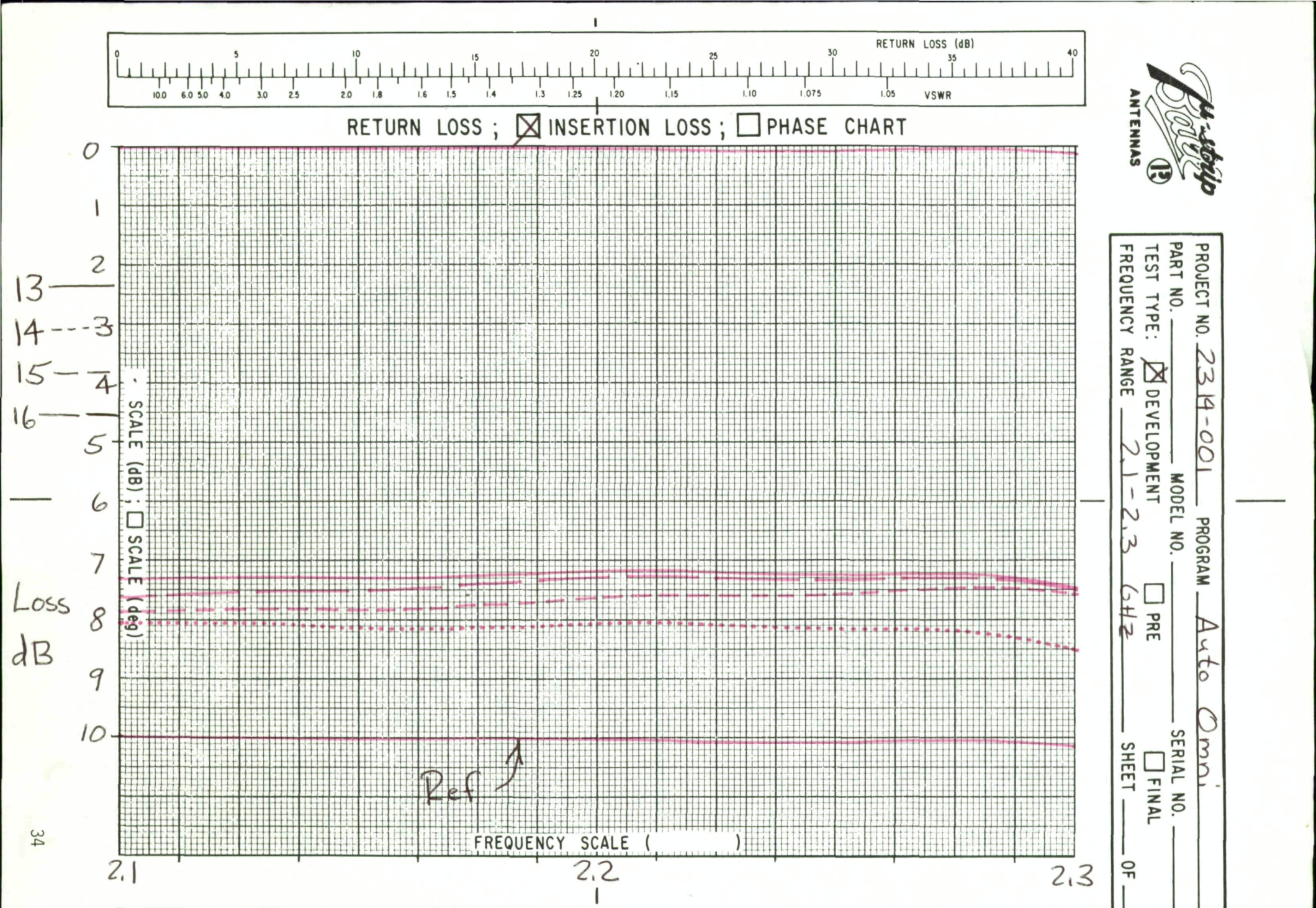
FREQUENCY RANGE 2.1 - 2.36 Hz SHEET ____ OF ____

BALL AEROSPACE SYSTEMS DIVISION

REMARKS SPD Insertion Loss

OPER. R.J. WITNESSED _____ DATE 7-1-82

Figure 3.2



Wilcox Electric ANTENNAS

PROJECT NO. 2314-001 PROGRAM Auto Omni

PART NO. _____ MODEL NO. _____ SERIAL NO. _____

TEST TYPE: ☒ DEVELOPMENT ☐ PRE ☐ FINAL

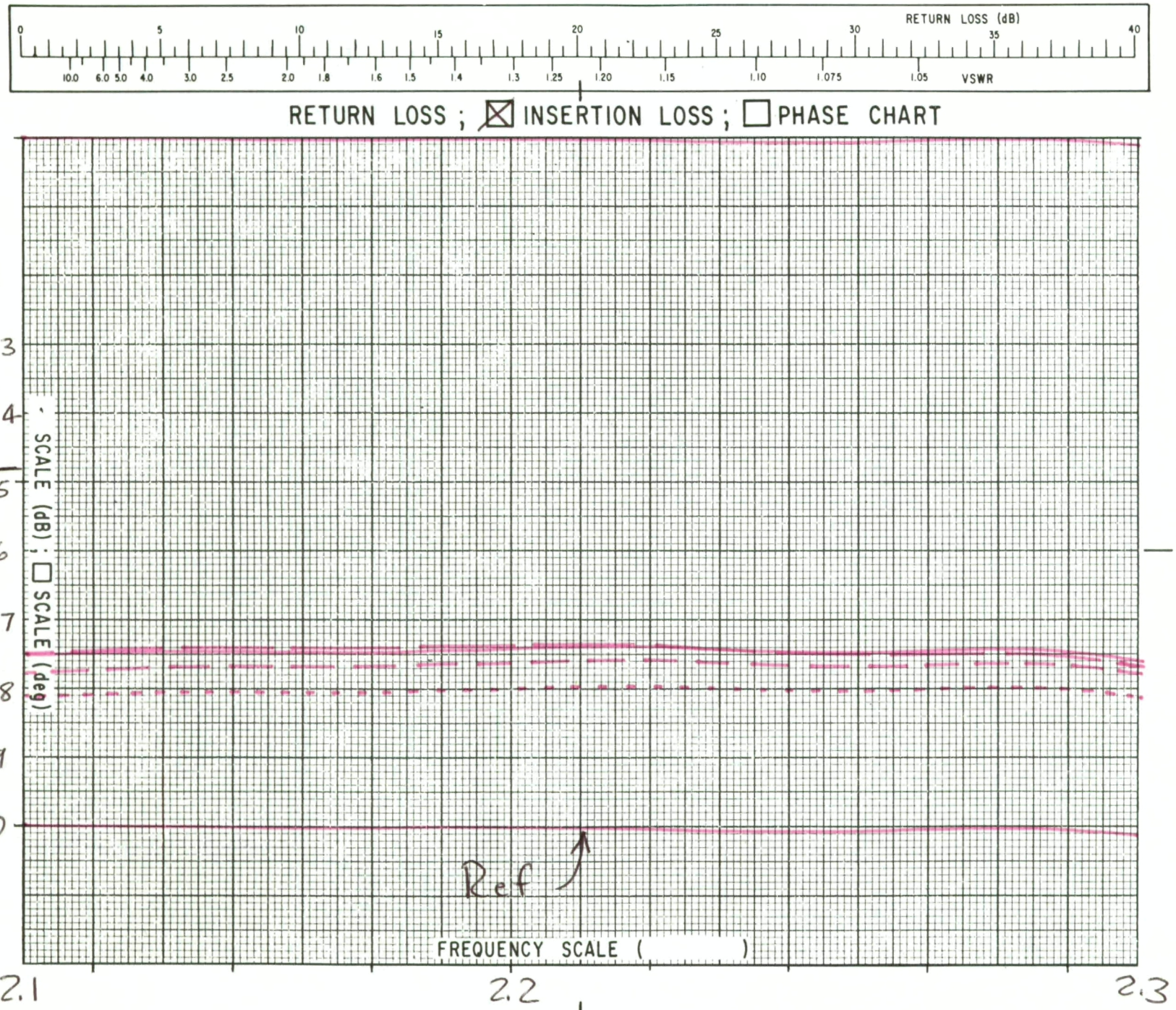
FREQUENCY RANGE 2.1-2.3 GHz SHEET ____ OF ____

BALL AEROSPACE SYSTEMS DIVISION

REMARKS SPD Insertion Loss

OPER. RJ. WITNESSED _____ DATE 7-1-82

Figure 3.3



Ball Antennas

PROJECT NO. 2314-001 PROGRAM Auto Omni

PART NO. _____ MODEL NO. _____ SERIAL NO. _____

TEST TYPE: ☒ DEVELOPMENT ☐ PRE ☐ FINAL

FREQUENCY RANGE 2.1 - 2.36 Hz SHEET _____ OF _____

BALL AEROSPACE SYSTEMS DIVISION

REMARKS SPD Insertion Loss

OPER. R.J. WITNESSED _____ DATE 7-1-82

Figure 3.4

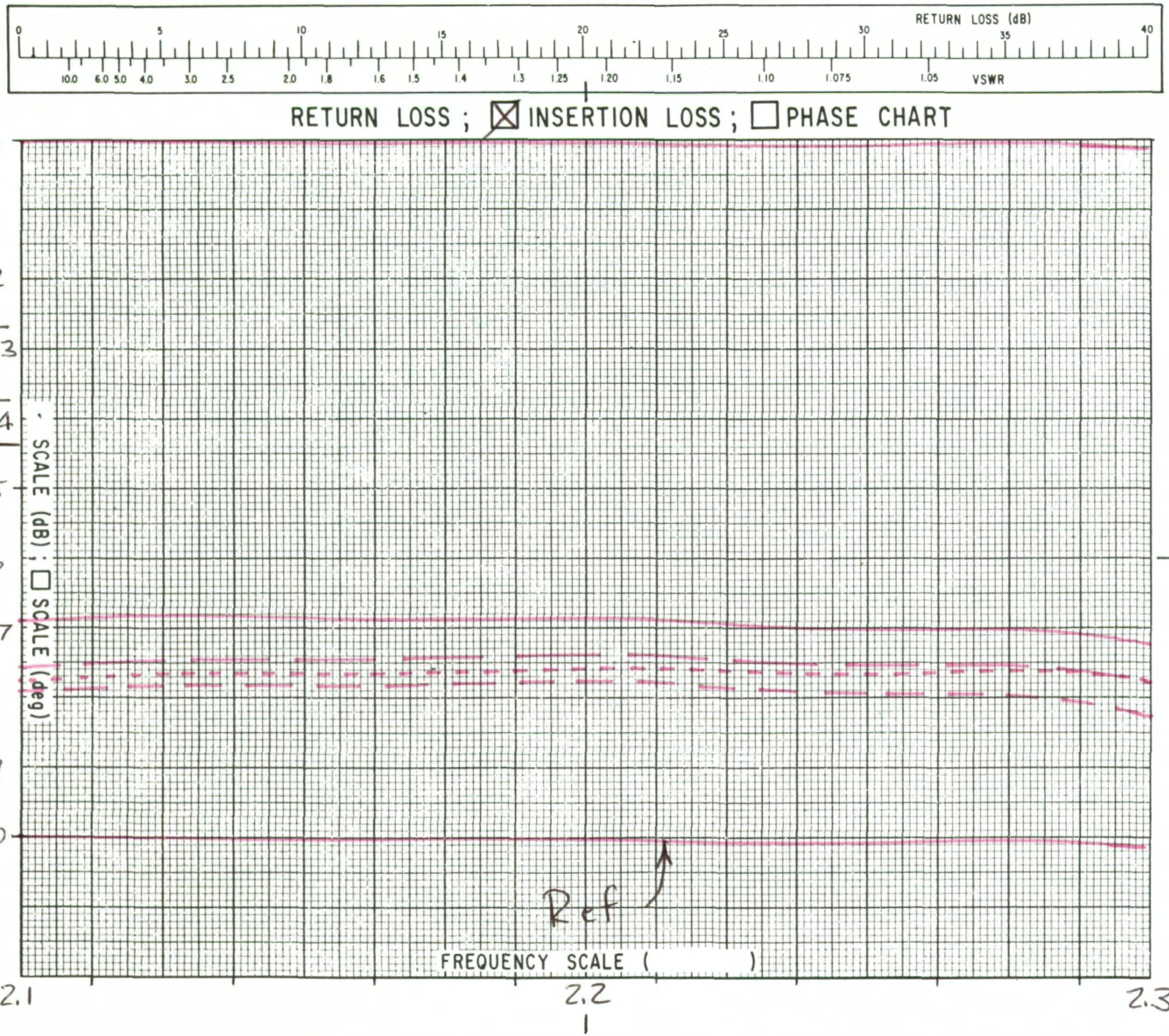

RETURN LOSS (dB)
0 5 10 15 20 25 30 35 40
10.0 6.0 5.0 4.0 3.0 2.5 2.0 1.8 1.6 1.5 1.4 1.3 1.25 1.20 1.15 1.10 1.075 1.05 VSWR
RETURN LOSS ; ☒ INSERTION LOSS ; ☐ PHASE CHART
0 1 2 3 4 5 6 7 8 9 10
25 26 27 28
SCALE (dB) ; ☐ SCALE (deg)
Loss dB
Ref
FREQUENCY SCALE ( )
2.1 2.2 2.3
PROJECT NO. 2314-001 PROGRAM Auto Omni
PART NO. MODEL NO. SERIAL NO.
TEST TYPE: ☒ DEVELOPMENT ☐ PRE ☐ FINAL
FREQUENCY RANGE 2.1 - 2.3 GHz SHEET OF
BALL AEROSPACE SYSTEMS DIVISION
REMARKS SPD Insertion Loss
OPER. R.J. WITNESSED DATE 7-1-82

Figure 3.5

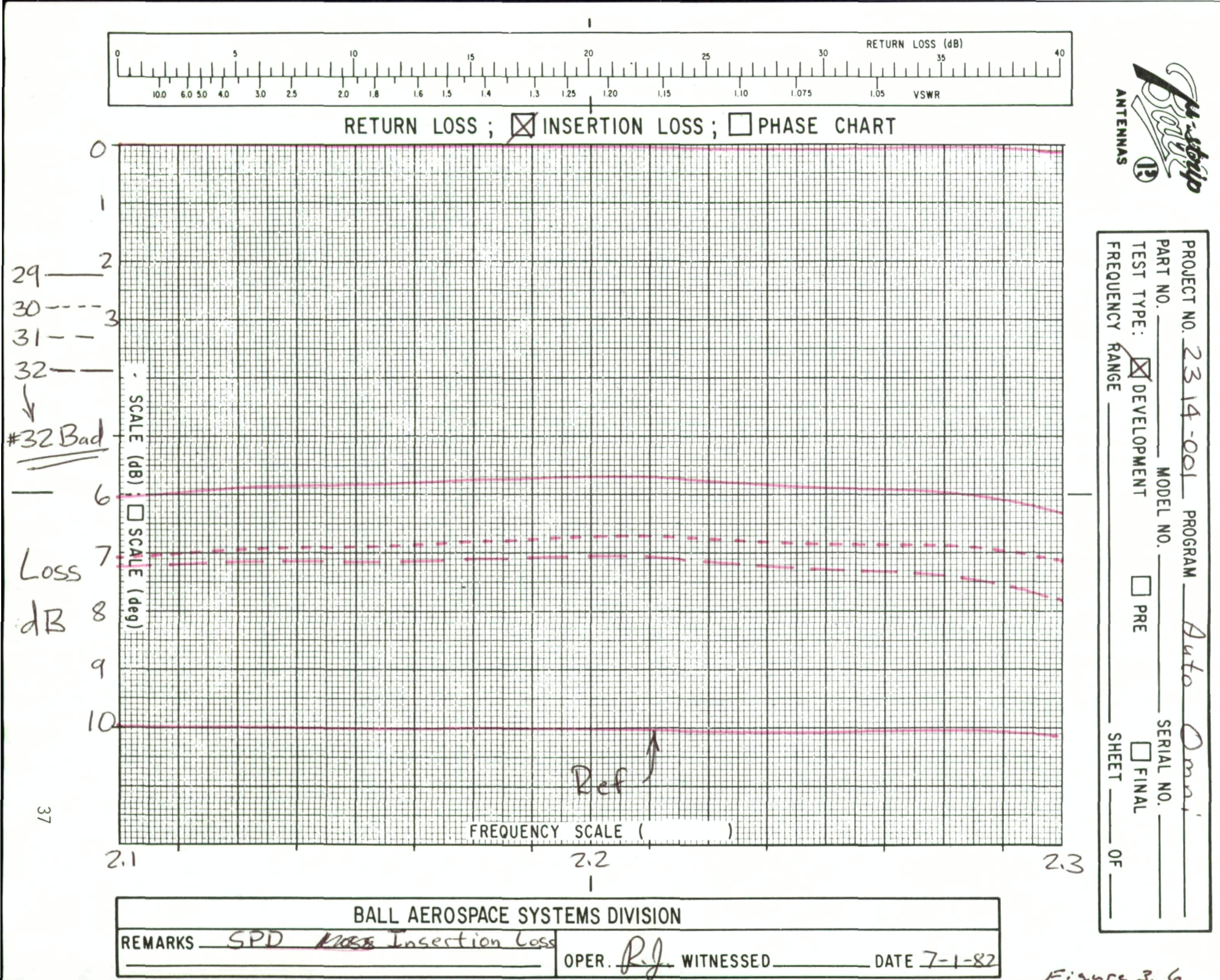
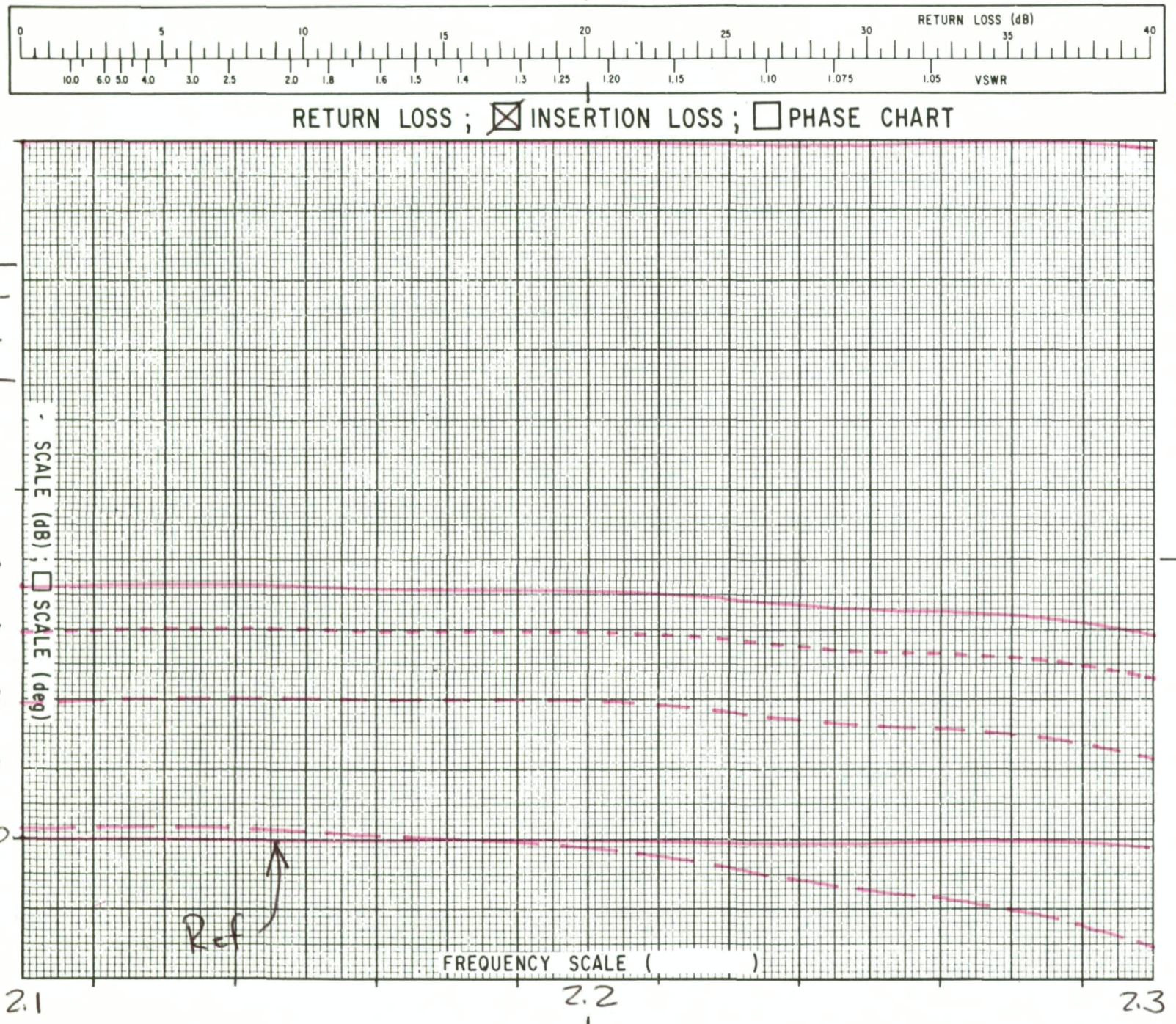

RETURN LOSS (dB)
0 5 10 15 20 25 30 35 40
10.0 6.0 5.0 4.0 3.0 2.5 2.0 1.8 1.6 1.5 1.4 1.3 1.25 1.20 1.15 1.10 1.075 1.05 VSWR
RETURN LOSS ; ☒ INSERTION LOSS ; ☐ PHASE CHART
0
1
2
3
6
7
8
9
10
29
30
31
32
#32 Bad
Loss
dB
SCALE (dB) ; ☐ SCALE (deg)
Ref
FREQUENCY SCALE ( )
2.1
2.2
2.3
37
Antennas
PROJECT NO. 2314-001 PROGRAM Auto Omni
PART NO. MODEL NO. SERIAL NO.
TEST TYPE: ☒ DEVELOPMENT ☐ PRE ☐ FINAL
FREQUENCY RANGE SHEET OF
BALL AEROSPACE SYSTEMS DIVISION
REMARKS SPD Insertion Loss
OPER. R.J. WITNESSED DATE 7-1-82

Figure 3.6



Wi-Lan Parks ANTENNAS

PROJECT NO. 2314-001 PROGRAM Auto Omni

PART NO. _____ MODEL NO. _____ SERIAL NO. _____

TEST TYPE: ☒ DEVELOPMENT ☐ PRE ☐ FINAL

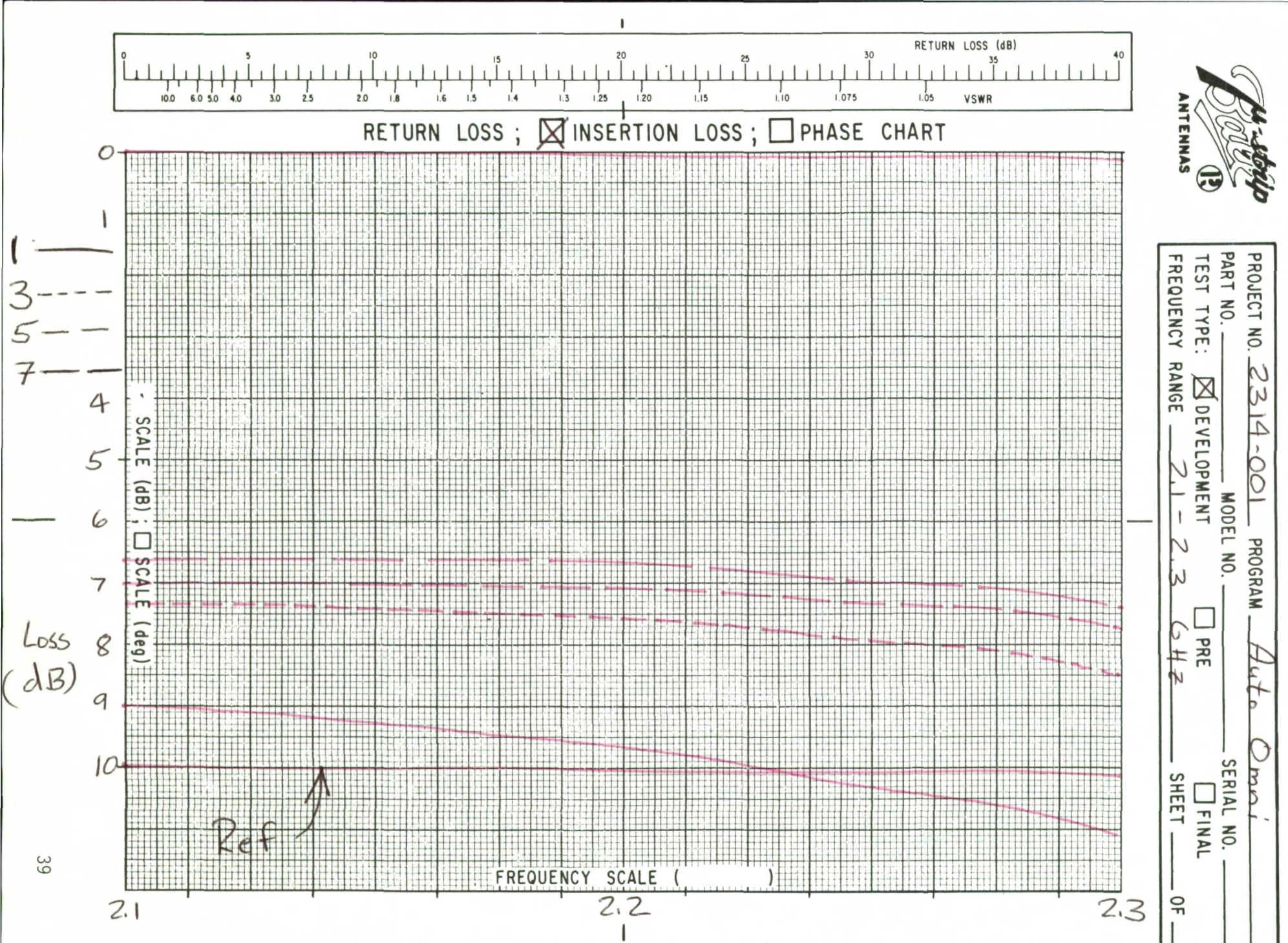
FREQUENCY RANGE 2.1-2.3 GHz SHEET ____ OF ____

BALL AEROSPACE SYSTEMS DIVISION

REMARKS SPD Insertion Loss

OPER. RJ. WITNESSED _____ DATE 7-1-87

Figure 3.7



Auto Omni ANTENNAS

PROJECT NO. 2314-001 PROGRAM Auto Omni

PART NO. _____ MODEL NO. _____ SERIAL NO. _____

TEST TYPE: ☒ DEVELOPMENT ☐ PRE ☐ FINAL

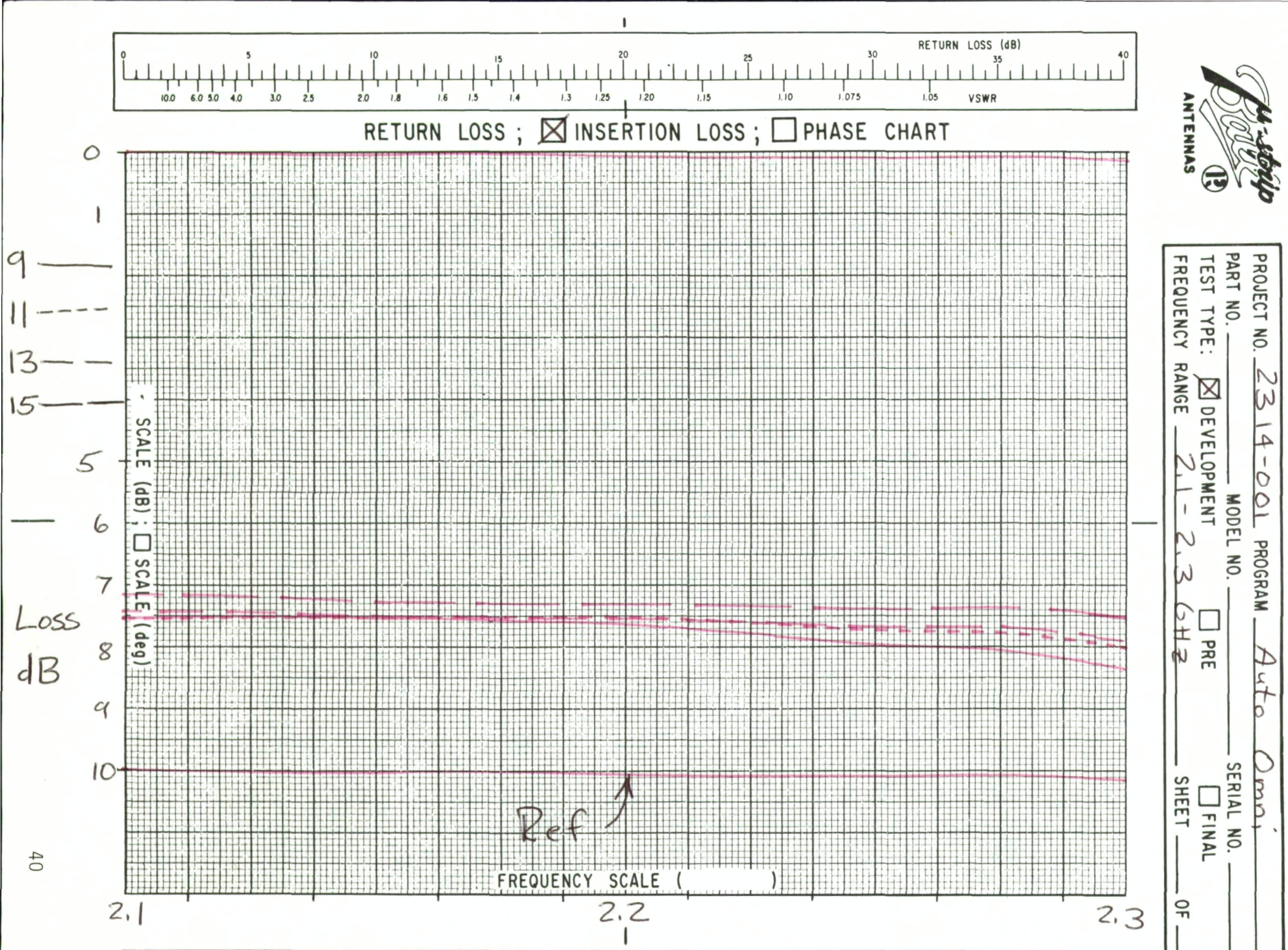
FREQUENCY RANGE 2.1 - 2.3 GHz SHEET _____ OF _____

BALL AEROSPACE SYSTEMS DIVISION

REMARKS SPD Insertion Loss

OPER. R.J. WITNESSED _____ DATE 7-1-82

Figure 3.8



PROJECT NO. 2314-001 PROGRAM Auto Omni

PART NO. _____ MODEL NO. _____ SERIAL NO. _____

TEST TYPE: ☒ DEVELOPMENT ☐ PRE ☐ FINAL

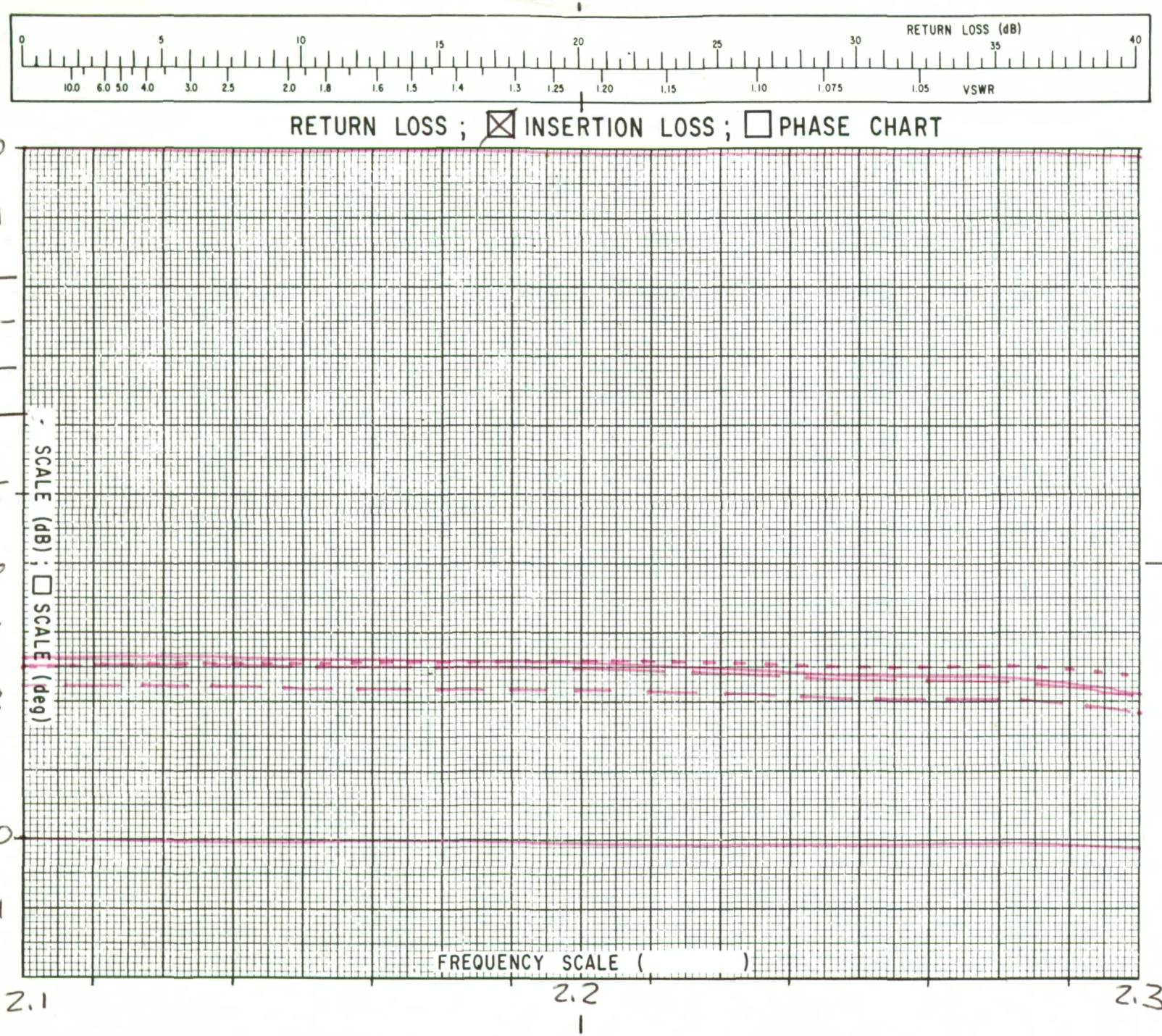
FREQUENCY RANGE 2.1 - 2.36Hz SHEET _____ OF _____

BALL AEROSPACE SYSTEMS DIVISION

REMARKS SPD Insection Loss

OPER. R.J. WITNESSED _____ DATE 7-1-82

Figure 3.9



ANTENNAS

PROJECT NO. 2314-001 PROGRAM Auto Omni

PART NO. _____ MODEL NO. _____ SERIAL NO. _____

TEST TYPE: ☒ DEVELOPMENT ☐ PRE ☐ FINAL

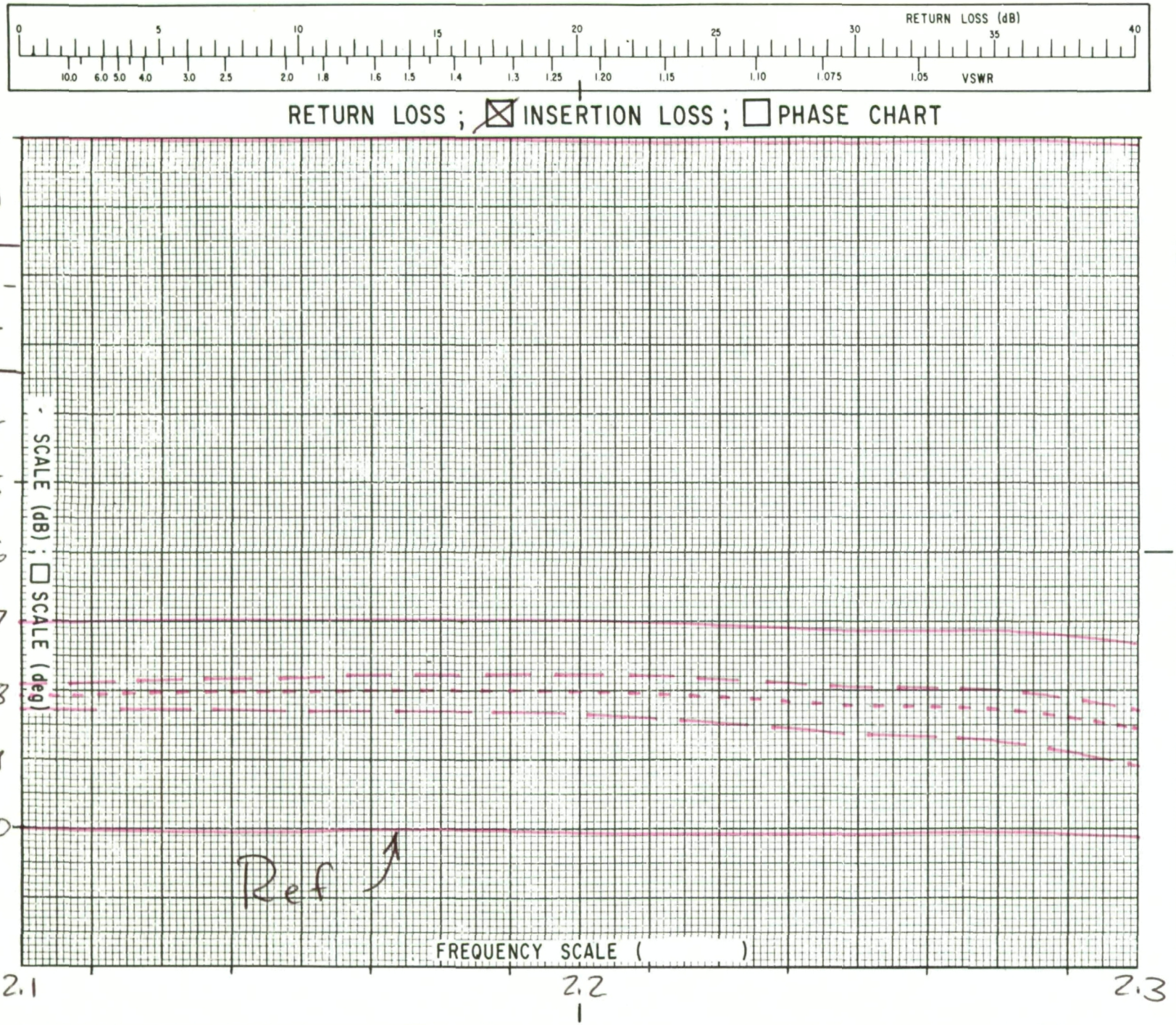
FREQUENCY RANGE 2.1 - 2.3 GHz SHEET _____ OF _____

BALL AEROSPACE SYSTEMS DIVISION

REMARKS SPD Insertion Loss

OPER. R.J. WITNESSED _____ DATE 7-1-82

Figure 3.10



Ball Antennas

PROJECT NO. 234-001 PROGRAM Auto Omni

PART NO. _____ MODEL NO. _____ SERIAL NO. _____

TEST TYPE: ☒ DEVELOPMENT ☐ PRE ☐ FINAL

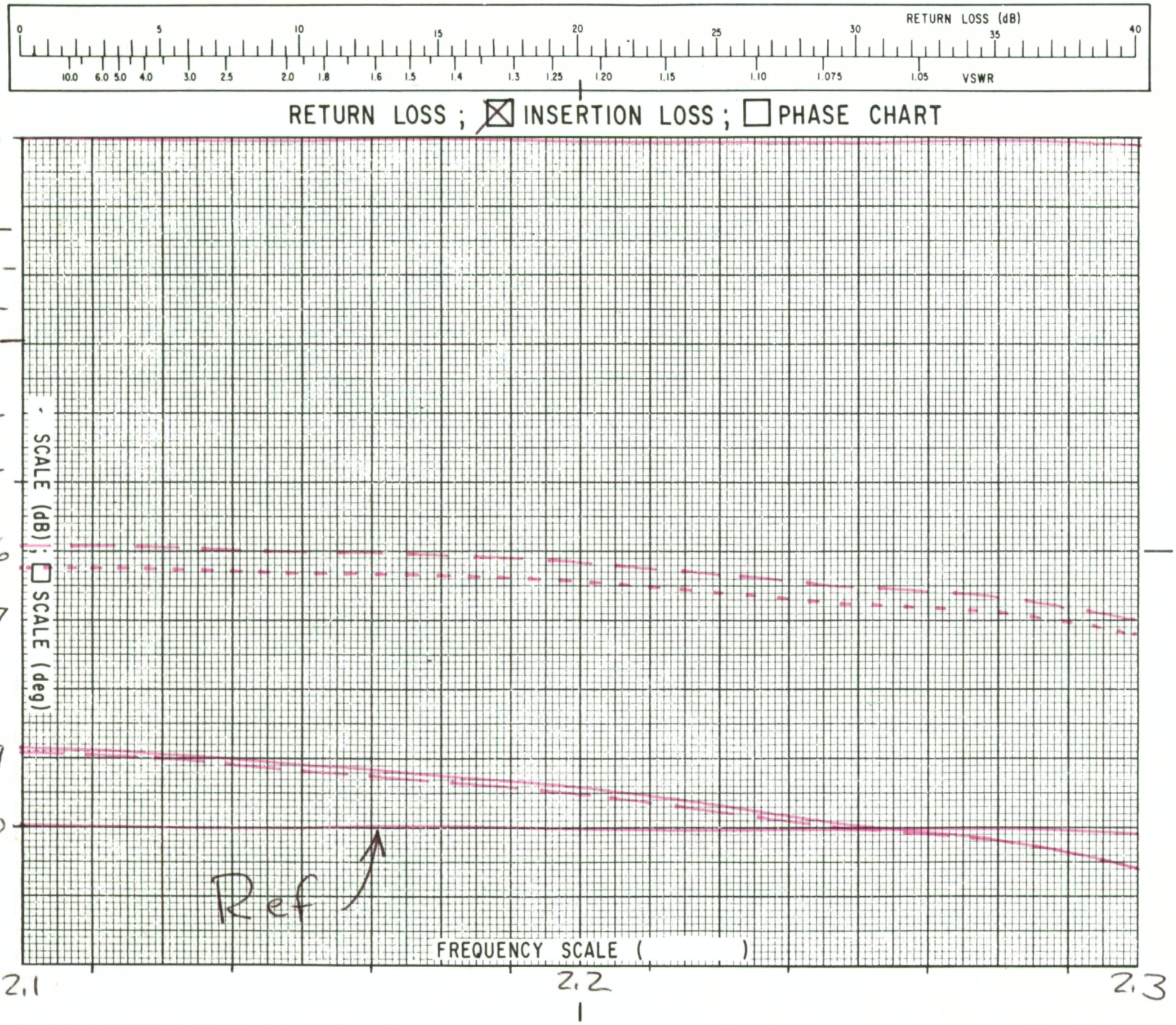
FREQUENCY RANGE 2.1 - 2.36 GHz SHEET ____ OF ____

BALL AEROSPACE SYSTEMS DIVISION

REMARKS SPD Insertion

OPER. R.J. WITNESSED _____ DATE 7-1-82

Figure 3.11



Wilkinson Dark ANTENNAS

PROJECT NO. 2314-001 PROGRAM Auto-Omni

PART NO. _____ MODEL NO. _____ SERIAL NO. _____

TEST TYPE: ☒ DEVELOPMENT ☐ PRE ☐ FINAL

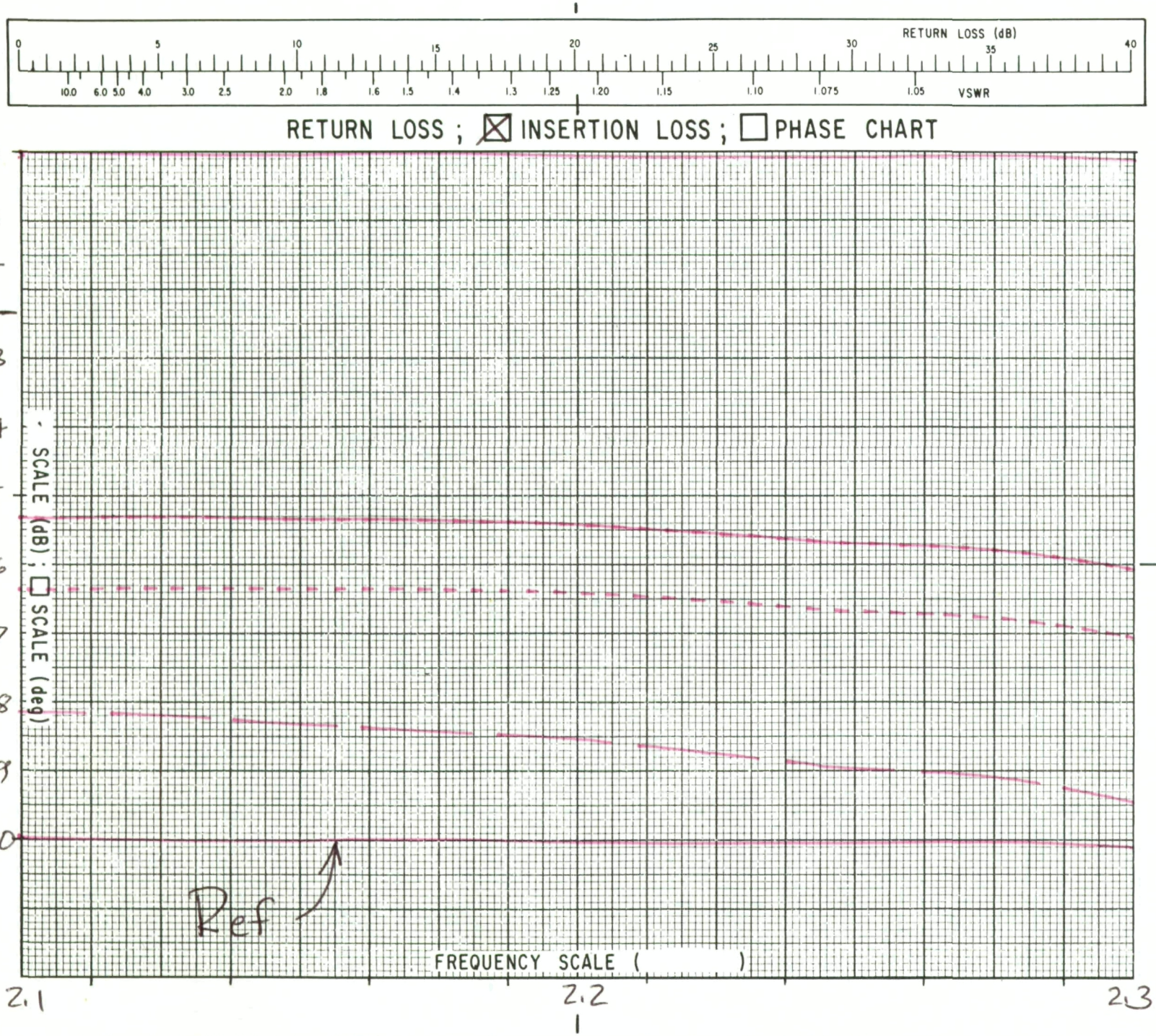
FREQUENCY RANGE 2.1-2.3 GHz SHEET _____ OF _____

BALL AEROSPACE SYSTEMS DIVISION

REMARKS SPD Insertion Loss

OPER. R.J. WITNESSED _____ DATE 7-1-82

Figure 3.12



Wi-Stoip Data ANTENNAS

PROJECT NO. 2314-001 PROGRAM Auto Omni

PART NO. _____ MODEL NO. _____ SERIAL NO. _____

TEST TYPE: ☒ DEVELOPMENT ☐ PRE ☐ FINAL

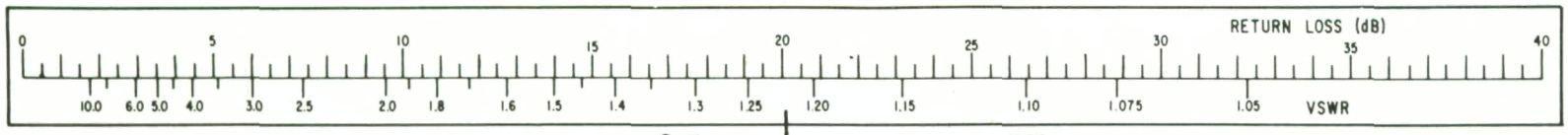
FREQUENCY RANGE 2.1 - 2.3 GHz SHEET ____ OF ____

BALL AEROSPACE SYSTEMS DIVISION

REMARKS SPD Insertion Loss

OPER. R.J. WITNESSED _____ DATE 7-1-82

Figure 3.13



RETURN LOSS ; ☒ INSERTION LOSS ; ☐ PHASE CHART

Scale-Dyne ANTENNAS

PROJECT NO. 2314-001 PROGRAM Auto Omni

PART NO. _____ MODEL NO. _____ SERIAL NO. _____

TEST TYPE: ☒ DEVELOPMENT ☐ PRE ☐ FINAL

FREQUENCY RANGE 2.1 - 2.3 GHz SHEET _____ OF _____

1 5 9 13

0 1 4 5 6 7 8 9 10

Loss dB

SCALE (dB) ; ☐ SCALE (deg)

Ref

FREQUENCY SCALE ( )

2.1 2.2 2.3

BALL AEROSPACE SYSTEMS DIVISION

REMARKS SPD Insertion Loss

OPER. R.J. WITNESSED _____ DATE 7-1-82

45

Figure 3.14

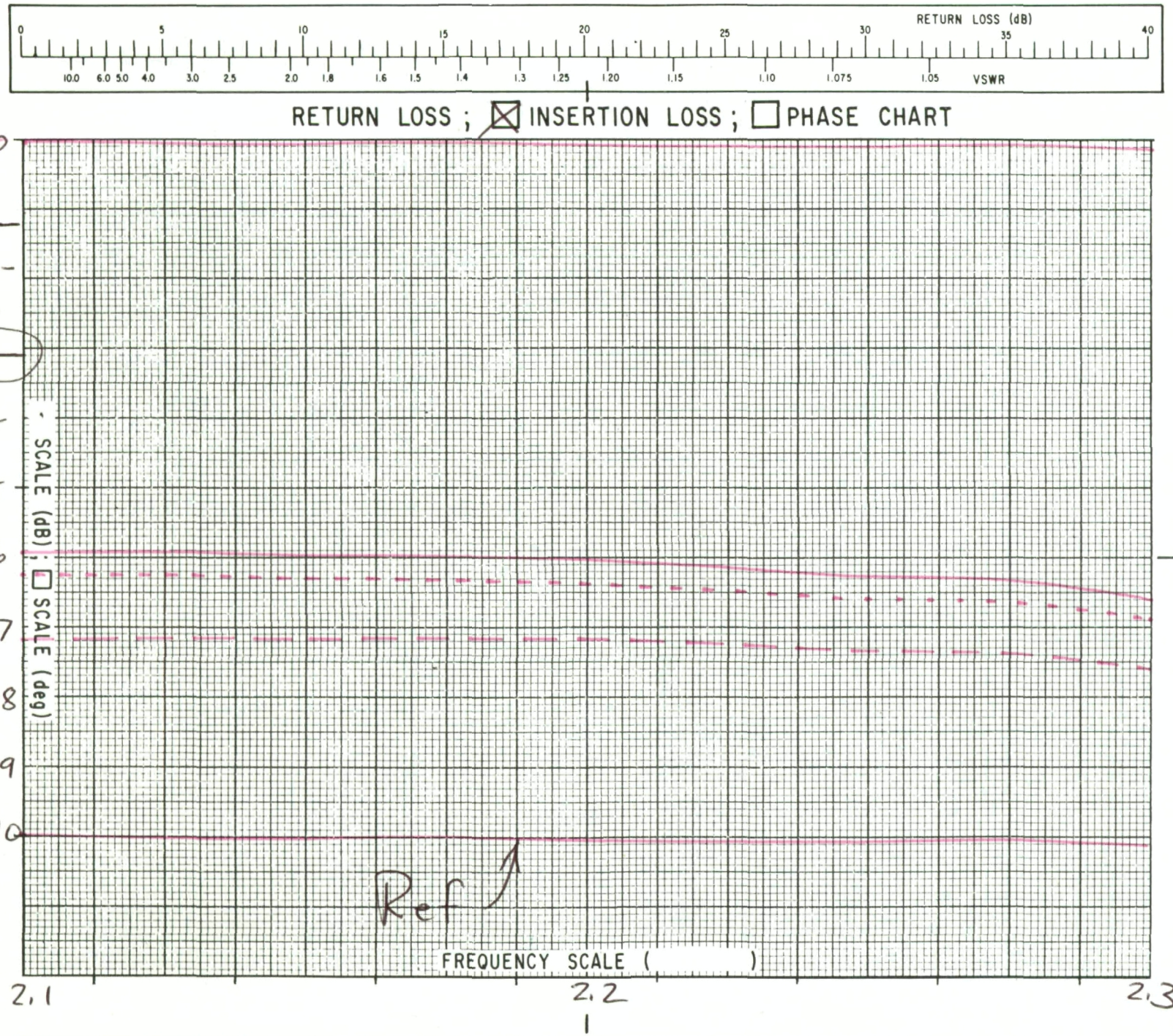

RETURN LOSS (dB)
0 5 10 15 20 25 30 35 40
10.0 6.0 5.0 4.0 3.0 2.5 2.0 1.8 1.6 1.5 1.4 1.3 1.25 1.20 1.15 1.10 1.075 1.05 VSWR
RETURN LOSS ; ☒ INSERTION LOSS ; ☐ PHASE CHART
0
18
23
28
32
4
5
6
7
8
9
10
Bad
Loss dB
SCALE (dB) ; ☐ SCALE (deg)
Ref 1
FREQUENCY SCALE ( )
2.1
2.2
2.3
PROJECT NO. 2314-001 PROGRAM Auto Omni
PART NO. MODEL NO. SERIAL NO.
TEST TYPE: ☒ DEVELOPMENT ☐ PRE ☐ FINAL
FREQUENCY RANGE 2.1-2.3 GHz SHEET OF
BALL AEROSPACE SYSTEMS DIVISION
REMARKS SPD Insertion Loss
OPER. RJ. WITNESSED DATE 7-1-82

Figure 3.15

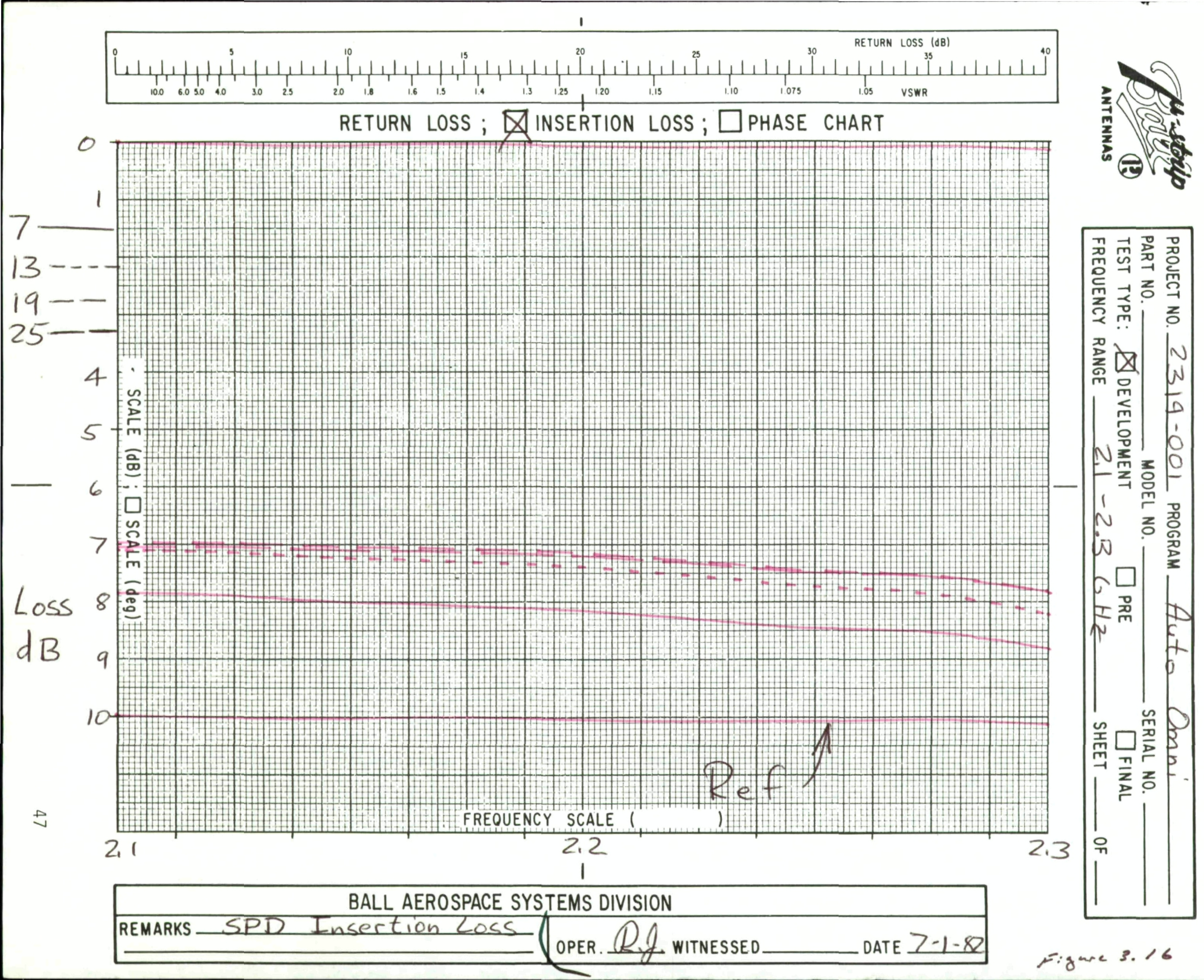
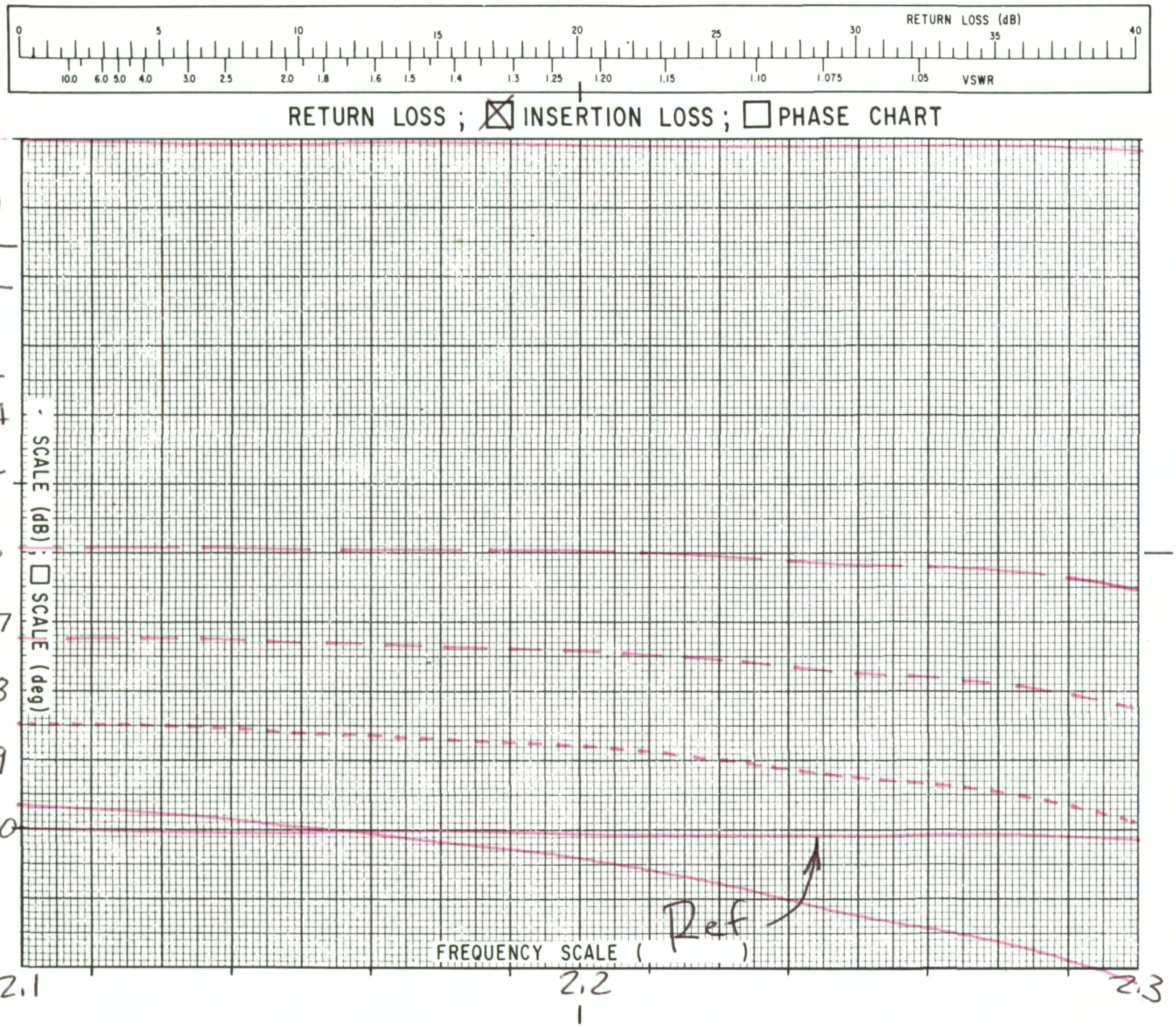

RETURN LOSS (dB)
0 5 10 15 20 25 30 35 40
10.0 6.0 5.0 4.0 3.0 2.5 2.0 1.8 1.6 1.5 1.4 1.3 1.25 1.20 1.15 1.10 1.075 1.05 VSWR
RETURN LOSS ; ☒ INSERTION LOSS ; ☐ PHASE CHART
0
1
7
13
19
25
4
5
6
7
8
9
10
Loss
dB
SCALE (dB) ; ☐ SCALE (deg)
Ref 1
FREQUENCY SCALE ( )
2.1
2.2
2.3
47
Ball Antennas
PROJECT NO. 2319-001 PROGRAM Auto Omni
PART NO. MODEL NO. SERIAL NO.
TEST TYPE: ☒ DEVELOPMENT ☐ PRE ☐ FINAL
FREQUENCY RANGE 2.1-2.3 GHz SHEET OF
BALL AEROSPACE SYSTEMS DIVISION
REMARKS SPD Insertion Loss
OPER. RJ WITNESSED DATE 7-1-82

Figure 3.16



Ball Antennas

PROJECT NO. 2314-001 PROGRAM Auto Omni

PART NO. _____ MODEL NO. _____ SERIAL NO. _____

TEST TYPE: ☒ DEVELOPMENT ☐ PRE ☐ FINAL

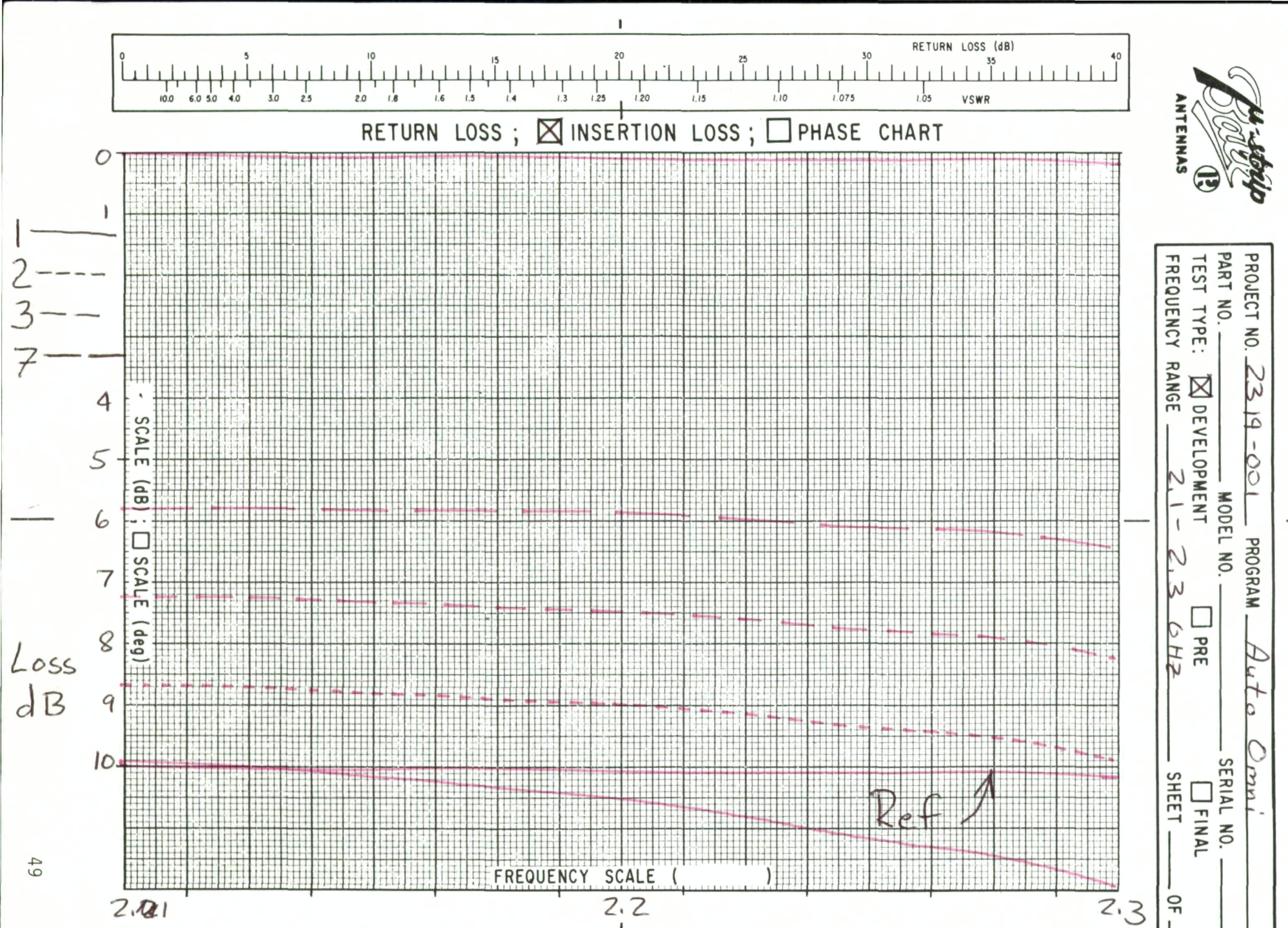
FREQUENCY RANGE 2.1-2.3 GHz SHEET ____ OF ____

BALL AEROSPACE SYSTEMS DIVISION

REMARKS SPD Insertion Loss

OPER. R.J. WITNESSED _____ DATE 7-1-82

Figure 3.17



Antenna Systems ANTENNAS

PROJECT NO. 2319-001 PROGRAM Auto Omni

PART NO. _____ MODEL NO. _____ SERIAL NO. _____

TEST TYPE: ☒ DEVELOPMENT ☐ PRE ☐ FINAL

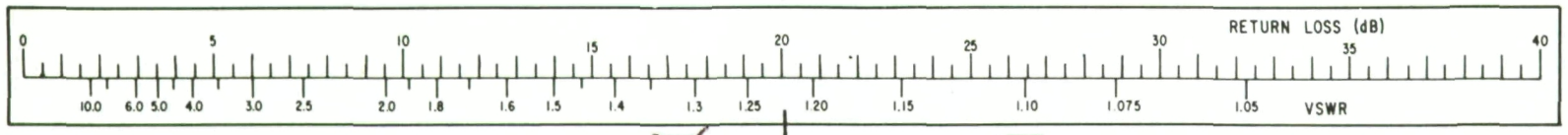
FREQUENCY RANGE 2.1 - 2.3 GHz SHEET _____ OF _____

BALL AEROSPACE SYSTEMS DIVISION

REMARKS SPD Insertion Loss

OPER. RJ. WITNESSED _____ DATE 7-1-82

Figure 3.18



RETURN LOSS ; ☒ INSERTION LOSS ; ☐ PHASE CHART

Antenna Dynamics ANTENNAS

PROJECT NO. 2319-001 PROGRAM Auto Omni
PART NO. _____ MODEL NO. _____ SERIAL NO. _____
TEST TYPE: ☒ DEVELOPMENT ☐ PRE ☐ FINAL
FREQUENCY RANGE 2.1-2.3 GHz SHEET ____ OF ____

0
1
2
3
7
12
4
5
6
7
8
9
10

Loss dB

SCALE (dB) ; ☐ SCALE (deg)

FREQUENCY SCALE ( )

2.1 2.2 2.3

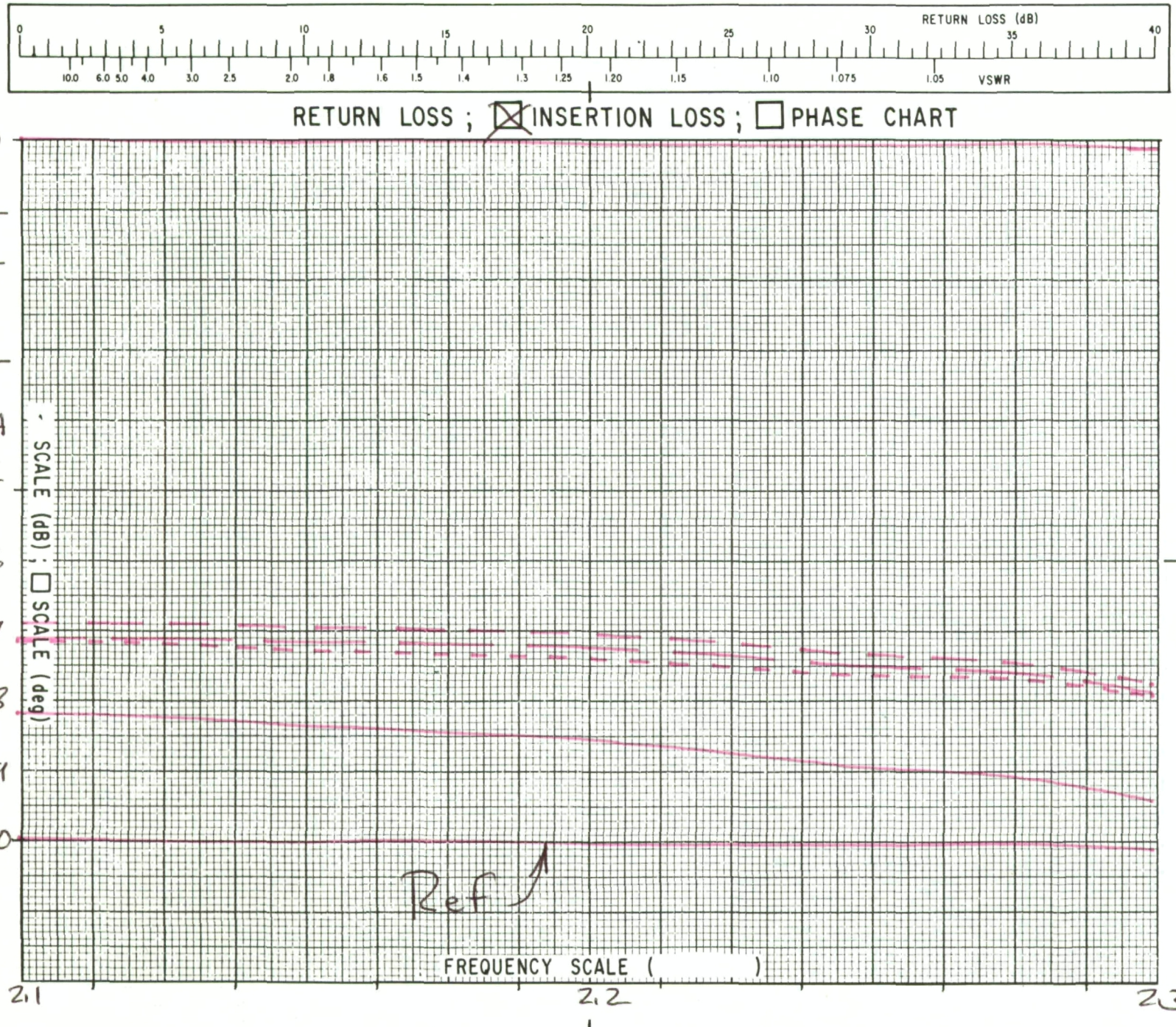
50

BALL AEROSPACE SYSTEMS DIVISION

REMARKS SPD Insertion Loss

OPER. R.J. WITNESSED _____ DATE 7-1-82

Figure 3.19



Wilson Laboratories ANTENNAS

PROJECT NO. 2314-001 PROGRAM Auto Omni

PART NO. _____ MODEL NO. _____ SERIAL NO. _____

TEST TYPE: ☒ DEVELOPMENT ☐ PRE ☐ FINAL

FREQUENCY RANGE 2.1-2.3 GHz SHEET _____ OF _____

BALL AEROSPACE SYSTEMS DIVISION

REMARKS SPD Insertion Loss

OPER. R.J. WITNESSED _____ DATE 7-1-82

Figure 3.20

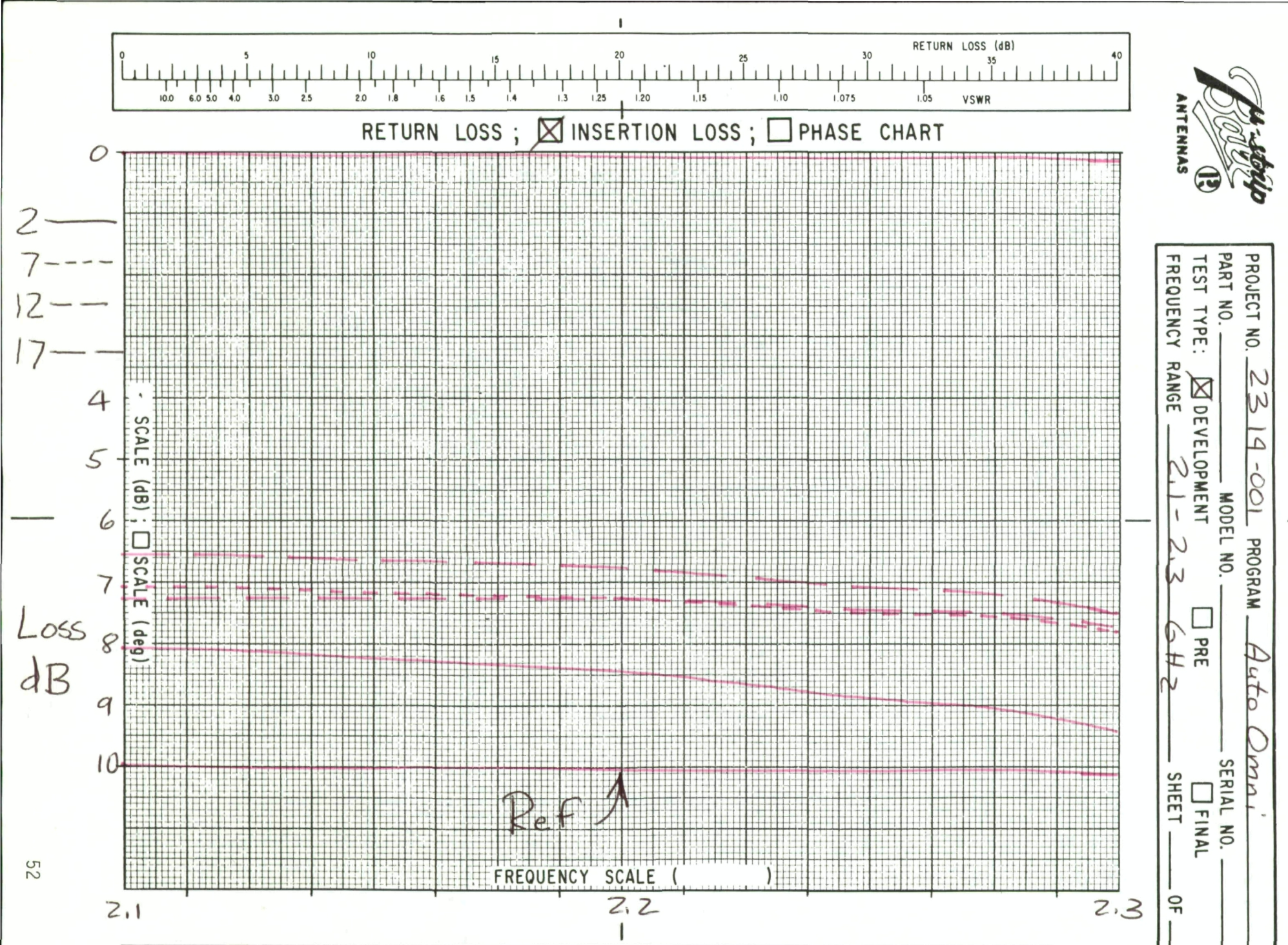

RETURN LOSS (dB)
0 5 10 15 20 25 30 35 40
10.0 6.0 5.0 4.0 3.0 2.5 2.0 1.8 1.6 1.5 1.4 1.3 1.25 1.20 1.15 1.10 1.075 1.05 VSWR
RETURN LOSS ; ☒ INSERTION LOSS ; ☐ PHASE CHART
0
2
7
12
17
4
5
6
7
8
9
10
Loss dB
SCALE (dB) ; ☐ SCALE (deg)
Ref 1
FREQUENCY SCALE ( )
2.1
2.2
2.3
PROJECT NO. 2319-001 PROGRAM Auto Omni
PART NO. MODEL NO. SERIAL NO.
TEST TYPE: ☒ DEVELOPMENT ☐ PRE ☐ FINAL
FREQUENCY RANGE 2.1 - 2.3 GHz SHEET OF
BALL AEROSPACE SYSTEMS DIVISION
REMARKS SPD Insertion Loss
OPER. R.J. WITNESSED DATE 7-1-82

Figure 3.21

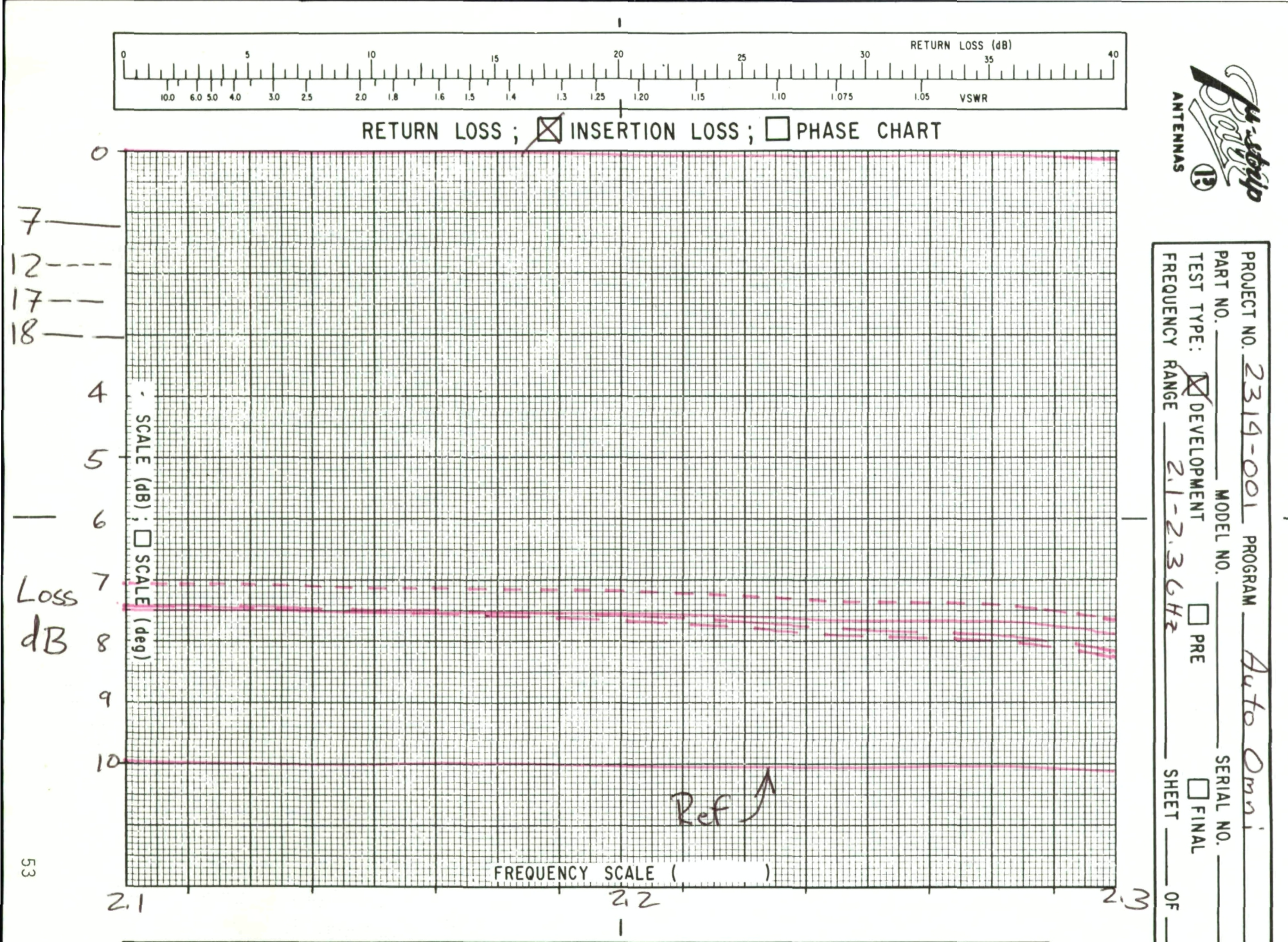
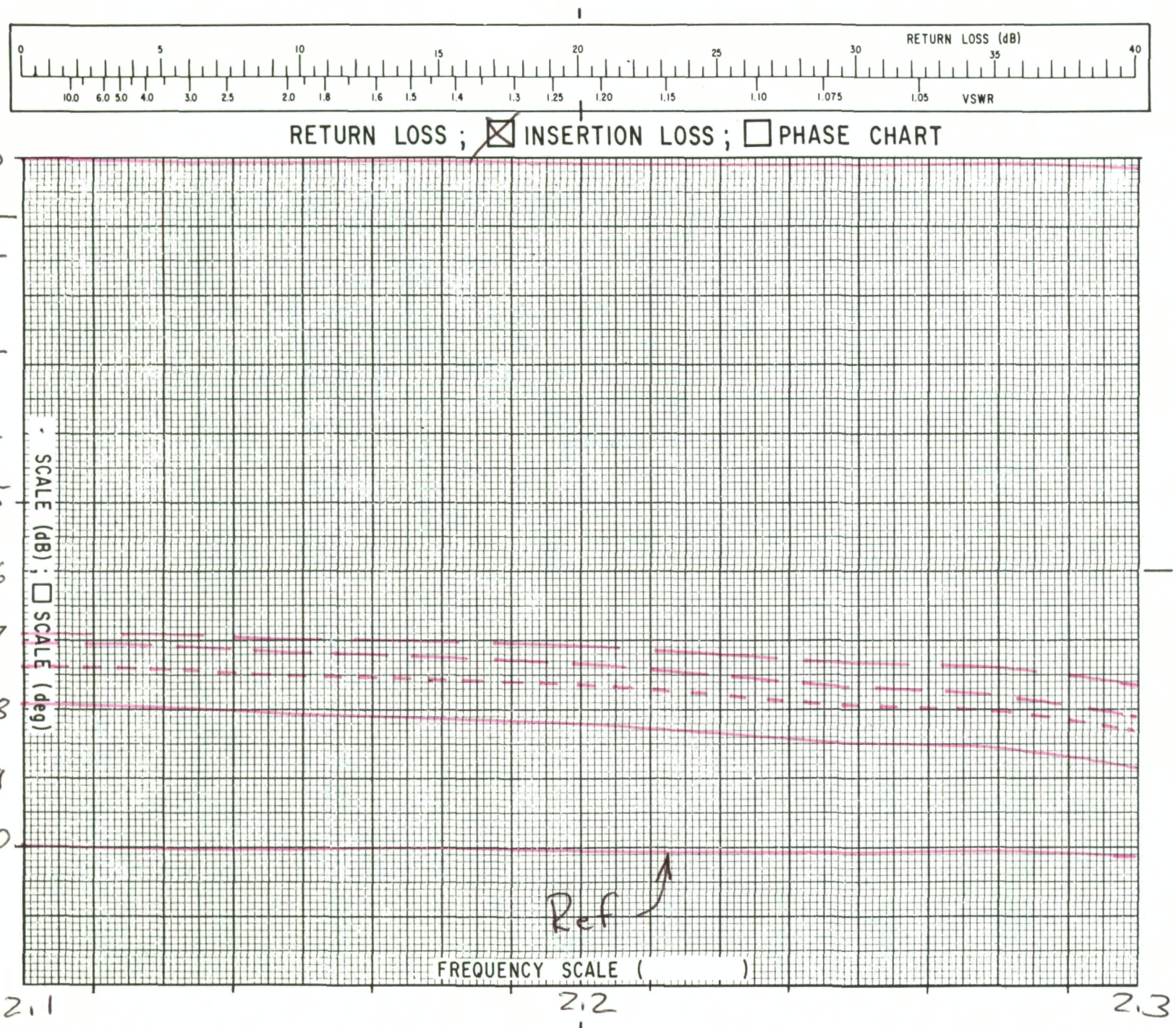

RETURN LOSS (dB)
0 5 10 15 20 25 30 35 40
10.0 6.0 5.0 4.0 3.0 2.5 2.0 1.8 1.6 1.5 1.4 1.3 1.25 1.20 1.15 1.10 1.075 1.05 VSWR
RETURN LOSS ; ☒ INSERTION LOSS ; ☐ PHASE CHART
0
7
12
17
18
4
5
6
7
8
9
10
Loss dB
SCALE (dB) ; ☐ SCALE (deg)
Ref
FREQUENCY SCALE ( )
2.1
2.2
2.3
PROJECT NO. 2319-001 PROGRAM Auto Omni
PART NO. MODEL NO. SERIAL NO.
TEST TYPE: ☒ DEVELOPMENT ☐ PRE ☐ FINAL
FREQUENCY RANGE 2.1-2.36 Hz SHEET OF
BALL AEROSPACE SYSTEMS DIVISION
REMARKS SPD Insertion Loss
OPER. R.J. WITNESSED DATE 7-1-82

Figure 3.22



Ball Antennas

PROJECT NO. 2314-201 PROGRAM Auto Omni

PART NO. _____ MODEL NO. _____ SERIAL NO. _____

TEST TYPE: ☒ DEVELOPMENT ☐ PRE ☐ FINAL

FREQUENCY RANGE 2.1-2.36 HZ SHEET _____ OF _____

BALL AEROSPACE SYSTEMS DIVISION

REMARKS SPD Insertion Loss

OPER. RJ. WITNESSED _____ DATE 7-1-82

Figure 3.23

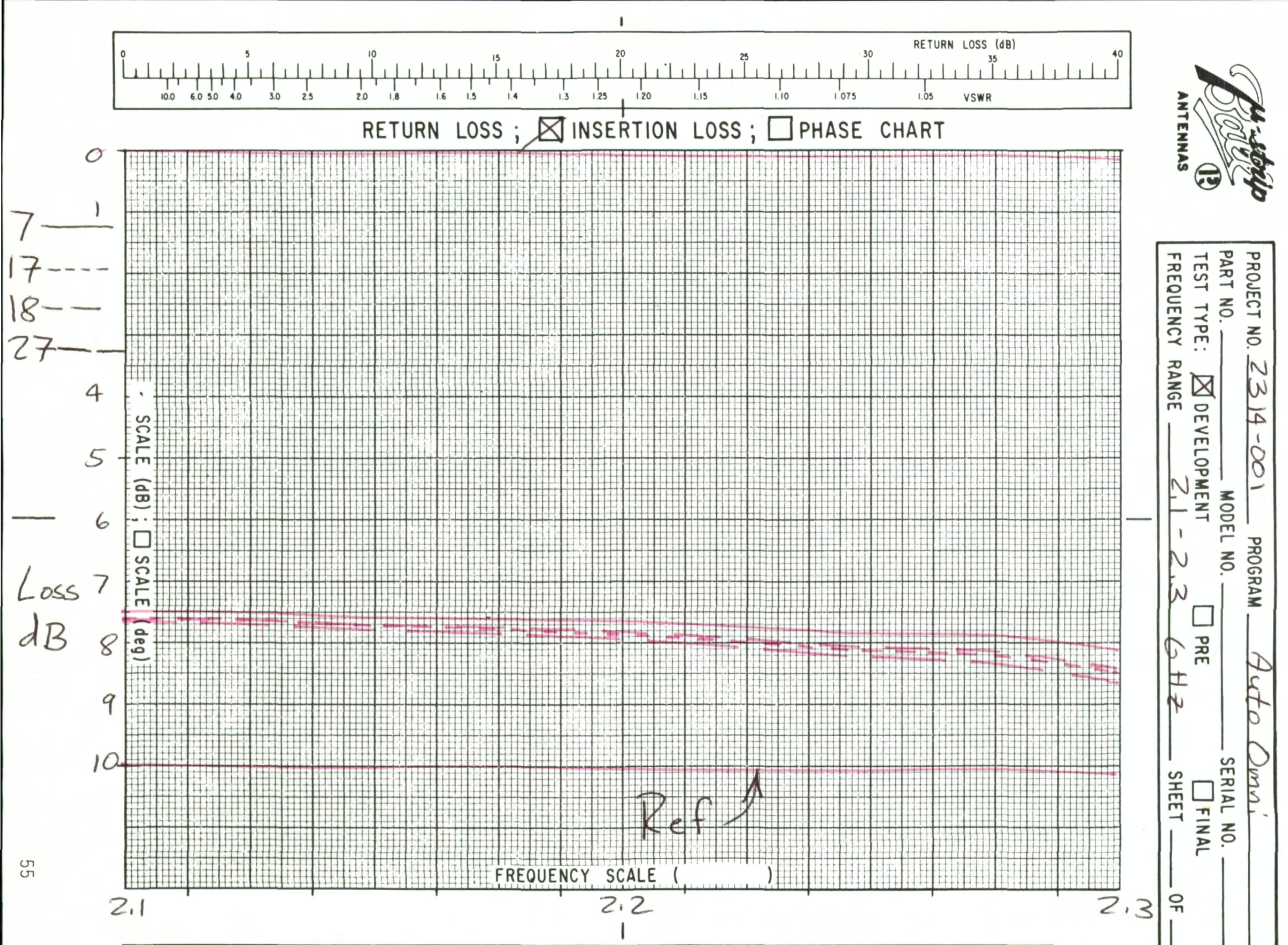
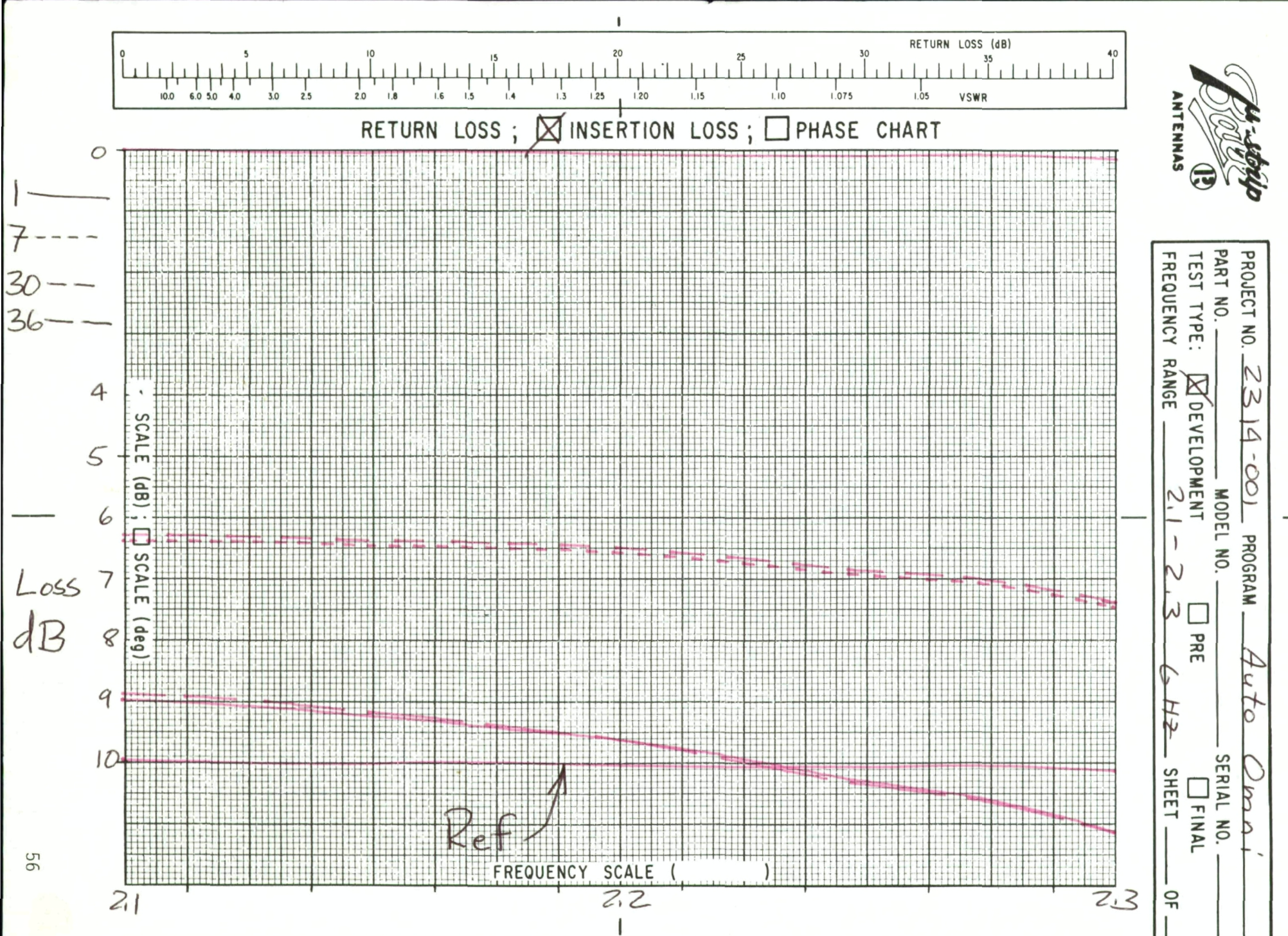

RETURN LOSS (dB)
0 5 10 15 20 25 30 35 40
10.0 6.0 5.0 4.0 3.0 2.5 2.0 1.8 1.6 1.5 1.4 1.3 1.25 1.20 1.15 1.10 1.075 1.05 VSWR
RETURN LOSS ; ☒ INSERTION LOSS ; ☐ PHASE CHART
0 1 2 3 4 5 6 7 8 9 10
SCALE (dB) ; ☐ SCALE (deg)
Loss dB
7
17
18
27
Ref 1
FREQUENCY SCALE ( )
2.1 2.2 2.3
PROJECT NO. 2314-001 PROGRAM Auto Omni
PART NO. MODEL NO. SERIAL NO.
TEST TYPE: ☒ DEVELOPMENT ☐ PRE ☐ FINAL
FREQUENCY RANGE 2.1 - 2.3 GHz SHEET OF
BALL AEROSPACE SYSTEMS DIVISION
REMARKS SPD Insertion Loss
OPER. RJ. WITNESSED DATE 7-1-82

Figure 3.24



Wa-Chop Data ANTENNAS

PROJECT NO. 2314-001 PROGRAM Auto Omni

PART NO. _____ MODEL NO. _____ SERIAL NO. _____

TEST TYPE: ☒ DEVELOPMENT ☐ PRE ☐ FINAL

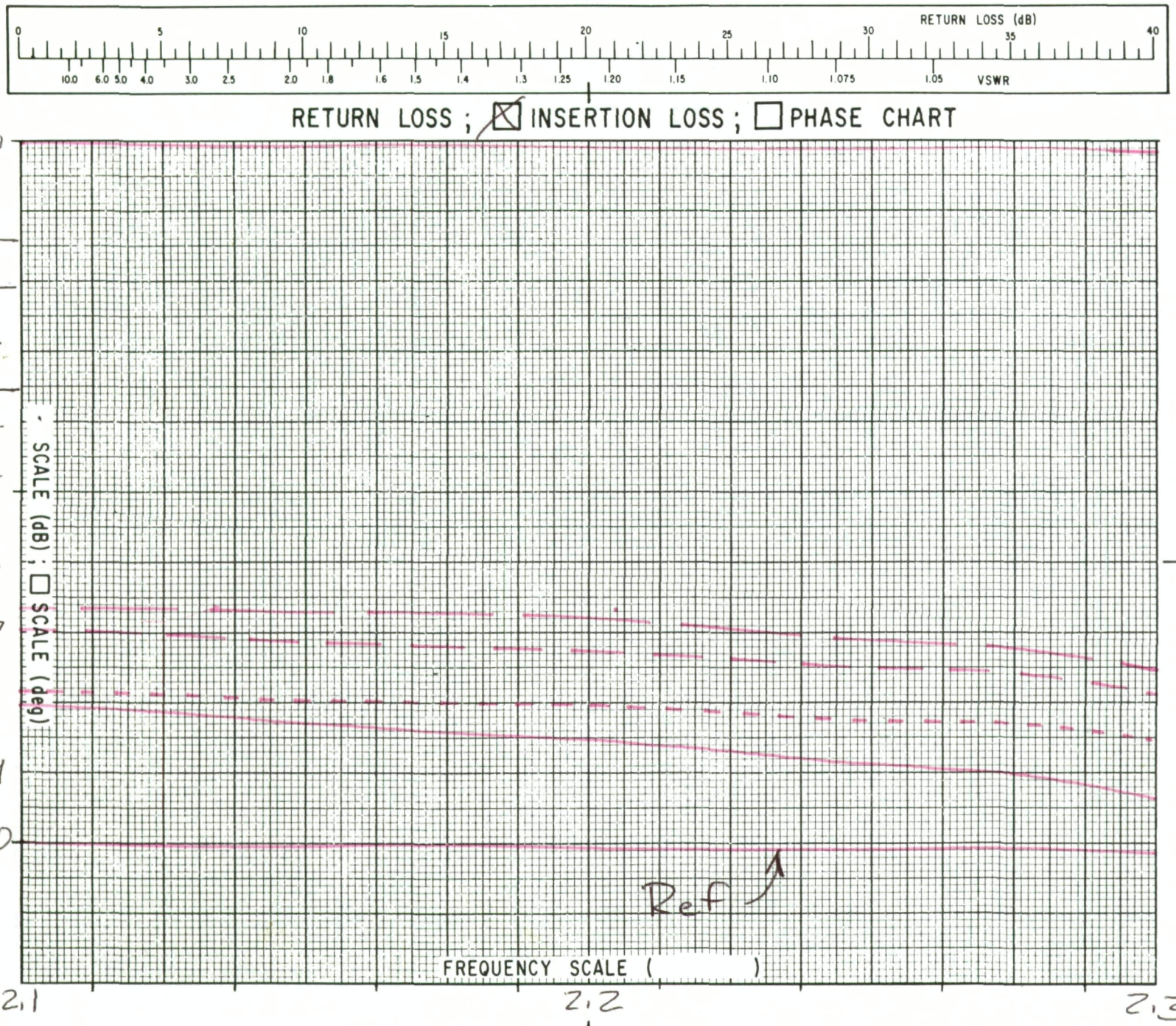
FREQUENCY RANGE 2.1 - 2.3 GHz SHEET _____ OF _____

BALL AEROSPACE SYSTEMS DIVISION

REMARKS SPD Insertion Loss

OPER. RJ WITNESSED _____ DATE 7-1-82

Figure 3.25



Antenna Dynamics ANTENNAS

PROJECT NO. 2314-001 PROGRAM Auto Omni
PART NO. ____ MODEL NO. ____ SERIAL NO. ____
TEST TYPE: ☒ DEVELOPMENT ☐ PRE ☐ FINAL
FREQUENCY RANGE 2.1 - 2.3 GHz SHEET ____ OF ____

BALL AEROSPACE SYSTEMS DIVISION

REMARKS SPD Insertion Loss

OPER. RJ. WITNESSED ____ DATE 7-1-82

Figure 3.26

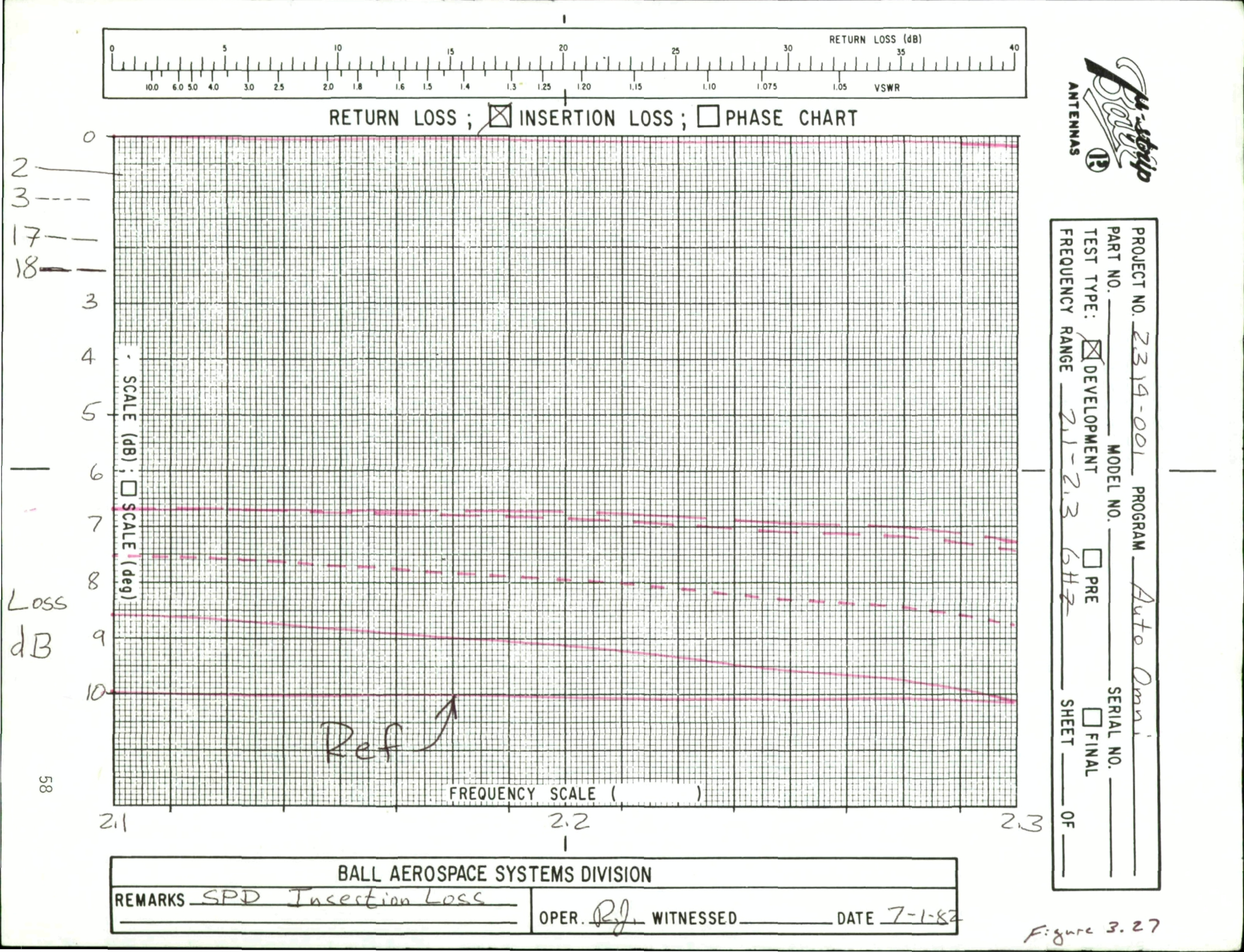

RETURN LOSS (dB)
0 5 10 15 20 25 30 35 40
10.0 6.0 5.0 4.0 3.0 2.5 2.0 1.8 1.6 1.5 1.4 1.3 1.25 1.20 1.15 1.10 1.075 1.05 VSWR
RETURN LOSS ; ☒ INSERTION LOSS ; ☐ PHASE CHART
2
3
17
18
0 3 4 5 6 7 8 9 10
SCALE (dB) ; ☐ SCALE (deg)
Loss
dB
Ref
FREQUENCY SCALE ( )
2.1 2.2 2.3
PROJECT NO. 2319-001 PROGRAM Auto Omni
PART NO. MODEL NO. SERIAL NO.
TEST TYPE: ☒ DEVELOPMENT ☐ PRE ☐ FINAL
FREQUENCY RANGE 2.1-2.3 GHz SHEET OF
BALL AEROSPACE SYSTEMS DIVISION
REMARKS SPD Insertion Loss
OPER. RJ. WITNESSED DATE 7-1-82

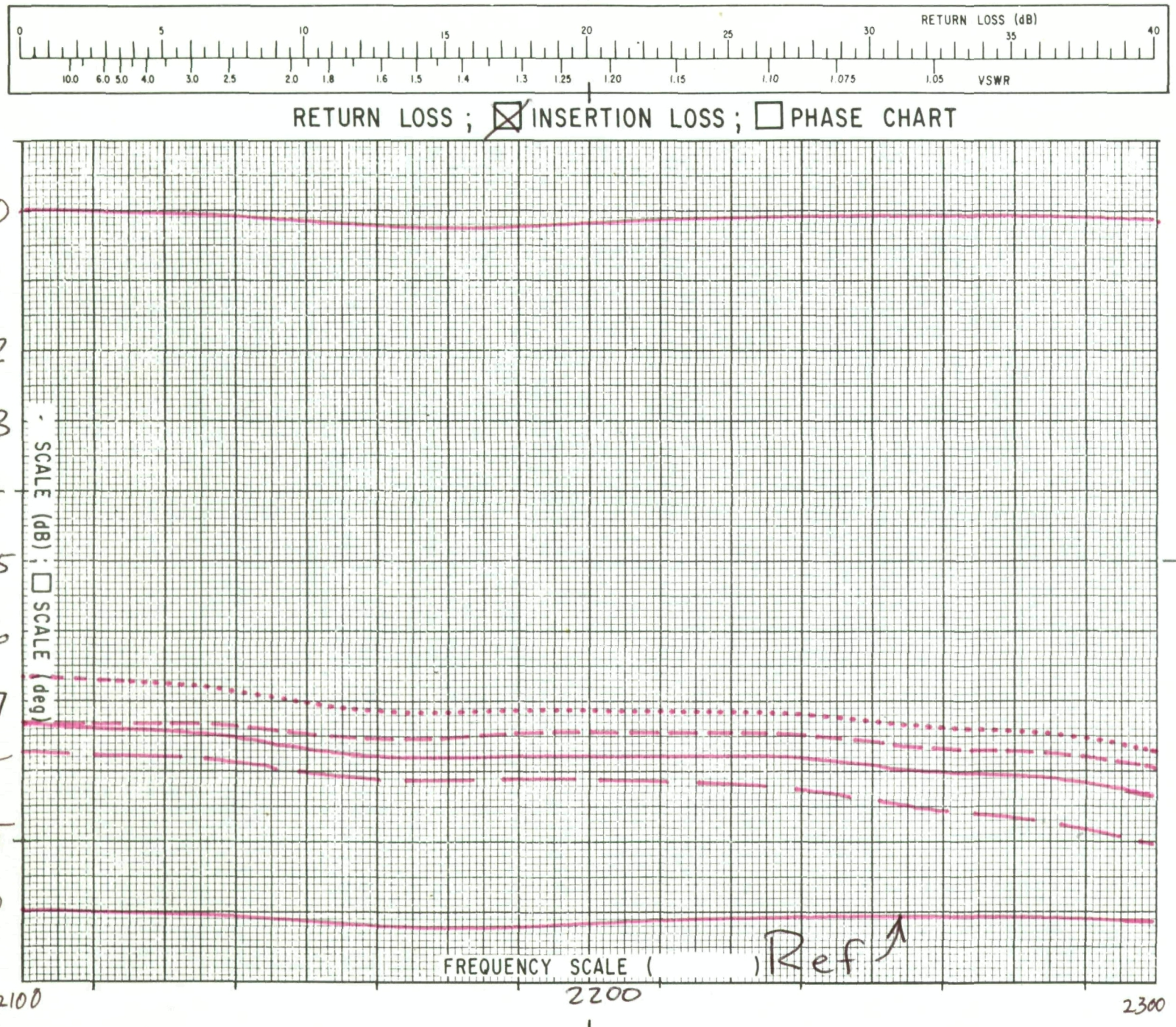
Figure 3.27

Case 2 (Raw Data)

SPD INSERTION LOSS DATA WITH RESISTIVE LOADS

(A Repeat of Selected Group I Clusters to Verify Test Validity)

Figure	Outputs			
3.29	6	15	19	20
3.30	7	15	19	20
3.31	7	12	15	20
3.32	7	11	12	20
3.33	7	12	17	20
3.34	7	12	17	18
3.35	7	12	17	26
3.36	7	17	18	27
3.37	12	16	17	26
3.38	16	17	26	27
3.39	16	17	18	27
3.40	7	13	15	18
3.41	15	17	18	20



Scientific-Atlanta ANTENNAS

PROJECT NO. 2314-001 PROGRAM Auto Omni

PART NO. ____ MODEL NO. ____ SERIAL NO. ____

TEST TYPE: ☒ DEVELOPMENT ☐ PRE ☐ FINAL

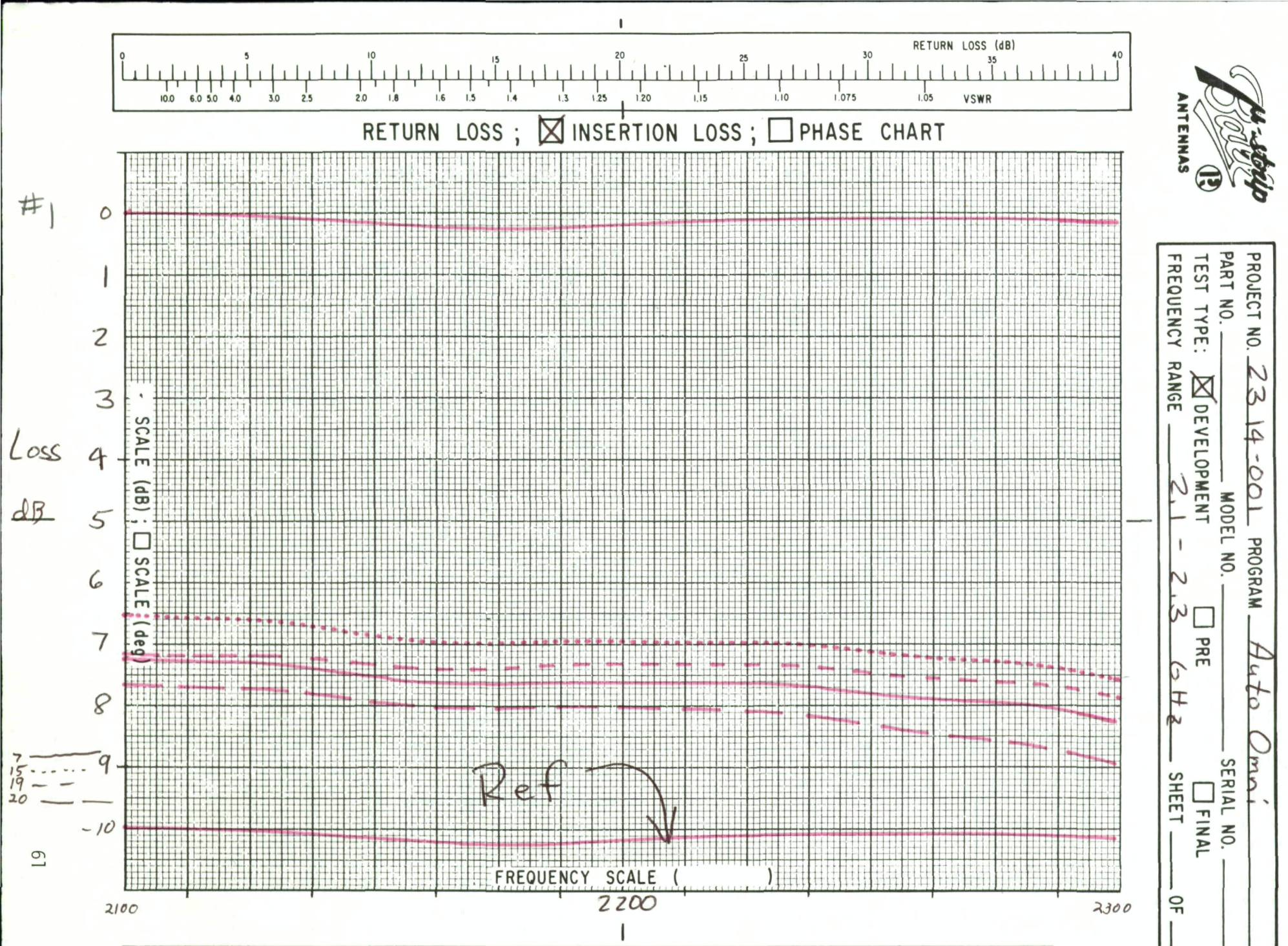
FREQUENCY RANGE 2.1 - 2.36 GHz SHEET ____ OF ____

BALL AEROSPACE SYSTEMS DIVISION

REMARKS SPD Insertion Loss

OPER. JB WITNESSED ____ DATE 7-6-82

Fig 3.29



Ball ANTENNAS

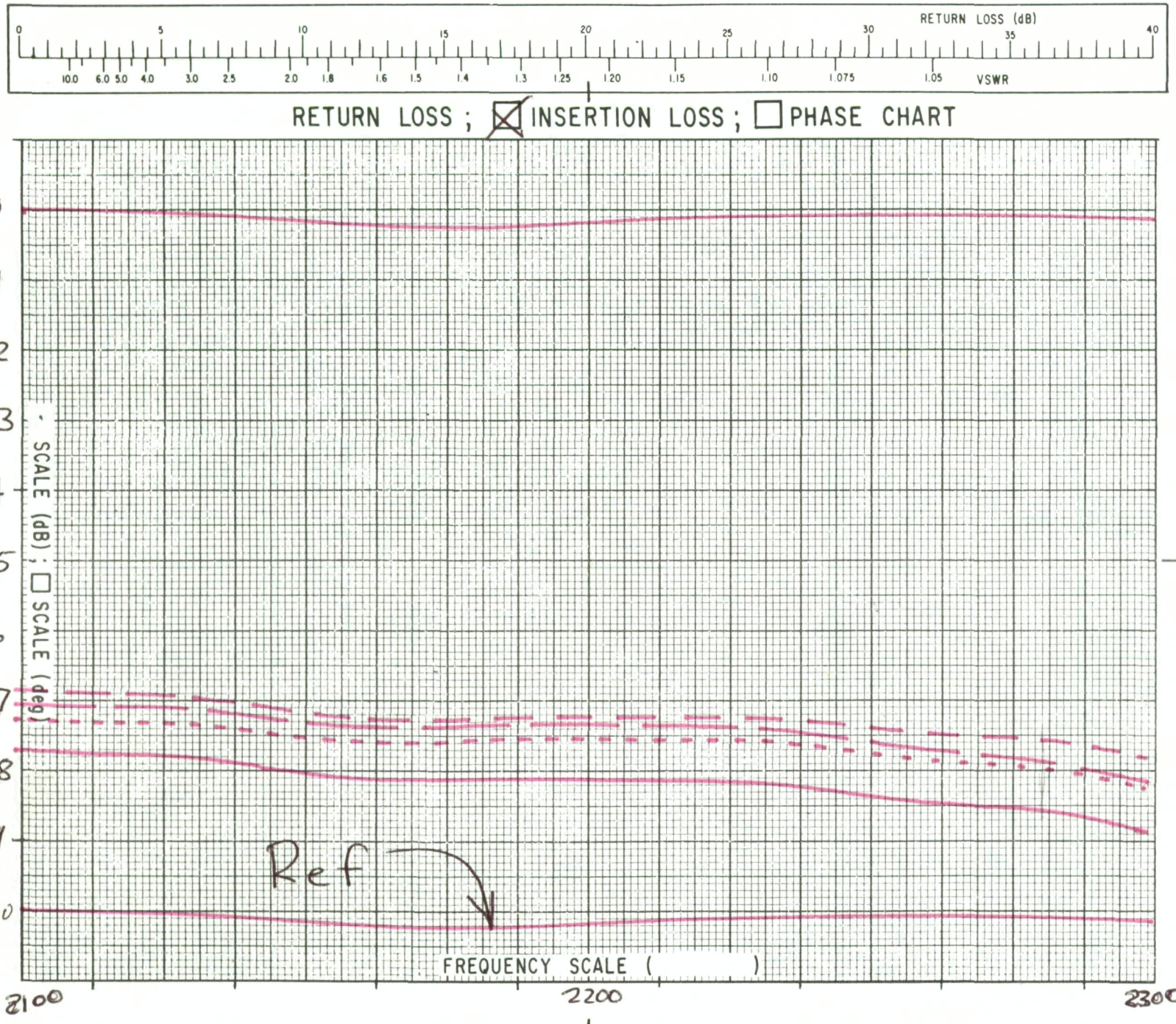
PROJECT NO. 2314-001 PROGRAM Auto Omni
PART NO. _____ MODEL NO. _____ SERIAL NO. _____
TEST TYPE: ☒ DEVELOPMENT ☐ PRE ☐ FINAL
FREQUENCY RANGE 2.1 - 2.3 GHz SHEET _____ OF _____

BALL AEROSPACE SYSTEMS DIVISION

REMARKS SPD Insertion Loss

OPER. JB WITNESSED _____ DATE 7-6-82

Fig 3.30



Hughes Aircraft Company ANTENNAS

PROJECT NO. 2314-001 PROGRAM Auto Omni

PART NO. _____ MODEL NO. _____ SERIAL NO. _____

TEST TYPE: ☒ DEVELOPMENT ☐ PRE ☐ FINAL

FREQUENCY RANGE 2.1-2.3 GHz SHEET _____ OF _____

BALL AEROSPACE SYSTEMS DIVISION

REMARKS SPD Insertion Loss

OPER. JB WITNESSED _____ DATE 7-6-82

Fig 3.31

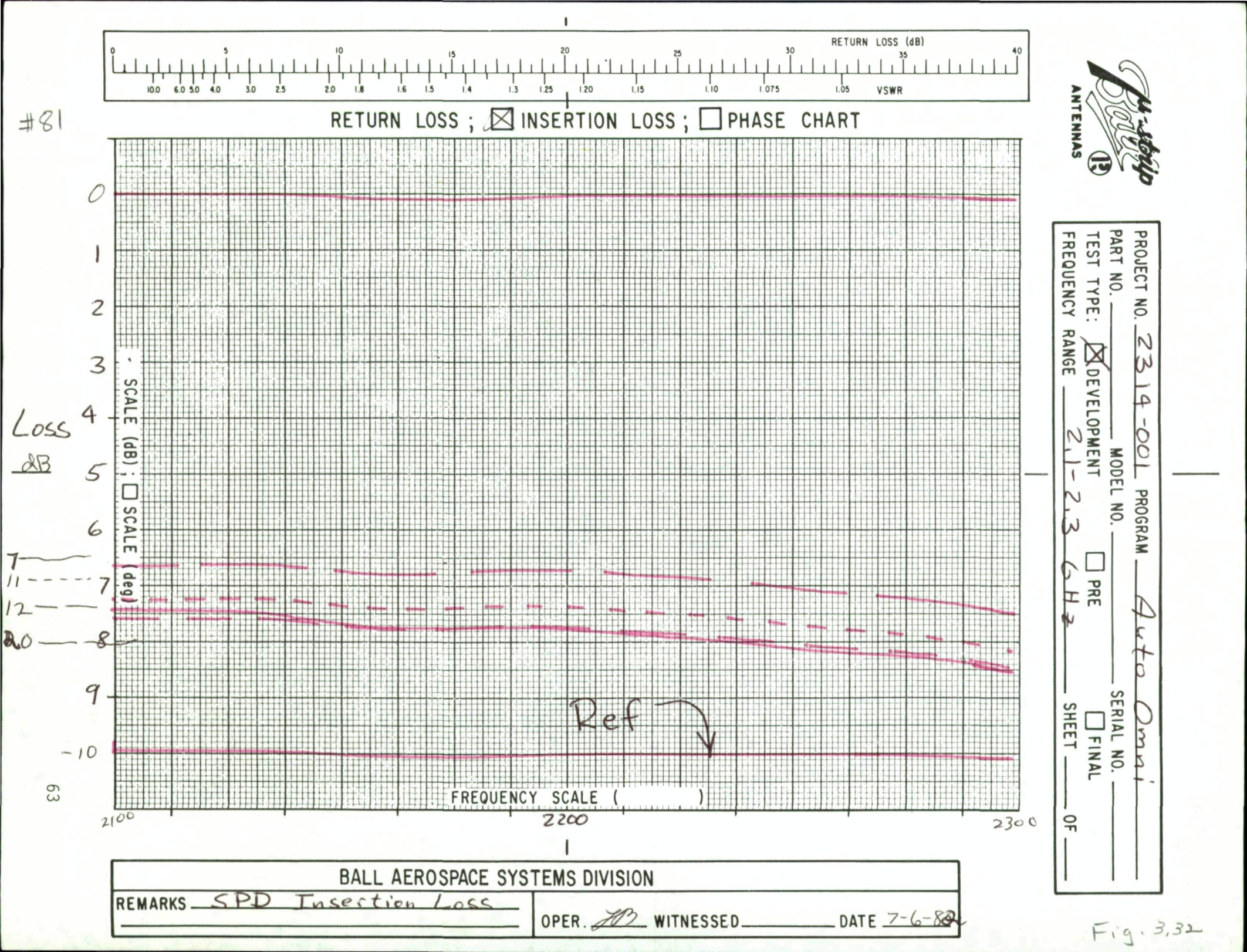

RETURN LOSS (dB)
0 5 10 15 20 25 30 35 40
10.0 6.0 5.0 4.0 3.0 2.5 2.0 1.8 1.6 1.5 1.4 1.3 1.25 1.20 1.15 1.10 1.075 1.05 VSWR
#81
RETURN LOSS ; ☒ INSERTION LOSS ; ☐ PHASE CHART
Loss dB
0 1 2 3 4 5 6 7 8 9 10
SCALE (dB) ; ☐ SCALE (deg)
7
11
12
2.0
Ref
FREQUENCY SCALE ( )
2100 2200 2300
63
Hughes Basic Antennas
PROJECT NO. 2314-001 PROGRAM Auto Omni
PART NO. MODEL NO. SERIAL NO.
TEST TYPE: ☒ DEVELOPMENT ☐ PRE ☐ FINAL
FREQUENCY RANGE 2.1-2.3 GHz SHEET OF
BALL AEROSPACE SYSTEMS DIVISION
REMARKS SPD Insertion Loss
OPER. WITNESSED DATE 7-6-82

Fig. 3,32

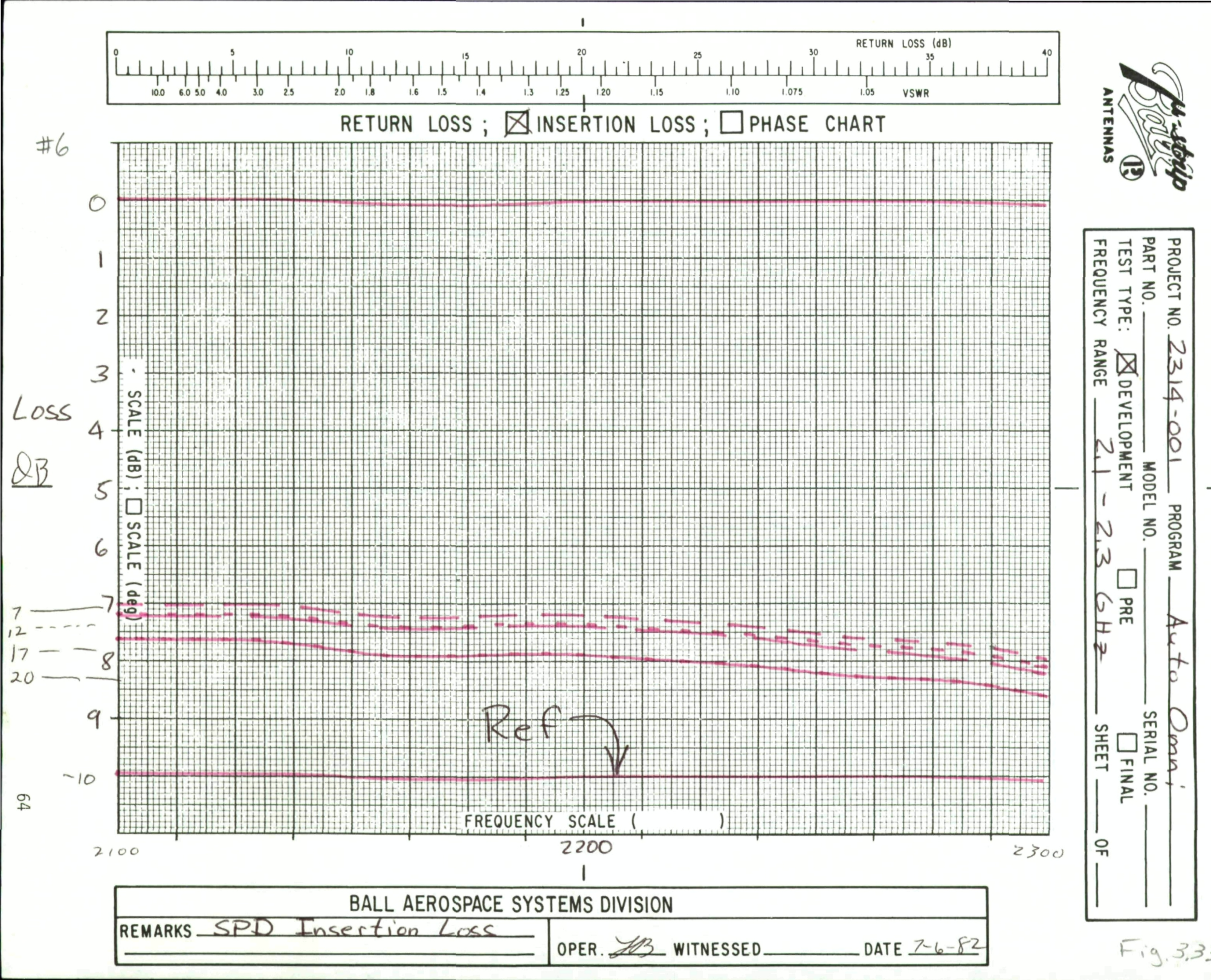

RETURN LOSS (dB)
0 5 10 15 20 25 30 35 40
10.0 6.0 5.0 4.0 3.0 2.5 2.0 1.8 1.6 1.5 1.4 1.3 1.25 1.20 1.15 1.10 1.075 1.05 VSWR
RETURN LOSS ; ☒ INSERTION LOSS ; ☐ PHASE CHART
#6
0 1 2 3 4 5 6 7 8 9 10
Loss
&B
7
12
17
20
SCALE (dB) ; ☐ SCALE (deg)
Ref
FREQUENCY SCALE ( )
2100 2200 2300
64
Hughes Basic 12 ANTENNAS
PROJECT NO. 2314-001 PROGRAM Auto Omni
PART NO. MODEL NO. SERIAL NO.
TEST TYPE: ☒ DEVELOPMENT ☐ PRE ☐ FINAL
FREQUENCY RANGE 2.1 - 2.36 GHz SHEET OF
BALL AEROSPACE SYSTEMS DIVISION
REMARKS SPD Insertion Loss
OPER. WITNESSED DATE 7-6-82

Fig. 3.33

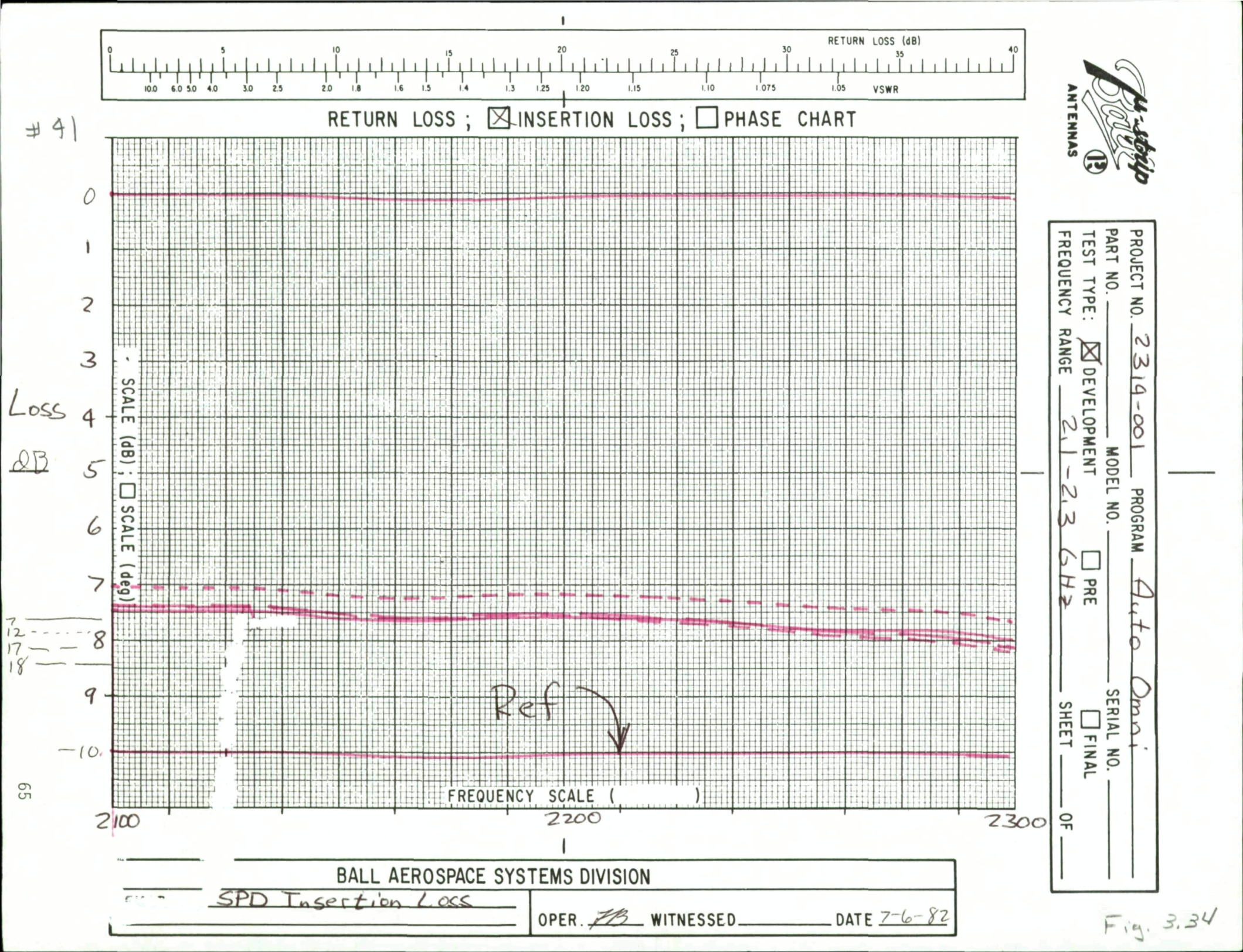
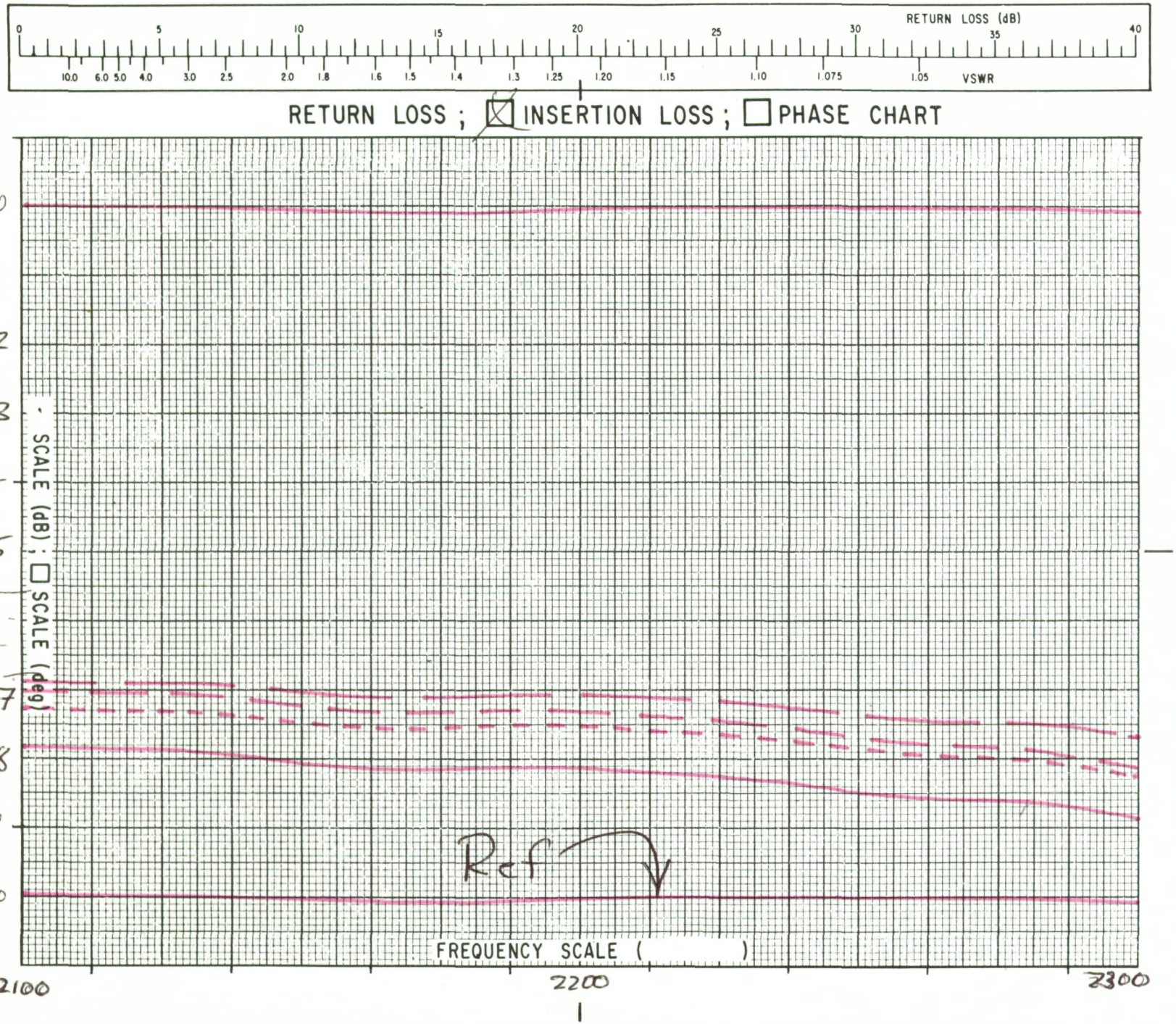

RETURN LOSS (dB)
0 5 10 15 20 25 30 35 40
10.0 6.0 5.0 4.0 3.0 2.5 2.0 1.8 1.6 1.5 1.4 1.3 1.25 1.20 1.15 1.10 1.075 1.05 VSWR
#41
RETURN LOSS ; ☒ INSERTION LOSS ; ☐ PHASE CHART
Loss
dB
0 1 2 3 4 5 6 7 8 9 10
SCALE (dB) ; ☐ SCALE (deg)
7 12 17 18
Ref
FREQUENCY SCALE ( )
2100 2200 2300
65
PROJECT NO. 2319-001 PROGRAM Auto Omni
PART NO. MODEL NO. SERIAL NO.
TEST TYPE: ☒ DEVELOPMENT ☐ PRE ☐ FINAL
FREQUENCY RANGE 2.1-2.36 GHz SHEET OF
BALL AEROSPACE SYSTEMS DIVISION
SPD Insertion Loss
OPER. WITNESSED DATE 7-6-82

Fig. 3.34



Ball Omni Antennas

PROJECT NO. 2314-001 PROGRAM Auto Omni
PART NO. _____ MODEL NO. _____ SERIAL NO. _____
TEST TYPE: ☒ DEVELOPMENT ☐ PRE ☐ FINAL
FREQUENCY RANGE 2.1-2.3 GHz SHEET ____ OF ____

BALL AEROSPACE SYSTEMS DIVISION

REMARKS SPD Insertion Loss

OPER. FB WITNESSED _____ DATE 2-6-82

Fig. 3.35

#17

RETURN LOSS (dB)
0 5 10 15 20 25 30 35 40
10.0 6.0 5.0 4.0 3.0 2.5 2.0 1.8 1.6 1.5 1.4 1.3 1.25 1.20 1.15 1.10 1.075 1.05 VSWR

RETURN LOSS ; ☒ INSERTION LOSS ; ☐ PHASE CHART

Scientific-Atlanta ANTENNAS

PROJECT NO. 2314-001 PROGRAM Auto Omni
PART NO. _____ MODEL NO. _____ SERIAL NO. _____
TEST TYPE: ☒ DEVELOPMENT ☐ PRE ☐ FINAL
FREQUENCY RANGE 2.1-2.36 GHz SHEET _____ OF _____

Loss dB

0 1 2 3 4 5 6 7 8 9 10

7 17 18 27

SCALE (dB) ; ☐ SCALE (deg)

Ref

FREQUENCY SCALE ( )
2100 2200 2300

67

BALL AEROSPACE SYSTEMS DIVISION

REMARKS SPD Insertion Loss

OPER. JB WITNESSED _____ DATE 7-6-82

Fig 3.34



#16

RETURN LOSS ; ☒ INSERTION LOSS ; ☐ PHASE CHART

Ball Stolle ANTENNAS

PROJECT NO. 2314-001 PROGRAM Auto Omni

PART NO. _____ MODEL NO. _____ SERIAL NO. _____

TEST TYPE: ☒ DEVELOPMENT ☐ PRE ☐ FINAL

FREQUENCY RANGE 2.1-2.36 GHz SHEET _____ OF _____

12
16
17
26
Loss
QB

SCALE (dB) ; ☐ SCALE (deg)

0
1
2
3
4
5
6
7
8
9
-10

Ref

FREQUENCY SCALE ( )

2100
2200
2300

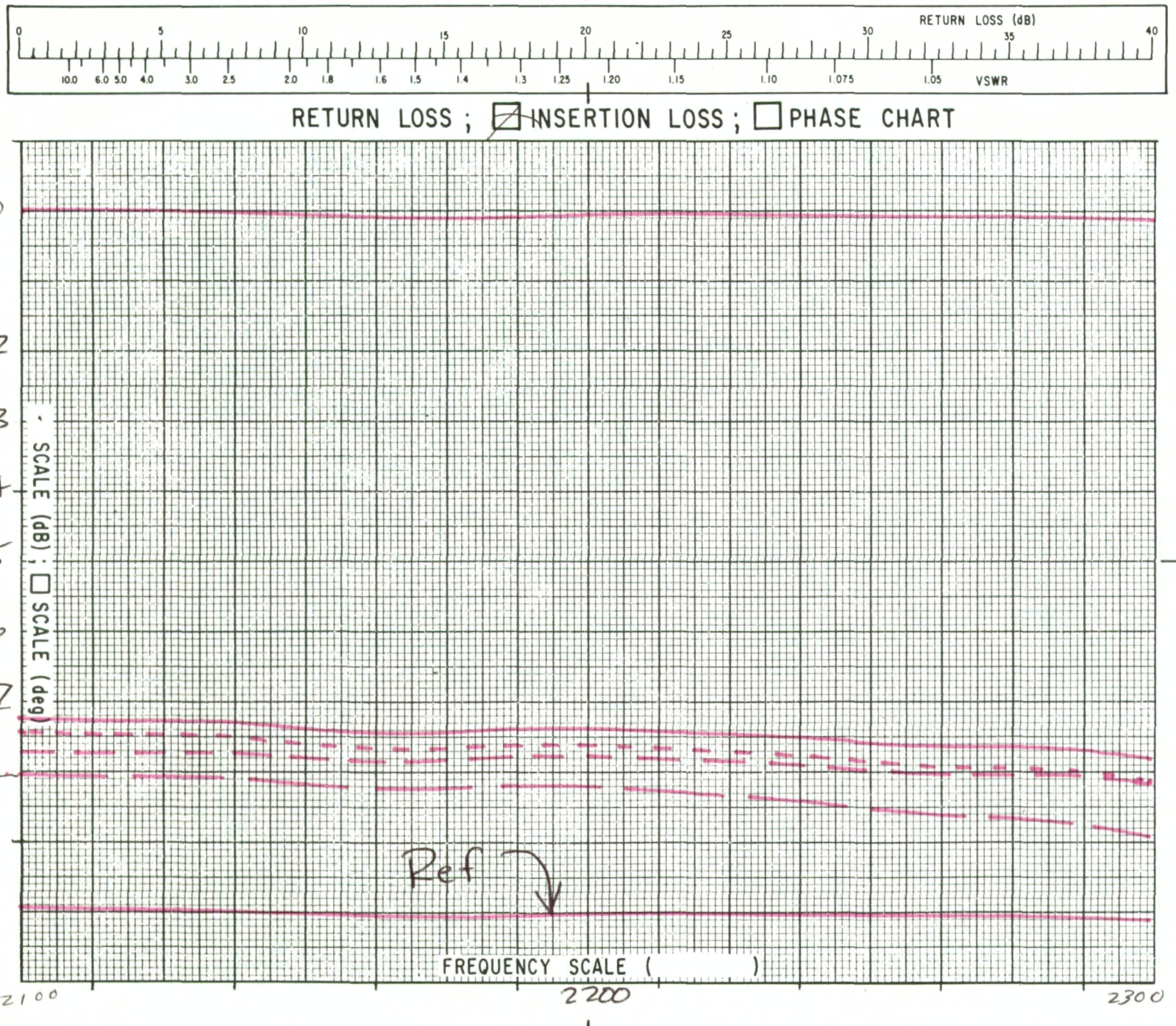
68

BALL AEROSPACE SYSTEMS DIVISION

REMARKS SPD Insertion Loss

OPER. JB WITNESSED _____ DATE 7-6-82

Fig 3.37



Hughes Aircraft Company ANTENNAS

PROJECT NO. 2314-001 PROGRAM Auto Omni

PART NO. _____ MODEL NO. _____ SERIAL NO. _____

TEST TYPE: ☒ DEVELOPMENT ☐ PRE ☐ FINAL

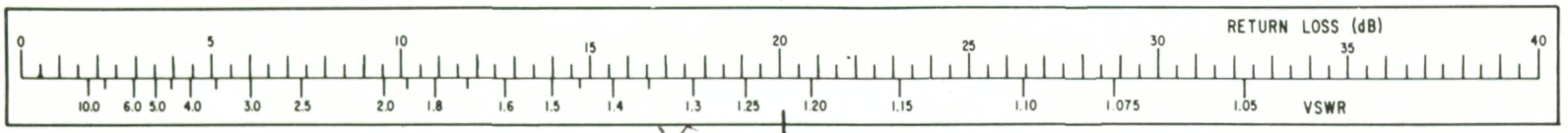
FREQUENCY RANGE 2.1 - 2.36 GHz SHEET _____ OF _____

BALL AEROSPACE SYSTEMS DIVISION

REMARKS SPD Insertion Loss

OPER. ZB WITNESSED _____ DATE 7-6-82

Fig 3.38



RETURN LOSS ; ☒ INSERTION LOSS ; ☐ PHASE CHART

#72

Loss dB

0 1 2 3 4 5 6 7 8 9 -10

-SCALE (dB) ; ☐ SCALE (deg)

Ref

FREQUENCY SCALE ( )

2100 2300

70

Ball Stop Patch ANTENNAS

PROJECT NO. 2314-001 PROGRAM Auto Omni

PART NO. _____ MODEL NO. _____ SERIAL NO. _____

TEST TYPE: ☒ DEVELOPMENT ☐ PRE ☐ FINAL

FREQUENCY RANGE 2.1 - 2.3 GHz SHEET _____ OF _____

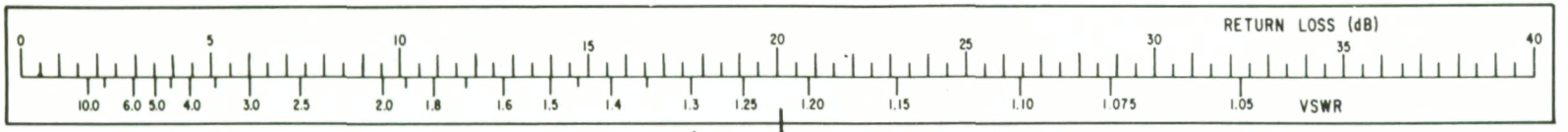
BALL AEROSPACE SYSTEMS DIVISION

REMARKS SPD Insertion Loss

OPER. [illegible] WITNESSED _____ DATE 7-6-82

Fig 3.39

#7



RETURN LOSS ; ☒ INSERTION LOSS ; ☐ PHASE CHART

Hughes Aircraft Company ANTENNAS

PROJECT NO. 2314-001 PROGRAM Auto Omni
PART NO. _____ MODEL NO. _____ SERIAL NO. _____
TEST TYPE: ☒ DEVELOPMENT ☐ PRE ☐ FINAL
FREQUENCY RANGE 2.1 - 2.36 GHz SHEET _____ OF _____

Loss dB

0 1 2 3 4 5 6 7 8 9 -10

7 13 15 18

- SCALE (dB) ; ☐ SCALE (deg)

Ref

FREQUENCY SCALE ( )

2100 2200 2300

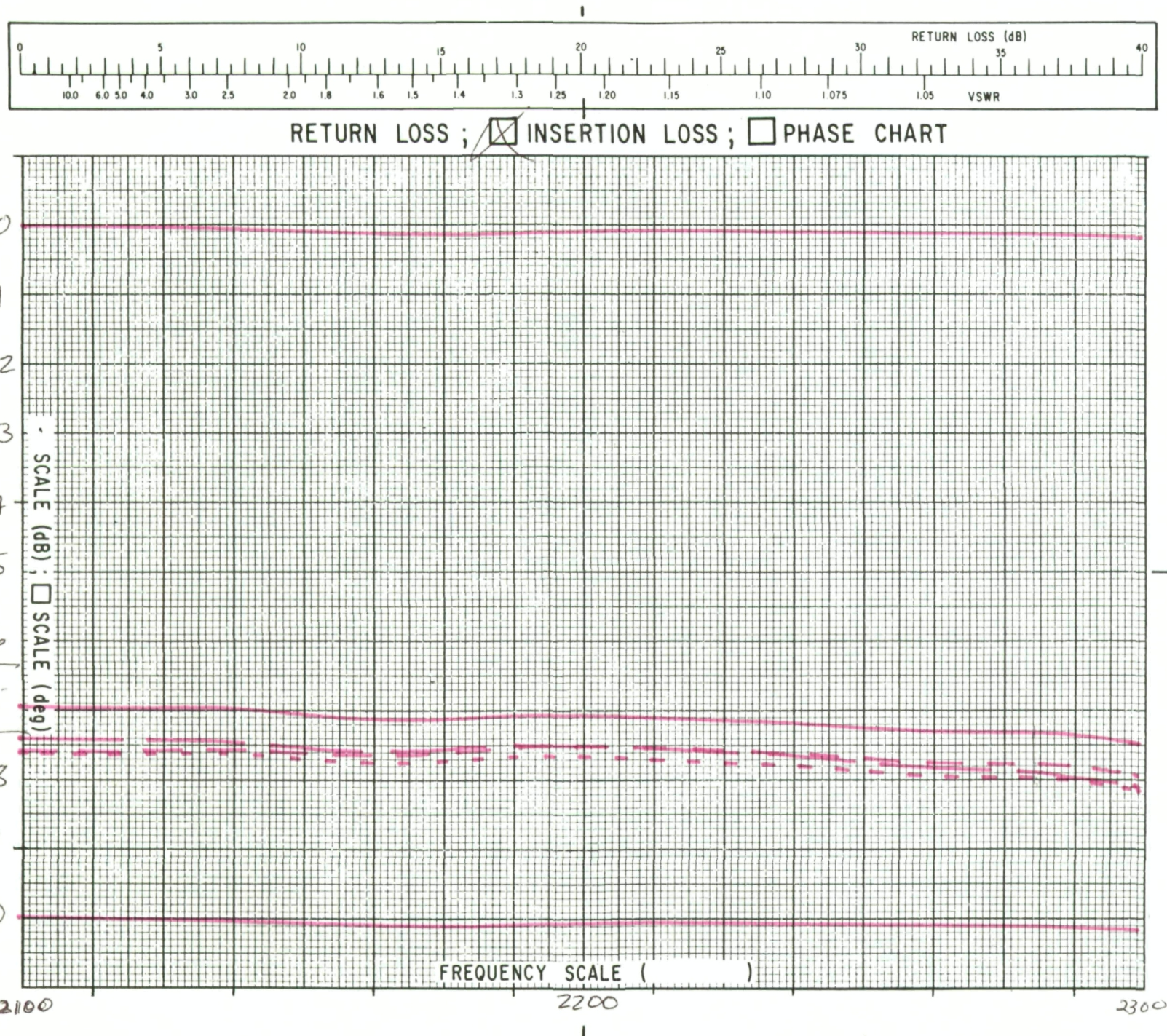
71

BALL AEROSPACE SYSTEMS DIVISION

REMARKS SPD Insertion Loss

OPER. ~~JB~~ WITNESSED _____ DATE 7-6-82

Fig 3.40



Q-Stop Patch ANTENNAS

PROJECT NO. 2314-001 PROGRAM Auto Omni

PART NO. _____ MODEL NO. _____ SERIAL NO. _____

TEST TYPE: ☒ DEVELOPMENT ☐ PRE ☐ FINAL

FREQUENCY RANGE 2.1 - 2.3 GHz SHEET _____ OF _____

BALL AEROSPACE SYSTEMS DIVISION

REMARKS SPD Insertion Loss

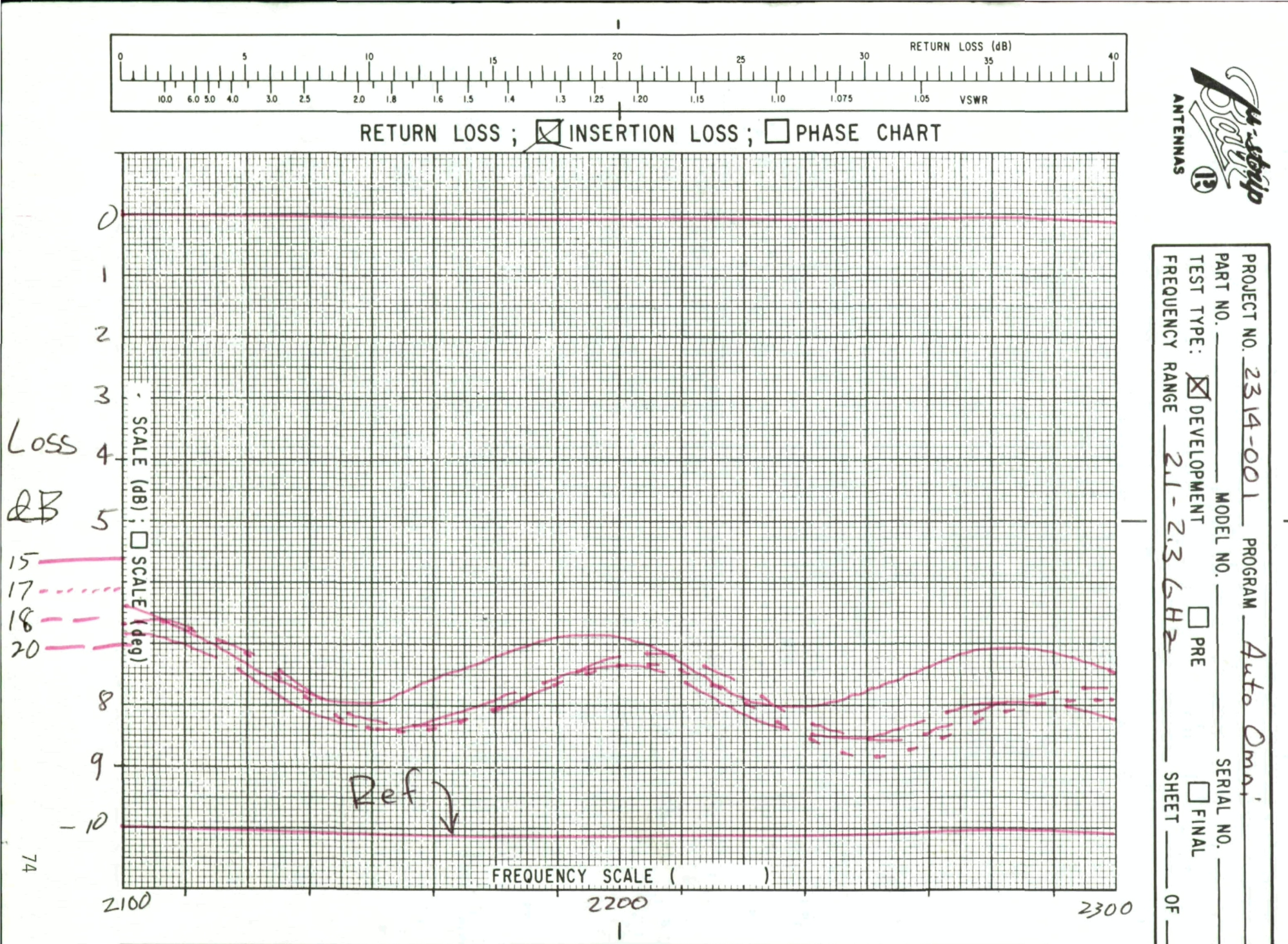
OPER. ZB WITNESSED _____ DATE 7-6-82

Fig. 3.4/

Case 3 (Raw Data)

SPD INSERTION LOSS DATA WITH ELEMENTS AS LOADS

Figure	Outputs			
3.42	15	17	18	20
3.43	7	13	15	18
3.44	16	17	18	27
3.45	16	17	26	27
3.46	12	16	17	26
3.47	7	17	18	27
3.48	7	12	17	26
3.49	7	12	17	18
3.50	7	12	17	20
3.51	7	11	12	20
3.52	7	12	15	20
3.53	6	15	19	20
3.54	7	15	19	20



Ball ANTENNAS

PROJECT NO. 2314-001 PROGRAM Auto Omni

PART NO. _____ MODEL NO. _____ SERIAL NO. _____

TEST TYPE: ☒ DEVELOPMENT ☐ PRE ☐ FINAL

FREQUENCY RANGE 2.1 - 2.36 GHz SHEET ____ OF ____

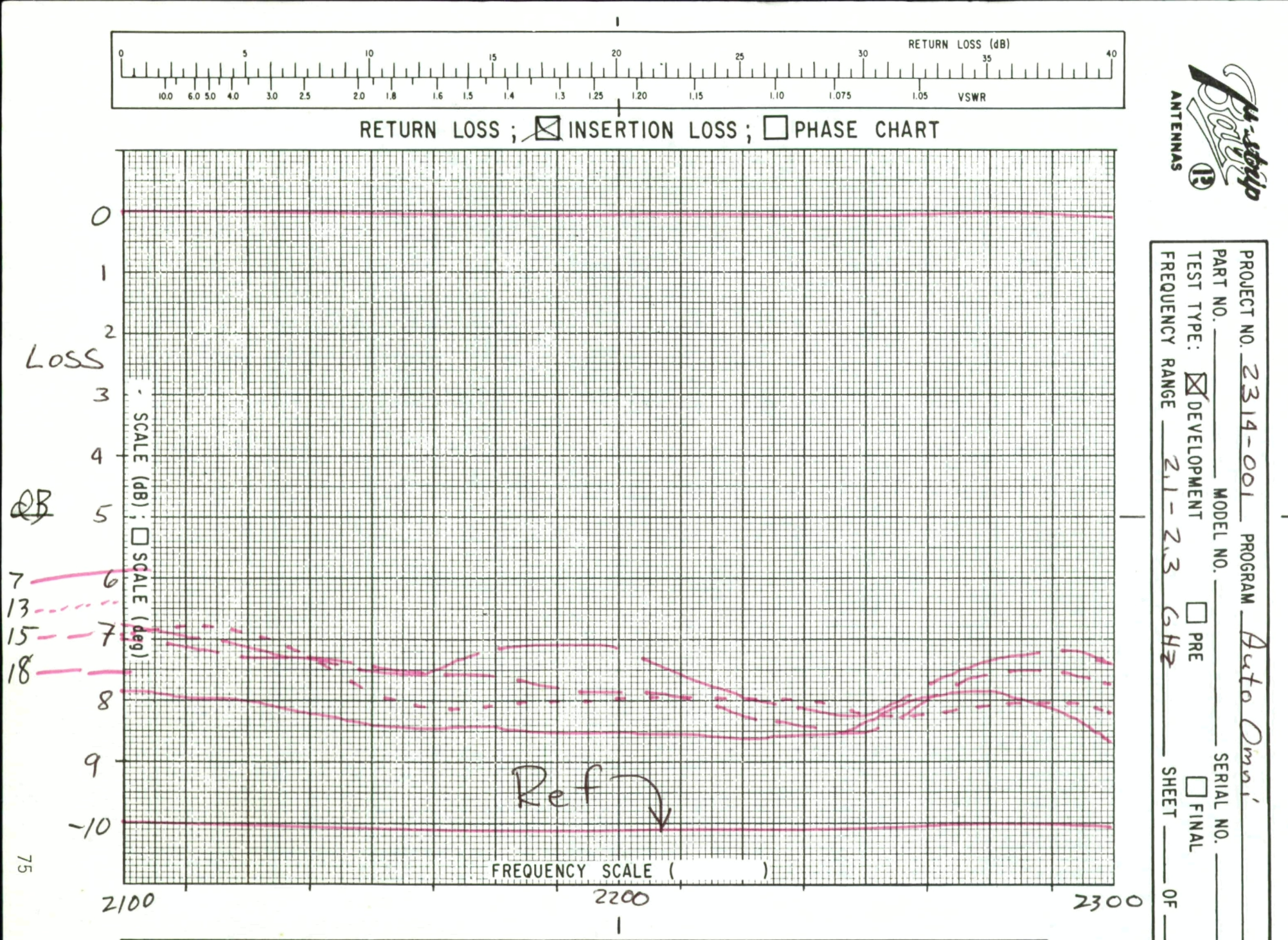
BALL AEROSPACE SYSTEMS DIVISION

REMARKS SPD Insertion Loss

OPER. [illegible] WITNESSED _____ DATE 2-14-82

74

Fig. 3.42



Hi-Stop Data ANTENNAS

PROJECT NO. 2314-001 PROGRAM Auto Omni

PART NO. _____ MODEL NO. _____ SERIAL NO. _____

TEST TYPE: ☒ DEVELOPMENT ☐ PRE ☐ FINAL

FREQUENCY RANGE 2.1 - 2.3 GHz SHEET _____ OF _____

BALL AEROSPACE SYSTEMS DIVISION

REMARKS SPD Insertion Loss

OPER. FB WITNESSED _____ DATE 2-14-82

Fig. 3.43

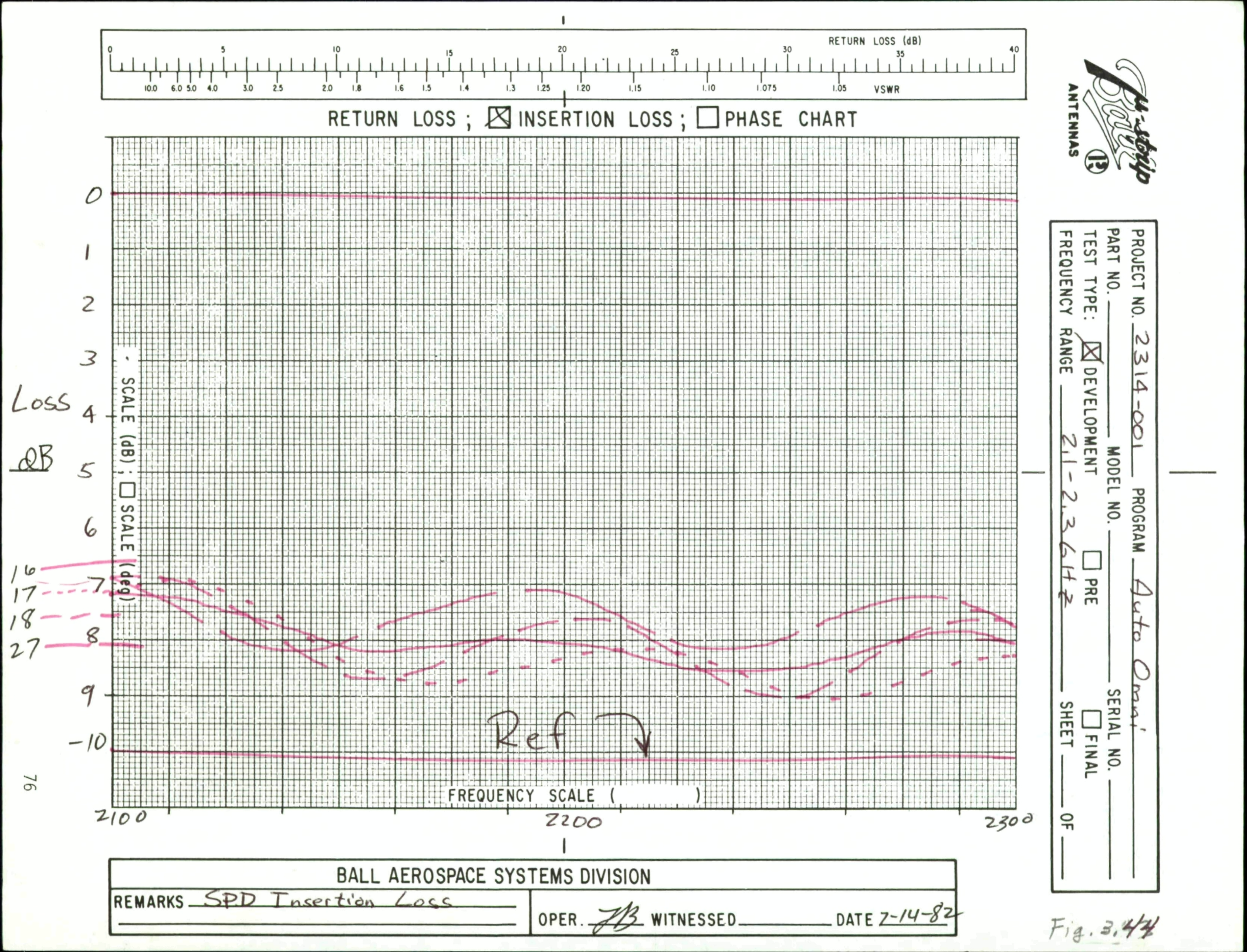
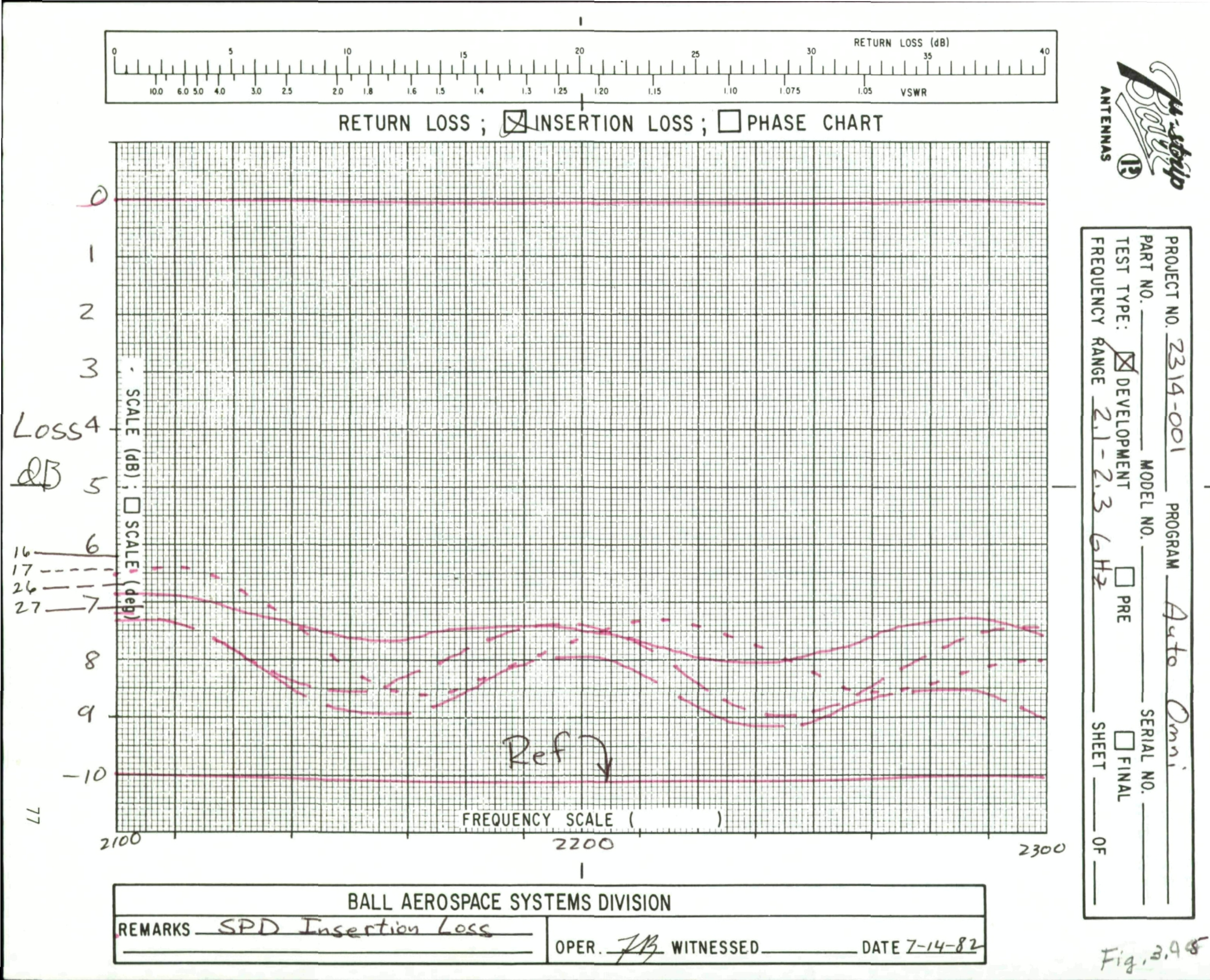

RETURN LOSS (dB)
0 5 10 15 20 25 30 35 40
10.0 6.0 5.0 4.0 3.0 2.5 2.0 1.8 1.6 1.5 1.4 1.3 1.25 1.20 1.15 1.10 1.075 1.05 VSWR
RETURN LOSS ; ☒ INSERTION LOSS ; ☐ PHASE CHART
Loss
dB
SCALE (dB) ; ☐ SCALE (deg)
0 1 2 3 4 5 6 7 8 9 -10
16
17
18
27
Ref
FREQUENCY SCALE ( )
2100 2200 2300
76
PROJECT NO. 2314-001 PROGRAM Auto Omni
PART NO. MODEL NO. SERIAL NO.
TEST TYPE: ☒ DEVELOPMENT ☐ PRE ☐ FINAL
FREQUENCY RANGE 2.1-2.36 GHz SHEET OF
BALL AEROSPACE SYSTEMS DIVISION
REMARKS SPD Insertion Loss
OPER. JB WITNESSED DATE 2-14-82

Fig. 3.4.4



Ball Antennas

PROJECT NO. 2314-001 PROGRAM Auto Omni

PART NO. _____ MODEL NO. _____ SERIAL NO. _____

TEST TYPE: ☒ DEVELOPMENT ☐ PRE ☐ FINAL

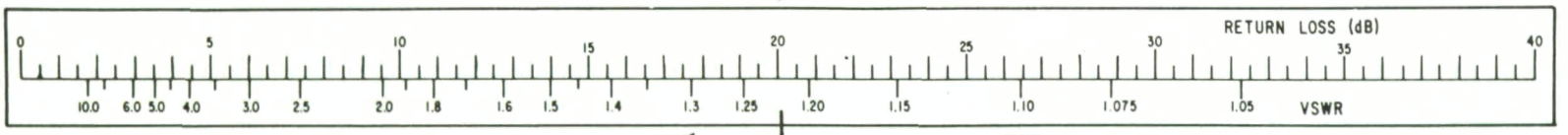
FREQUENCY RANGE 2.1 - 2.3 GHz SHEET _____ OF _____

BALL AEROSPACE SYSTEMS DIVISION

REMARKS SPD Insertion Loss

OPER. JB WITNESSED _____ DATE 7-14-82

Fig. 2.9.5



RETURN LOSS ; ☒ INSERTION LOSS ; ☐ PHASE CHART

Ball ANTENNAS

PROJECT NO. 2314-001 PROGRAM Auto Omni

PART NO. _____ MODEL NO. _____ SERIAL NO. _____

TEST TYPE: ☒ DEVELOPMENT ☐ PRE ☐ FINAL

FREQUENCY RANGE 2.1 - 2.3 GHz SHEET ____ OF ____

Loss

dB

0
1
2
3
4
5
7
8
9
10

12
16
17
26

SCALE (dB) ; ☐ SCALE (deg)

Ref

FREQUENCY SCALE ( )

2100
2200
2300

78

BALL AEROSPACE SYSTEMS DIVISION

REMARKS SPP Insertion Loss

OPER. JB WITNESSED _____ DATE 7-14-82

Fig. 3.46



RETURN LOSS ; ☒ INSERTION LOSS ; ☐ PHASE CHART

Loss dB

0 1 2 3 4 5 6 7 8 9 -10

7
17
18
27

· SCALE (dB) ; ☐ SCALE (deg)

Ref

FREQUENCY SCALE ( )

2100 2200 2300

79

PROJECT NO. 2314-001 PROGRAM Auto Omni

PART NO. _____ MODEL NO. _____ SERIAL NO. _____

TEST TYPE: ☒ DEVELOPMENT ☐ PRE ☐ FINAL

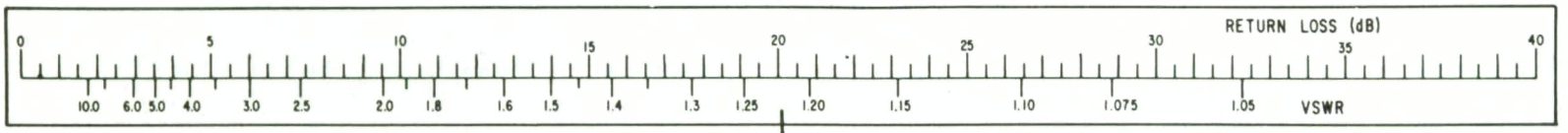
FREQUENCY RANGE 2.1-2.3 GHz SHEET ____ OF ____

BALL AEROSPACE SYSTEMS DIVISION

REMARKS SPD Insertion Loss

OPER. JB WITNESSED _____ DATE 7-14-82

Fig. 3.47



RETURN LOSS ; ☒ INSERTION LOSS ; ☐ PHASE CHART

Ball Stolle ANTENNAS

PROJECT NO. 2314-001 PROGRAM Auto Omni

PART NO. _____ MODEL NO. _____ SERIAL NO. _____

TEST TYPE: ☒ DEVELOPMENT ☐ PRE ☐ FINAL

FREQUENCY RANGE 2.1-2.3 GHz SHEET ____ OF ____

0
1
2
3
4
dB 5
6
7
8
9
10

7
12
17
26

· SCALE (dB) ; ☐ SCALE (deg)

FREQUENCY SCALE ( )

2100 2200 2300

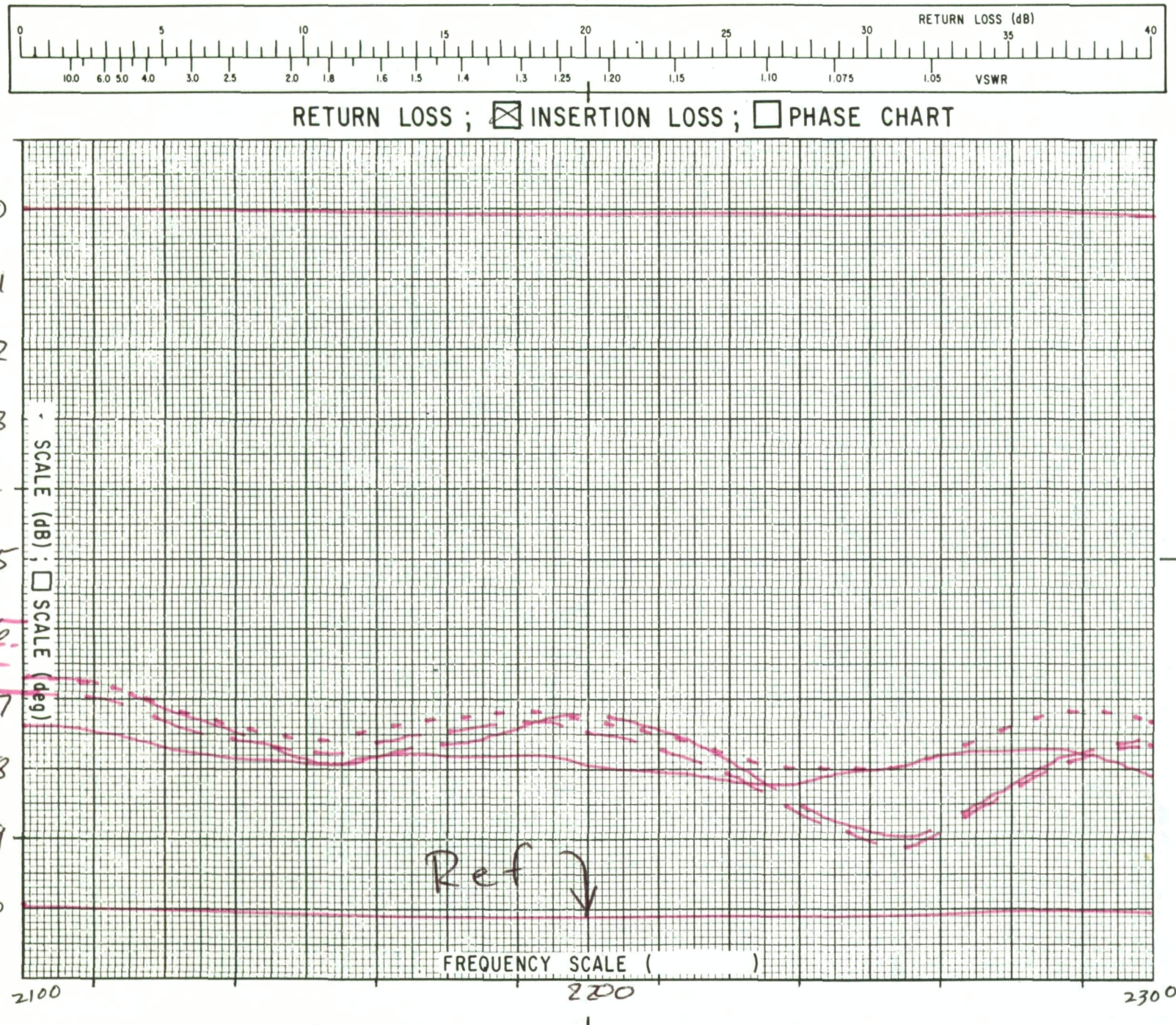
80

BALL AEROSPACE SYSTEMS DIVISION

REMARKS Insertion Loss of SPD

OPER. ZB WITNESSED _____ DATE 7-14-82

Fig. 3.98



Auto Omni

PROJECT NO. 2314-001 PROGRAM _____

PART NO. _____ MODEL NO. _____ SERIAL NO. _____

TEST TYPE: ☒ DEVELOPMENT ☐ PRE ☐ FINAL

FREQUENCY RANGE 2.1 - 2.3 GHz SHEET ____ OF ____

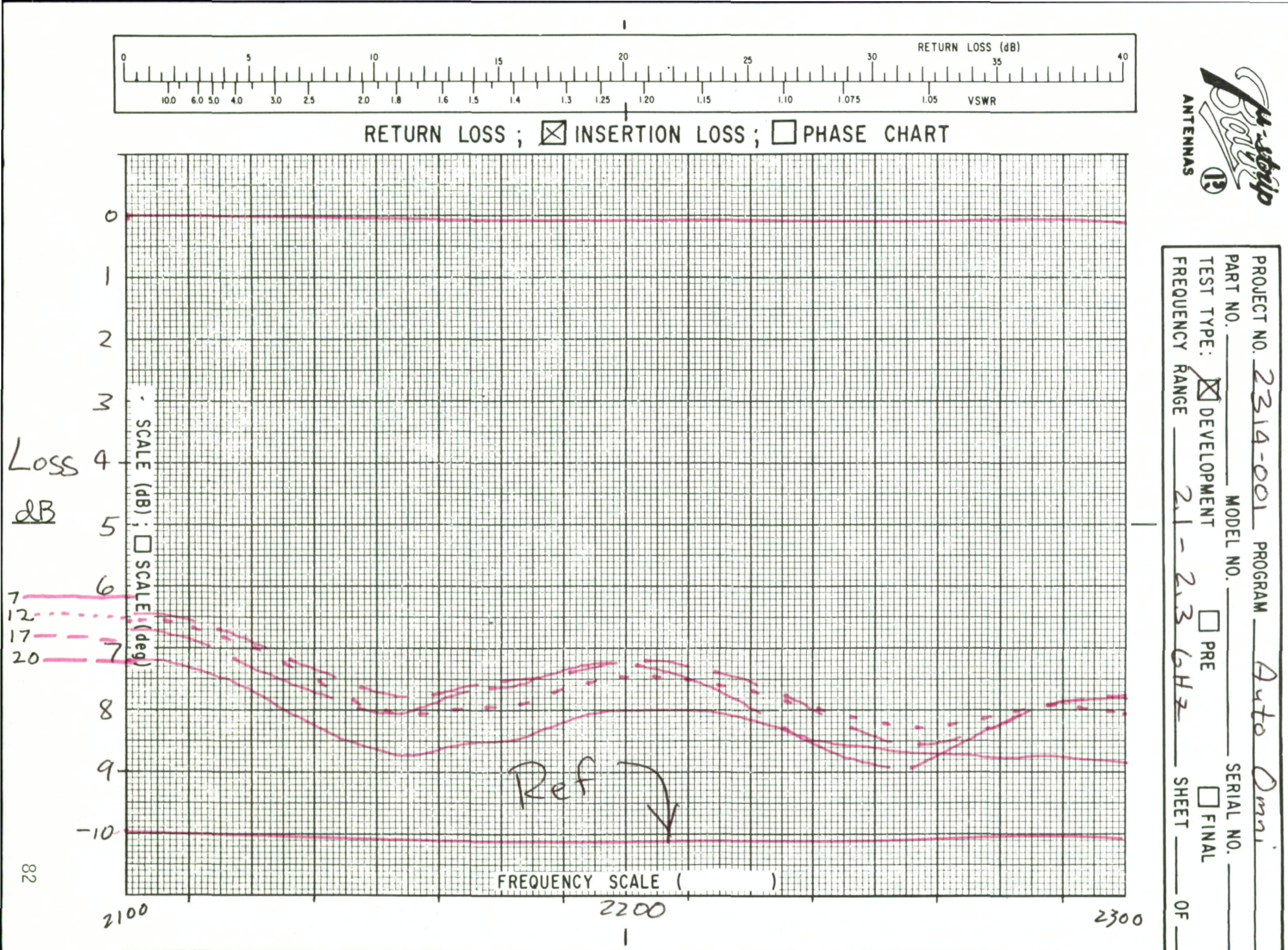
BALL AEROSPACE SYSTEMS DIVISION

REMARKS SPD Insertion Loss

OPER. ZB WITNESSED _____ DATE 7-14-82

81

Fig. 3.9



Hughes Aircraft Co. ANTENNAS

PROJECT NO. 2314-001 PROGRAM Auto Omni

PART NO. _____ MODEL NO. _____ SERIAL NO. _____

TEST TYPE: ☒ DEVELOPMENT ☐ PRE ☐ FINAL

FREQUENCY RANGE 2.1 - 2.36 GHz SHEET _____ OF _____

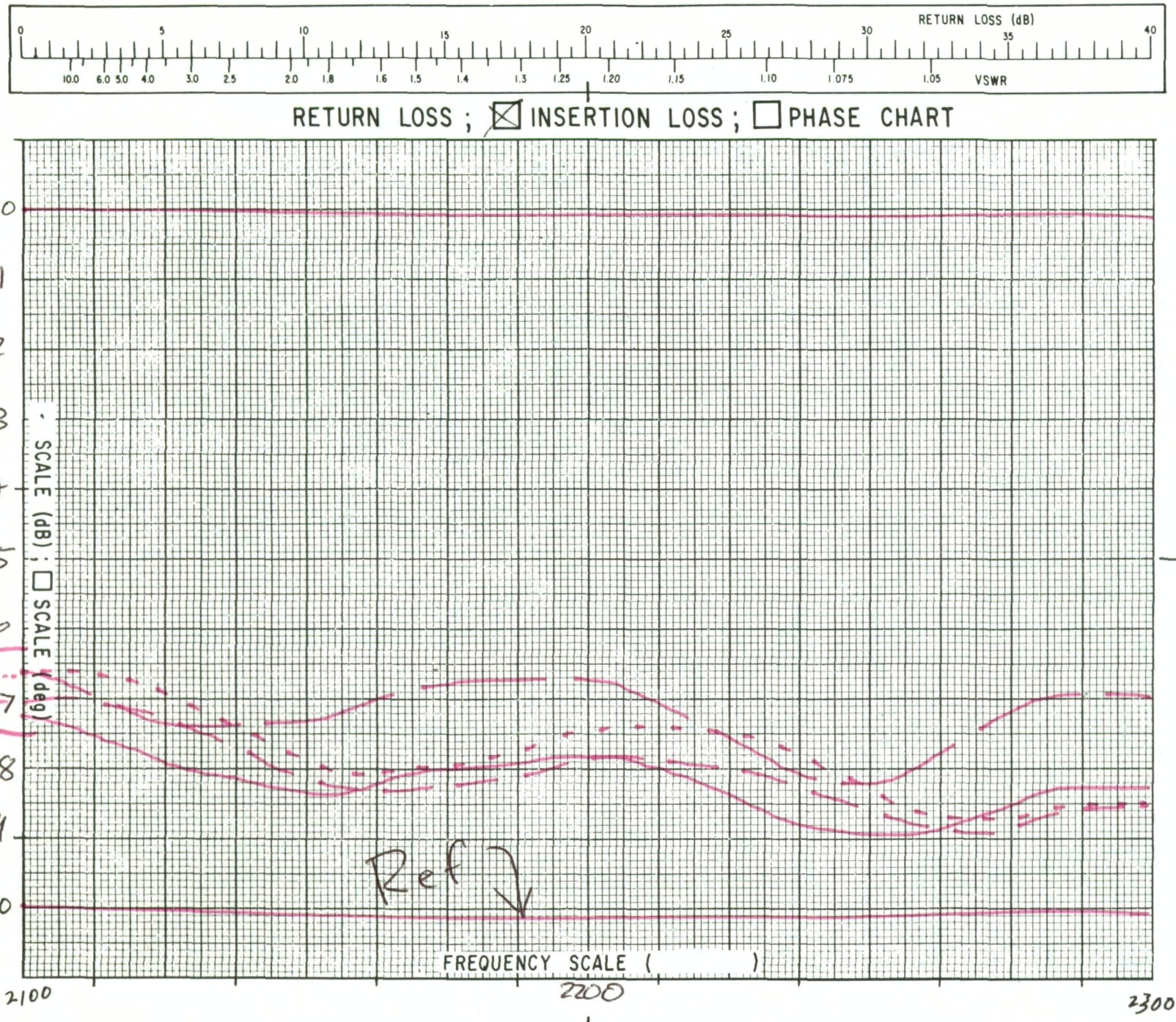
BALL AEROSPACE SYSTEMS DIVISION

REMARKS SPD Insertion Loss

OPER. JB WITNESSED _____ DATE 7-14-82

82

Fig. 3.50



Hughes Aircraft Co. ANTENNAS

PROJECT NO. 2314-001 PROGRAM Auto Omni

PART NO. _____ MODEL NO. _____ SERIAL NO. _____

TEST TYPE: ☒ DEVELOPMENT ☐ PRE ☐ FINAL

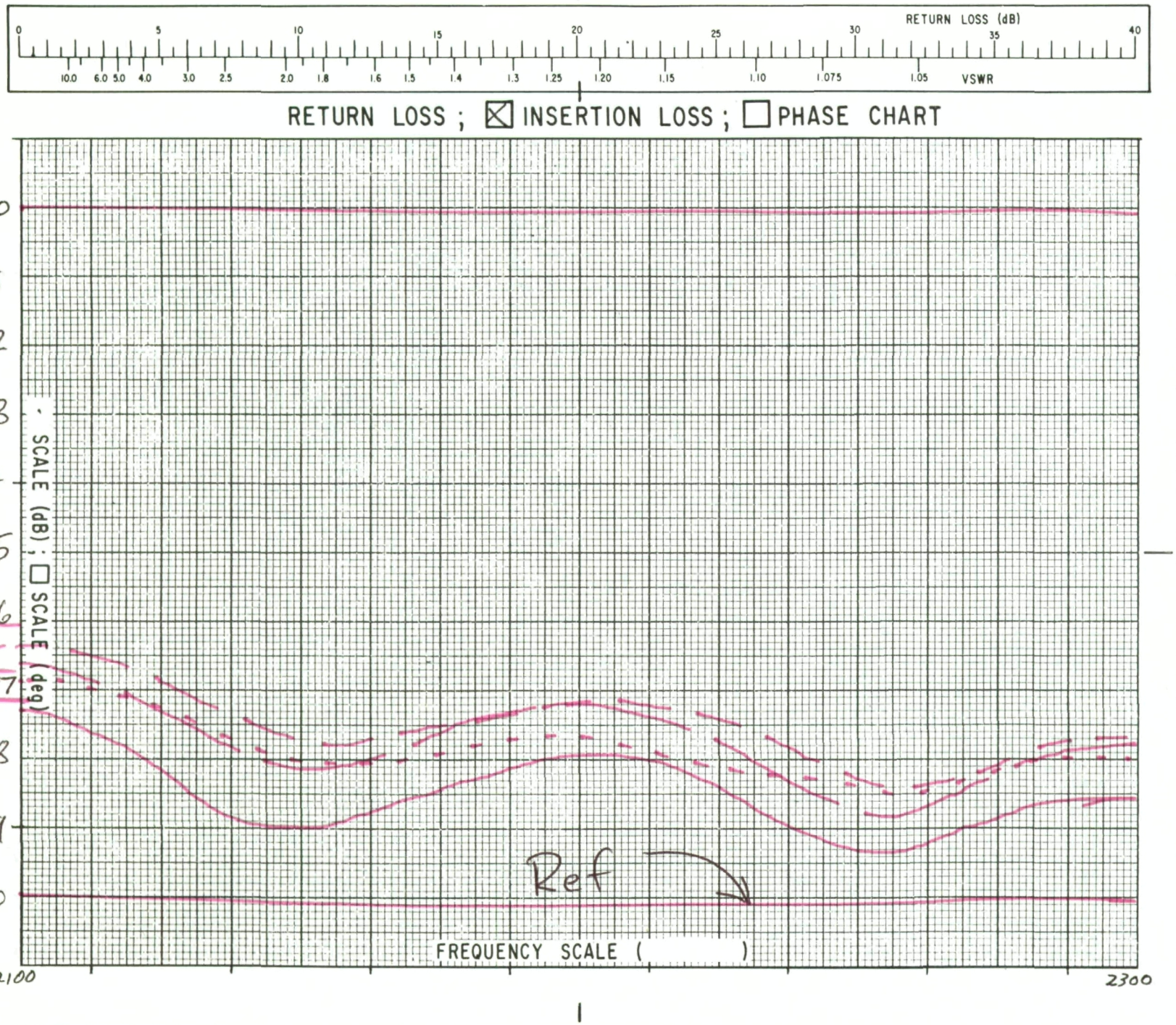
FREQUENCY RANGE 2.1-2.3 GHz. SHEET ____ OF ____

BALL AEROSPACE SYSTEMS DIVISION

REMARKS SPD Insertion Loss

OPER. JB WITNESSED _____ DATE 7-14-82

Fig. 3.5p



PROJECT NO. 2314-001 PROGRAM Auto Omni
PART NO. ____ MODEL NO. ____ SERIAL NO. ____
TEST TYPE: ☒ DEVELOPMENT ☐ PRE ☐ FINAL
FREQUENCY RANGE 2.1 - 2.36 GHz SHEET ____ OF ____

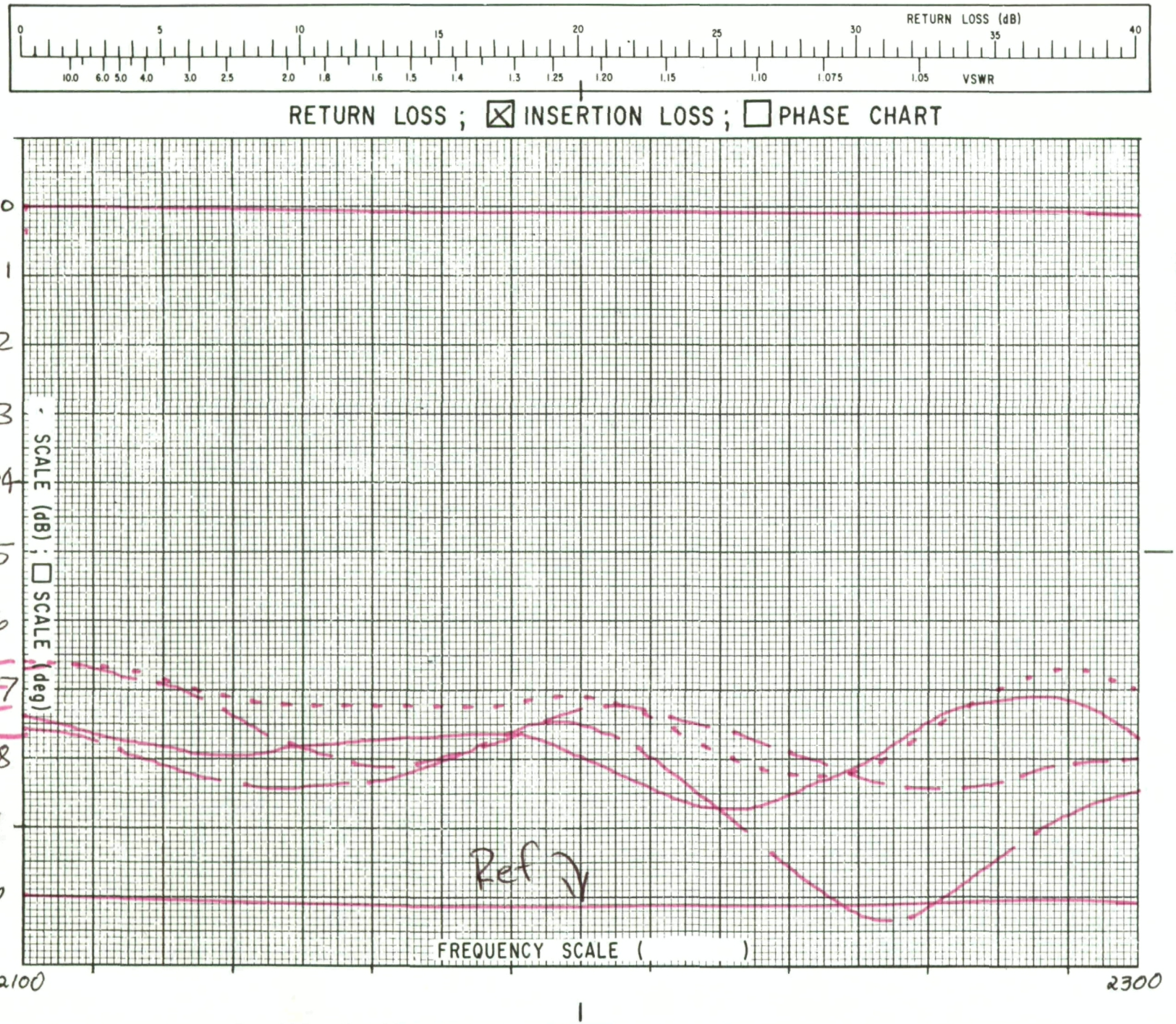
BALL AEROSPACE SYSTEMS DIVISION

REMARKS SPD Insertion Loss

OPER. JB WITNESSED ____ DATE 7-14-82

84

Fig. 352



Auto Omni

PROJECT NO. 2314-001 PROGRAM _____

PART NO. _____ MODEL NO. _____ SERIAL NO. _____

TEST TYPE: ☒ DEVELOPMENT ☐ PRE ☐ FINAL

FREQUENCY RANGE 2.1-2.36Hz SHEET ____ OF ____

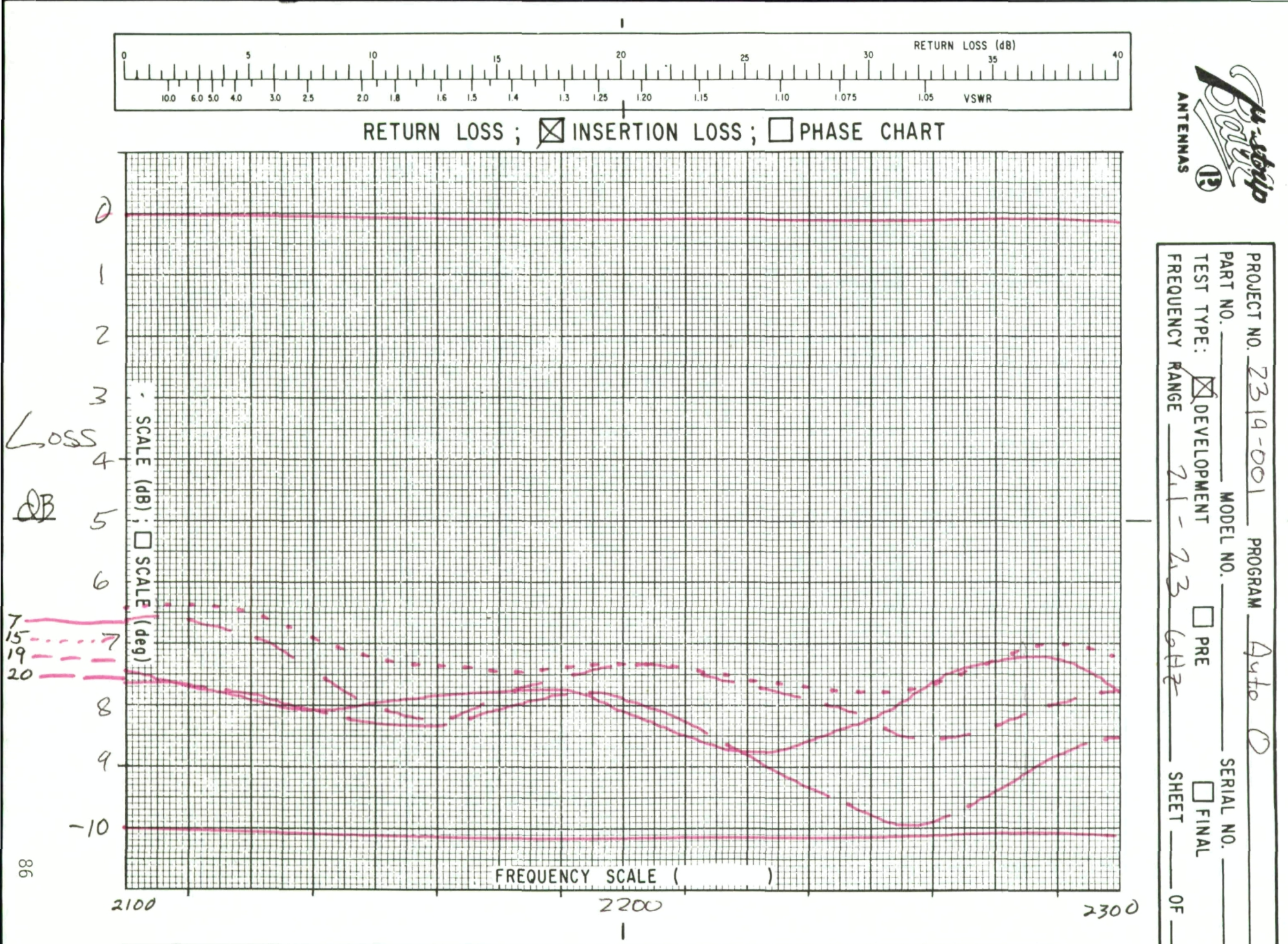
BALL AEROSPACE SYSTEMS DIVISION

REMARKS SPD Insertion Loss

OPER. JM WITNESSED _____ DATE 7-14-82

85

Fig. 3.53



PROJECT NO. 2319-001 PROGRAM Ayte C

PART NO. _____ MODEL NO. _____ SERIAL NO. _____

TEST TYPE: ☒ DEVELOPMENT ☐ PRE ☐ FINAL

FREQUENCY RANGE 21 - 23 GHz SHEET ____ OF ____

BALL AEROSPACE SYSTEMS DIVISION

REMARKS SPD Insertion Loss

OPER. JB WITNESSED _____ DATE 7-14-82

Fig. 3.54

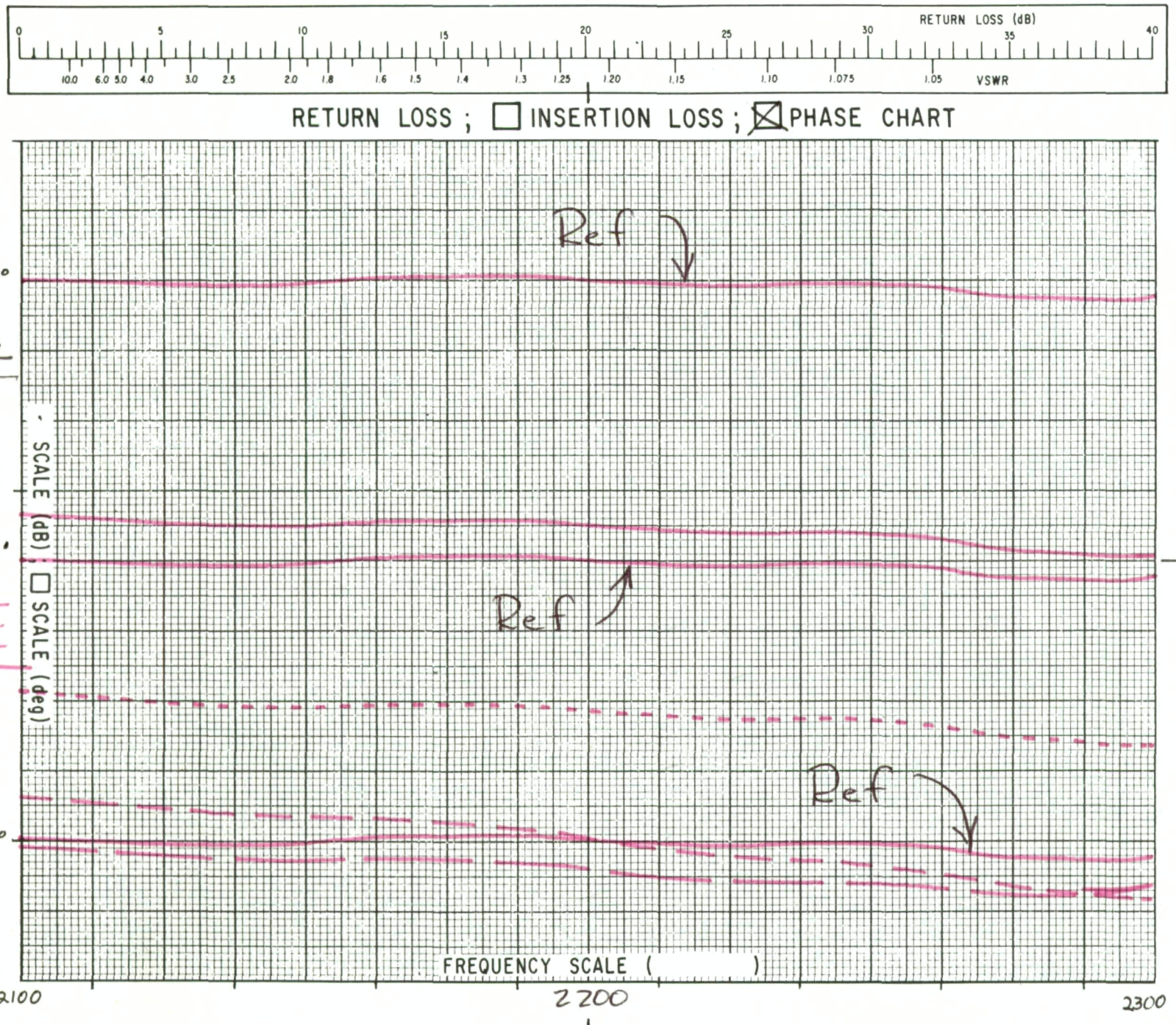
Case 2

Case 2 (Raw Data)

SPD INSERTION PHASE DATA WITH RESISTIVE LOADS

Output seven used as reference for phase

Figure	Outputs			
3.55	6	15	19	20
3.56	15	17	18	20
3.57	7	13	15	18
3.58	16	17	18	27
3.59	16	17	26	27
3.60	12	16	17	26
3.61	7	17	18	27
3.62	7	12	17	26
3.63	7	12	17	18
3.64	7	12	17	20
3.65	7	11	12	20
3.66	7	12	15	20
3.67	7	15	19	20



PROJECT NO. 2314-001 PROGRAM Auto Omni

PART NO. _____ MODEL NO. _____ SERIAL NO. _____

TEST TYPE: ☒ DEVELOPMENT ☐ PRE ☐ FINAL

FREQUENCY RANGE 2.1 - 2.3 GHz SHEET ___ OF ___

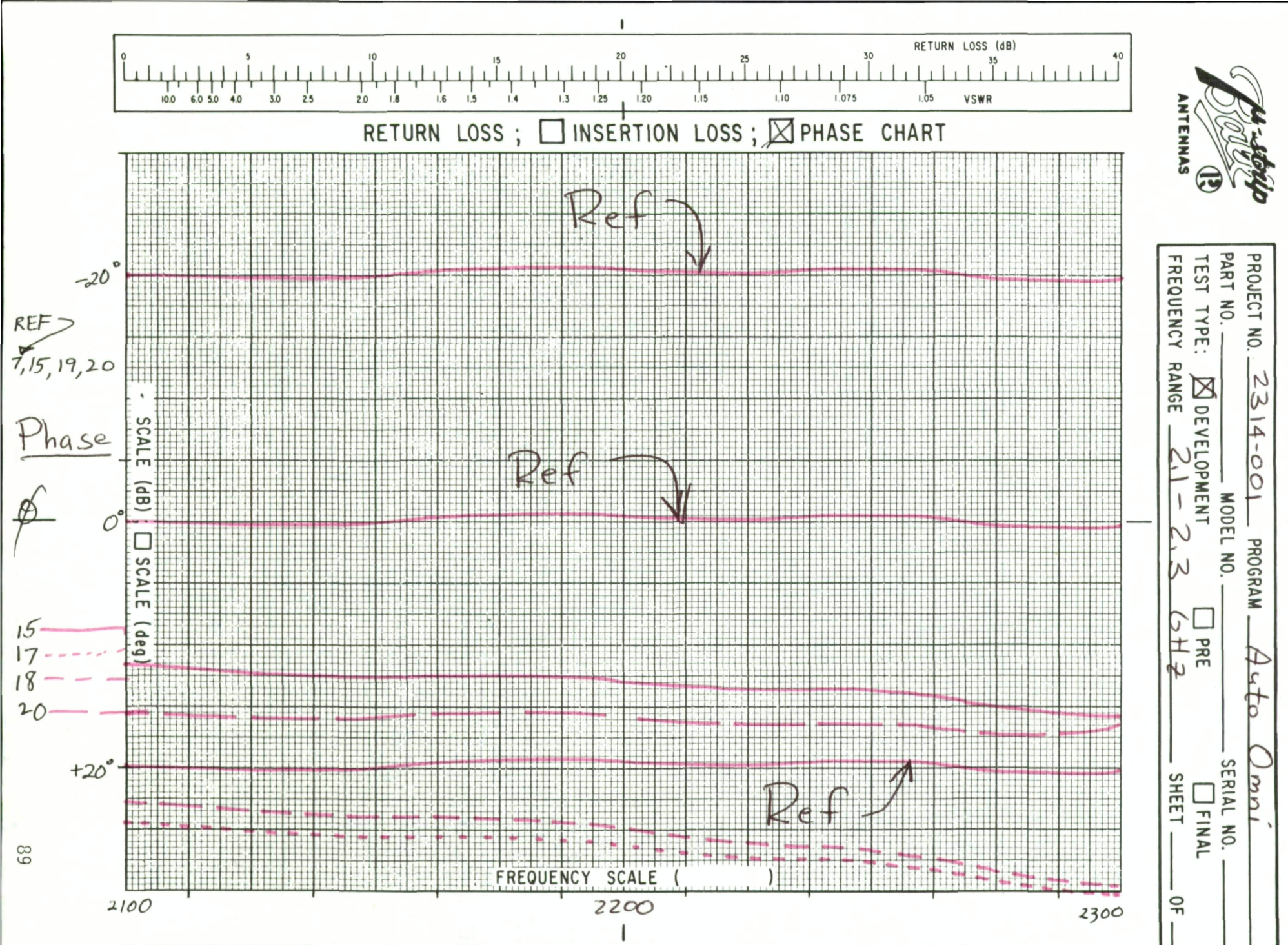
BALL AEROSPACE SYSTEMS DIVISION

REMARKS SPD Insertion Phase

OPER. JB WITNESSED _____ DATE 7-9-82

88

Fig. 3.5



Hughes Ball 12 ANTENNAS

PROJECT NO. 2314-001 PROGRAM Auto Omni

PART NO. _____ MODEL NO. _____ SERIAL NO. _____

TEST TYPE: ☒ DEVELOPMENT ☐ PRE ☐ FINAL

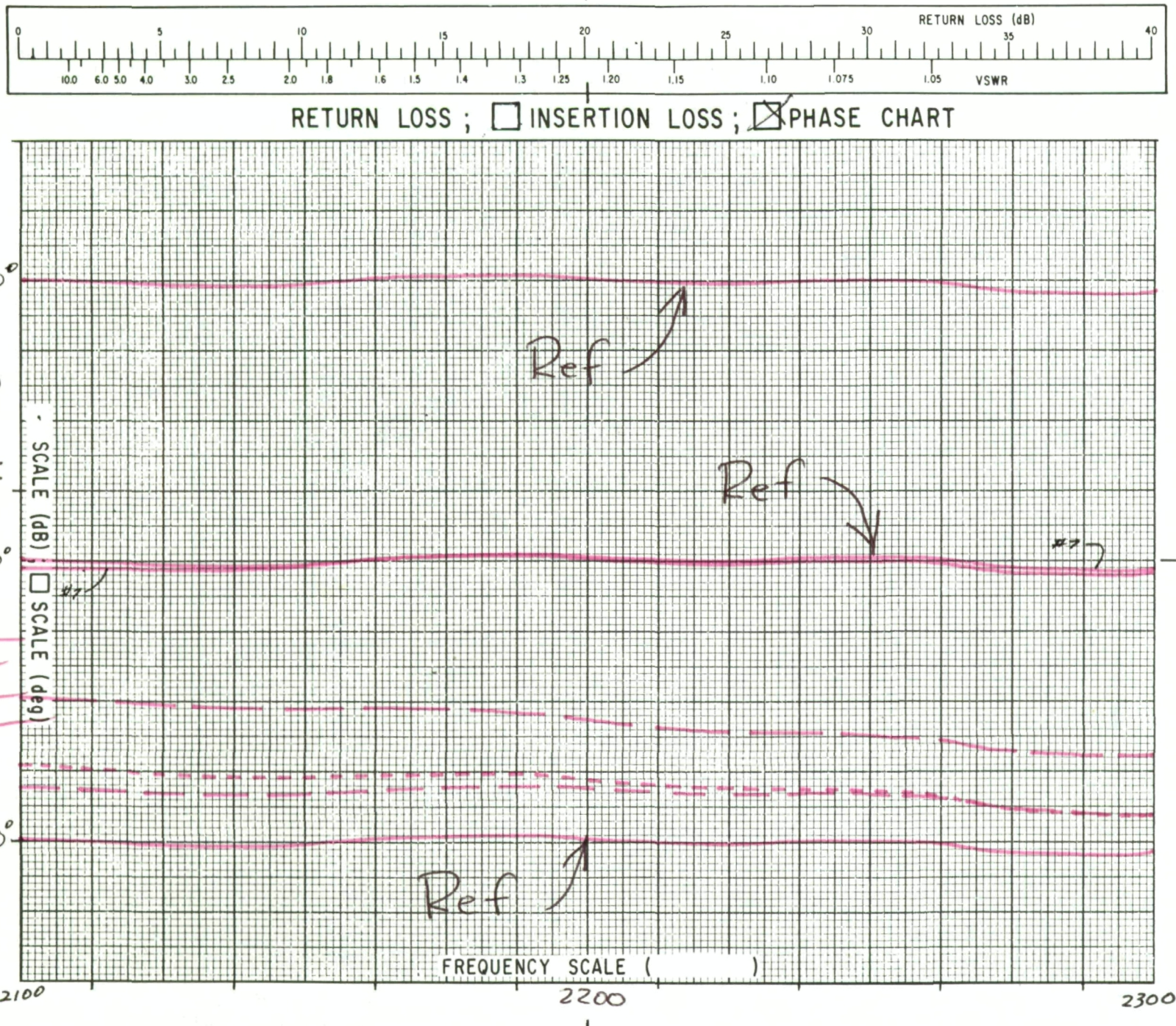
FREQUENCY RANGE 2.1 - 2.3 GHz SHEET ____ OF ____

BALL AEROSPACE SYSTEMS DIVISION

REMARKS SPD Insertion Phase

OPER. JB. WITNESSED _____ DATE 7-9-82

Fig 3.56



PROJECT NO. 2314-001 PROGRAM Auto Omni

PART NO. _____ MODEL NO. _____ SERIAL NO. _____

TEST TYPE: ☒ DEVELOPMENT ☐ PRE ☐ FINAL

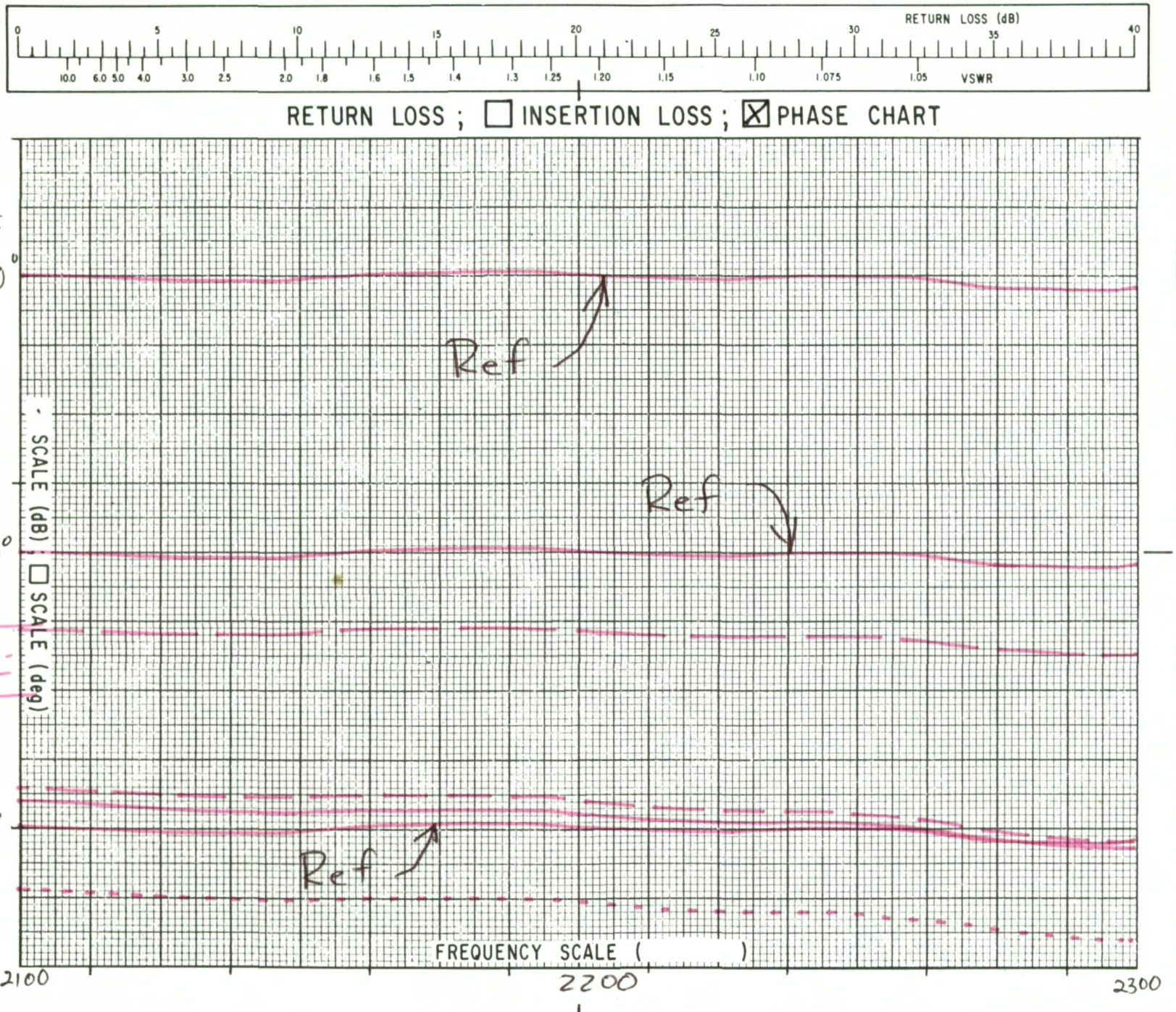
FREQUENCY RANGE 2.1-2.3 GHz SHEET ____ OF ____

BALL AEROSPACE SYSTEMS DIVISION

REMARKS SPD Insertion Loss

OPER. ZB WITNESSED _____ DATE 7-9-82

Fig 3.5.2



PROJECT NO. 2314-001 PROGRAM Auto Omni

PART NO. _____ MODEL NO. _____ SERIAL NO. _____

TEST TYPE: ☒ DEVELOPMENT ☐ PRE ☐ FINAL

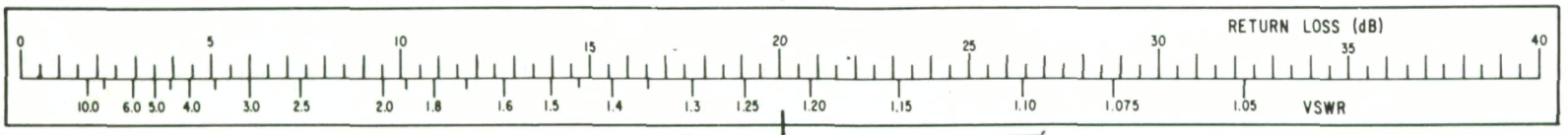
FREQUENCY RANGE 2.1-2.3 GHz SHEET ____ OF ____

BALL AEROSPACE SYSTEMS DIVISION

REMARKS SPD Insertion ~~Mags~~ Phase

OPER. YB WITNESSED _____ DATE 7-9-82

Fig. 3.5 8



RETURN LOSS ; ☐ INSERTION LOSS ; ☒ PHASE CHART

Scale Antennas

PROJECT NO. 2314-001 PROGRAM Auto Omni

PART NO. _____ MODEL NO. _____ SERIAL NO. _____

TEST TYPE: ☒ DEVELOPMENT ☐ PRE ☐ FINAL

FREQUENCY RANGE 2.1-2.3 GHz SHEET ____ OF ____

Phase

−20°

REF : 7, 15, 19, 20

Ref

Ref

Ref

SCALE (dB) ☐ SCALE (deg)

Φ 0°

16
17
26
27

+20°

FREQUENCY SCALE ( )

2100 2200 ~~2300~~ 2300

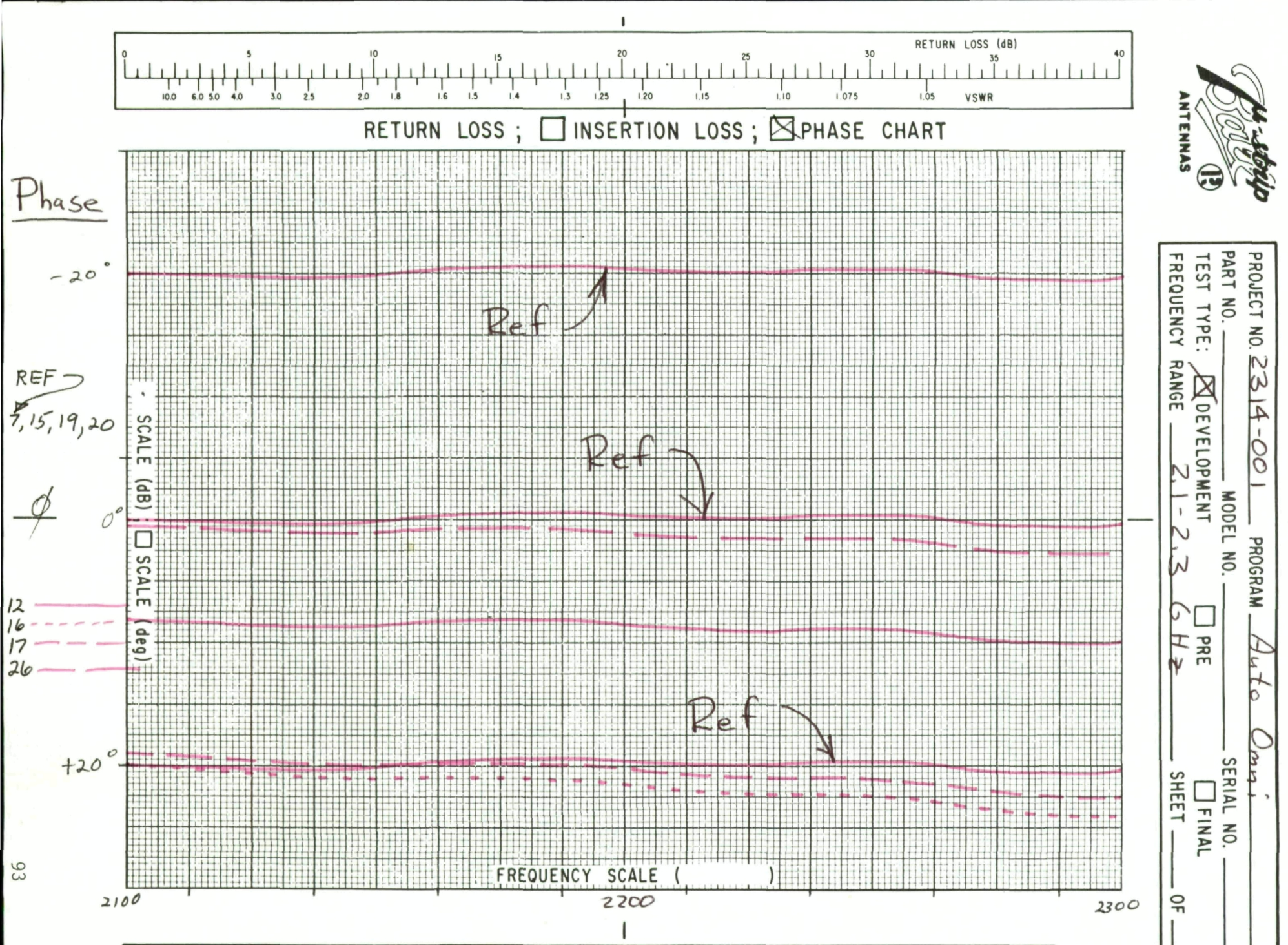
92

BALL AEROSPACE SYSTEMS DIVISION

REMARKS SPD Insertion ~~Loss~~ Phase

OPER. ZB. WITNESSED _____ DATE 7-9-82

Fig. 3.59



PROJECT NO. 2314-001 PROGRAM Auto Omni

PART NO. _____ MODEL NO. _____ SERIAL NO. _____

TEST TYPE: ☒ DEVELOPMENT ☐ PRE ☐ FINAL

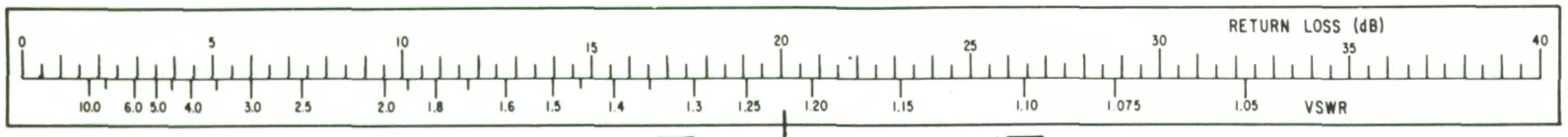
FREQUENCY RANGE 2.1-2.3 GHz SHEET ____ OF ____

BALL AEROSPACE SYSTEMS DIVISION

REMARKS SPD Insertion ~~Loss~~ Phase

OPER. ZB WITNESSED _____ DATE 7-9-82

Fig. 3.60



RETURN LOSS ; ☐ INSERTION LOSS ; ☒ PHASE CHART

Phase

-20°

REF

7,15,19,20

Ø 0°

7
17
18
27

+20°

Ref

Ref

Ref

SCALE (dB) ; ☐ SCALE (deg)

FREQUENCY SCALE ( )

2100 2200 2300

94

Hughes Ball (12) ANTENNAS

PROJECT NO. 2314-001 PROGRAM Auto Omni

PART NO. _____ MODEL NO. _____ SERIAL NO. _____

TEST TYPE: ☒ DEVELOPMENT ☐ PRE ☐ FINAL

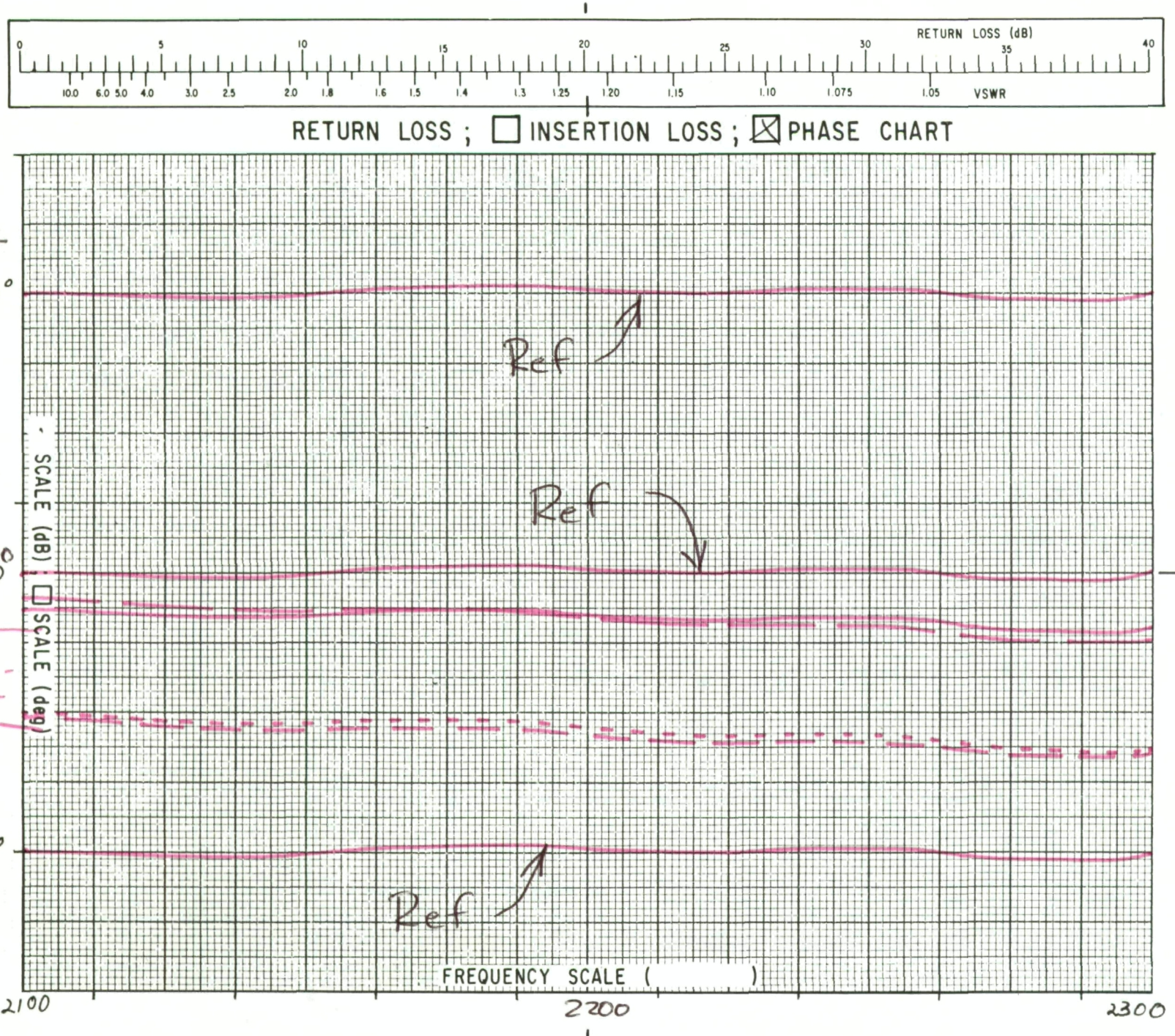
FREQUENCY RANGE 2.1-2.3 GHz SHEET ____ OF ____

BALL AEROSPACE SYSTEMS DIVISION

REMARKS SPD Insertion Phase

OPER. ZB WITNESSED _____ DATE 7-9-82

Fig. 3,6d



PROJECT NO. 2314-001 PROGRAM Auto Omni

PART NO. _____ MODEL NO. _____ SERIAL NO. _____

TEST TYPE: ☒ DEVELOPMENT ☐ PRE ☐ FINAL

FREQUENCY RANGE 2.1-2.36 GHz SHEET _____ OF _____

BALL AEROSPACE SYSTEMS DIVISION

REMARKS SPD Insertion Phase

OPER. JB WITNESSED _____ DATE 7-9-82

95

Fig. 3.62

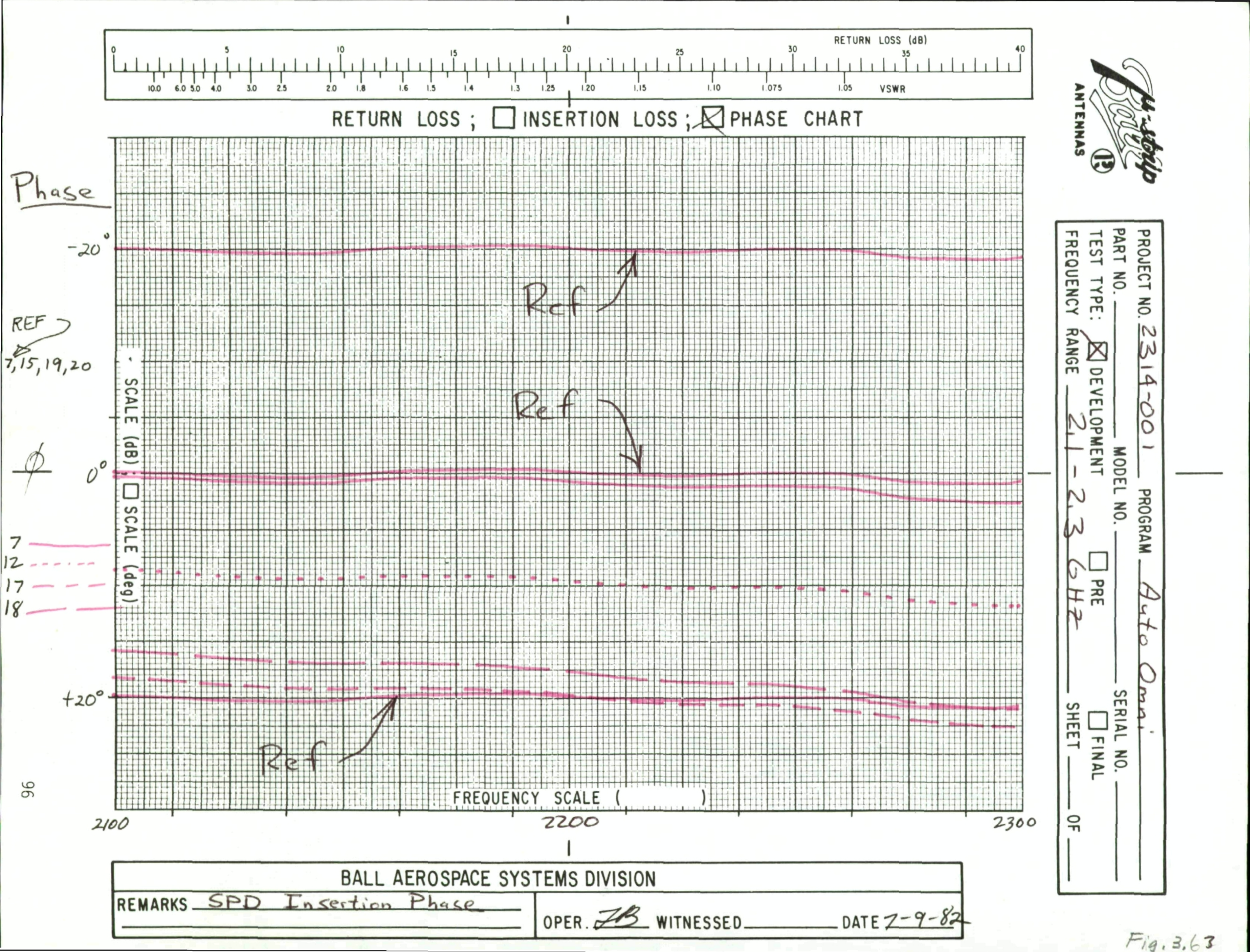
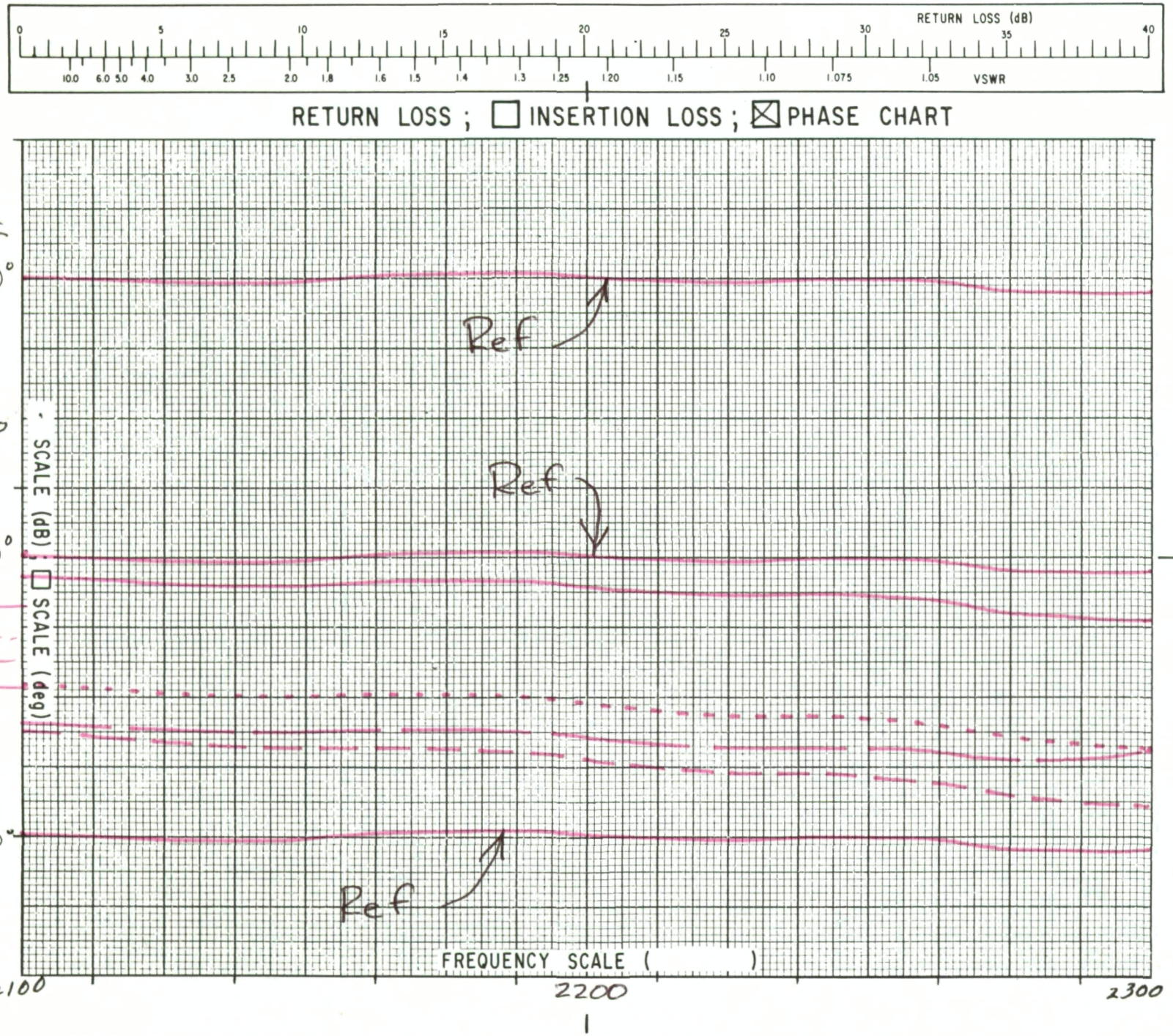

RETURN LOSS (dB)
0 5 10 15 20 25 30 35 40
10.0 6.0 5.0 4.0 3.0 2.5 2.0 1.8 1.6 1.5 1.4 1.3 1.25 1.20 1.15 1.10 1.075 1.05 VSWR
RETURN LOSS ; ☐ INSERTION LOSS ; ☒ PHASE CHART
Phase
-20°
REF
7, 15, 19, 20
Ref
Ref
0°
SCALE (dB) ; ☐ SCALE (deg)
7
12
17
18
+20°
Ref
FREQUENCY SCALE ( )
2100
2200
2300
96
PROJECT NO. 2314-001 PROGRAM Auto Omni
PART NO. MODEL NO. SERIAL NO.
TEST TYPE: ☒ DEVELOPMENT ☐ PRE ☐ FINAL
FREQUENCY RANGE 21-2.36 GHz SHEET OF
BALL AEROSPACE SYSTEMS DIVISION
REMARKS SPD Insertion Phase
OPER. JB WITNESSED DATE 7-9-82

Fig. 3.63



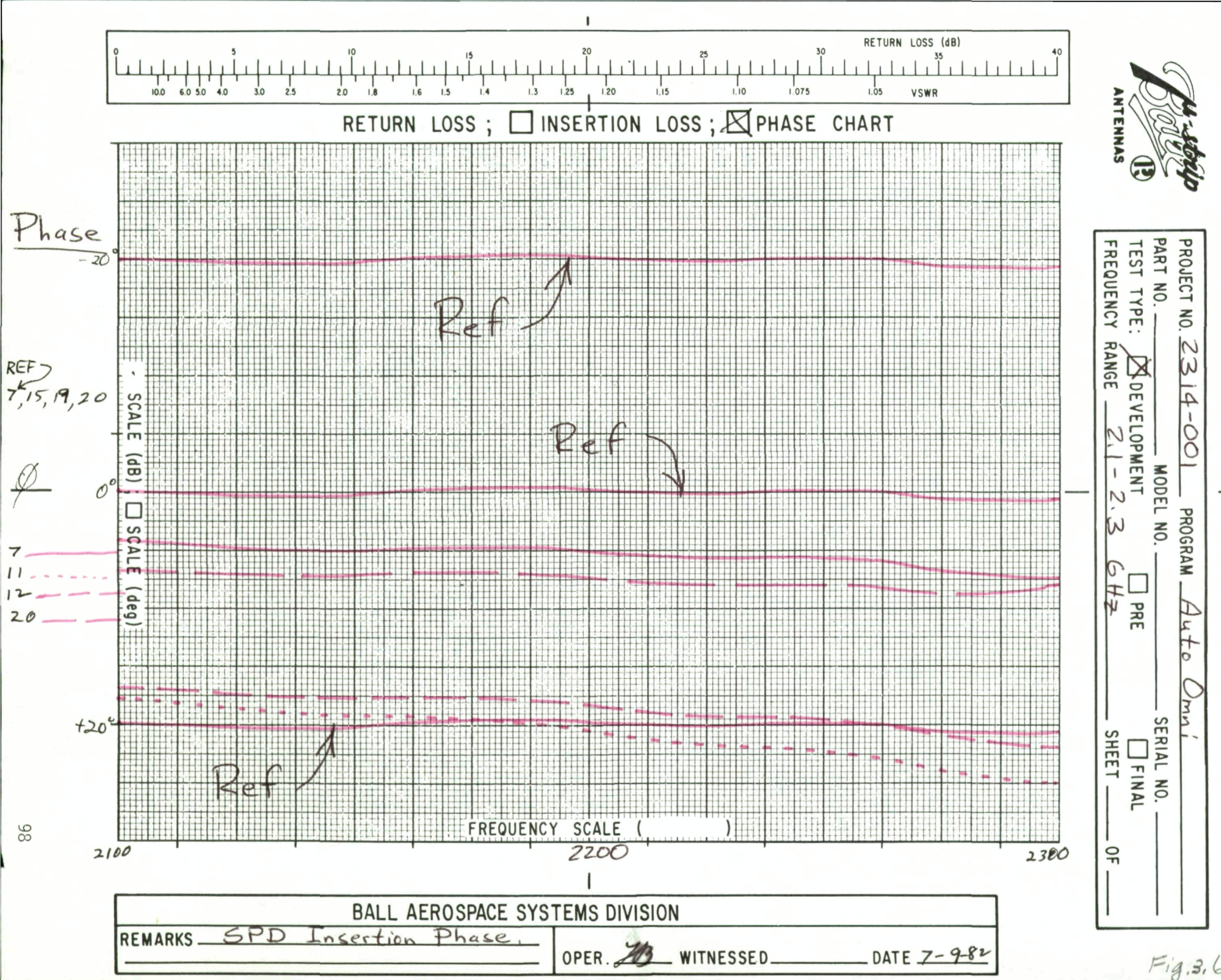
PROJECT NO. 2314-001 PROGRAM Auto Omni
PART NO. _____ MODEL NO. _____ SERIAL NO. _____
TEST TYPE: ☒ DEVELOPMENT ☐ PRE ☐ FINAL
FREQUENCY RANGE 2.1 - 2.3 GHz SHEET ____ OF ____

BALL AEROSPACE SYSTEMS DIVISION

REMARKS SPD Insertion Phase

OPER. ZB WITNESSED _____ DATE 7-9-82

Fig. 3, 68



Hughes Aircraft Co. ANTENNAS

PROJECT NO. 2314-001 PROGRAM Auto Omni

PART NO. _____ MODEL NO. _____ SERIAL NO. _____

TEST TYPE: ☒ DEVELOPMENT ☐ PRE ☐ FINAL

FREQUENCY RANGE 2.1 - 2.3 GHz SHEET _____ OF _____

BALL AEROSPACE SYSTEMS DIVISION

REMARKS SPD Insertion Phase.

OPER. [illegible] WITNESSED _____ DATE 7-9-82

Fig. 3.6.5

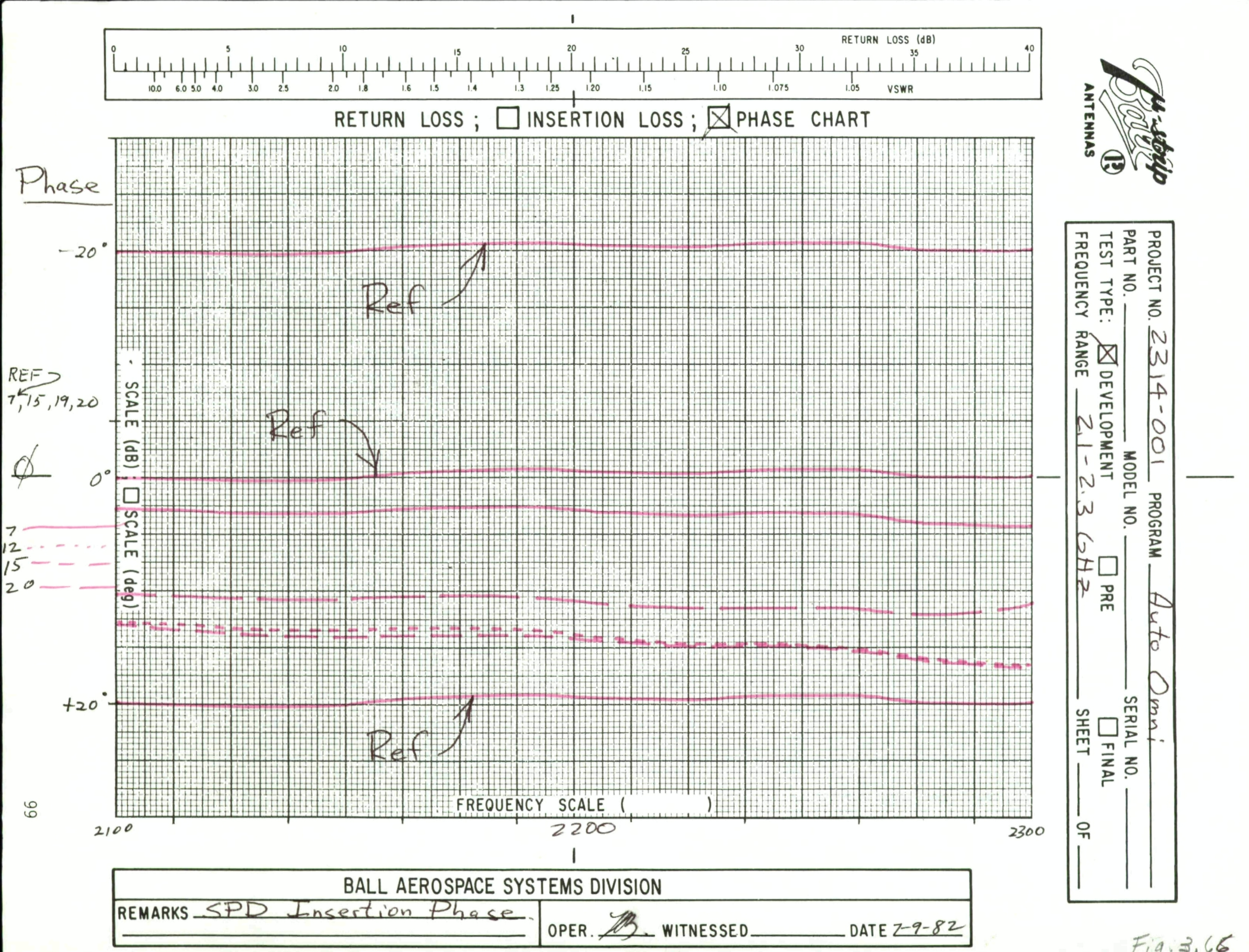
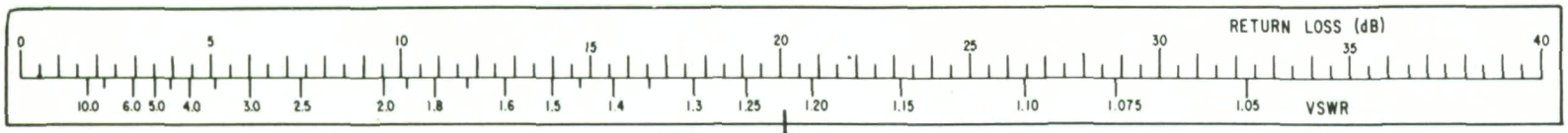

RETURN LOSS (dB)
0 5 10 15 20 25 30 35 40
10.0 6.0 5.0 4.0 3.0 2.5 2.0 1.8 1.6 1.5 1.4 1.3 1.25 1.20 1.15 1.10 1.075 1.05 VSWR
RETURN LOSS ; ☐ INSERTION LOSS ; ☒ PHASE CHART
Phase
-20°
Ref
REF 7, 15, 19, 20
Ø
0°
Ref
SCALE (dB) ☐ SCALE (deg)
7
12
15
20
+20°
Ref
FREQUENCY SCALE ( )
2100
2200
2300
99
PROJECT NO. 2314-001 PROGRAM Auto Omni
PART NO. MODEL NO. SERIAL NO.
TEST TYPE: ☒ DEVELOPMENT ☐ PRE ☐ FINAL
FREQUENCY RANGE 2.1-2.3 GHz SHEET OF
BALL AEROSPACE SYSTEMS DIVISION
REMARKS SPD Insertion Phase
OPER. WITNESSED DATE 2-9-82

Fig. 3.66



RETURN LOSS ; ☐ INSERTION LOSS ; ☒ PHASE CHART

Phase

-20°

Ref

Ref

Ø

0

7 REF
15
19
20

Ref

+20°

- SCALE (dB) ; ☐ SCALE (deg)

100

FREQUENCY SCALE ( )

2100 2200 2300

PROJECT NO. 2314-001 PROGRAM Auto Omni

PART NO. _____ MODEL NO. _____ SERIAL NO. _____

TEST TYPE: ☒ DEVELOPMENT ☐ PRE ☐ FINAL

FREQUENCY RANGE 2.1 - 2.3 GHz SHEET _____ OF _____

BALL AEROSPACE SYSTEMS DIVISION

REMARKS SPD Insertion Phase

OPER. FB. WITNESSED _____ DATE 7-9-82

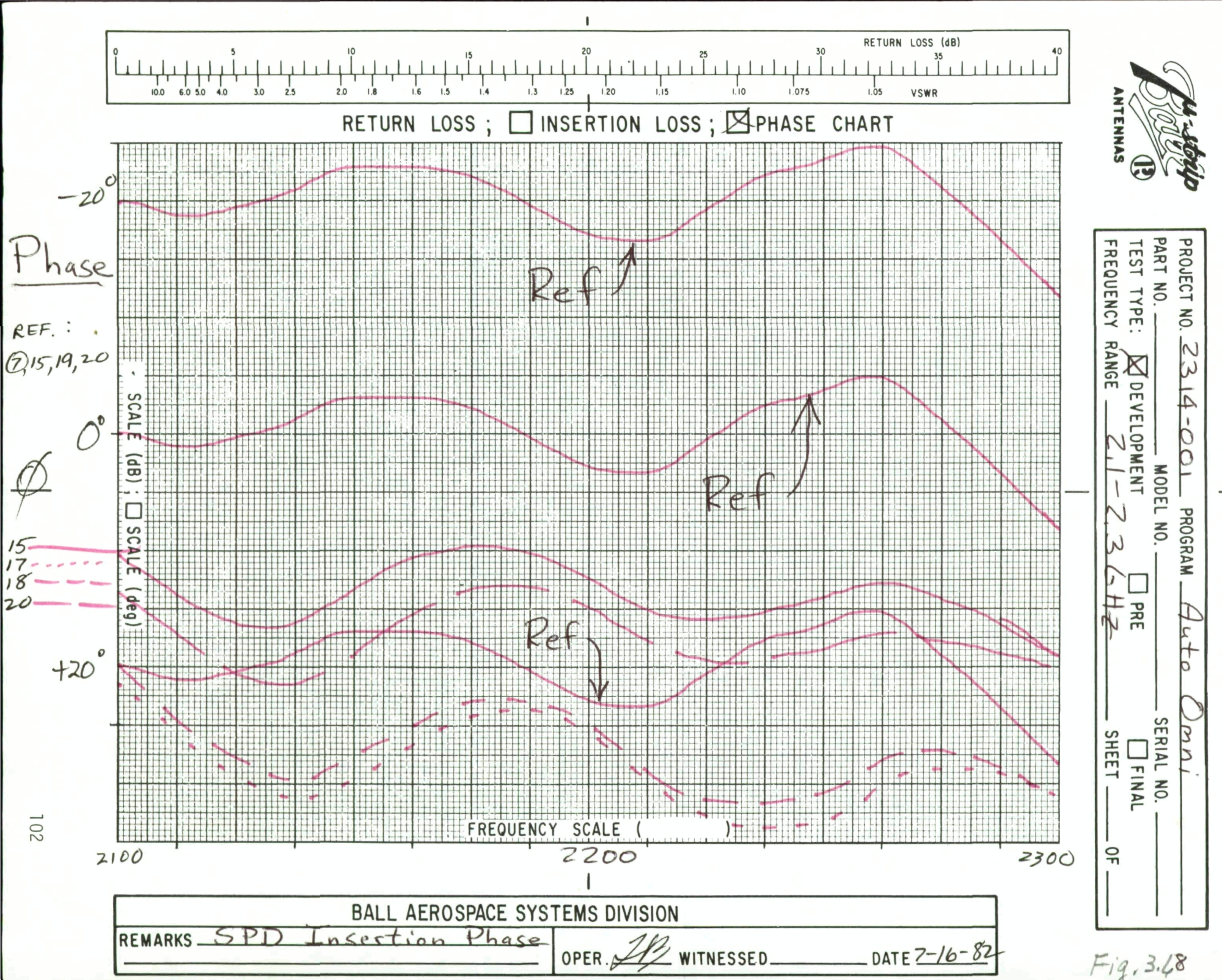
Fig. 3.60

Case 3 (Raw Data)

SPD INSERTION PHASE DATA WITH ELEMENTS AS LOADS

Output seven used as reference

Figure	Outputs			
3.68	15	17	18	20
3.69	7	13	15	18
3.70	16	17	18	27
3.71	16	17	26	27
3.72	12	16	17	26
3.73	7	17	18	27
3.74	7	12	17	26
3.75	7	12	17	18
3.76	7	12	17	20
3.77	7	11	12	20
3.78	7	12	15	20
3.79	7	15	19	20
3.80	6	15	19	20



PROJECT NO. 2314-001 PROGRAM Auto Omni

PART NO. _____ MODEL NO. _____ SERIAL NO. _____

TEST TYPE: ☒ DEVELOPMENT ☐ PRE ☐ FINAL

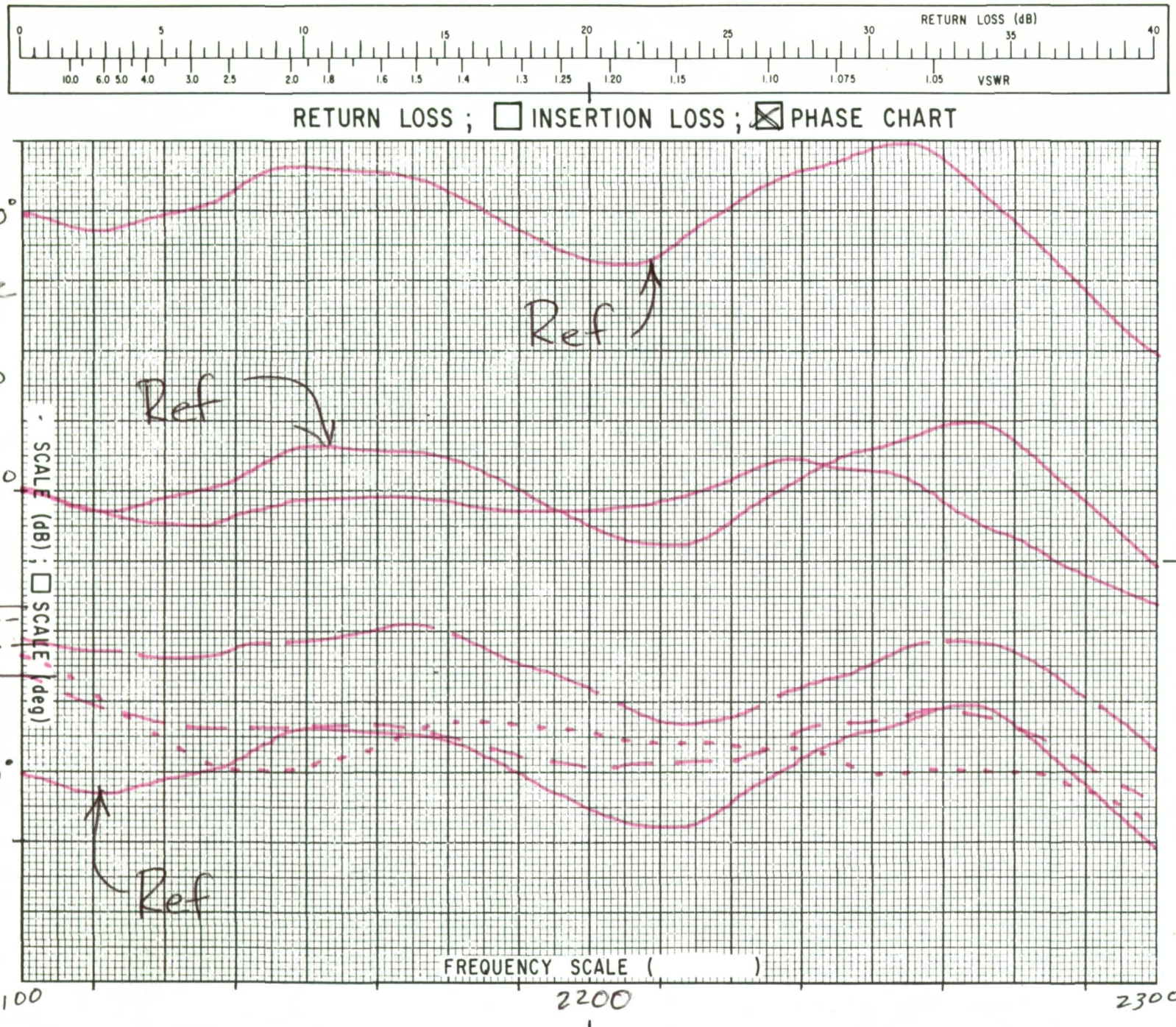
FREQUENCY RANGE 2.1-2.36 GHz SHEET _____ OF _____

BALL AEROSPACE SYSTEMS DIVISION

REMARKS SPD Insertion Phase

OPER. JB WITNESSED _____ DATE 7-16-82

Fig. 3.68



Auto Omni

PROJECT NO. 2314-001 PROGRAM Auto Omni
PART NO. _____ MODEL NO. _____ SERIAL NO. _____
TEST TYPE: ☒ DEVELOPMENT ☐ PRE ☐ FINAL
FREQUENCY RANGE 2.1 - 2.36 GHz SHEET _____ OF _____

BALL AEROSPACE SYSTEMS DIVISION

REMARKS SPD Insertion Phase

OPER. [illegible] WITNESSED _____ DATE 7-15-82

103

Fig 3.69

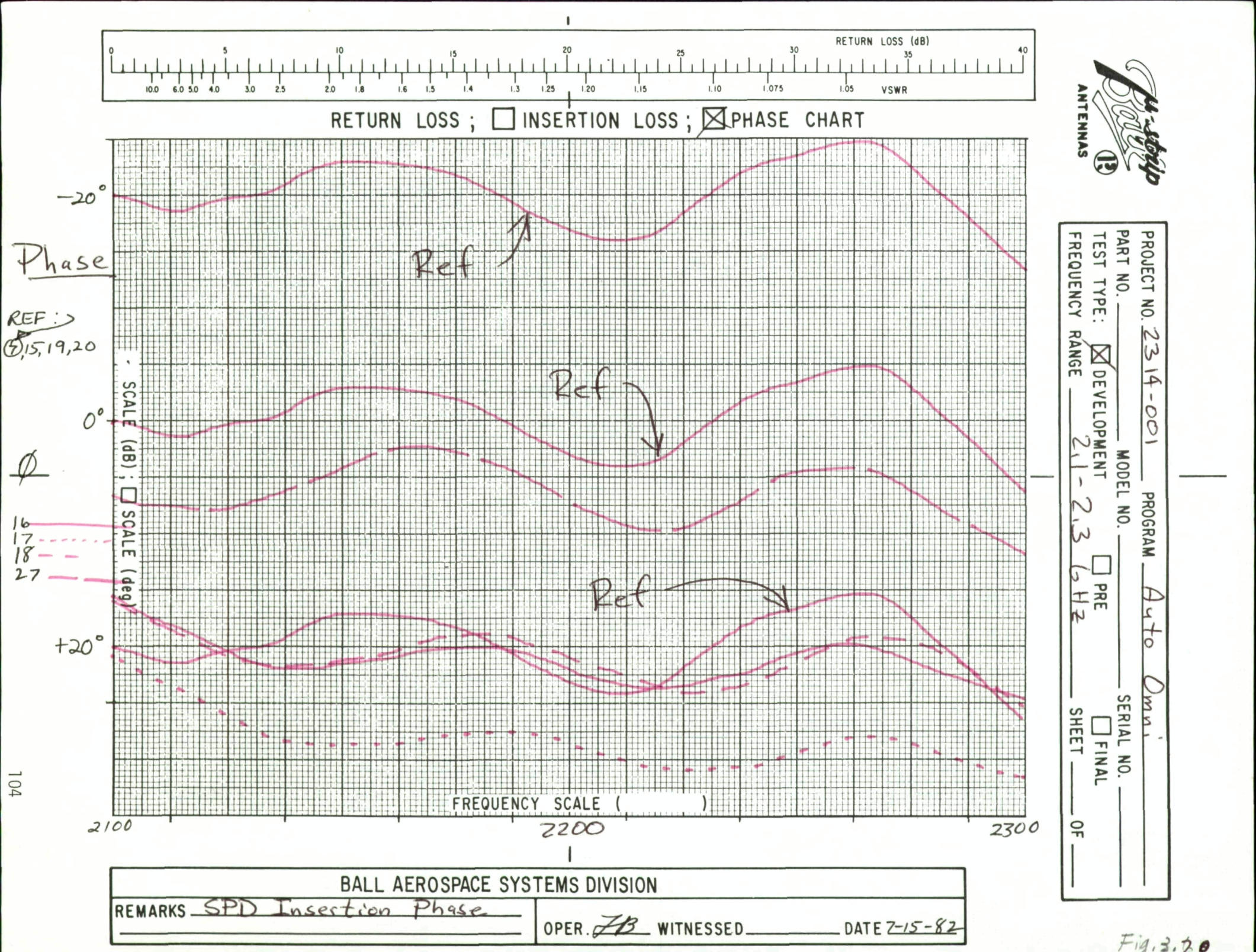
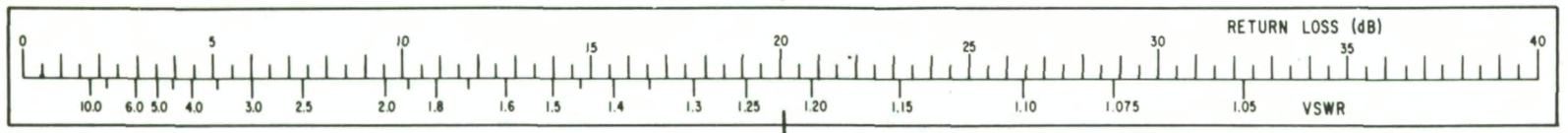

RETURN LOSS (dB)
0 5 10 15 20 25 30 35 40
10.0 6.0 5.0 4.0 3.0 2.5 2.0 1.8 1.6 1.5 1.4 1.3 1.25 1.20 1.15 1.10 1.075 1.05 VSWR
RETURN LOSS ; ☐ INSERTION LOSS ; ☒ PHASE CHART
-20°
Phase
REF : 5, 15, 19, 20
0°
Ø
16
17
18
27
+20°
SCALE (dB) ; ☐ SCALE (deg)
Ref
Ref
Ref
FREQUENCY SCALE ( )
2100
2200
2300
PROJECT NO. 2314-001 PROGRAM Auto Omni
PART NO. MODEL NO. SERIAL NO.
TEST TYPE: ☒ DEVELOPMENT ☐ PRE ☐ FINAL
FREQUENCY RANGE 2.1 - 2.3 GHz SHEET OF
BALL AEROSPACE SYSTEMS DIVISION
REMARKS SPD Insertion Phase
OPER. ZB WITNESSED DATE 7-15-82

Fig. 3.7.0



RETURN LOSS ; ☐ INSERTION LOSS ; ☒ PHASE CHART

Ball Omni Antennas

PROJECT NO. 2314-001 PROGRAM Auto Omni

PART NO. _____ MODEL NO. _____ SERIAL NO. _____

TEST TYPE: ☒ DEVELOPMENT ☐ PRE ☐ FINAL

FREQUENCY RANGE 2.1-2.3 GHz SHEET _____ OF _____

-20°

Phase

REF :
7, 15, 19, 20

Ref

0°

Ref

Φ

SCALE (dB) ; ☐ SCALE (deg)

16
17
26
27

+20°

Ref

FREQUENCY SCALE ( )

2100 2200 2300

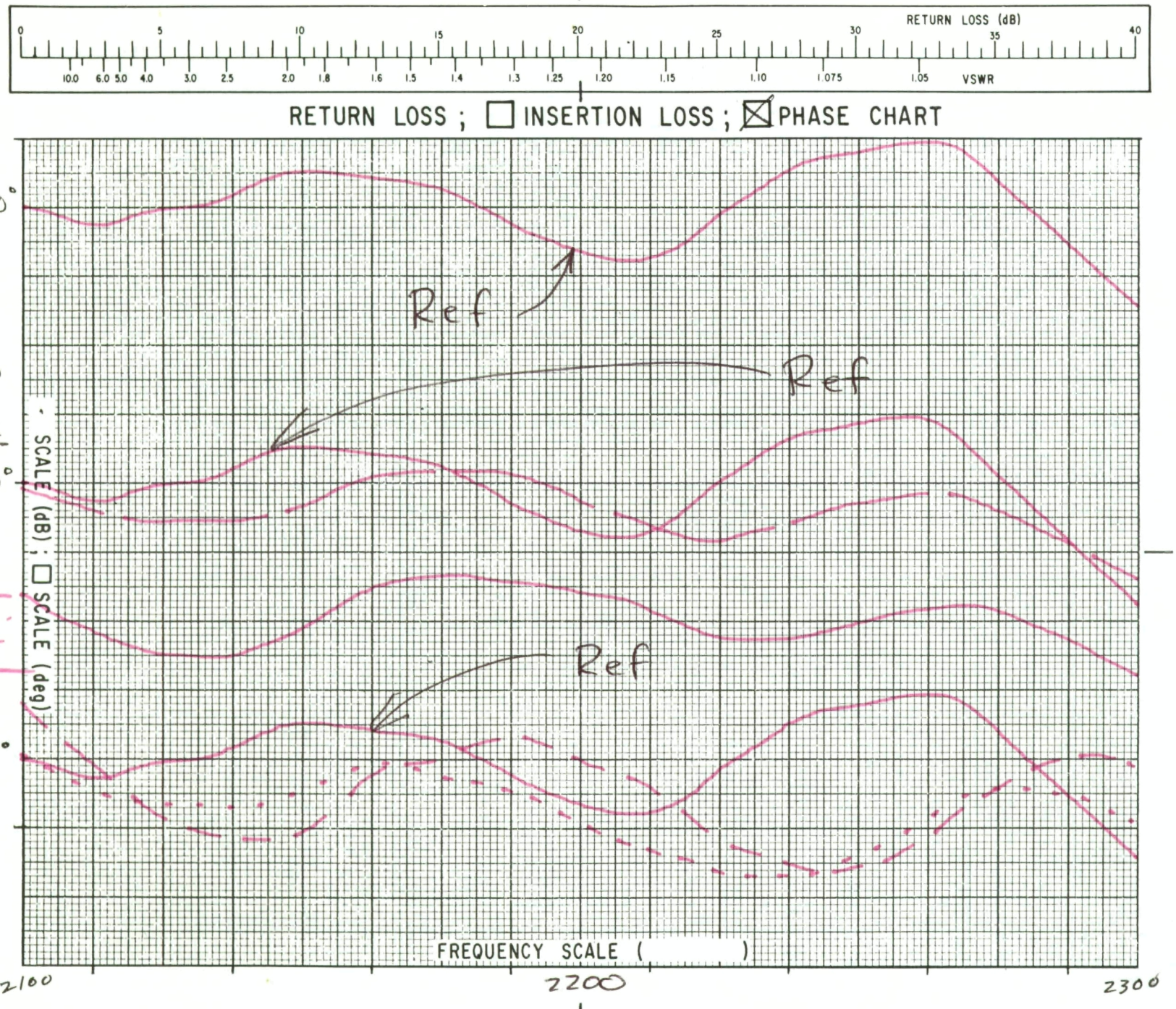
105

BALL AEROSPACE SYSTEMS DIVISION

REMARKS SPD Insertion Phase

OPER. JB WITNESSED _____ DATE 7-15-82

Fig. 3.7 Φ



PROJECT NO. 2314-001 PROGRAM Auto Omni

PART NO. _____ MODEL NO. _____ SERIAL NO. _____

TEST TYPE: ☒ DEVELOPMENT ☐ PRE ☐ FINAL

FREQUENCY RANGE 2.1 - 2.3 GHz SHEET _____ OF _____

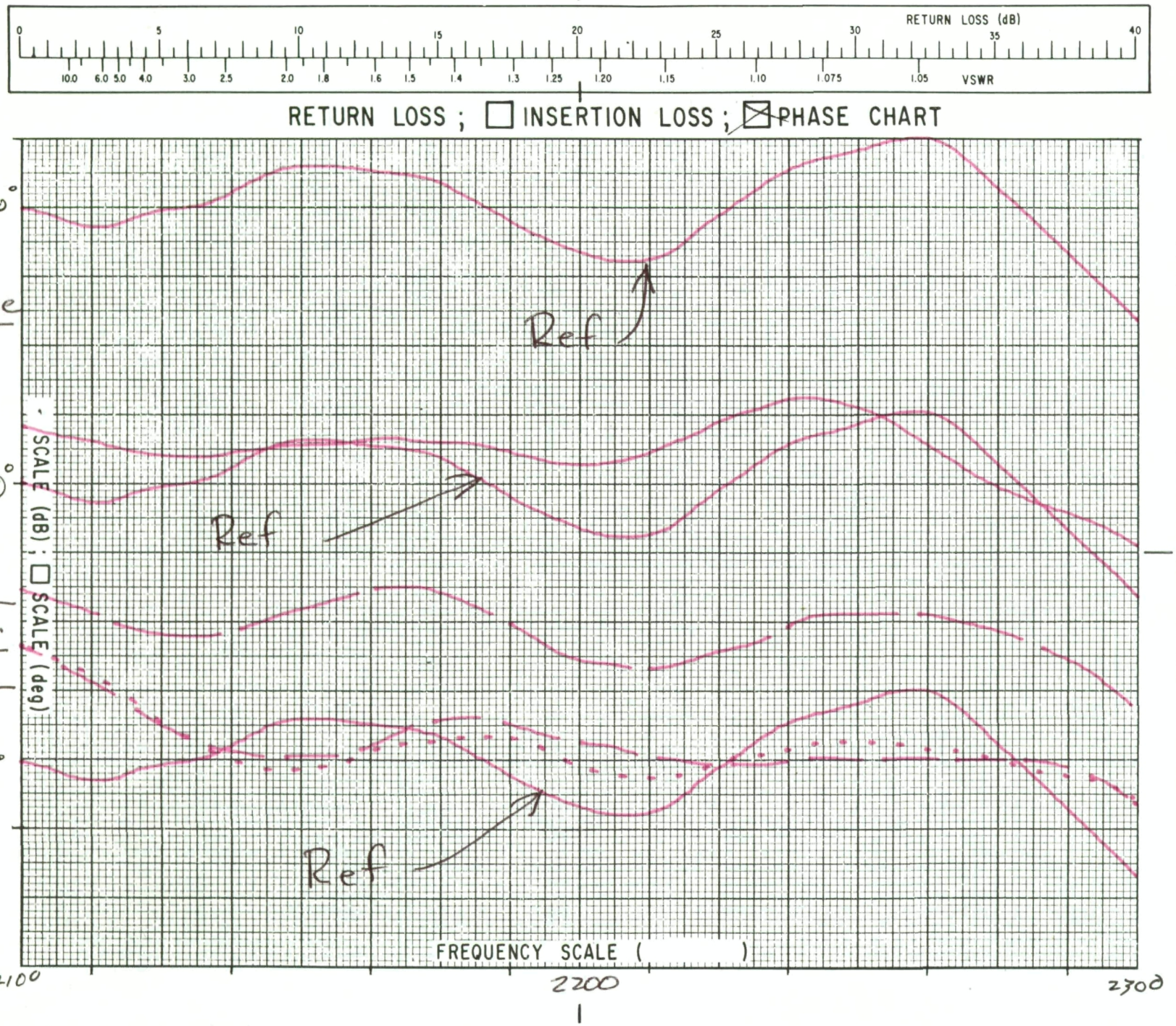
BALL AEROSPACE SYSTEMS DIVISION

REMARKS SPD Insertion Phase

OPER. JB WITNESSED _____ DATE 7-15-82

106

Fig. 3.72



PROJECT NO. 2314-001 PROGRAM Auto Omni

PART NO. _____ MODEL NO. _____ SERIAL NO. _____

TEST TYPE: ☒ DEVELOPMENT ☐ PRE ☐ FINAL

FREQUENCY RANGE 2.1 - 2.3 GHz SHEET ____ OF ____

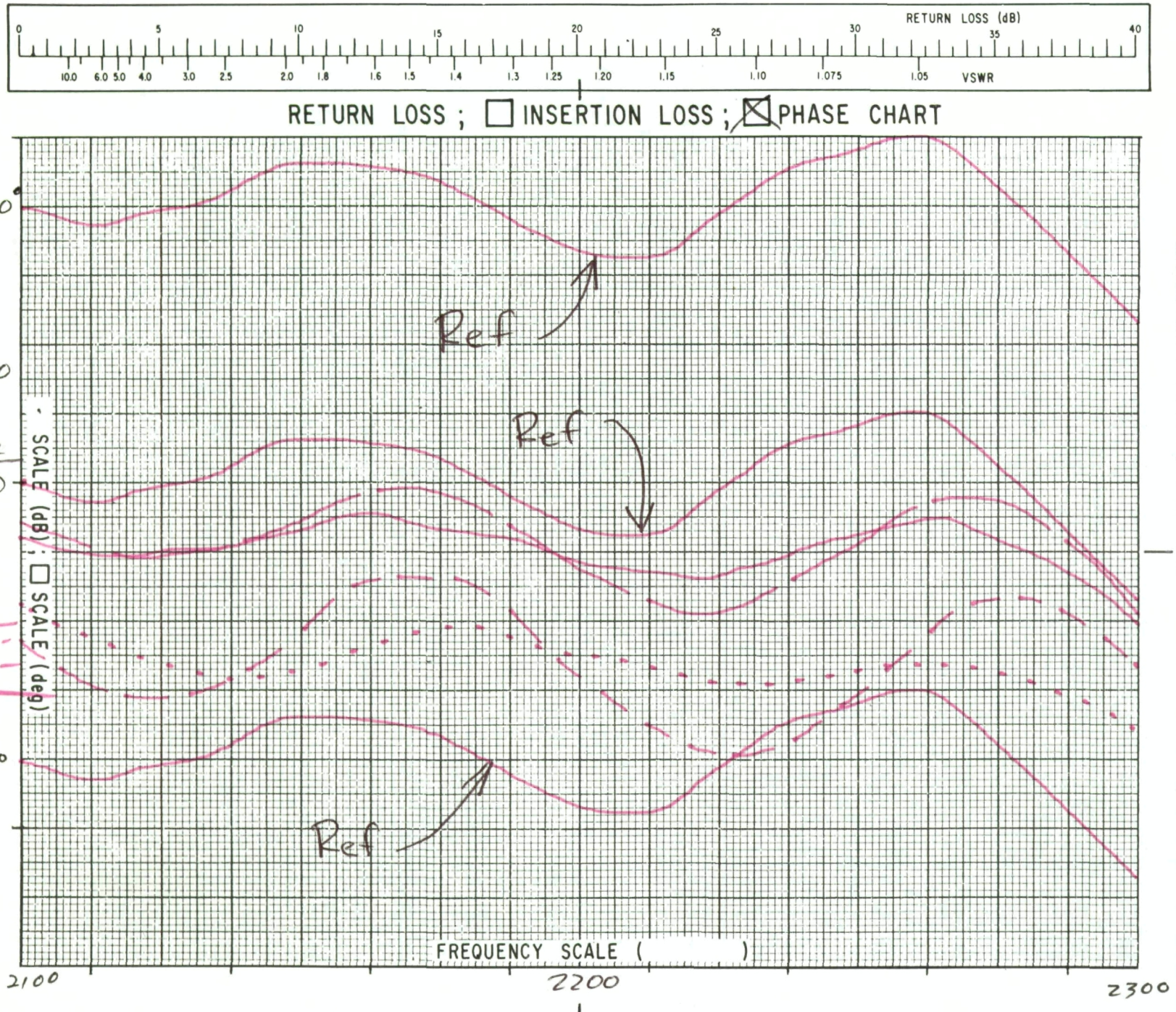
BALL AEROSPACE SYSTEMS DIVISION

REMARKS SPD Insection Phase

OPER JB WITNESSED _____ DATE 2-15-82

107

Fig. 3.73



PROJECT NO. 2314-001 PROGRAM Auto Omni
PART NO. ____ MODEL NO. ____ SERIAL NO. ____
TEST TYPE: ☒ DEVELOPMENT ☐ PRE ☐ FINAL
FREQUENCY RANGE 2.1 - 2.36 GHz SHEET ____ OF ____

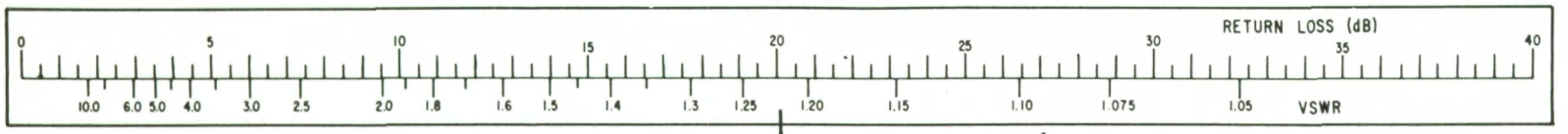
BALL AEROSPACE SYSTEMS DIVISION

REMARKS SPD Insertion Phase

OPER. ZB WITNESSED ____ DATE 2-15-82

108

Fig. 3.7.4



RETURN LOSS ; ☐ INSERTION LOSS ; ☒ PHASE CHART

Ball Stolo ANTENNAS

PROJECT NO. 2314-001 PROGRAM Auto Omni

PART NO. _____ MODEL NO. _____ SERIAL NO. _____

TEST TYPE: ☒ DEVELOPMENT ☐ PRE ☐ FINAL

FREQUENCY RANGE 2.1 - 2.3 GHz SHEET ____ OF ____

-20°

Phase

REF :
⑦, 15, 19, 20

Ref

0°

Ref

7
12
17
18

+20°

Ref

SCALE (dB) ; ☐ SCALE (deg)

FREQUENCY SCALE ( )

2100 2200 2300

109

BALL AEROSPACE SYSTEMS DIVISION

REMARKS SPD Insertion Phase

OPER. JB WITNESSED _____ DATE 7-15-82

Fig. 3.75

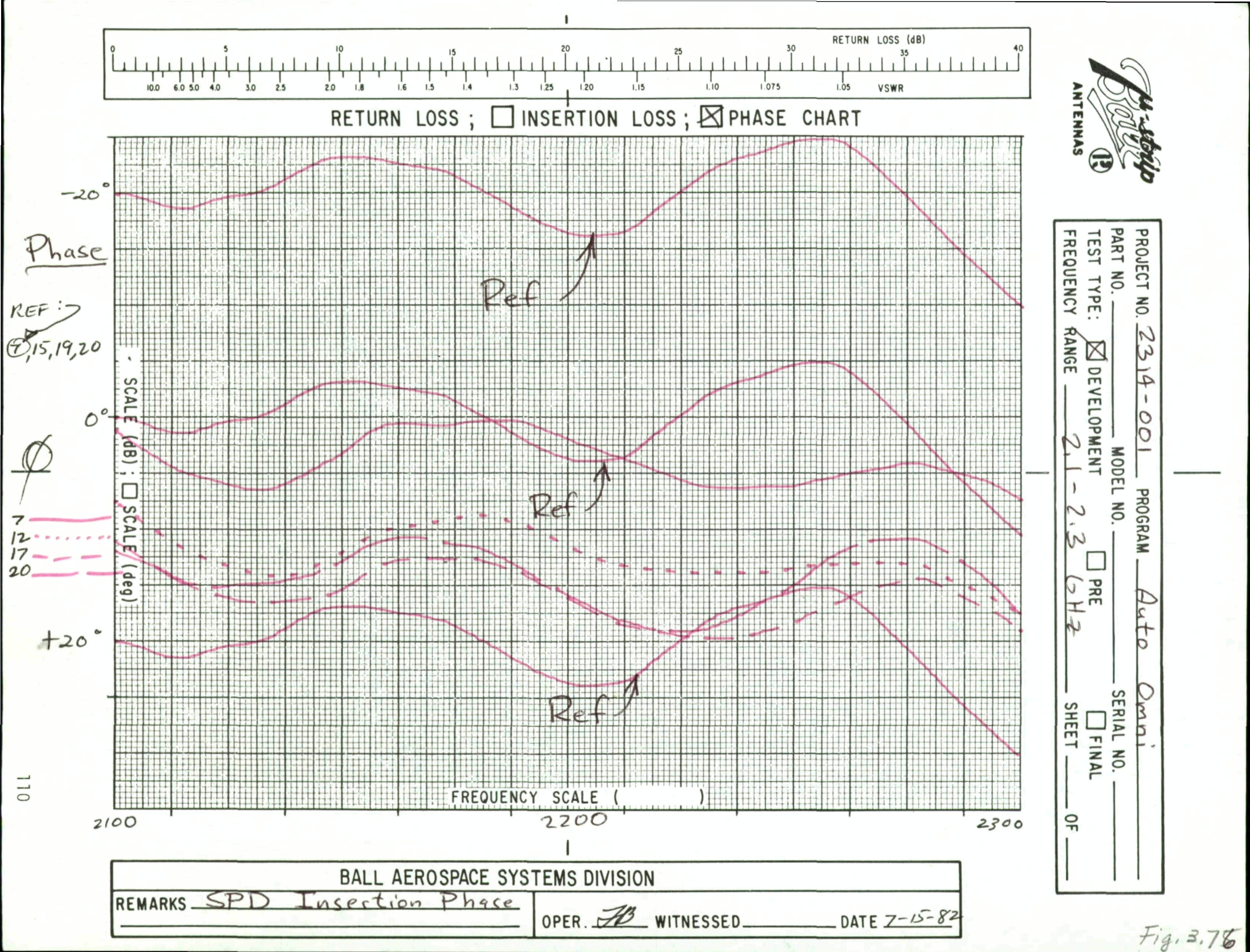
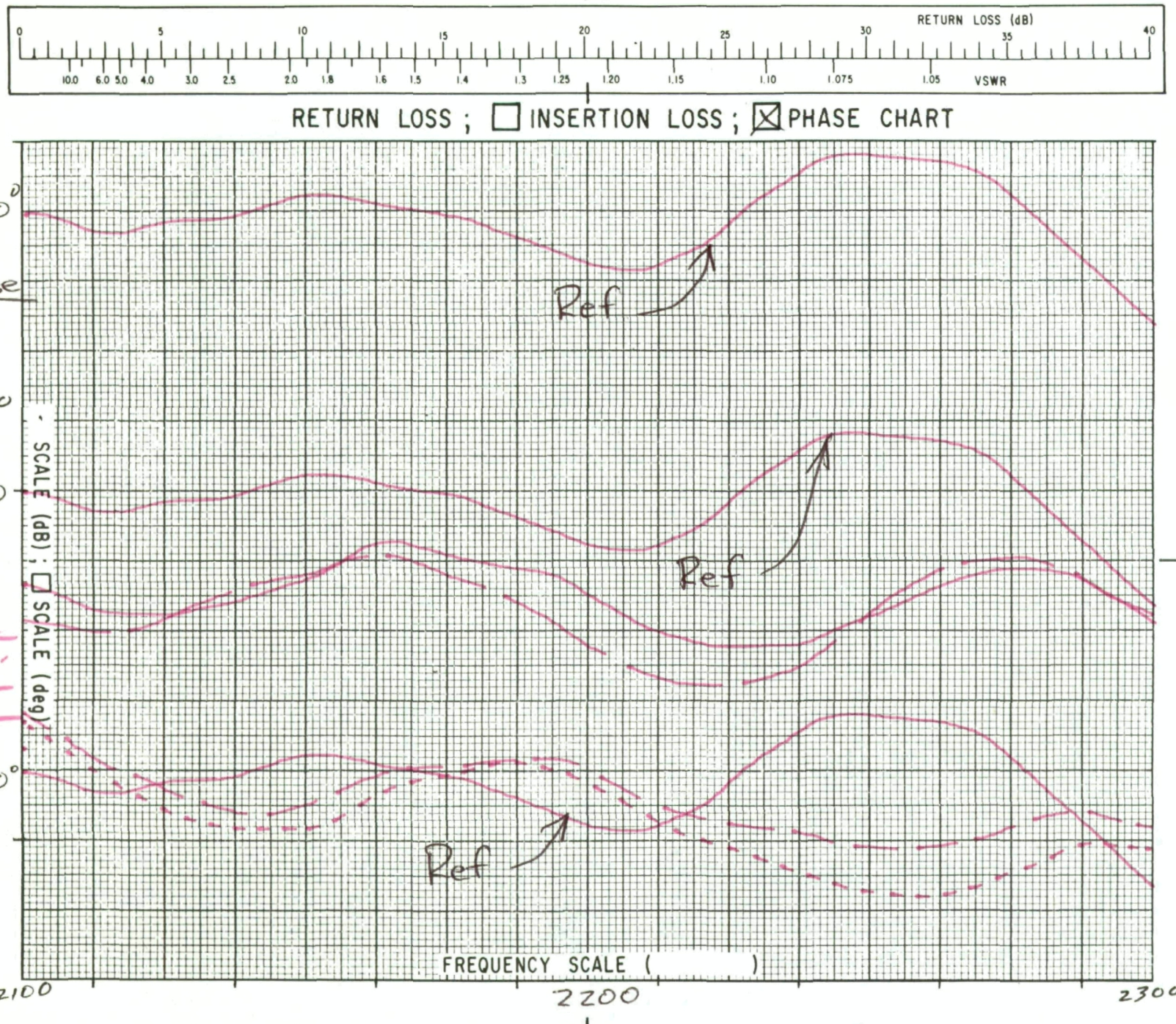

RETURN LOSS (dB)
0 5 10 15 20 25 30 35 40
10.0 6.0 5.0 4.0 3.0 2.5 2.0 1.8 1.6 1.5 1.4 1.3 1.25 1.20 1.15 1.10 1.075 1.05 VSWR
RETURN LOSS ; ☐ INSERTION LOSS ; ☒ PHASE CHART
-20°
Phase
REF : 7, 15, 19, 20
0°
+20°
Ref
Ref
Ref
SCALE (dB) ; ☐ SCALE (deg)
7
12
17
20
FREQUENCY SCALE ( )
2100
2200
2300
110
PROJECT NO. 2314-001 PROGRAM Auto Omni
PART NO. MODEL NO. SERIAL NO.
TEST TYPE: ☒ DEVELOPMENT ☐ PRE ☐ FINAL
FREQUENCY RANGE 2.1 - 2.3 GHz SHEET OF
BALL AEROSPACE SYSTEMS DIVISION
REMARKS SPD Insertion Phase
OPER. WITNESSED DATE 7-15-82

Fig. 3.76



PROJECT NO. 2314-001 PROGRAM Auto Omni

PART NO. _____ MODEL NO. _____ SERIAL NO. _____

TEST TYPE: ☒ DEVELOPMENT ☐ PRE ☐ FINAL

FREQUENCY RANGE 2.1 - 2.3 GHz SHEET _____ OF _____

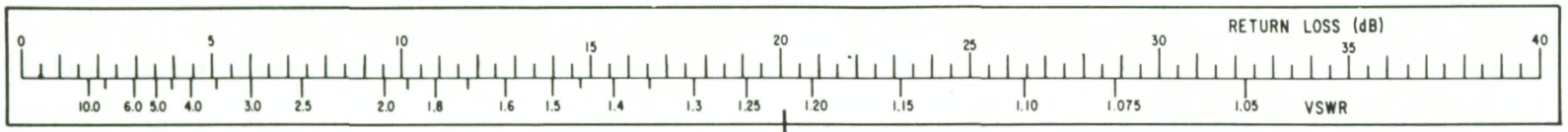
BALL AEROSPACE SYSTEMS DIVISION

REMARKS SPD Insertion Phase

OPER. JM WITNESSED _____ DATE 7-15-82

111

Fig. 3.77



RETURN LOSS ; ☐ INSERTION LOSS ; ☒ PHASE CHART

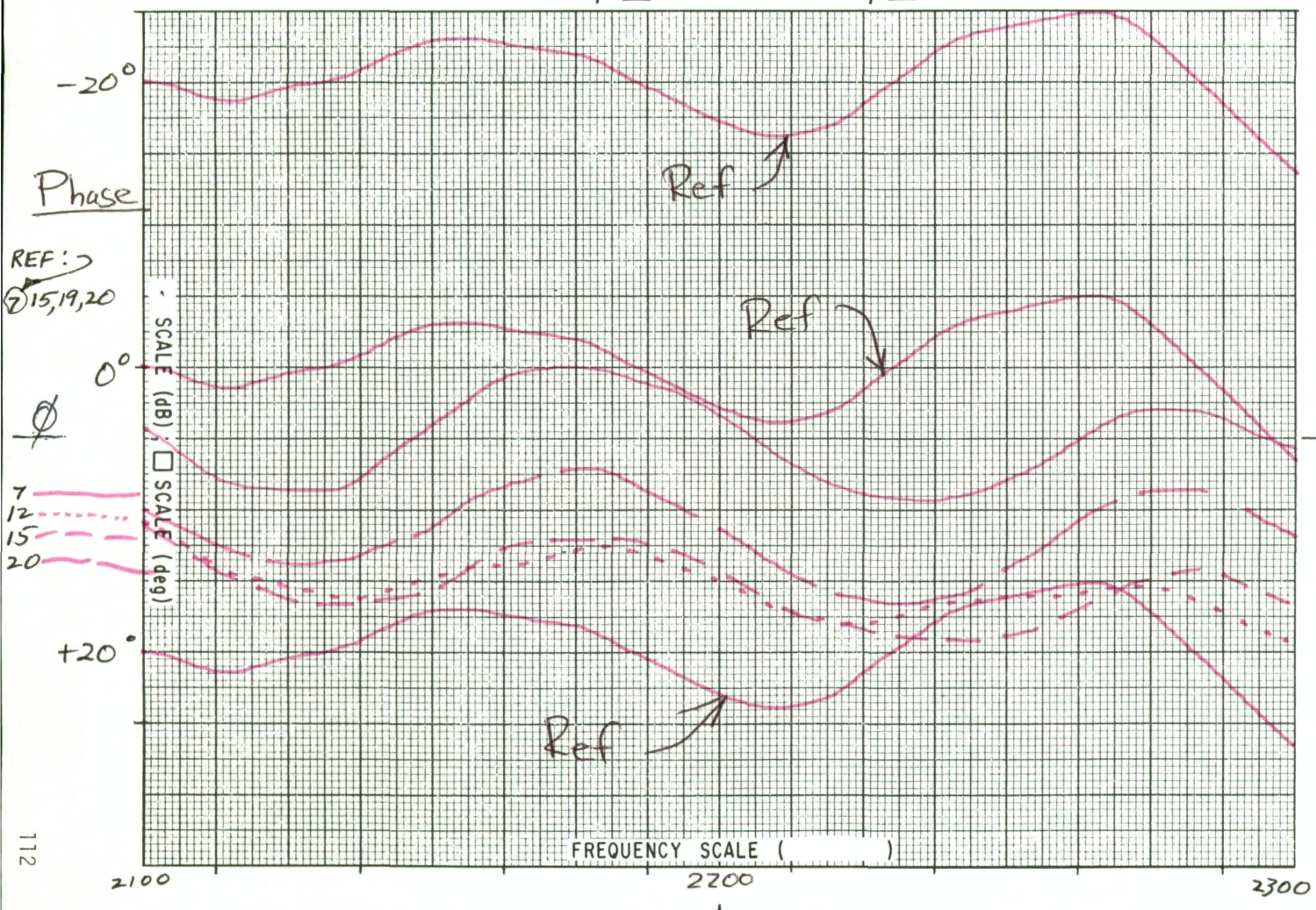
Scale-Loop ANTENNAS

PROJECT NO. 2314-001 PROGRAM Auto Omni

PART NO. _____ MODEL NO. _____ SERIAL NO. _____

TEST TYPE: ☒ DEVELOPMENT ☐ PRE ☐ FINAL

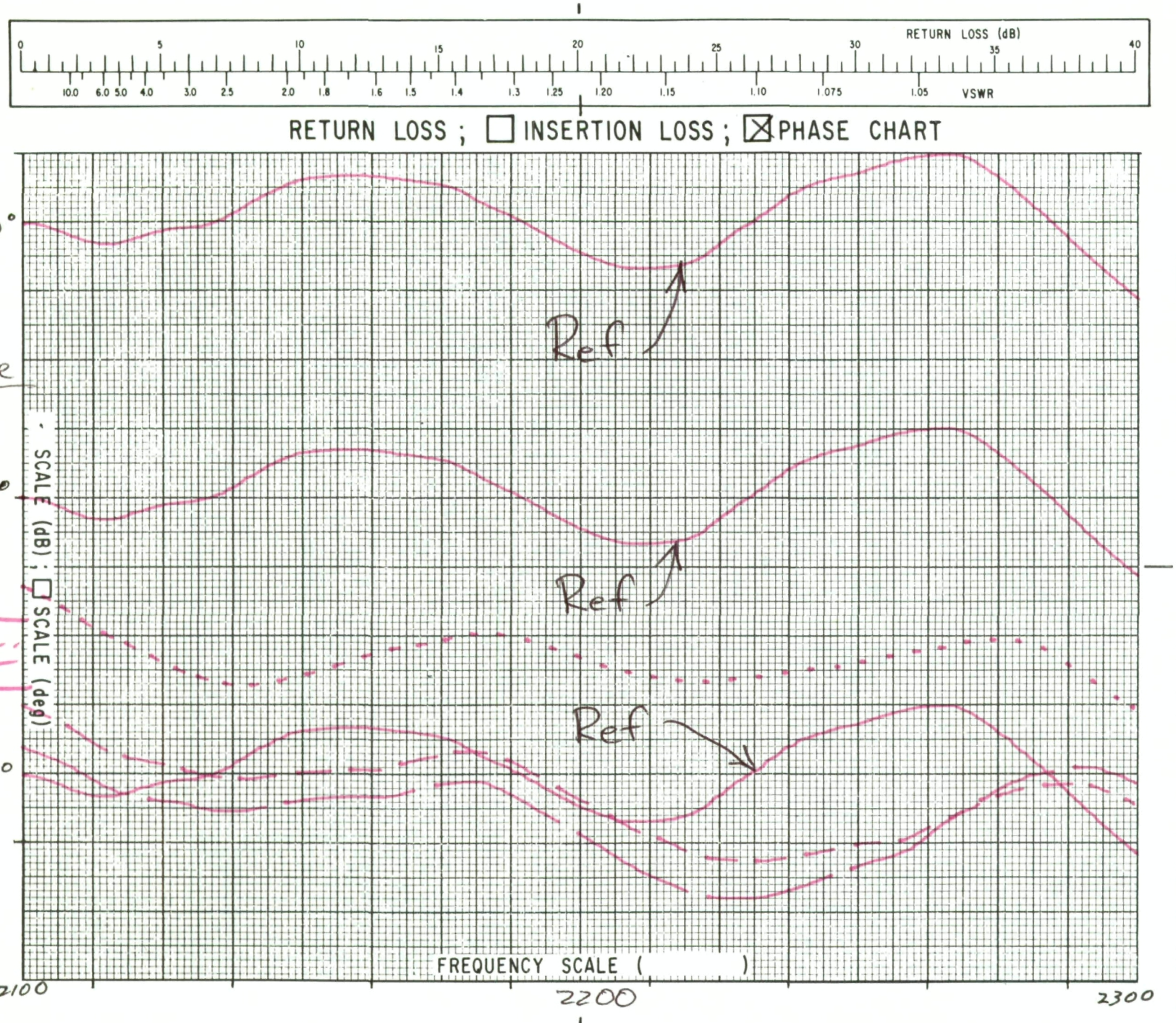
FREQUENCY RANGE 2.1 - 2.3 GHz SHEET _____ OF _____



BALL AEROSPACE SYSTEMS DIVISION	
REMARKS SPD Insertion Phase	OPER. JB WITNESSED _____ DATE 7-15-82

112

Fig. 3.78



Wi-Lan Inc. ANTENNAS

PROJECT NO. 2314-001 PROGRAM Auto Omni

PART NO. _____ MODEL NO. _____ SERIAL NO. _____

TEST TYPE: ☒ DEVELOPMENT ☐ PRE ☐ FINAL

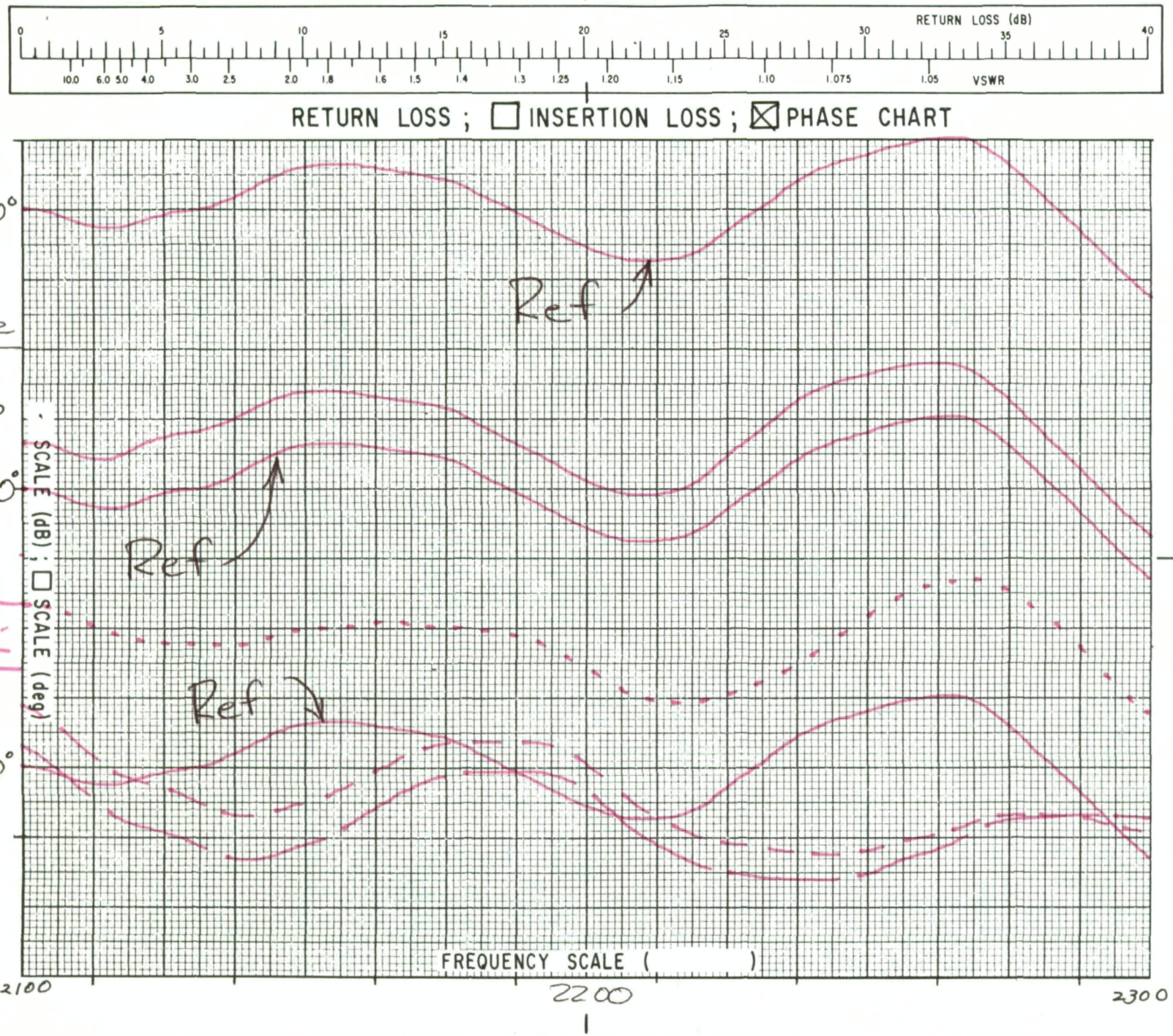
FREQUENCY RANGE 2.1 - 2.3 GHz SHEET ___ OF ___

BALL AEROSPACE SYSTEMS DIVISION

REMARKS SPD Insertion Phase

OPER. AB WITNESSED _____ DATE 7-15-82

Fig. 3.79



PROJECT NO. 2314-001 PROGRAM Auto Omni

PART NO. _____ MODEL NO. _____ SERIAL NO. _____

TEST TYPE: ☒ DEVELOPMENT ☐ PRE ☐ FINAL

FREQUENCY RANGE 2.1-2.3 GHz SHEET _____ OF _____

BALL AEROSPACE SYSTEMS DIVISION

REMARKS SPD Insertion Phase

OPER. TB WITNESSED _____ DATE 7-15-82

114

Fig. 3.80

Chapter 4
GAIN AND PHASE PERFORMANCE COMPARED TO PHASE ONE DATA

Abstract

This chapter discusses the measured performance of the Auto Omni antenna taken during phase two with the switching power divider. This performance is also compared to the phase one data which was taken with a laboratory type power divider in place of the switching power divider.

4.1 INTRODUCTION

The Icosahedron geometry which is used to locate the Auto Omni elements on the sphere repeats itself as five identical spherical segments. Upon further examination of one of these spherical segments it is evident that the segment consists of two mirror image segments. Therefore, by characterizing one-tenth of the sphere, the entire antenna may be characterized. During phase one of NAS5-26240 the Auto Omni antenna was characterized by selecting element clusters within one-tenth of the sphere which would be representative of the entire sphere $0° \leq \theta \leq 120°; 0° \leq \phi \leq 36°$. The results of this test were documented by Interim Report on NAS5-26240 called RF Test Data Phase One, 4 August 1981. During phase one the switching power divider was not available. Therefore, in place of the SPD a commercial four-way power divider was used. Each set of four elements was connected to the power divider by coax connectors and the gain radiation distribution pattern (RDP) was taken. During this test the power divider was well matched and had an insertion loss of 6.5 dB.

4.2 PHASE ONE PERFORMANCE

During phase one, thirteen element clusters were thought to be sufficient to characterize the coverage region $0° \leq \theta \leq 120°$; $0° \leq \phi \leq 36°$. These element clusters are listed in Table 4.1. An array number has been assigned to each cluster in Table 4.1 as an element cluster reference number. The array number is also used in Table 4.2. That table summarizes the phase one gain test data. From that data the Auto Omni peak gain is seen to be 9.61 dB at 2150 MHz and 9.96 dB at 2280 MHz.

4.3 PHASE TWO PERFORMANCE

To verify the impact of the use of the switching power divider, data was taken during phase two for the same element clusters selected during phase one. Table 4.3 lists the peak gains measured during phase two for these clusters with the microstrip switching power divider installed. Table 4.3 shows that the average element cluster gain is 8.66 dB at 2106 MHz and 9.28 dB at 2287 MHz. If, however, the average peak gain is computed from

only those element clusters which do not include the higher loss SPD outputs 1, 2, 35 or 36 the average peak gain increases to 9.16 dB at 2106 MHz and 9.64 dB at 2287 MHz.

The lower gains during phase two testing are believed to be directly attributable to the higher loss of the switching power divider. Figures 4.1 through 4.26 are the sector RDP's taken during phase two from which the Table 4.3 data was taken.

4.4 PHASE TWO COMPARED TO PHASE ONE

The differences in the peak of the beam locations and the gain taken during phases one and two are shown in Table 4.4. This comparison shows that (excluding the elements associated with SPD outputs which are known to be higher loss) the average difference in pointing direction is (θ,ϕ) = (-0.3°, 4.3°) at 2106 MHz and (4.33°, -3.7°) at 2287 MHz. Table 4.4 also shows that the average peak gain is lower in phase two by 0.4 dB at 2106 MHz and 0.6 dB at 2287 MHz.

Table 4.1 SELECTED ELEMENT GROUPS FOR RDP MEASUREMENTS

Array #	Elements				RDP Limits (Degrees) θ	RDP Limits (Degrees) φ
26	1	2	3	6	0, 40	0,180
1	1	2	3	7	10, 50	0, 80
36	2	3	7	12	20, 64	-10, 50
81	2	7	11	12	26, 74	-30, 30
6	2	7	12	17	36, 80	-20, 50
41	7	12	17	18	54,150	10, 70
51	7	12	17	26	50,100	-30, 40
17	7	17	18	27	66,100	14, 60
16	12	17	26	32	70,104	-30, 30
61	17	26	27	32	80,130	-20, 40
72	17	18	27	32	80,130	0, 90
7	3	7	13	18	36, 80	16, 66
106	2	3	17	18	36, 80	6, 66

Table 4.2 PEAK GAIN (dBic) AND BEAM PEAK LOCATIONS
MEASURED WITH A FIXED 4-WAY POWER DIVIDER

Array Number (Frequency)	Beam Maximum Location θ	Beam Maximum Location ϕ	Peak Gain (dBic)
#26 (2100)	15°	0°	9.30
#26 (2280)	16°	0°	9.10
#1 (2100)	25°	38°	10.10
#1 (2280)	27°	38°	9.50
#36 (2100)	40°	26°	9.30
#36 (2280)	41°	24°	10.00
#81 (2100)	54°	-5°	9.70
#81 (2280)	42°	-7°	9.70
#6 (2100)	56°	12°	9.40
#6 (2280)	56°	12°	10.10
#41 (2100)	81°	25°	9.80
#41 (2280)	71°	22°	10.70
#51 (2100)	77°	8°	9.30
#51 (2280)	79°	3°	10.40
#17 (2100)	83°	32°	10.00
#17 (2280)	83°	32°	10.20
Average Peak (2100)	--	--	9.61
Gain (2280)	--	--	9.96

Table 4.3 PEAK GAIN AND BEAM PEAK LOCATIONS

Array Number (Frequency)	Beam Maximum Location θ	Beam Maximum Location φ	Peak Gain (dBic)
#26 (2106) *	16°	6°	7.80
#26 (2287) *	16°	2°	7.70
#1 (2106) *	32°	34°	8.10
#1 (2287) *	34°	32°	9.20
#36 (2106) *	46°	22°	8.10
#36 (2287) *	46°	20°	9.30
#81 (2106) *	52°	-10°	8.80
#81 (2287) *	58°	-13°	9.20
#6 (2106) *	66°	10°	8.90
#6 (2287) *	66°	10°	9.90
#41 (2106)	78°	20°	9.40
#41 (2287)	76°	18°	10.00
#51 (2106)	80°	2°	9.60
#51 (2287)	76°	2°	9.50
#17 (2106)	90°	26°	9.00
#17 (2287)	88°	26°	9.90
#16 (2106)	90°	-4°	9.10
#16 (2287)	90°	4°	9.90
#61 (2106)	104°	-4°	8.80
#61 (2287)	104°	-4°	9.40
#72 (2106)	104°	18°	9.30
#72 (2287)	100°	18°	9.10

Table 4.3 (Continued)

Array Number (Frequency)	Beam Maximum Location θ	Beam Maximum Location φ	Peak Gain (dBic)
#7 (2106)	66°	54°	8.90
#7 (2287)	64°	50°	9.70
#106 (2106) *	62°	28°	6.80
#106 (2287) *	58°	30°	7.90
Average Gain (2106)	--	--	8.66
Average Gain (2287)	--	--	9.28
Average Gain (2106) Excluding Weak Channels (2287)	--	--	9.16 9.64

* These groups include a higher insertion loss channel.

Table 4.4 DIFFERENCES IN PEAK GAIN AND BEAM POINTING ANGLE PRODUCED BY THE SPD. A FIXED 4-WAY POWER DIVIDER IS USED AS THE REFERENCE.

Array Number (Frequency)	Angular Difference $\Delta\theta$	$\Delta\phi$	Difference in Peak Gain (dB)
#26 (2106) *	1°	6°	-1.5
#26 (2287) *	0°	2°	-1.4
#1 (2106) *	7°	-4°	-2.0
#1 (2287) *	7°	-6°	-0.3
#36 (2106) *	6°	-4°	-1.2
#36 (2287) *	5°	-4°	-0.7
#81 (2106) *	-2°	-5°	-0.9
#81 (2287) *	16°	-6°	-0.5
#6 (2106) *	10°	-2°	-0.5
#6 (2287) *	10°	-2°	-0.2
#41 (2106)	3°	-5°	-0.4
#41 (2287)	5°	-4°	-0.7
#51 (2106)	3°	12°	0.3
#51 (2287)	3°	-1°	-0.9
#17 (2106)	-7°	6°	-1.0
#17 (2287)	5°	-6°	-0.3
Average (2106)	2.6°	0.5°	-0.9
Results (2287)	6.4°	-3.4°	-0.6
Average Values Excluding (2106)	-0.3°	4.3	-0.4
Weak Channels (2287)	4.33°	-3.7°	-0.6

* A higher insertion loss SPD channel was located in these groups.

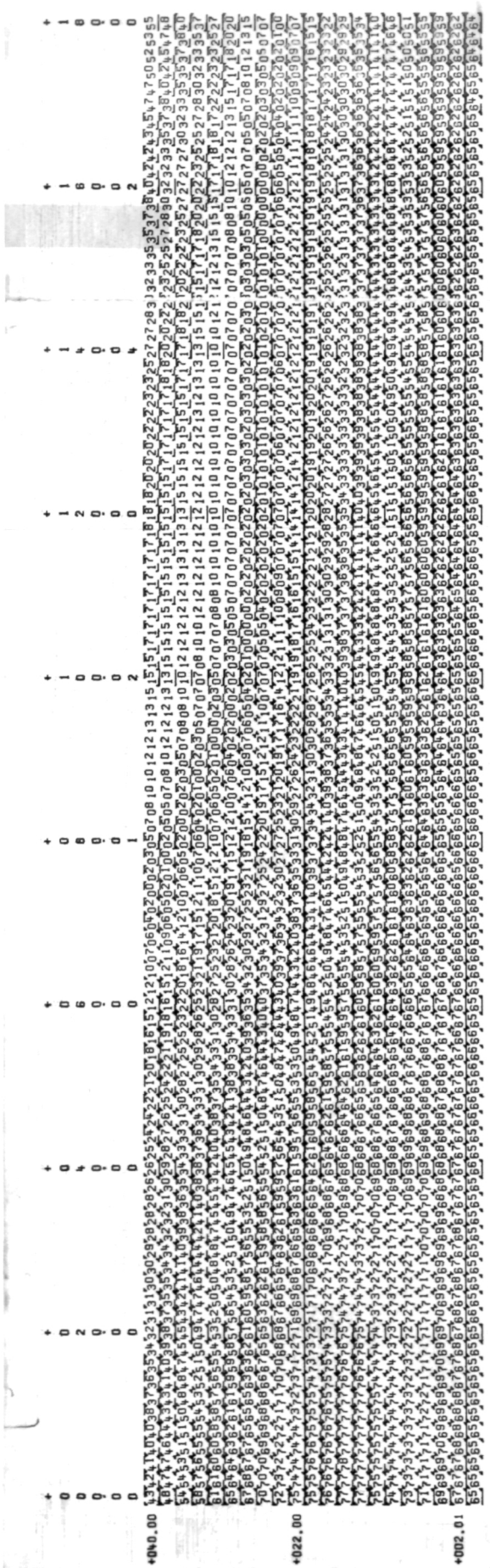
RAW DATA

AUTONOMOUS OMNI

Phase II Gain (with SPD)

Frequency = 2106 MHz

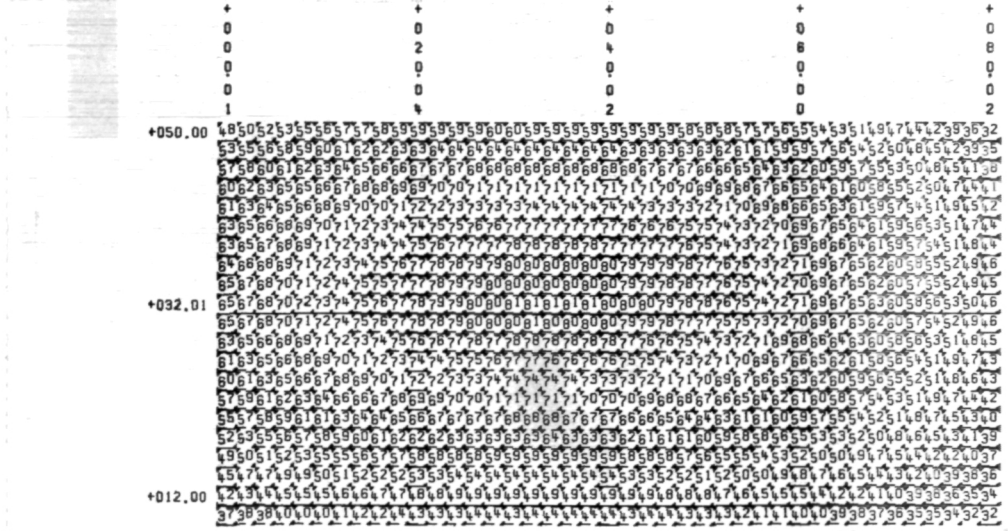
Figure	Array Number
4.1	26
4.2	1
4.3	36
4.4	81
4.5	6
4.6	41
4.7	51
4.8	17
4.9	16
4.10	61
4.11	72
4.12	7
4.13	106



#26
F = 2106 MHz

Elements
1, 2, 3, 6

Figure 4.1



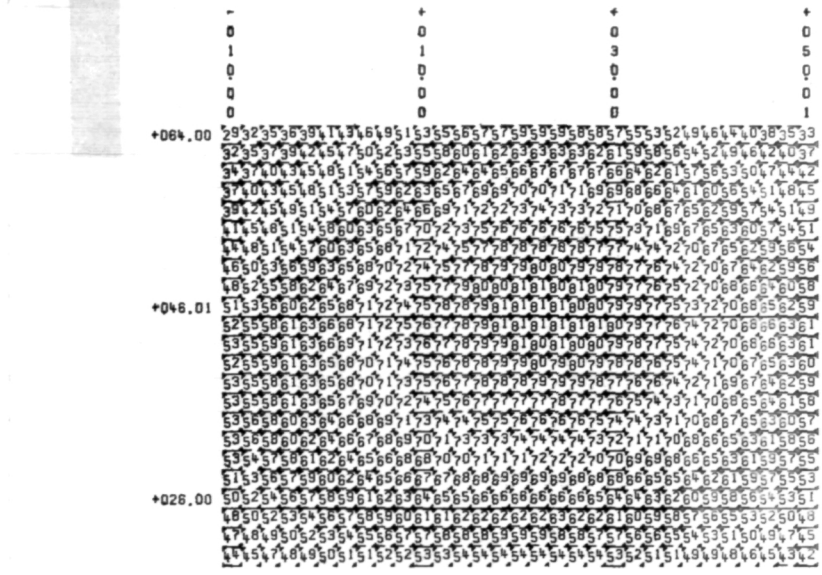
#1

F = 2106

Elements

1, 2, 3, 7

Figure 4.2



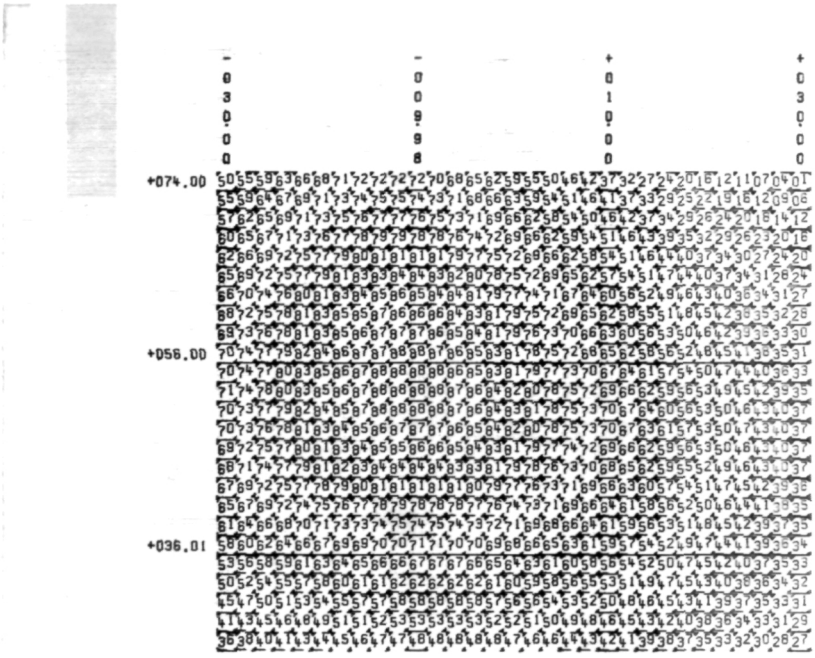
#36

F = 2106

Elements

2, 7, 12, 15

Figure 4.3



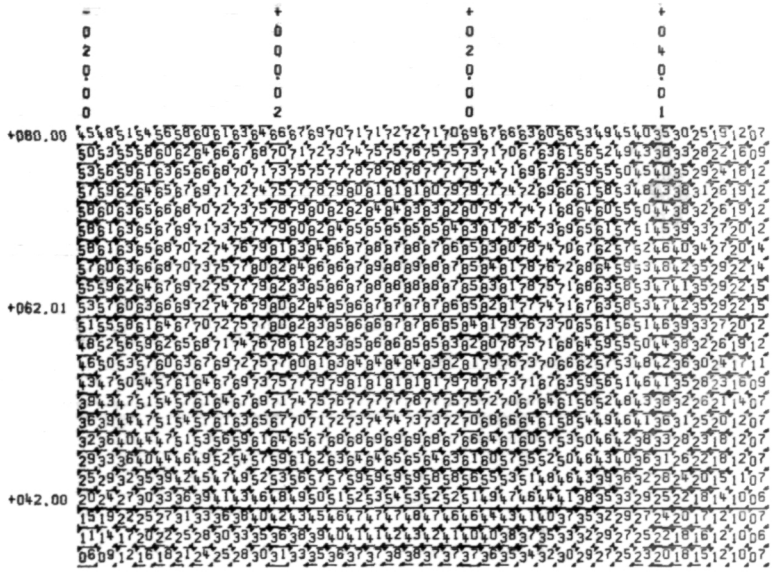
#81

F = 2106

Elements

2, 7, 11, 12

Figure 4.4



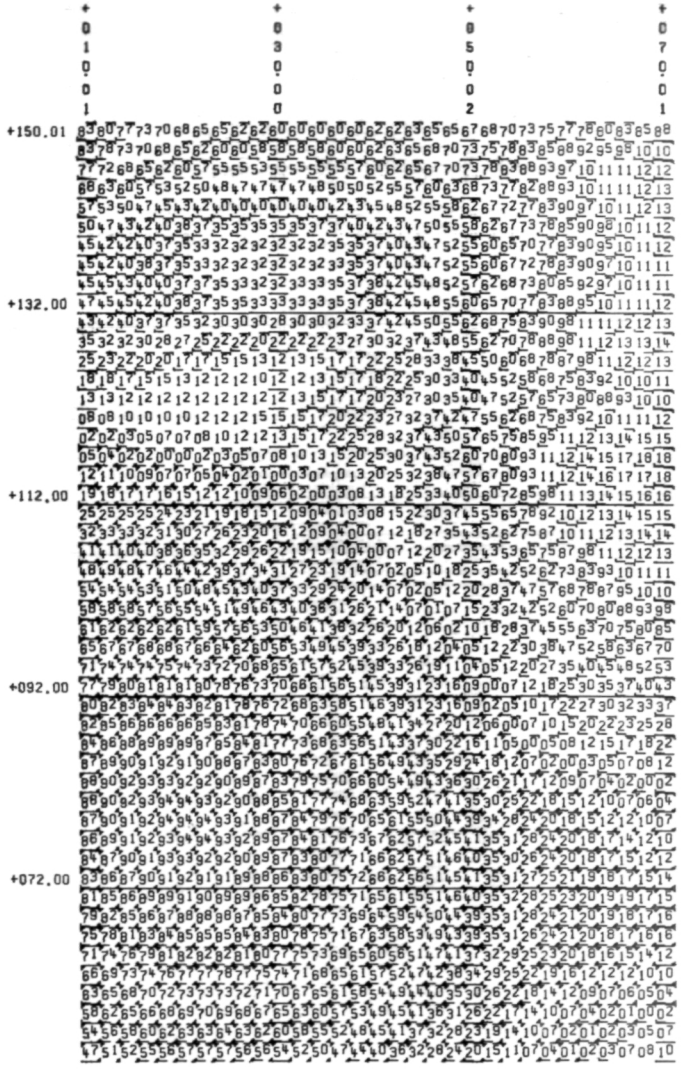
#6

F = 2106

Elements

2, 7, 12, 17

Figure 4.5



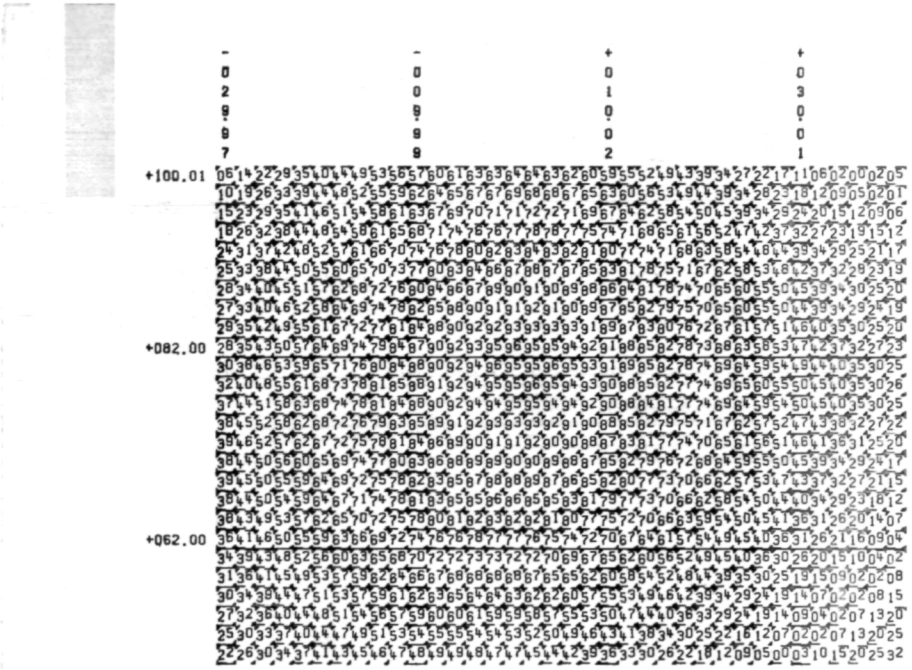
#41

F = 2106

Elements

7, 12, 17, 18

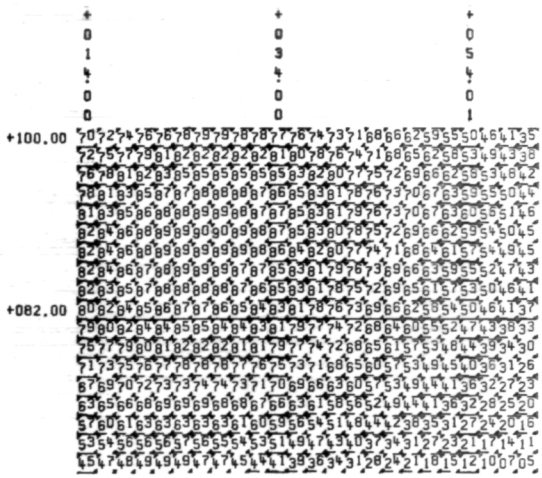
Figure 4.6



#51
F = 2106

Elements
7, 12, 17, 26

Figure 4.7



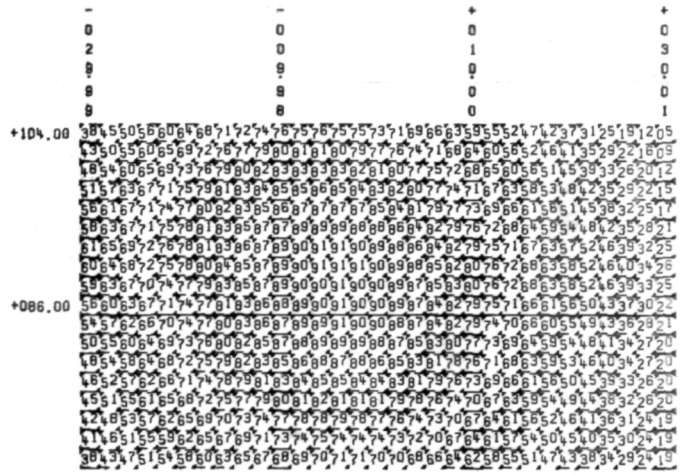
#17

F = 2106

Elements

7, 17, 18, 27

Figure 4.8



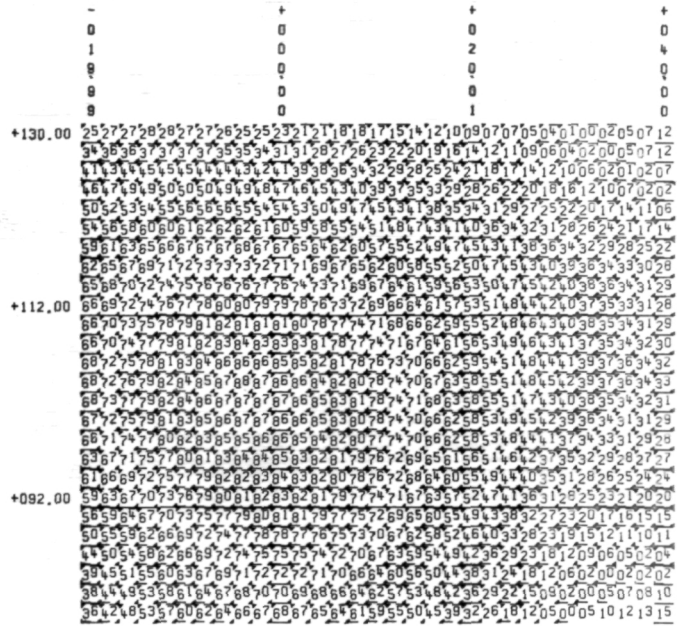
#16

F = 2106

Elements

12, 17, 26, 32

Figure 4.9



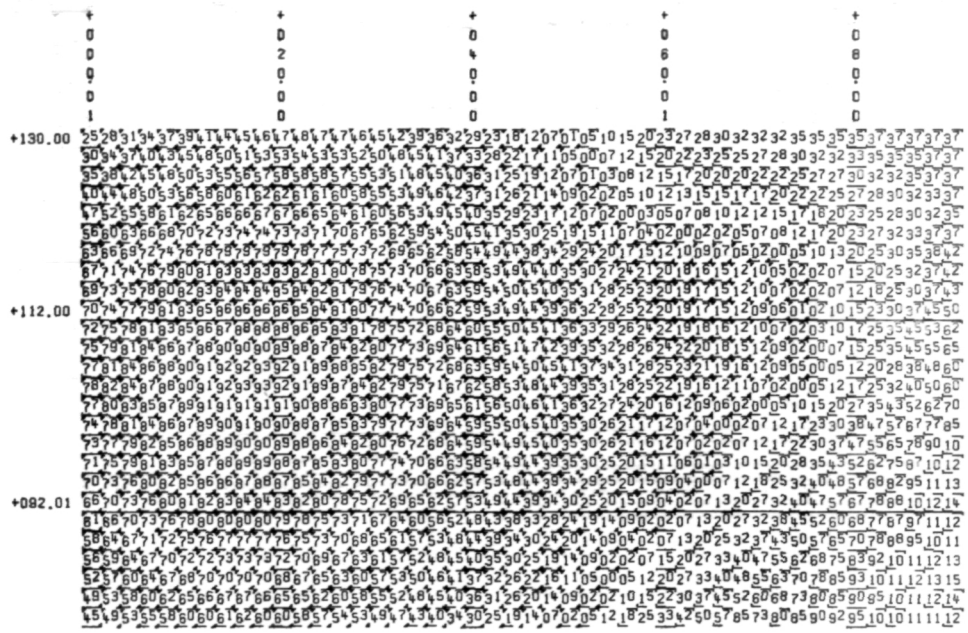
#61

F = 2106

Elements

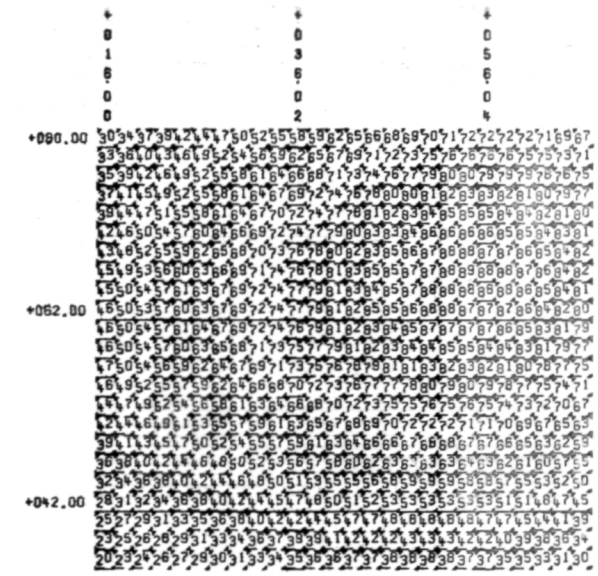
17, 26, 27, 32

Figure 4.10



#72
F = 2106
Elements
17, 18, 27, 32

Figure 4.11



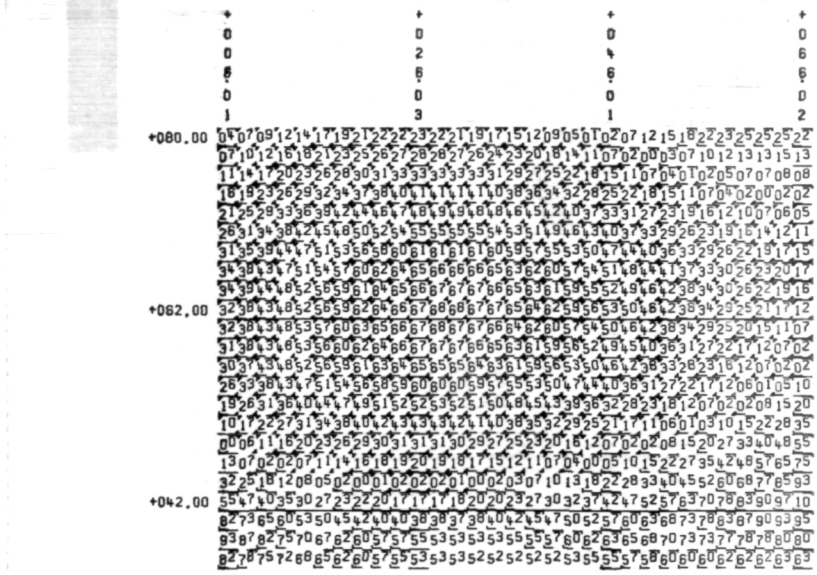
#7

F = 2106

Elements

3, 7, 13, 18

Figure 4.12



#106

F = 2106

Elements

2, 3, 17, 18

Figure 4.13

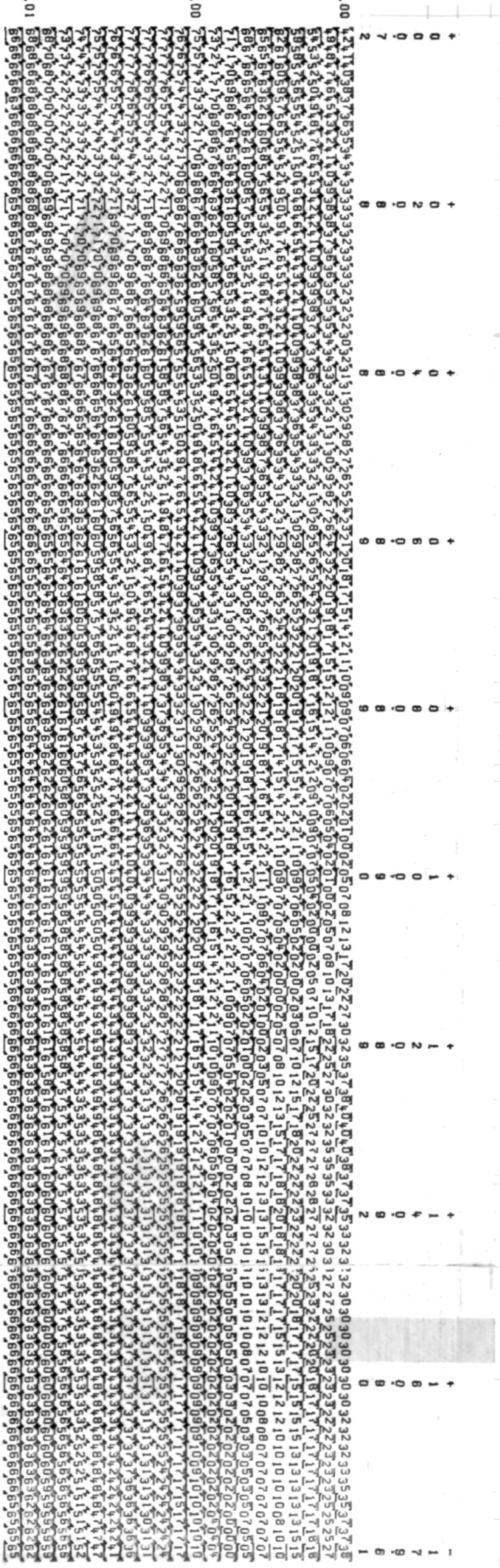
RAW DATA

AUTONOMOUS OMNI

Phase II Gain (with SPD)

Frequency = 2287 MHz

Figure	Array
4.14	26
4.15	1
4.16	36
4.17	81
4.18	6
4.19	41
4.20	51
4.21	17
4.22	16
4.23	61
4.24	72
4.25	7
4.26	106



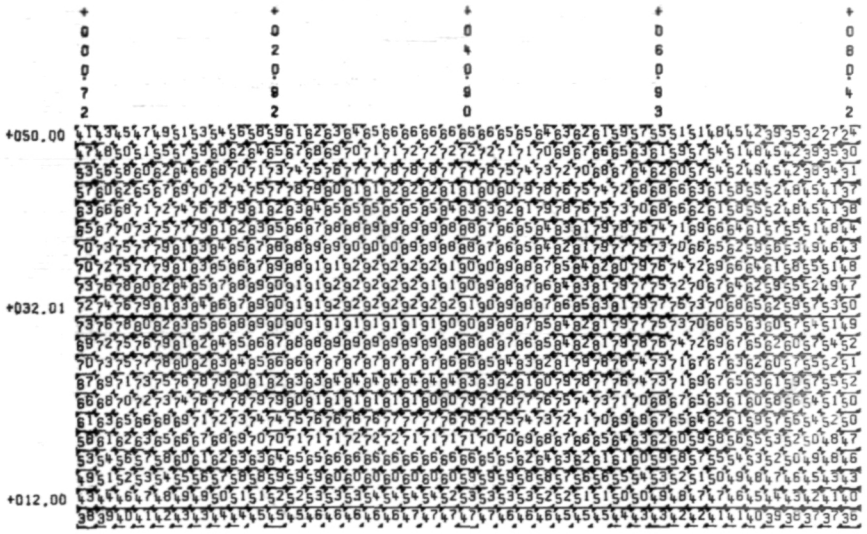
26

F= 2287 MHz

ELEMENTS

1,2,3,6

FIGURE 4.14



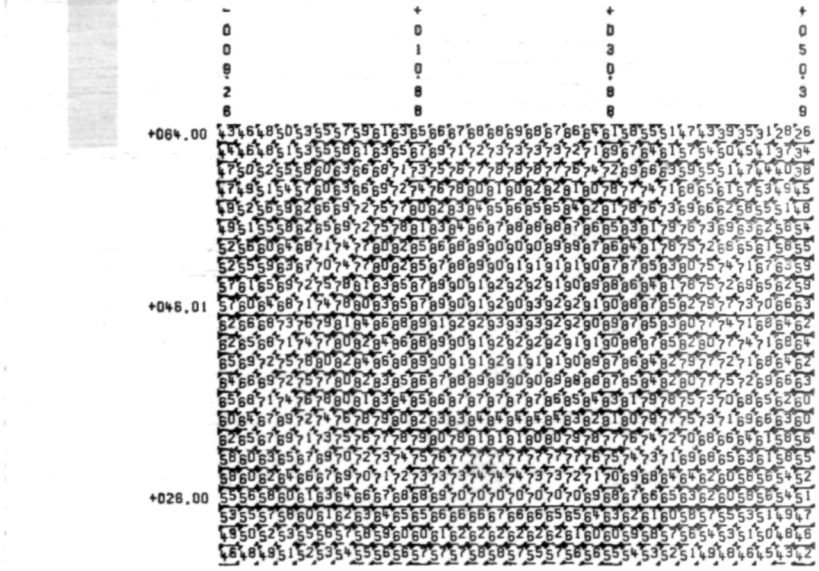
#1

F = 2287

Elements

1, 2, 3, 7

Figure 4.15



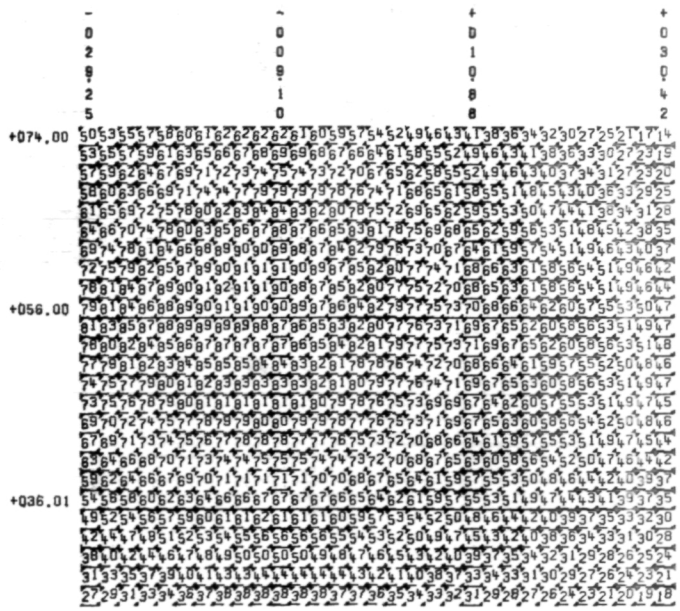
#36

F = 2287

Elements

2, 7, 12, 15

Figure 4.16



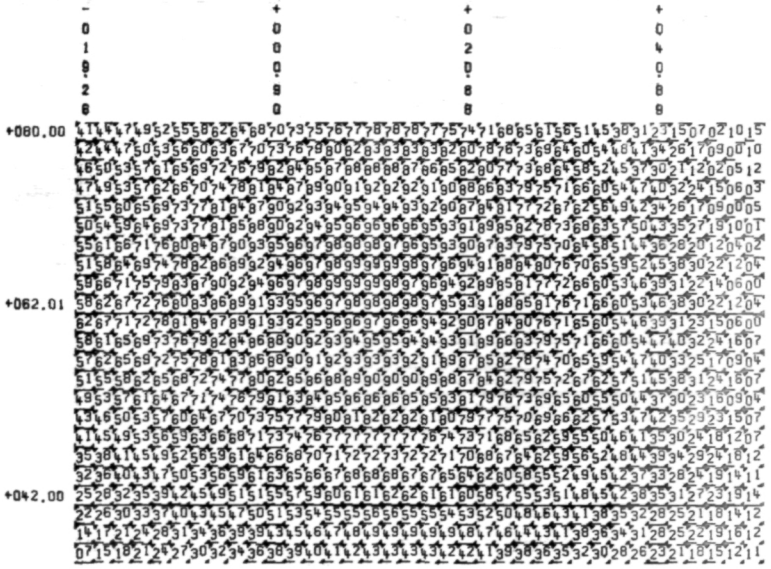
#81

F = 2287

Elements

2, 7, 11, 12

Figure 4.17



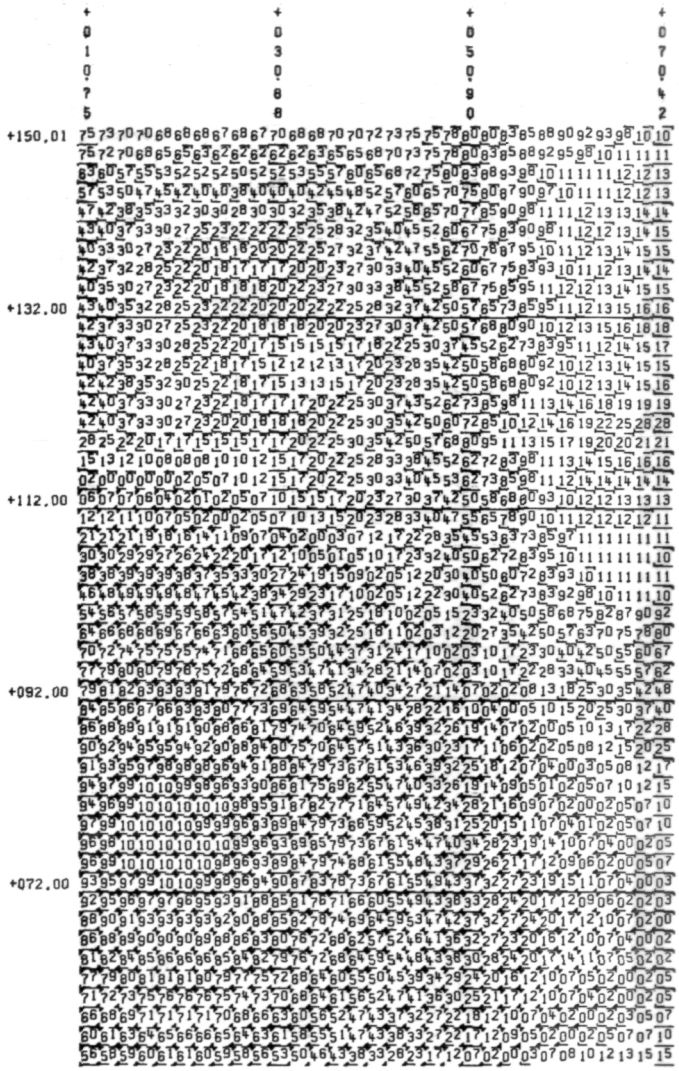
#6

F = 2287

Elements

2, 7, 12, 17

Figure 4.18



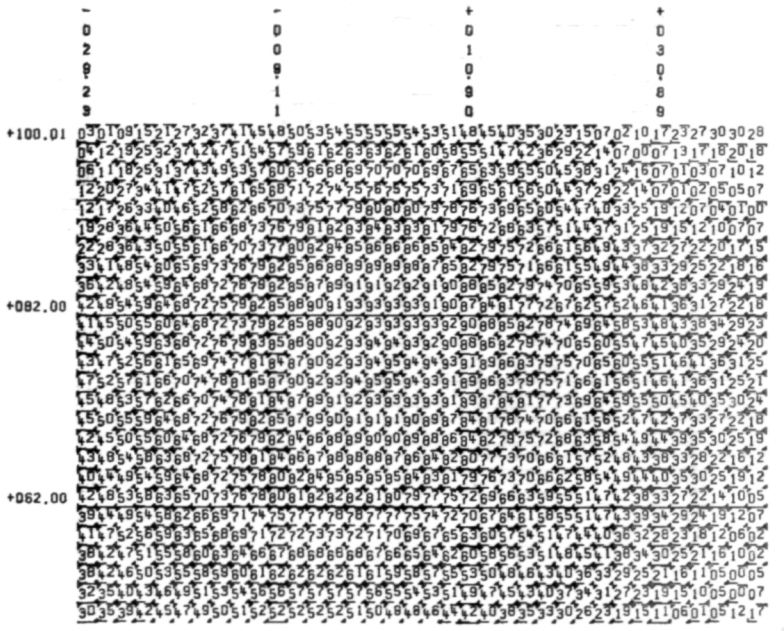
#41

F = 2287

Elements

7, 12, 17, 18

Figure 4.19



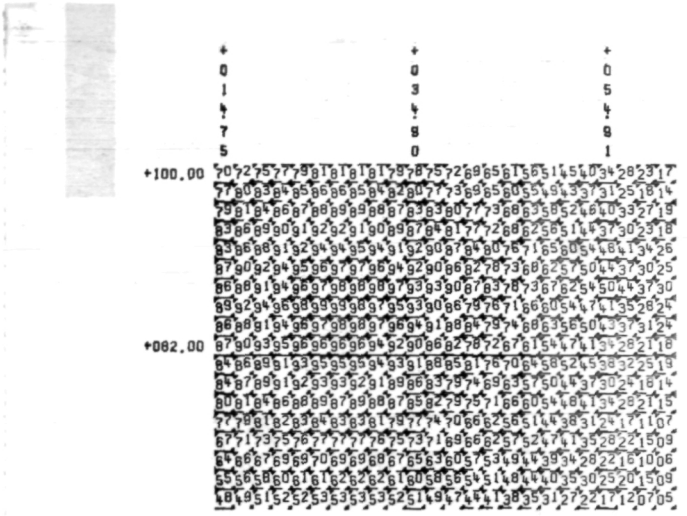
#51

F = 2287

Elements

7, 12, 17, 26

Figure 4.20



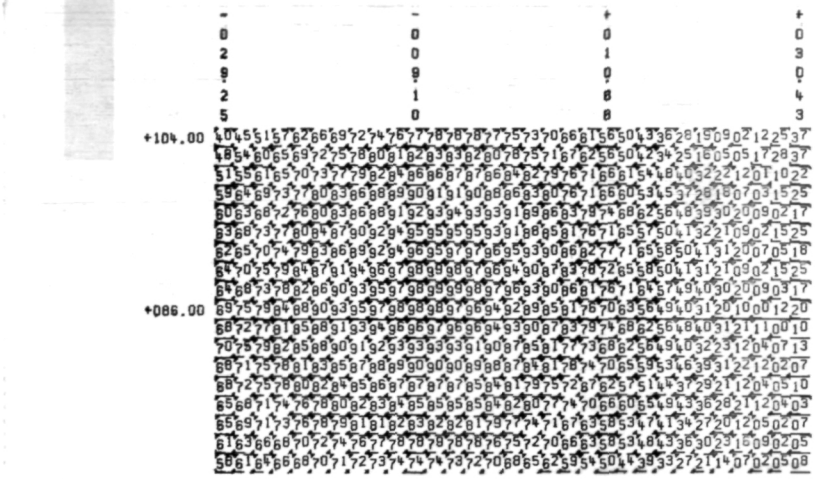
#17

F = 2287

Elements

7, 17, 18, 27

Figure 4.21



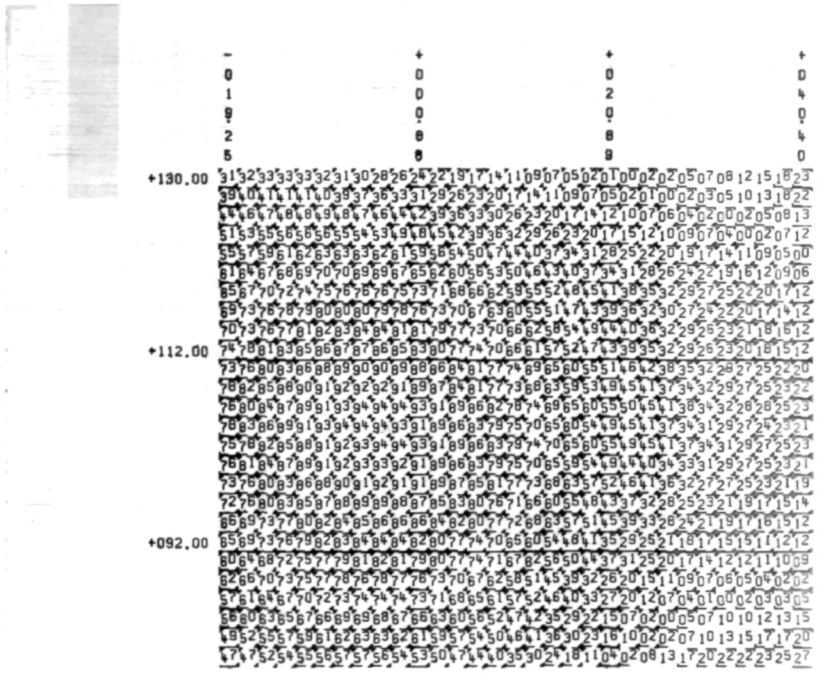
#16

F = 2287

Elements

12, 17, 26, 32

Figure 4.22



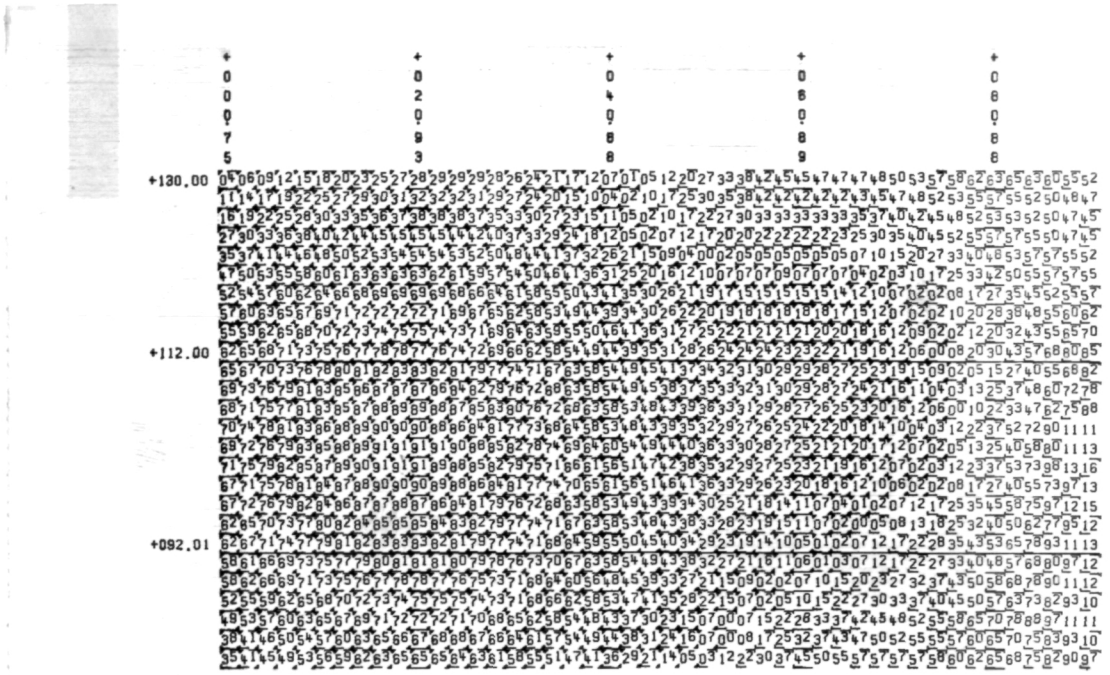
#61

F = 2287

Elements

17, 26, 27, 32

Figure 4.23



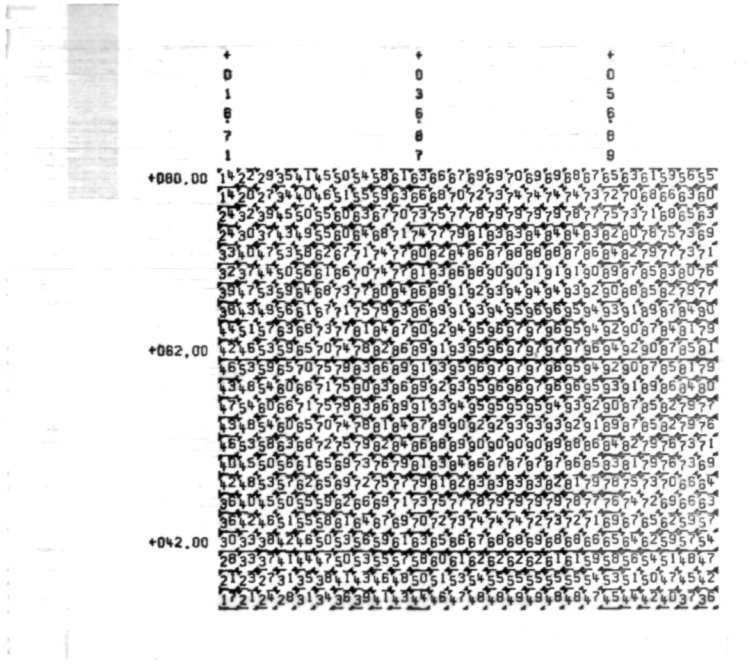
#72

F = 2287

Elements

17, 18, 27, 32

Figure 4.24



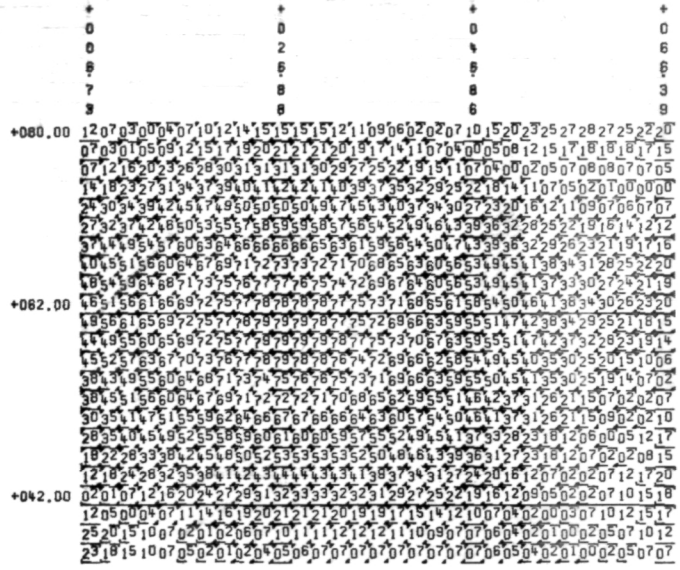
#7

F = 2287

Elements

3, 7, 13, 18

Figure 4.25



#106

F = 2287

Elements

2, 3, 17, 18

Figure 4.26

Chapter 5
RANGE INTERFACED GAIN MEASUREMENTS

Abstract

This chapter discusses the gain data taken on Auto Omni when operated in the range interface mode. In this mode, the signal's direction of arrival is provided by the range computer to the antenna. The antenna then directs its beam towards the range test horn. As a result, the radiation distribution pattern shows the directed beam gain throughout its coverage region.

5.1 INTRODUCTION

The range interface test allows the gain of the Auto Omni antenna to be mapped throughout the coverage region. This mapping is accomplished by interfacing the antenna range measurement computer with the Auto Omni microprocessor. Through this interface, the antenna is instructed to continually direct the beam towards the range test horn even as the antennas's theta and phi are varied.

5.2 TEST RESULTS

Composite radiation distribution patterns (RDP's) were taken in the range interface mode. These RDP's are shown in Figure 5.1 (2106 MHz) and Figure 5.3 (2287 MHz). Figures 5.2 (2106 MHz) and 5.4 (2287 MHz) are shaded for the coverage areas with less than 7.0 dBic gain.

5.3 TEST CONCLUSIONS

It is readily apparent from Figures 5.2 and 5.4 that there are substantial areas which have less than 7.0 dB gain. These areas may be treated as three categories:

Category 1 - area near pole
Category 2 - area $50° < \theta < 90°$; $-180° \leq \phi \leq -90°$
Category 3 - area near each element

The following paragraphs discuss each of these areas.

5.3.1 Category 1 - Area Near Pole, Coordinates (0°, 0°)

The area near the pole has low gain as the result of including SPD output 1 (which has a high insertion loss) in a cluster. The algorithm used for the selection of Auto Omni elements chooses the four elements which lie closest to the desired pointing direction. Should the angular separation from an element to the pointing direction be two degrees or less, that element is

excluded from the cluster and another element is chosen. The impact of this algorithm is clearly seen in Figures 5.3 and 5.5 where the gain at the pole (excluding element 1) is higher than the gain just off the pole (includes element 1). The area in Figure 5.3 between elements 1 and 2 would be expected to be lower than is shown. It is believed that in this region the power which would have gone to elements 1 and 2 is transferred to the other two selected elements. As a result, the gain is not as low as might be expected since the gain does drop rapidly in this region.

When element 1 is turned on, the gain is expected to be much higher if the SPD outputs to elements 1 and 2 had normal insertion losses. For this same reason, the gain in the area of element 2 is low.

It should be noted that the projection of the coverage regions in Figures 5.1 through 5.4 is misleading. That is, the area near the pole which has gain less than 7 dB is no where near so large a proportion of the coverage region as it appears.

5.3.2 Category 2; Area $50° < \theta < 90°$; $-180° < \phi < -90°$

During the handling of the Auto Omni antenna, elements 22, 23 and 35 were inadvertently moved so that they were no longer being properly connected to their polarization hybrids. This interconnection problem was not discovered during a VSWR check of the elements prior to the range interface test since their VSWR had only degraded to 1.7:1 from 1.5:1 when properly connected. From Figure 5.3 it becomes apparent that most of the beams within the Category 2 area use one or more of these non-circularly polarized elements. If these elements were properly connected, the gain would be expected to increase to an acceptable level.

5.3.3 Category 3 - Area Near to Elements

The Auto Omni element selection algorithm has been designed to exclude elements from the cluster which are within a two degree solid angle of the desired pointing direction. Examination of Figure 5.3 leads one to believe that this algorithm may not be optimum. In particular, the gain is obviously lower in the vicinity of elements 7, 8, 9, 10, 11, 14, 15, 16, 17, 18, 19, 20, 21, 24 and 25.

Low gain probably occurs around other elements as well, but it is masked by the Categories 1 and 2 problems discussed previously.

After a careful study of the low gain areas, the problem seems to be created by the microprocessor algorithm that chooses the elements on the basis of the pointing direction. This problem is illustrated in the following example. Consider a pointing direction that is approaching element 21 in the manner of Figure 5.5(a). As long as the pointing direction is more than two degrees away from element 21, the algorithm selects elements 14, 20, 21, and 34. The resulting cluster has a symmetric diamond shape that produces a reasonable amount of gain. Once the pointing direction is within two degrees of element 21, the algorithm excludes this element, and the subarray consists of elements 9, 14, 29 and 34. In this cluster (see Figure 5.5(b)), the elements form a widely spaced rectangle and a lower gain results than that produced by a diamond-shaped cluster. As the pointing direction moves across element 21 (still within two degrees of the element), element 22 becomes closer than 34, and the selected subarray becomes the oddly shaped cluster depicted in Figure 5.5(c). Because of the asymmetry of this array, the resulting gain is lower than that of a diamond-shaped cluster. Once the pointing angle progresses more than two degrees away from 21, a diamond-shaped cluster (with higher gain) results. This cluster is shown in Figure 5.5(d), and it includes element 21.

Thus, the problem of low gain in the vicinity of element locations, is due to the algorithm which appears to have a major defect. When the pointing direction is within two degrees (solid angle) of an antenna element, the algorithm excludes it from the subarray cluster. The result of this is either a widely-spaced symmetrical subarray or an oddly shaped asymmetrical lattice. These conditions result in gains that are lower than the more compact diamond-shaped array. The discussion of possible solutions to this algorithm is in Chapter 6.

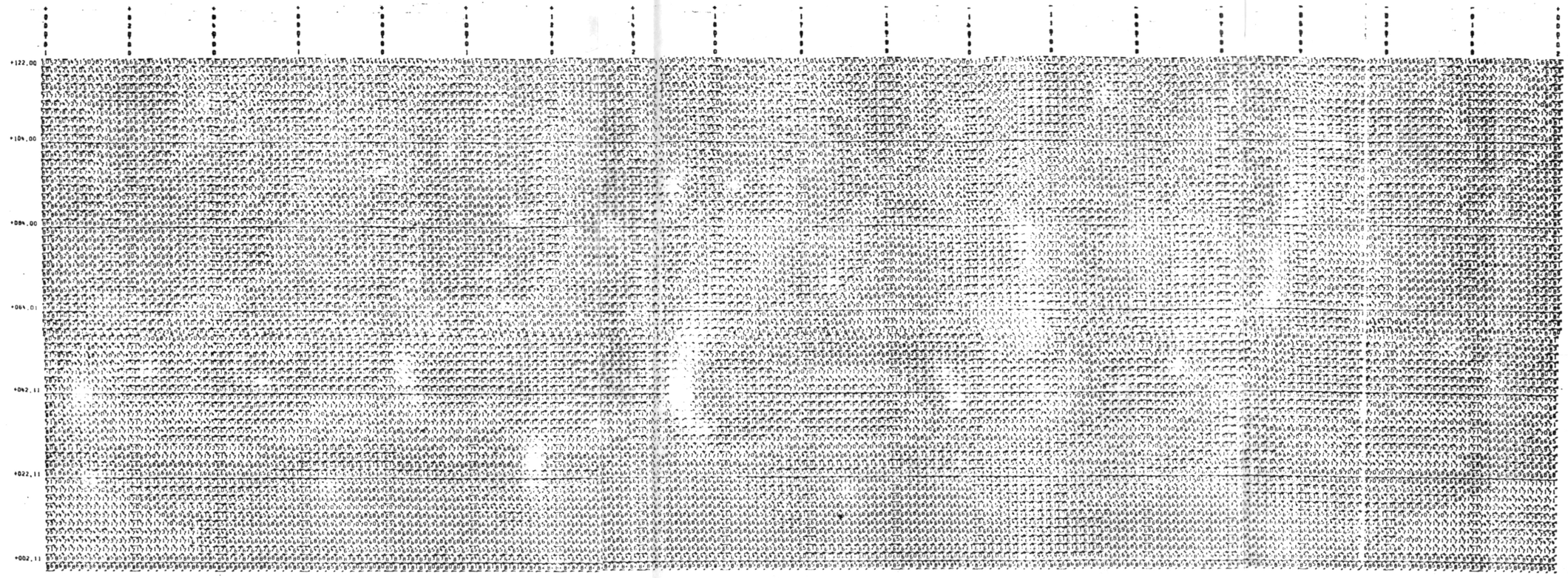


Figure 5.1 Range Interfaced Mode

Gain at 2106 MHz

FILE: DF##11 FREQ= . MHZ
FREQ NR: 1
PLOT DATA: AA

2106 Composite RDP

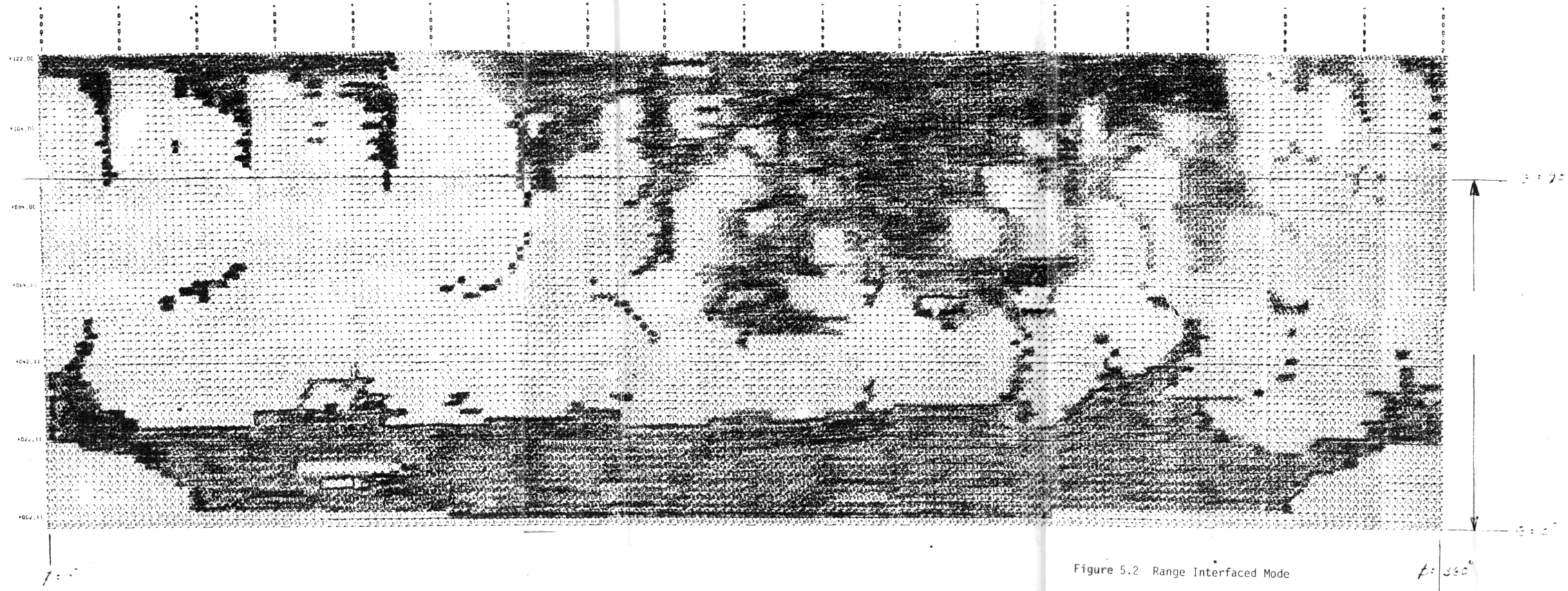


Figure 5.2 Range Interfaced Mode

Gain Greater than 7 dB at 2106 MHz

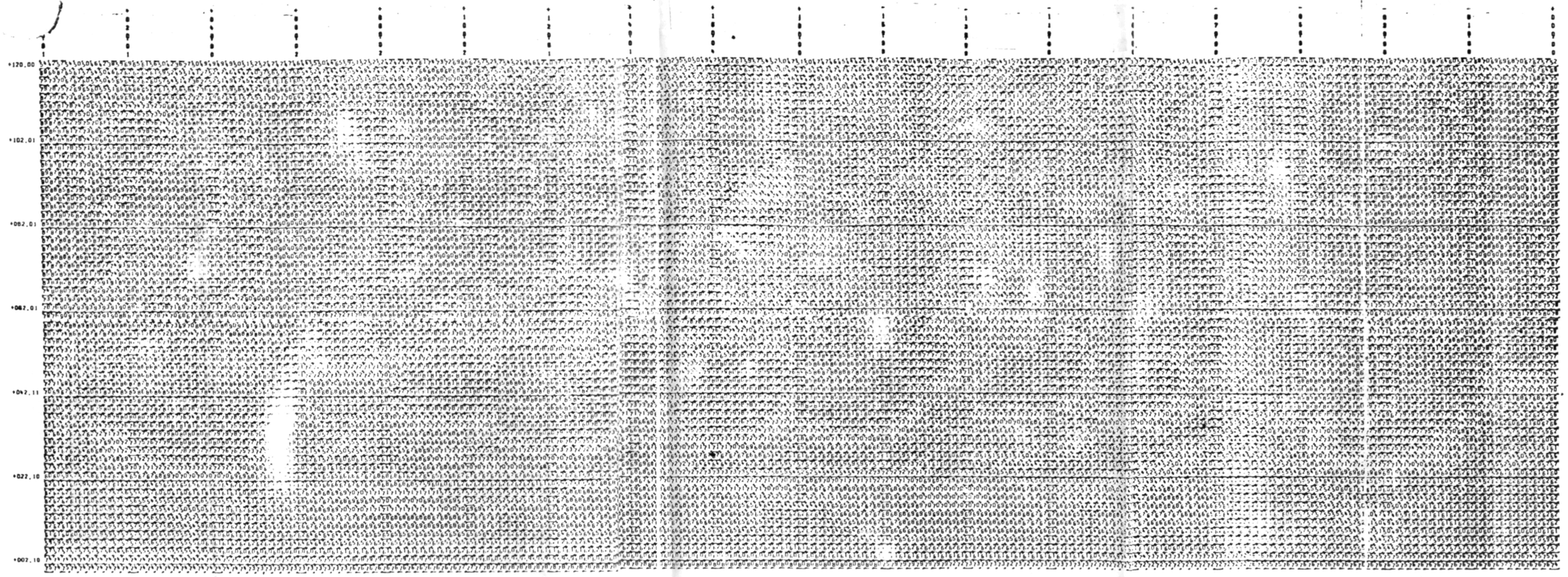


Figure 5.3 Range Interfaced Mode Gain at 2287 MHz

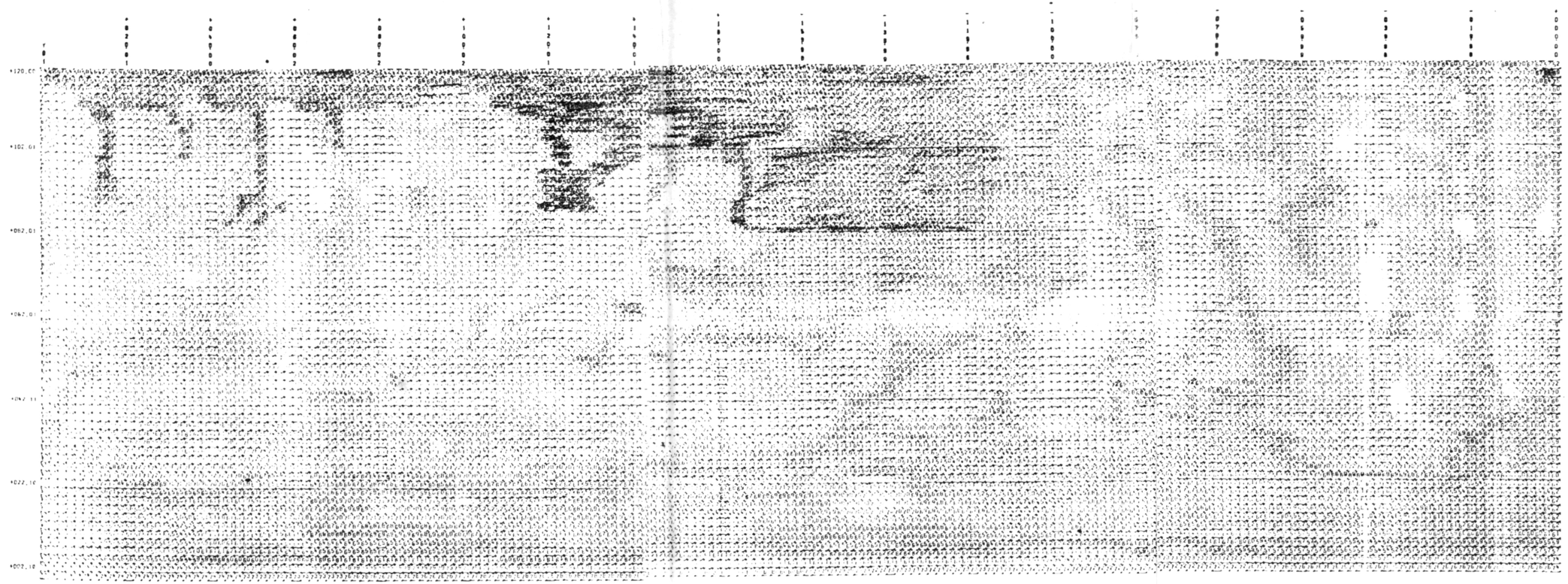


Figure 5.4 Range Interfaced Mode

Gain Greater than 7 dB at 2287 MHz

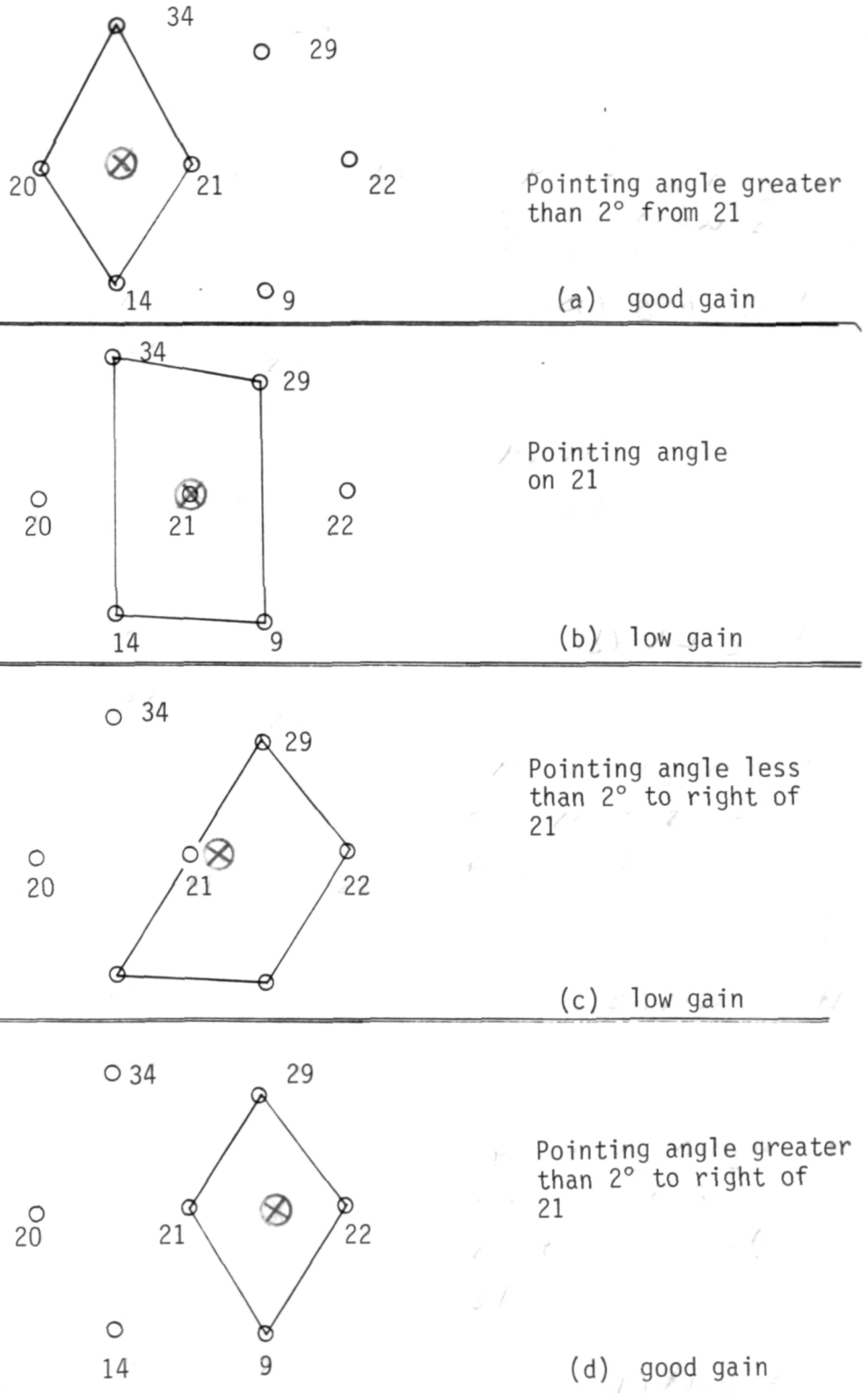


Figure 5.5 Element clusters shape changes with pointing angles.

Chapter 6
MODIFICATION OF ELEMENT SELECTION ALGORITHM

Abstract

The Auto Omni element selection algorithm does not include any element which is within two degrees of the desired pointing angle. Changes to this algorithm are discussed in this chapter.

6.1 INTRODUCTION

The element selection algorithm may be optimized by improvements in two areas. These areas are discussed in the following paragraphs.

6.2 MODIFICATION TO INCLUDE MORE THAN FOUR ELEMENTS IN A CLUSTER

To propose an improvement to the element selection algorithm, a series of RDP's were taken around element locations where Figure 5.3 indicated a gain of less than 7.0 dB. These RDP's were taken around elements 2, 3, 6, 9, 10, and 22. Various element clusters were selected around these locations to investigate the effects of element clusters on the gain. These sector RDP's are shown as Figures 6.1 through 6.6.

A summary of peak gains for the various element clusters is displayed in Table 6.1. In this table, the first cluster at each position was chosen by entering the coordinates of the element under consideration into the microcomputer's directed beam mode. These clusters always excluded the element whose coordinates were entered. The clusters also had a widely spaced rectangular lattice. After the initial cluster was determined, additional combinations of four, five and six elements were tried to see if any gain improvement would result. After this test was performed, elements 22, 23 and 35 were found to be improperly connected to their polarization hybrids. As a result, those clusters which include these elements is presently thought to be invalid. As a result, the only valid test clusters in Table 6.1 are around elements 2, 3 and 6. With such a small sampling the data is inconclusive. It should be noted, however, that the selection of five or six element clusters always improves the gain. For example, with five element clusters, the gain improves 0.4 dB at 2106 MHz and 1 dB at 2287 MHz. The one element cluster tested shows an improved gain of 0.2 dB at 2106 MHz and 1.1 dB at 2287 MHz. Additional testing should be performed to verify the initial conclusion that the element selection algorithm should be modified to use five element clusters when the pointing direction is "close" to the elements coordinates.

6.3 MODIFICATION TO PROVIDE SYMMETRICAL CLUSTERS

Another area for further investigation is the modification of the element selection algorithm to provide symmetrical clusters. When the pointing direction is close to an element's coordinates, the set of elements used in the cluster changes rapidly with the present algorithm. This results from the distances from the desired pointing direction to each of several elements being very similar. One consequence of this similarity in distances is that the cluster shape rapidly changes with some shapes being lower than that of the preferred "diamond" shape lattice. Additional investigation into this effect should be performed and software modifications made to choose those element clusters which are closest to a "diamond" shape. (It should be noted that "non-diamond" clusters are found most often at theta locations greater than 70°.

Table 6.1

GAIN CHANGES WITH DIFFERENT NUMBER OF ELEMENTS IN A CLUSTER

Element whose Pointing is the Pointing Direction	Selected Elements	Gain (2106 MHz) dBic	Gain (2287 MHz) dBic	Gain Compared to First Cluster in each Group (2106 MHz)	Gain Compared to First Cluster in each Group (2287 MHz)	Raw Data Figure
2	1,3,6,12	6.6	6.2	---	---	6.1
	1,3,6,12,2	7.4	6.4	0.8	0.2	
	3,6,11,7	7.3	7.1	0.7	0.9	
	2,7,11,12	6.6	5.7	0.0	-0.5	
3	1,2,4,13	6.8	5.7			6.2
	1,2,4,13,3	7.1	6.7	0.3	1.0	
	1,4,7,13	6.6	6.5	-0.2	0.8	
	2,8,7,13	7.8	6.2	1.0	0.5	
6	1,2,5,16	6.9	5.0	---	---	6.3
	1,2,5,6,16	7.1	6.7	0.2	1.7	
	2,5,10,11	5.7	5.6	-1.2	0.6	
	1,2,5,6,10,11	7.1	6.1	0.2	1.1	
	6,10,11,16	6.6	5.6	-0.3	0.6	
9 *	14,15,21,22	7.9	5.5	---	---	6.4
	9,14,15,21,22	6.6	5.2	-1.3	-0.3	
	4,5,14,15	6.6	5.2	-1.3	0.0	
22 *	15,21,23,29	7.4	5.0	---	---	6.5
	15,21,23,29,22	6.6	6.0	-0.8	1.0	
	9,15,29,35	7.3	5.2	-0.1	0.2	
10 *	15,16,23,24	6.1	5.2	---	---	6.6
	15,16,23,24,10	4.6	6.6	-1.5	1.4	
	5,6,23,24	4.4	4.9	-1.7	-0.3	
	10,16,23,24	6.8	7.3	0.7	2.1	

* possibly invalid data

RAW DATA

SECTOR RDP's

NOTE: All RDP's in this section are in a 2° by 2° matrix. Horizontal is phi, vertical is theta. A gain correction number of 0 dB must be added to each number to give true gain in dBic.

Figure	Pointing Direction (θ,ϕ)
6.1	(31°, 0°)
6.2	(31°, 72°)
6.3	(31°, 288°)
6.4	(58°, 180°)
6.5	(90°, 198°)
6.6	(58°, 252°)

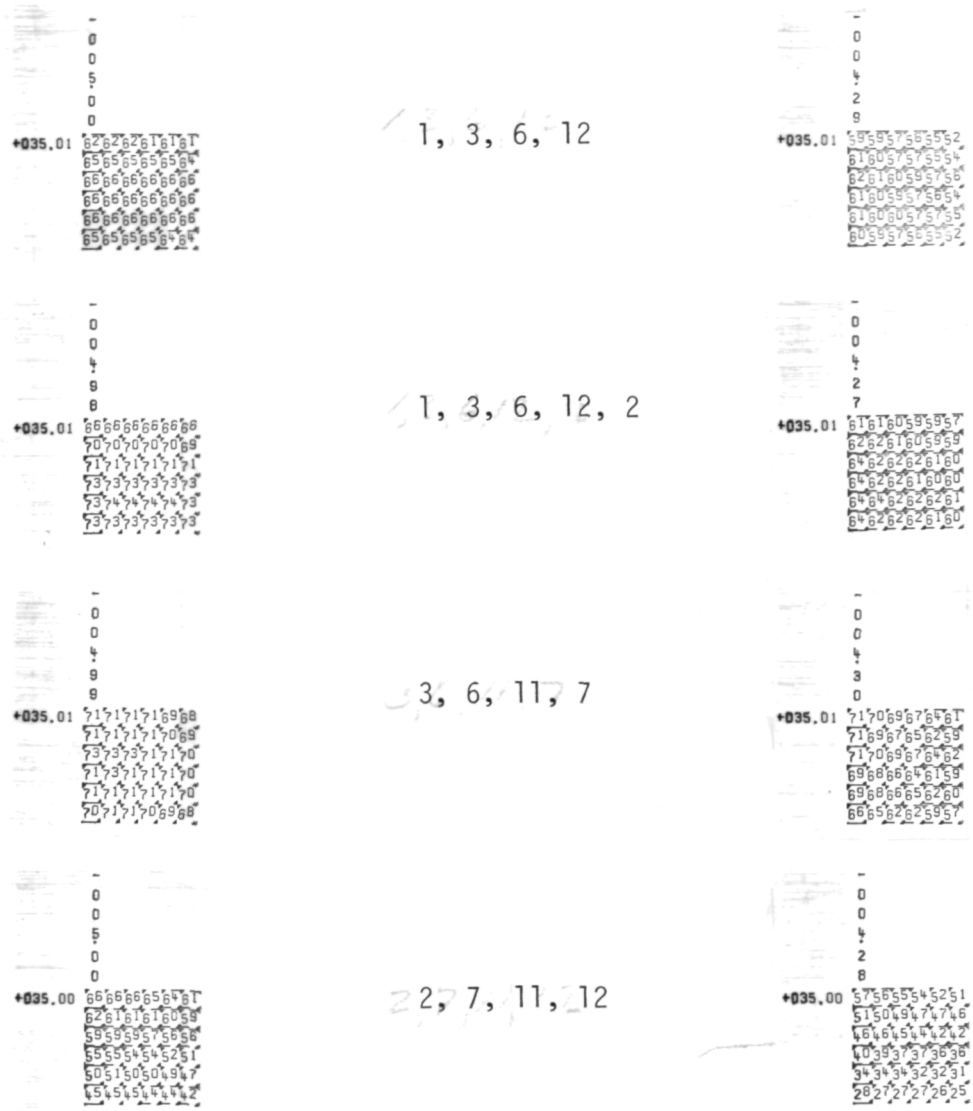


Figure 6.1

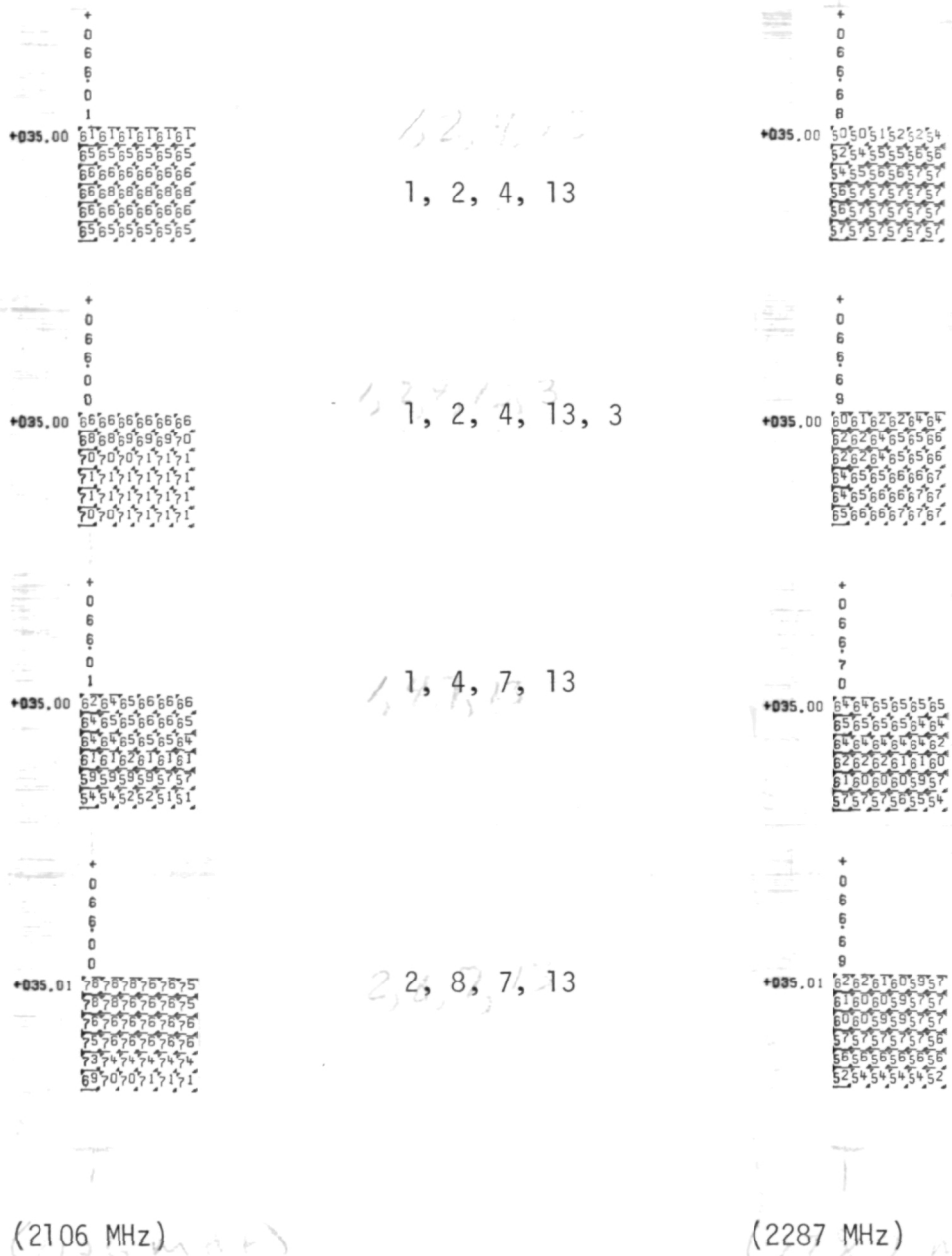


Figure 6.2

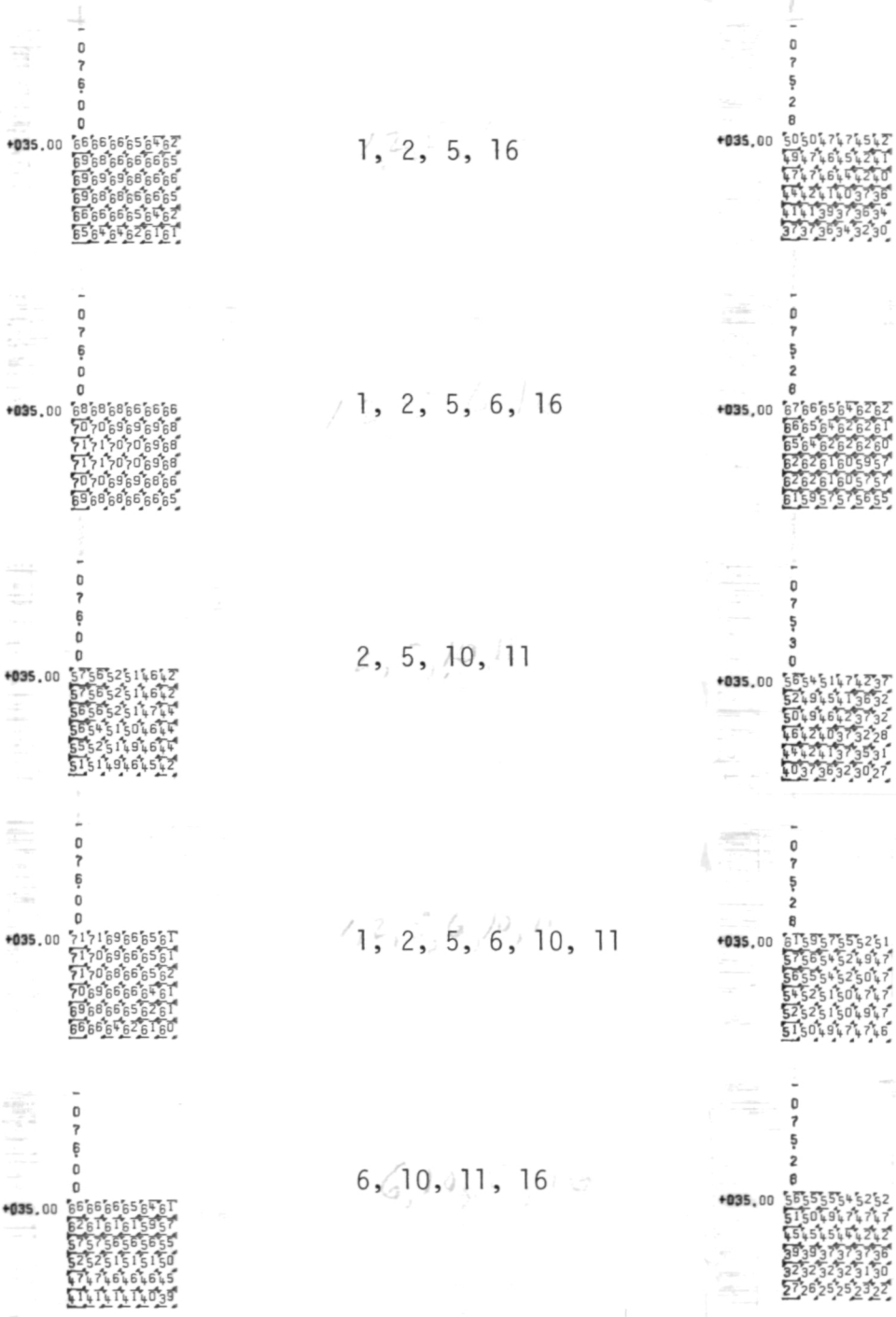
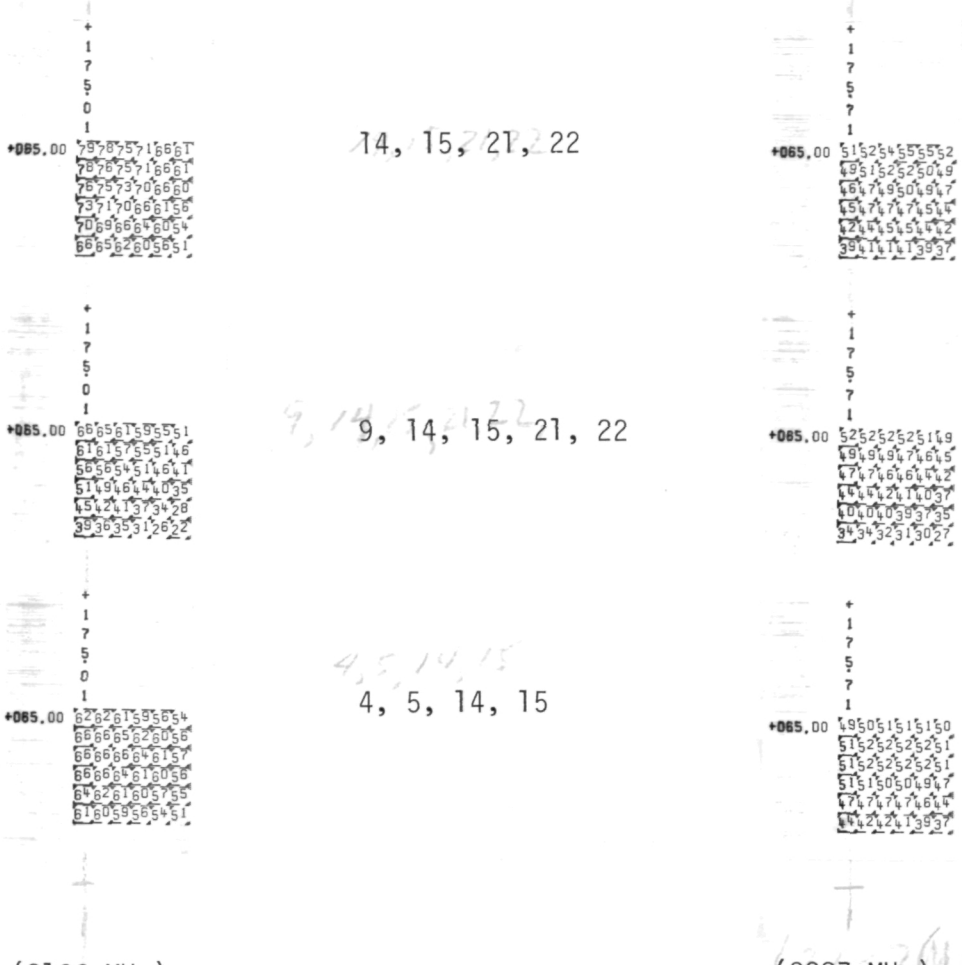

+035.00
1, 2, 5, 16
+035.00
+035.00
1, 2, 5, 6, 16
+035.00
+035.00
2, 5, 10, 11
+035.00
+035.00
1, 2, 5, 6, 10, 11
+035.00
+035.00
6, 10, 11, 16
+035.00
(2106 MHz)
(2287 MHz)

Figure 6.3



(2106 MHz)

(2287 MHz)

Figure 6.4

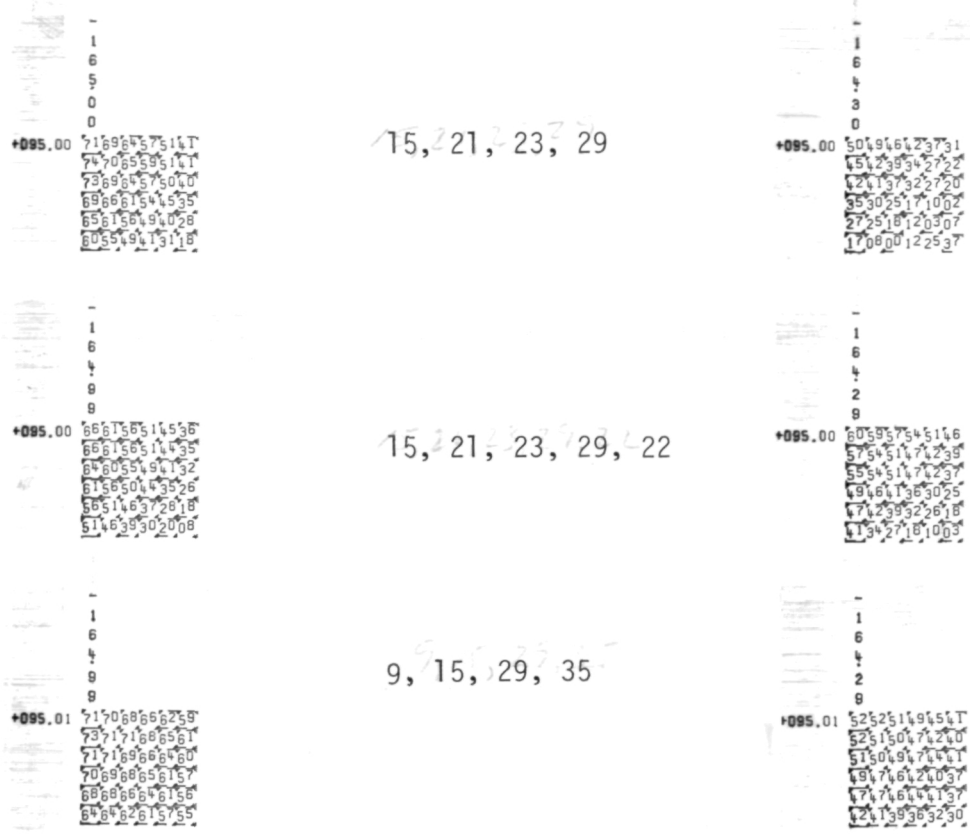


Figure 6.5

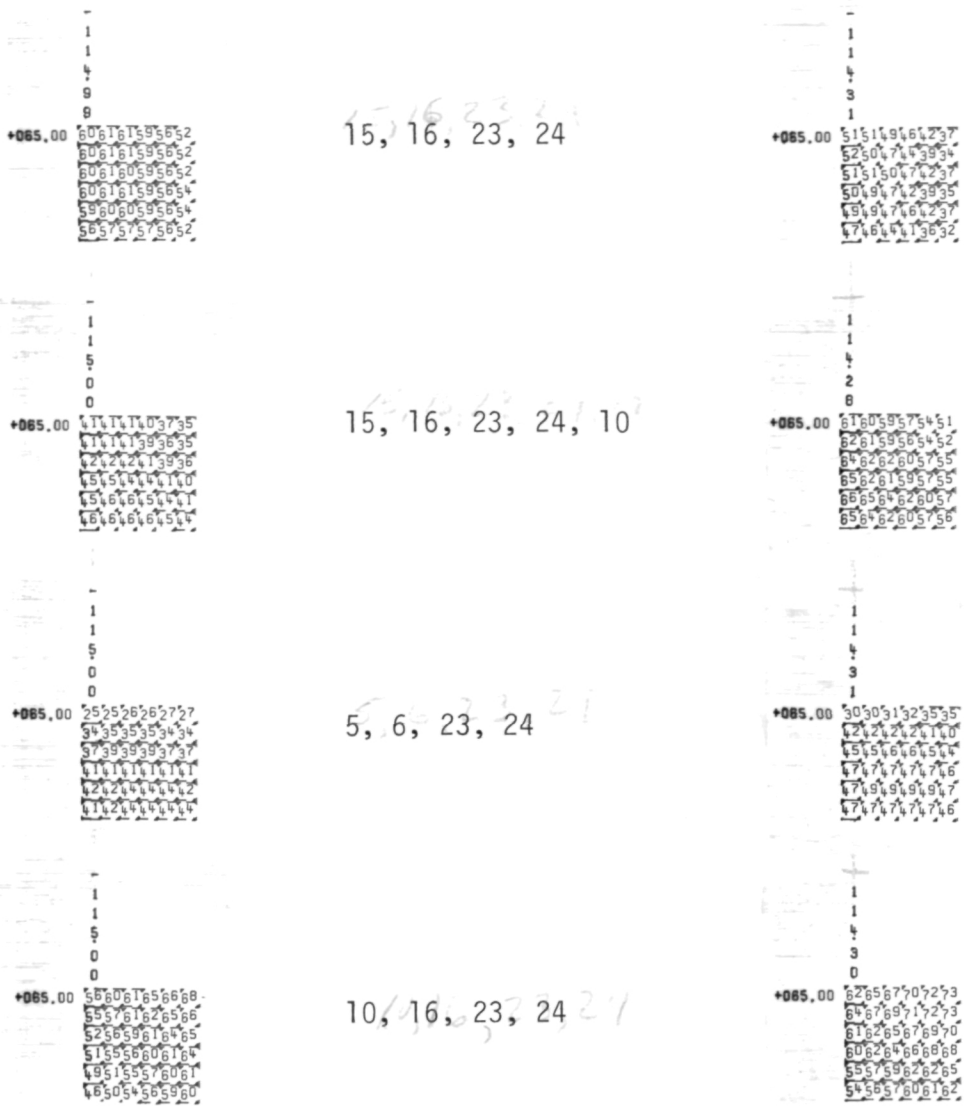


Figure 6.6

Chapter 7
OMNIDIRECTIONAL GAIN COVERAGE

Abstract

This chapter describes the results of the omnidirectional mode testing.

7.1 INTRODUCTION

In the omnidirectional mode the Auto Omni antenna turns on elements 7 through 16. This 10 element subarray is to provide a gain of -5 dBic or greater throughout the hemisphere. This coverage was measured at 98.3% of the region at 2106 MHz and 82.2% at 2287 MHz during phase one testing.

7.2 TEST RESULTS

Gain radiation distribution patterns were taken in the omnidirectional mode at both 2106 MHz and 2287 MHz. These RDP's are shown as Figures 7.1 and 7.2. As shown by these figures, the MHz gain is generally highest at the pole (0°, 0°) and lowest at the equator (θ = 90°). This gain taper results from the use of elements whose patterns are able to combine without blockage at the pole and with blockage at the equator.

Omnidirectional gain at 2106 MHz varies from 4.5 dBic at the pole to a low of -6 dBic at the equator.

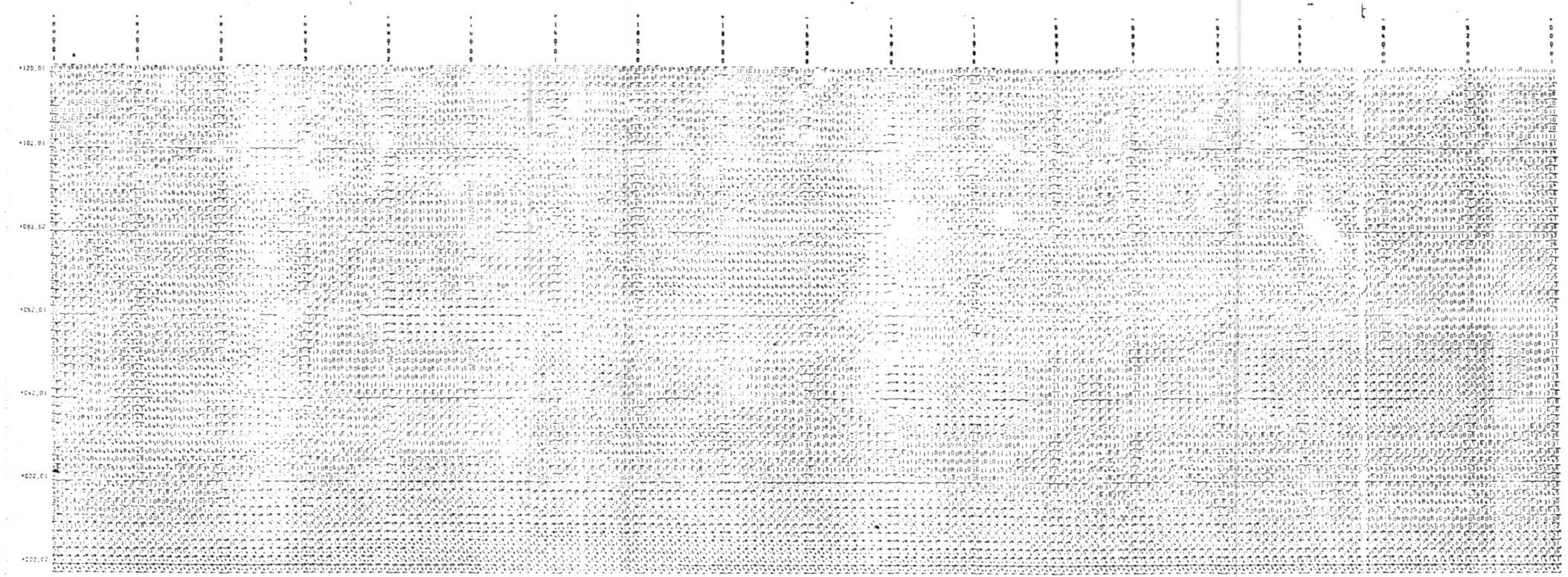


Figure 7.1 Omni Mode

Gain at 2106 MHz

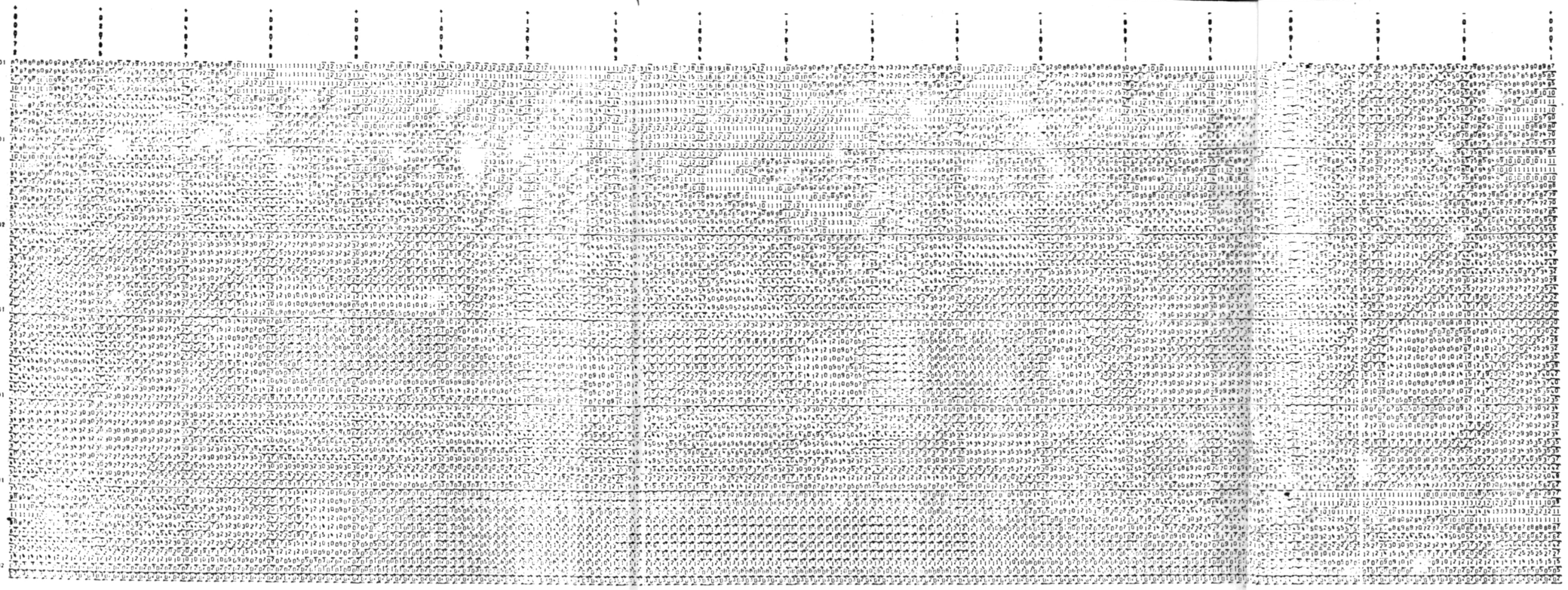


Figure 7.2 Omni Mode

Gain at 2287 MHz

Omni
FILE: DF0852
FREQ NR: 1 FREQ= 2287. MHZ
PLOT DATA: AA

Chapter 8
PHASE DATA
OMNIDIRECTIONAL MODE AND RANGE INTERFACE MODE

Abstract

Phase data radiation distribution patterns were taken in both the omnidirectional and range interface operating modes at 2106 MHz and 2287 MHz. This chapter discusses this data and shows that the insertion phase varies smoothly between pointing directions.

8.1 INTRODUCTION

While the gain radiation distribution patterns discussed in the previous chapters were being taken, the phase RDP's shown as Figures 7.1 through 7.4 were also being taken. These RDP's show that the Auto Omni insertion phase varies slowly between beams.

8.2 TEST DATA - RANGE INTERFACED OPERATING MODE

Figures 8.1 and 8.2 are phase RDP's for the range interfaced operating mode. As such, these RDP's show the insertion phase changes which occur as the antenna pointing direction changes. It is interesting to note that while small phase changes exist between adjacent pointing directions, phase changes as much as 180° as phi is varied through 360°. This peculiarity in performance results from the relative orinetation of the elements on the sphere. This orientation causes the elements at phi equal 0° to be 180° out of phase with the elements at phi equal 180°. It also causes the antenna to have a smoothly varying phase as a function of azimuth.

8.3 TEST DATA - OMNIDIRECTIONAL MODE

The phase test data (Figures 8.3 and 8.4) for the omni mode is similar to that of the range interfaced mode. Except for small coverage regions, the omni mode phase varies very slowly.

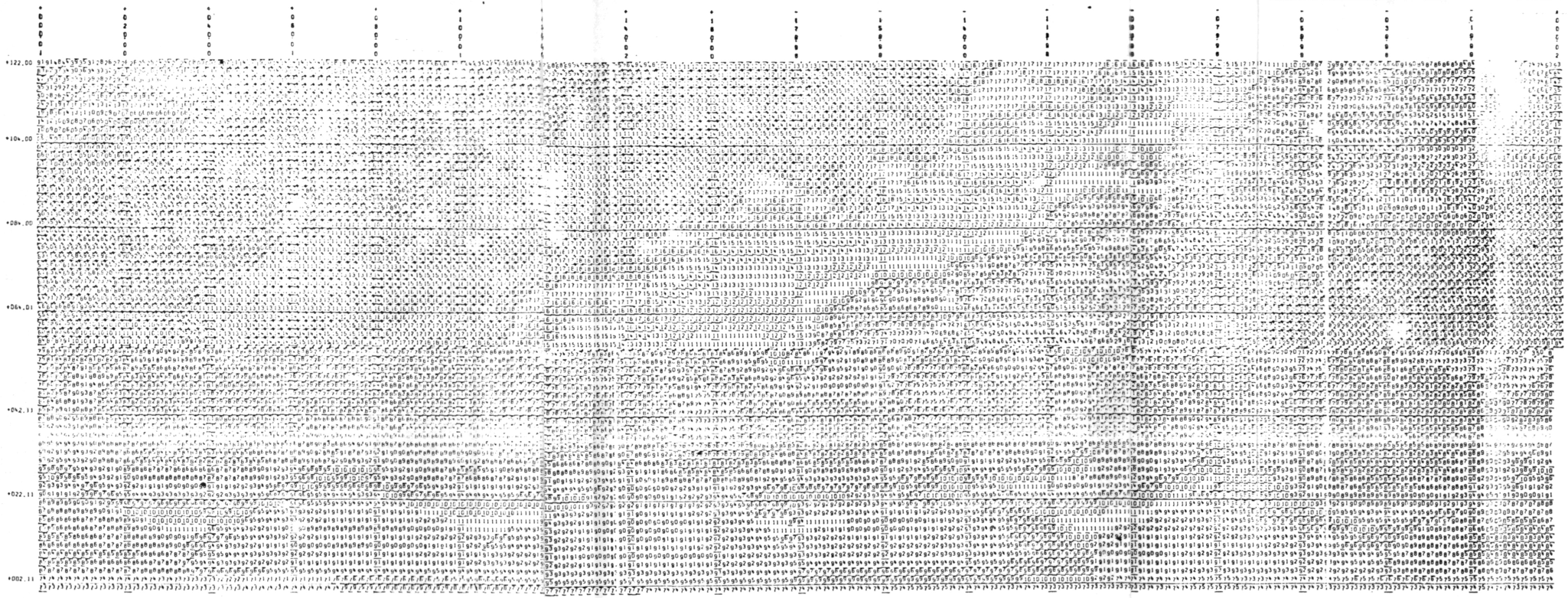


Figure 8.1 Range Interfaced Mode

Composite Face at 2106 MHz

FILE: DF001
REQ NR: 1 FREQ= [redacted] MHZ
LOT DATA: AA 4706

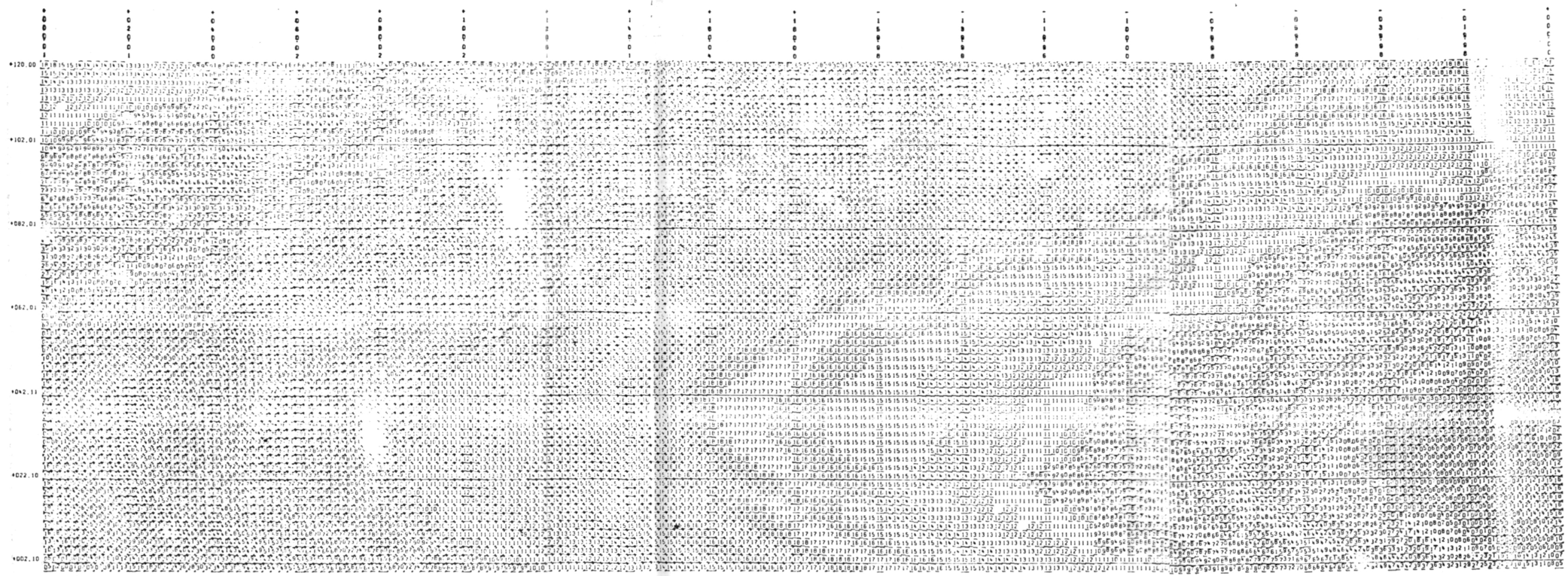


Figure 8.2 Range Interfaced Mode

Composite Face at 2287 MHz

2287 Composite Phase
FILE: DF8831 FREQ= 4883. MHZ
FREQ NR: 1
PLOT DATA: PA

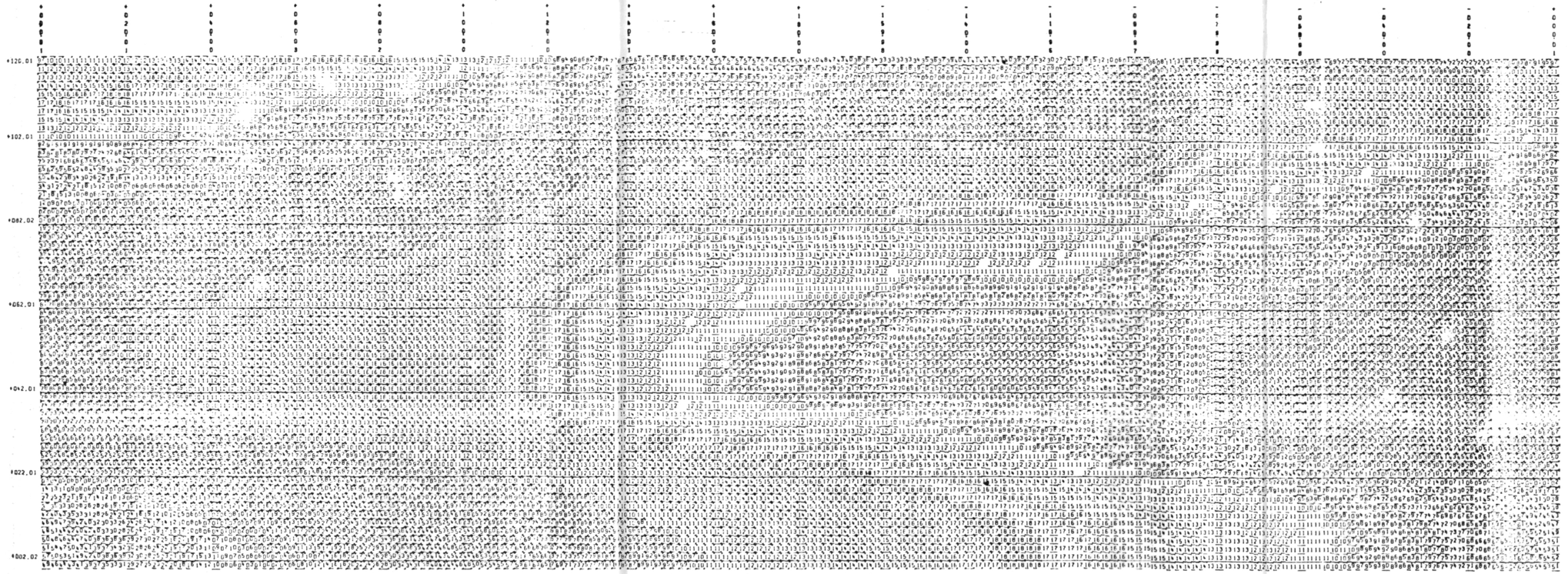


Figure 8.3 Omni Mode

Phase at 2106 MHz

Omni Phase [redacted]

FILE: DF005I
FREQ NR: 1 FREQ= 2106. MHZ
PLOT DATA: PA

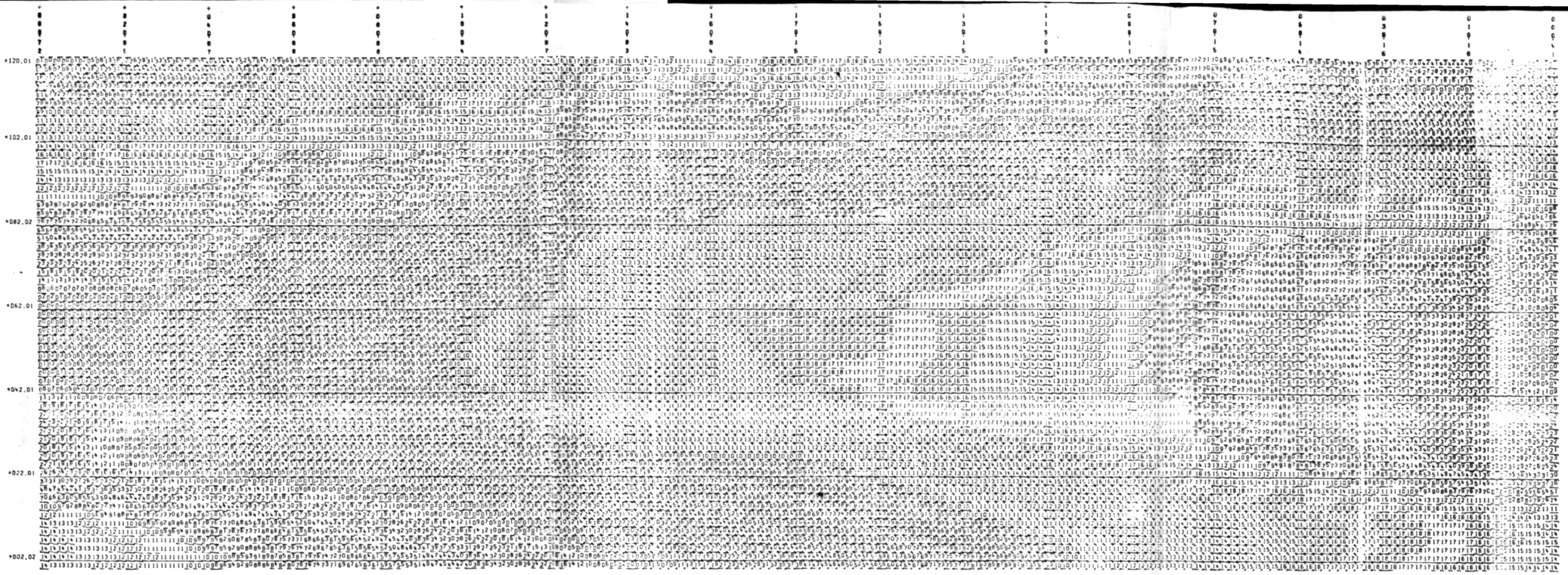


Figure 8.4 Omni Mode

Phase at 2287 MHz

Chapter 9
RETRODIRECTIVE MODE TESTING
(with NASA Standard Transponder)

Abstract

This chapter discusses the performance of the Auto Omni antenna when operated in the retrodirective mode. In this mode, the antenna uses a signal level estimate from the NASA standard transponder as an input to a search algorithm. This algorithm determines the direction of arrival of the received signal.

Testing of the final algorithm implementation was not performed because of restricted travel funds for NASA personnel involved in the test. This funding limitation forced a curtailment of the testing one day from completion.

9.1 INTRODUCTION

The objective of this series of tests was to obtain performance data on the Auto Omni antenna when operated in the retrodirective mode. In this mode, the Auto Omni antenna and microcomputer were interfaced with the signal level estimator (SLE) and NASA standard transponder (supplied by Motorola) and transmitter simulator (provided by NASA/GSFC).

The retrodirective mode testing consisted of three test phases:

Phase 1 - Gain calibration
Phase 2 - Retrodirective mode tests -- "weak"
Signal level ~ -115 dBm incident
Phase 3 - Retrodirective mode tests -- "strong"
Signal level ~ -100 dBm incident

These test phases were performed in the BASD 48-foot anechoic chamber.

9.2 PHASE 1 GAIN CALIBRATION

The gain calibration setup is shown in Figure 9.1. Gain calibration was performed to determine the relationship between gain and the transponder AGC TLM voltage. For this calibration, a standard gain horn antenna was installed on the range and the synthesizer power level driving the PN modulator was varied in 1 dB steps from -65 dBm to -40 dBm. At each power level, the transponder AGC TLM voltage was recorded. The results of this calibration procedure are shown in Figure 9.2. Figure 9.2 shows that the AGC TLM varies linearly with power level and may, therefore, be used as an accurate indication of relative gain. The AGC TLM's voltage slope is -54 mV/dB.

The Auto Omni was then installed on the range to establish the absolute gain reference AGC TLM voltage level. Figure 9.2 shows the range hardware interconnection. The range then positioned the Auto Omni antenna at theta and phi equal 0.1° and the omni range selected. At this pointing angle the Auto Omni gain is 4.4 dBic (2106 MHz). The AGC TLM level was then measured to be:

2.79V = 4.4 dBic gain with transmitter set to -50 dBm
2.06V = 4.4 dBic gain with transmitter set to -35 dBm

With this data, the absolute gain of the Auto Omni antenna could be determined for each acquired pointing angle based solely on the AGC TLM voltage.

9.3 PHASE 2 - RETRODIRECTIVE MODE TESTS - "WEAK"

Signal level ~ -115 dBm incident

Having calibrated the setup, the Auto Omni was put into position as shown in Figure 9.3. The transmitter was then set to -50 dBm which equates to an incident power level of -115 dBm. An arbitrary set of 61 pointing angles were then used to check out the antenna's direction finding capability. The antenna was allowed to determine the signal's direction of arrival four times at each of the 61 positions to verify the algorithm's repeatability. The Auto Omni microcomputer printed out the (theta, phi) coordinates during its six search phases followed by its final predicted direction of arrival. The set of elements in the final cluster were then recorded along with the AGC TLM voltage.

Table 9.1 shows the results of the weak signal retrodirective mode test. Included in this table are:

- Actual direction of arrival
- Elements which directed beam mode would use
- Elements and AGC TLM voltage from best of four acquisitions
- Elements and AGC TLM voltage from last of four acquisitions

along with calculated values:

- solid angle error
- gain

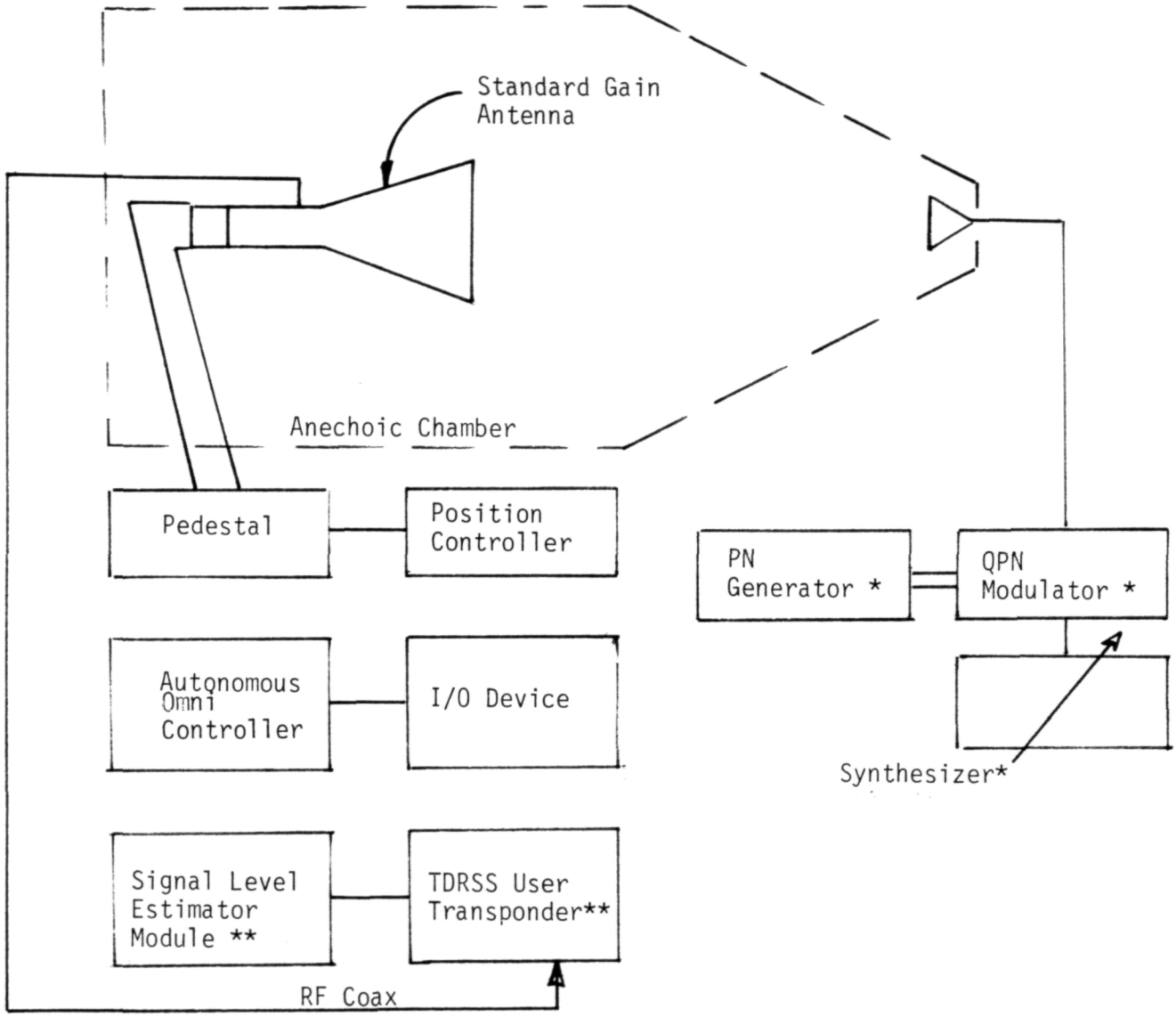
Based on the 61 pointing angles tested, the best acquisitions had a pointing angle error of 7.3° (solid angle) and a gain of 7.4 dBic. Using only the final acquisition at each position, Auto Omni had a pointing angle error of 11.6° (solid angle) and a gain of 6.8 dBic.

It should be noted the search algorithm has been modified so that the pointing angle used will be the same as the best pointing angle encountered during the six search phases. This improvement to the search algorithm will improve the accuracy of the acquisition.

9.4 PHASE 3 - RETRODIRECTIVE MODE TESTS -- "STRONG" SIGNAL LEVEL ~ -100 dBm INCIDENT

During phase three the transmitter level was increased by 15 dB from Phase 2. The data in Table 9.2 is the same as was in Table 9.1, except that the best of the four acquisitions and the last of the four acquisitions were the same. Also, the set of beam directions used only every fifth direction of Phase 2. As shown in Table 9.2, with a strong signal Auto Omni acquired with an average predicted solid angle error of 10.3° and gain of 7.0 dB.

To verify the accuracy of the acquisition, the beam directions were also entered into the directed beam mode and the gains measured. The average gains in this test case were 7.3 dB; only 0.3 dB better than found from the retro-directive mode.



* NASA Supplied
** Motorola Supplied

NOTE: The synthesizer has an internal variable attenuator

Figure 9.1 Gain Calibration Setup

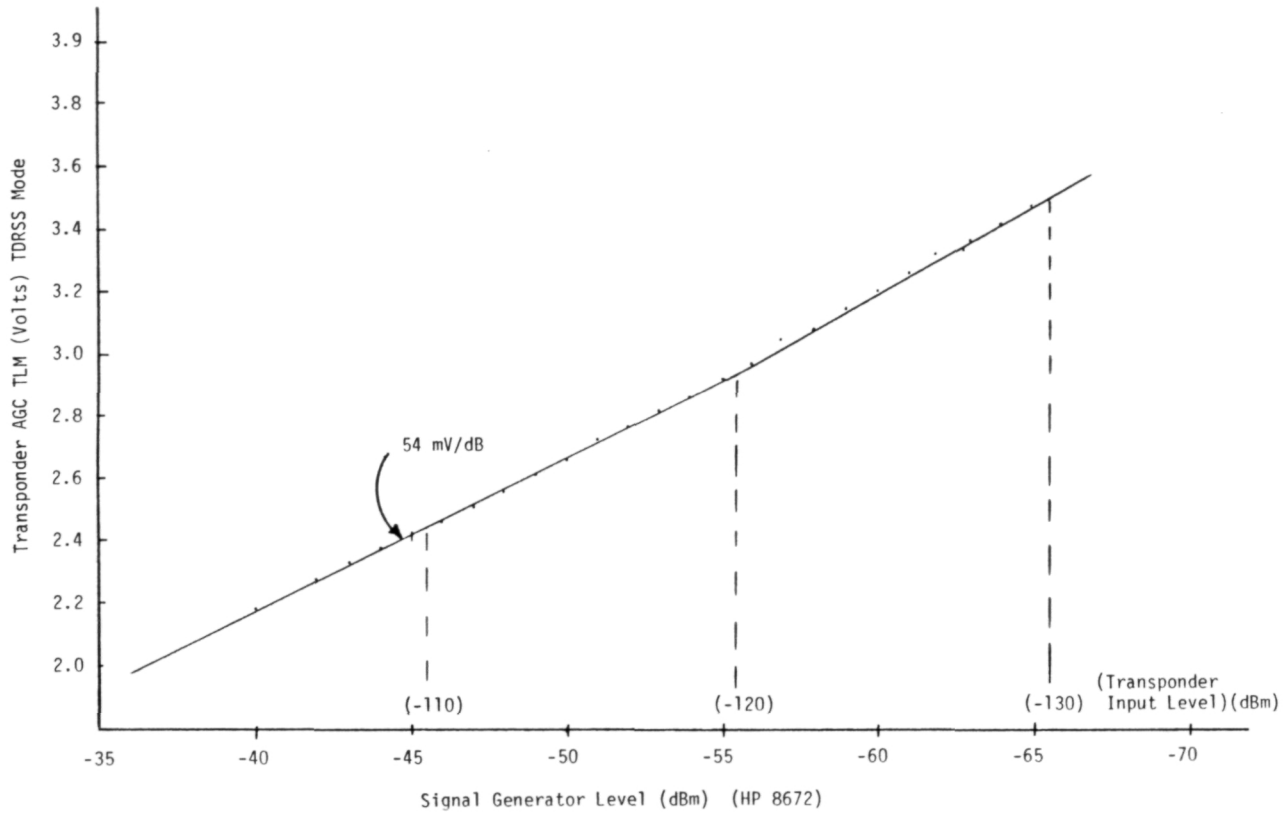
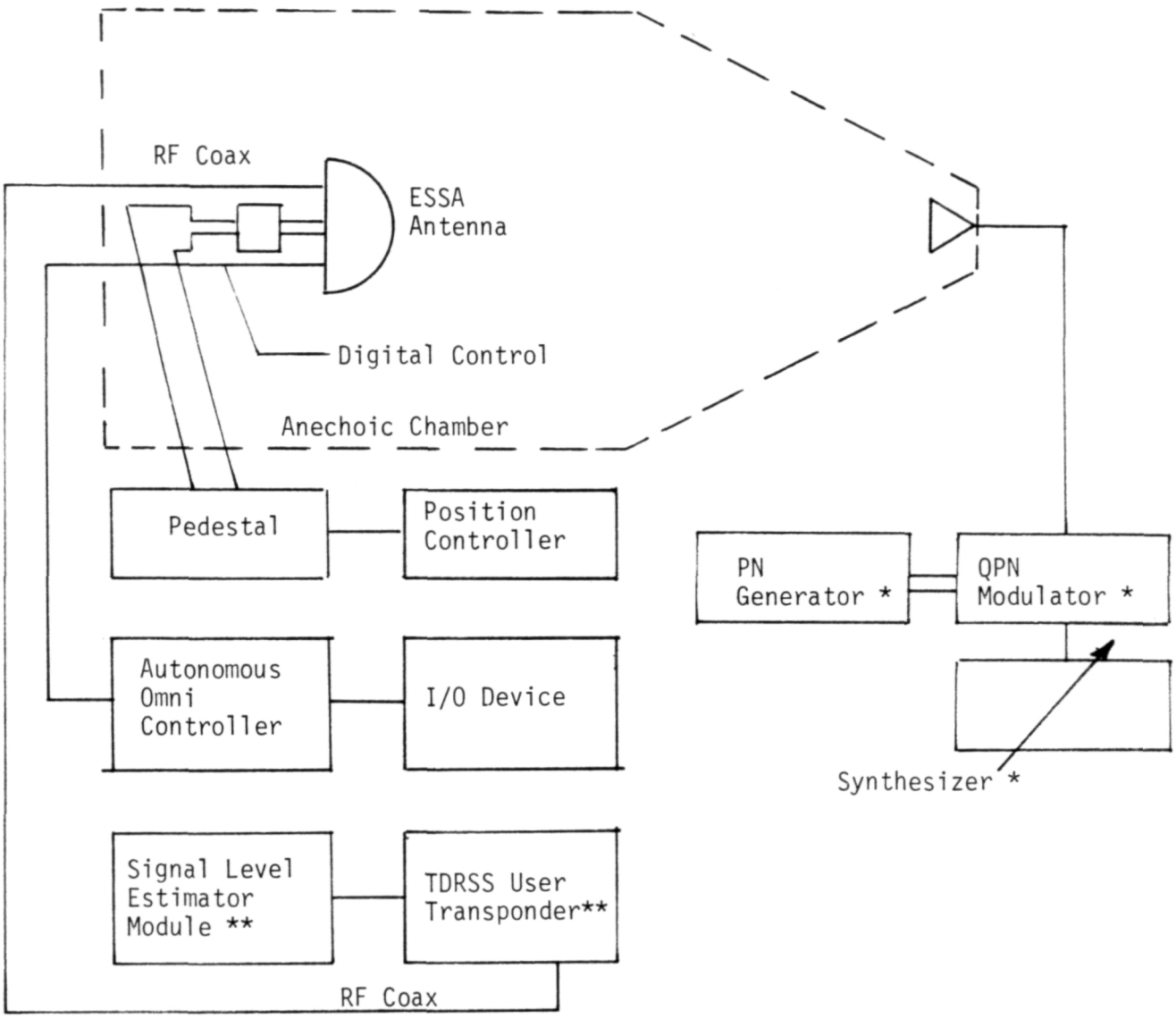


Figure 9.2 Transponder AGC TLM vs Test Signal Generator Level with Standard Antenna



* NASA Supplied
** Motorola Supplied

NOTE: The synthesizer has an internal variable attenuator

Figure 9.3 Autonomous Omni Range Test Setup

	DATA FOR LAST OF FOUR ACQUISITIONS									DATA FOR BEST OF FOUR ACQUISITIONS						
	True Direction			Calculated Direction						Calculated Direction Max. Gain Beam				A.O. Gain (dBic)		
Beam No.	ϑ	φ	Directed Beam Elements	ϑ	φ	Solid Angle Error	AGC TLM Voltage	A.O. Gain (dBic)	Final Antenna Elements	ϑ	φ	Solid Angle Error	AGC TLM Voltage	Max. Gain Beam	Final Elements Max. Gain Beam	
1	0.1	0.1	2, 3, 5, 6	3.7	179.0	3.8°	2.73	5.5	1, 4, 5, 6	13.2	338.6	13.1°	2.67	6.6	1, 2, 3, 6	
2	1.5	45.0	2, 3, 4, 6	5.0	175.0	6.1°	2.75	5.1	1, 4, 5, 6	4.2	8.1	3.1°	2.64	7.2	1, 2, 3, 6	
3	3.0	90.0	1, 2, 3, 4	0.1	195.5	3.0°	2.67	6.6	1, 2, 3, 6	*	*	*	*	*	*	
4	4.5	135.0	1, 3, 4, 5	7.2	358.4	10.9°	2.69	5.3	1, 2, 3, 6	*	*	*	*	*	*	
5	6.0	180.0	1, 2, 3, 4	10.9	177.3	4.9°	2.67	6.6	1, 4, 5, 6	*	*	*	*	*	*	
6	7.5	225.0	1, 4, 5, 6	1.8	174.9	6.5°	2.73	5.5	1, 3, 4, 5	0.5	346.9	7.8°	2.67	6.6	1, 4, 5, 6	
7	9.0	270.0	1, 2, 5, 6	10.1	348.2	12.0°	2.70	6.1	1, 2, 3, 6	*	*	*	*	*	*	
8	10.5	315.0	1, 2, 5, 6	10.5	325.8	2.0°	2.65	7.0	1, 2, 3, 6	*	*	*	*	*	*	
9	12.0	5.0	1, 2, 3, 6	18.4	352.1	7.2°	2.62	7.5	1, 2, 3, 6	*	*	*	*	*	*	
10	13.5	50.0	1, 2, 3, 4	14.5	9.4	9.7°	2.67	6.6	1, 2, 3, 6	*	*	*	*	*	*	
11	15.0	95.0	1, 2, 3, 4	11.3	18.1	16.5°	2.77	4.8	1, 2, 3, 6	*	*	*	*	*	*	
12	16.5	140.0	1, 3, 4, 5	6.0	172.5	11.9°	2.76	5.0	1, 4, 5, 6	8.9	162.1	8.9°	2.65	7.0	1, 3, 4, 5	
13	18.0	185.0	4, 5, 6, 9	14.7	191.8	3.8°	2.65	7.0	4, 5, 6, 9	*	*	*	*	*	*	
14	19.5	230.0	1, 4, 5, 6	9.2	241.9	10.7°	2.66	6.8	1, 4, 5, 6	*	*	*	*	*	*	
15	21.0	275.0	1, 2, 5, 6	14.3	272.0	6.8°	2.67	6.6	1, 2, 5, 6	*	*	*	*	*	*	
16	22.5	320.0	1, 2, 6, 11	27.9	324.8	5.8°	2.62	7.5	1, 2, 6, 11	*	*	*	*	*	*	
17	24.0	10.0	1, 2, 3, 7	23.8	332.3	15.0°	2.77	4.8	1, 2, 6, 11	17.6	374.2	7.0°	2.64	7.2	1, 2, 3, 7	
18	25.5	55.0	1, 2, 3, 7	24.4	100.0	18.6°	2.68	6.4	3, 4, 8, 13	*	*	*	*	*	*	
19	27.0	100.0	1, 3, 4, 8	30.9	156.1	26.5°	2.68	6.4	3, 5, 9, 14	30.7	112.4	7.0°	2.67	6.6	3, 4, 8, 14	
20	28.5	145.0	3, 5, 9, 14	26.0	190.9	20.7°	2.62	7.5	4, 5, 9, 15	29.8	156.0	5.5°	2.62	7.5	4, 5, 9, 14	
21	30.0	190.0	4, 5, 9, 15	38.3	216.5	16.9°	2.62	7.5	5, 9, 10, 15	*	*	*	*	*	*	
22	31.5	235.0	5, 6, 10, 15	24.4	100.0	51.4°	2.75	5.1	3, 4, 8, 13	*	*	*	*	*	*	
23	33.0	280.0	5, 6, 10, 16	24.8	263.1	11.5°	2.73	5.5	1, 5, 6, 10	33.6	261.5	10.1°	2.67	6.6	5, 6, 10, 16	
24	34.5	325.0	1, 2, 6, 11	28.6	337.7	8.9°	2.62	7.5	1, 2, 6, 11	*	*	*	*	*	*	
25	36.0	15.0	2, 3, 7, 12	40.5	368.4	6.1°	2.74	5.3	2, 7, 11, 12	*	*	*	*	*	*	
26	37.5	60.0	2, 3, 7, 13	43.2	73.7	10.5°	2.65	7.0	3, 7, 8, 13	*	*	*	*	*	*	
27	39.0	105.0	3, 4, 8, 13	30.4	115.9	10.6°	2.60	7.9	3, 4, 8, 14	*	*	*	*	*	*	
28	40.5	150.0	4, 8, 9, 14	46.9	123.5	19.3°	2.73	5.5	3, 4, 8, 14	*	*	*	*	*	*	
29	42.0	195.0	4, 5, 9, 15	45.0	212.9	12.6°	2.60	7.9	5, 9, 10, 15	*	*	*	*	*	*	
30	43.5	240.0	5, 6, 10, 15	51.2	232.4	9.5°	2.74	5.3	5, 10, 15, 23	*	*	*	*	*	*	
31	45.0	285.0	6, 10, 11, 16	42.0	302.5	12.4°	2.60	7.9	2, 6, 11, 16	*	*	*	*	*	*	
32	46.5	330.0	2, 6, 11, 12	44.5	336.5	5.0°	2.60	7.9	2, 6, 11, 12	*	*	*	*	*	*	
33	48.0	20.0	2, 3, 7, 12	49.1	336.5	32.3°	2.74	5.3	2, 6, 11, 12	40.2	382.5	8.0°	2.59	8.1	2, 3, 7, 12	
34	49.5	65.0	3, 7, 8, 13	39.0	77.3	13.5°	2.57	8.5	3, 7, 8, 13	*	*	*	*	*	*	
35	51.0	110.0	3, 4, 8, 14	50.8	103.8	4.8°	2.67	5.6	3, 8, 13, 14	46.3	111.9	4.9°	2.59	8.1	3, 4, 8, 14	
36	52.5	155.0	4, 9, 14, 21	49.8	128.2	21.0°	2.72	5.7	4, 8, 9, 14	60.6	149.2	9.4°	2.61	7.1	4, 9, 14, 21	
37	54.0	200.0	5, 9, 15, 22	55.1	200.6	1.2°	2.65	7.0	5, 9, 15, 22	*	*	*	*	*	*	
38	55.5	245.0	5, 10, 15, 23	43.1	232.2	15.7°	2.69	6.3	6, 5, 10, 15	52.9	261.5	13.6°	2.65	7.0	5, 10, 16, 24	
39	57.0	290.0	6, 10, 11, 16	42.0	303.2	18.0°	2.63	7.4	2, 6, 11, 16	53.3	304.6	9.4°	2.54	9.0	6, 11, 16, 25	
40	58.5	335.0	2, 11, 12, 26	56.5	333.4	8.1°	2.63	7.4	11, 12, 25, 26	*	*	*	*	*	*	
41	60.0	25.0	2, 7, 12, 17	59.9	367.3	15.3°	2.60	7.9	2, 7, 12, 17	*	*	*	*	*	*	
42	61.5	70.0	3, 7, 8, 18	54.0	78.8	10.6°	2.56	8.7	3, 8, 13, 19	*	*	*	*	*	*	
43	63.0	115.0	8, 14, 19, 20	54.4	118.9	9.2°	2.55	8.8	4, 8, 14, 20	*	*	*	*	*	*	
44	64.5	160.0	4, 9, 14, 21	58.2	161.1	6.4°	2.60	7.9	4, 9, 14, 21	*	*	*	*	*	*	
45	66.0	205.0	9, 9, 15, 22	60.1	215.5	11.1°	2.69	6.3	5, 10, 15, 23	58.5	206.7	3.0°	2.64	7.2	9, 15, 22, 23	
46	67.5	250.0	10, 15, 23, 24	58.5	261.8	11.0°	2.65	7.0	10, 16, 23, 24	*	*	*	*	*	*	
47	69.0	295.0	11, 16, 24, 25	63.3	304.9	10.7°	2.64	7.2	11, 16, 25, 26	60.5	305.0	12.4°	2.60	7.9	6, 11, 16, 25	
48	70.5	340.0	11, 12, 25, 26	68.7	337.4	2.8°	2.61	7.7	11, 12, 25, 26	*	*	*	*	*	*	
49	72.0	30.0	7, 12, 17, 18	74.3	28.3	2.8°	2.57	8.5	7, 12, 17, 18	73.1	26.3	3.7°	2.56	8.7	7, 12, 17, 18	
50	73.5	75.0	8, 13, 18, 19	78.9	65.4	10.8°	2.70	6.1	13, 18, 19, 33	79.5	74.4	6.0°	2.55	8.8	8, 13, 18, 19	
51	75.0	120.0	8, 14, 19,	30.0	131.4	12.2°	2.58	8.3	8, 14, 20, 21	*	*	*	*	*	*	
52	76.5	165.0	19, 14, 21, 22	70.0	170.4	12.7°	2.62	7.5	9, 14, 21, 22	*	*	*	*	*	*	
53	78.0	210.0	9, 15, 22, 23	52.1	211.5	25.9°	2.77	4.8	5, 9, 10, 15	78.4	211.0	1.1°	2.70	6.1	9, 15, 22, 23	
54	79.0	255.0	10, 16, 23, 24	82.8	256.1	4.0°	2.62	7.5	10, 23, 24, 30	80.8	264.7	9.7°	2.61	7.7	10, 16, 23, 24	
55	80.5	300.0	11, 16, 24, 25	79.3	324.0	23.7°	2.67	6.6	11, 25, 26, 31	*	*	*	*	*	*	
56	82.0	345.0	11, 12, 17, 26	86.0	350.3	6.6°	2.59	8.1	12, 17, 28, 31	*	*	*	*	*	*	
57	83.5	30.0	7, 17, 18, 27	88.5	29.9	5.0°	2.57	8.5	7, 17, 18, 27	*	*	*	*	*	*	
58	85.0	75.0	13, 18, 19, 33	93.7	66.6	12.1°	2.57	8.5	13, 18, 19, 33	*	*	*	*	*	*	
59	86.5	120.0	8, 19, 20, 28	81.2	121.6	5.5°	2.65	7.0	8, 14, 19, 20	*	*	*	*	*	*	
60	88.0	165.0	14, 21, 22, 29	89.8	175.4	10.6°	2.60	7.9	9, 21, 22, 29	*	*	*	*	*	*	
61	89.5	210.0	15, 22, 23, 35	83.1	215.1	8.2°	2.72	5.7	15, 22, 23, 25	*	*	*	*	*	*	
Average Values						11.6°		6.8				7.3°		7.4		

* No better beam found

Table 9.1 Phase 1 - Retrodirective Mode Testing with "Weak" Signal ~ -115 dBm Incident

Beam No.	True Direction θ	True Direction φ	Directed Beam Elements	Calculated Direction θ	Calculated Direction φ	Solid Angle Error	AGC TLM Voltage	A.O. Gain (dBic)	Final Antenna Elements	Directed Beam Gain (dBic)
1	0.1	0.1	2, 3, 5, 6	14.8	348.0	14.7°	1.95	6.4	1, 2, 3, 6	---
6	7.5	225.0	1, 4, 5, 6	10.0	161.8	9.4°	2.00	5.5	1, 3, 4, 5	6.6
11	15.0	95.0	1, 2, 3, 4	10.1	71.2	15.5°	2.05	4.6	1, 2, 3, 6	---
16	22.5	320.0	1, 2, 6, 11	20.7	316.9	2.1°	1.89	7.5	1, 2, 6, 11	7.5
21	30.0	190.0	4, 5, 9, 15	25.6	192.2	4.5°	1.90	7.4	4, 5, 9, 15	7.4
26	37.5	60.0	2, 3, 7, 13	38.5	76.1	9.9°	1.92	7.0	3, 7, 8, 13	7.5
31	45.0	285.0	6, 10, 11, 16	45.8	297.9	9.2°	1.89	7.5	6, 10, 11, 16	7.5
36	52.5	155.0	4, 9, 14, 21	51.9	131.9	18.2°	2.17	7.5	4, 8, 14, 20	7.5
41	60.0	25.0	2, 7, 12, 17	59.7	367.1	15.5°	1.88	7.7	2, 7, 12, 17	7.7
46	67.5	250.0	10, 15, 23, 24	68.3	263.4	12.4°	1.93	6.8	10, 16, 23, 24	5.5
51	75.0	120.0	8, 4, 19, 20	73.0	131.3	11.0°	1.87	7.9	8, 14, 20, 21	7.0
57	83.5	30.0	7, 17, 18, 27	84.6	29.7	1.1°	1.84	8.5	7, 17, 18, 27	8.5
Average						10.3°		7.0		7.3

Table 9.2 Retrodirective Mode Performance
Strong Signal Case (-100 dBm)



APPENDIX A

ESSA/ERBS TDRS
TRACKING PROGRAM



ESSA/ERBS TDRS
TRACKING PROGRAM

TN 82-06

Prepared by:

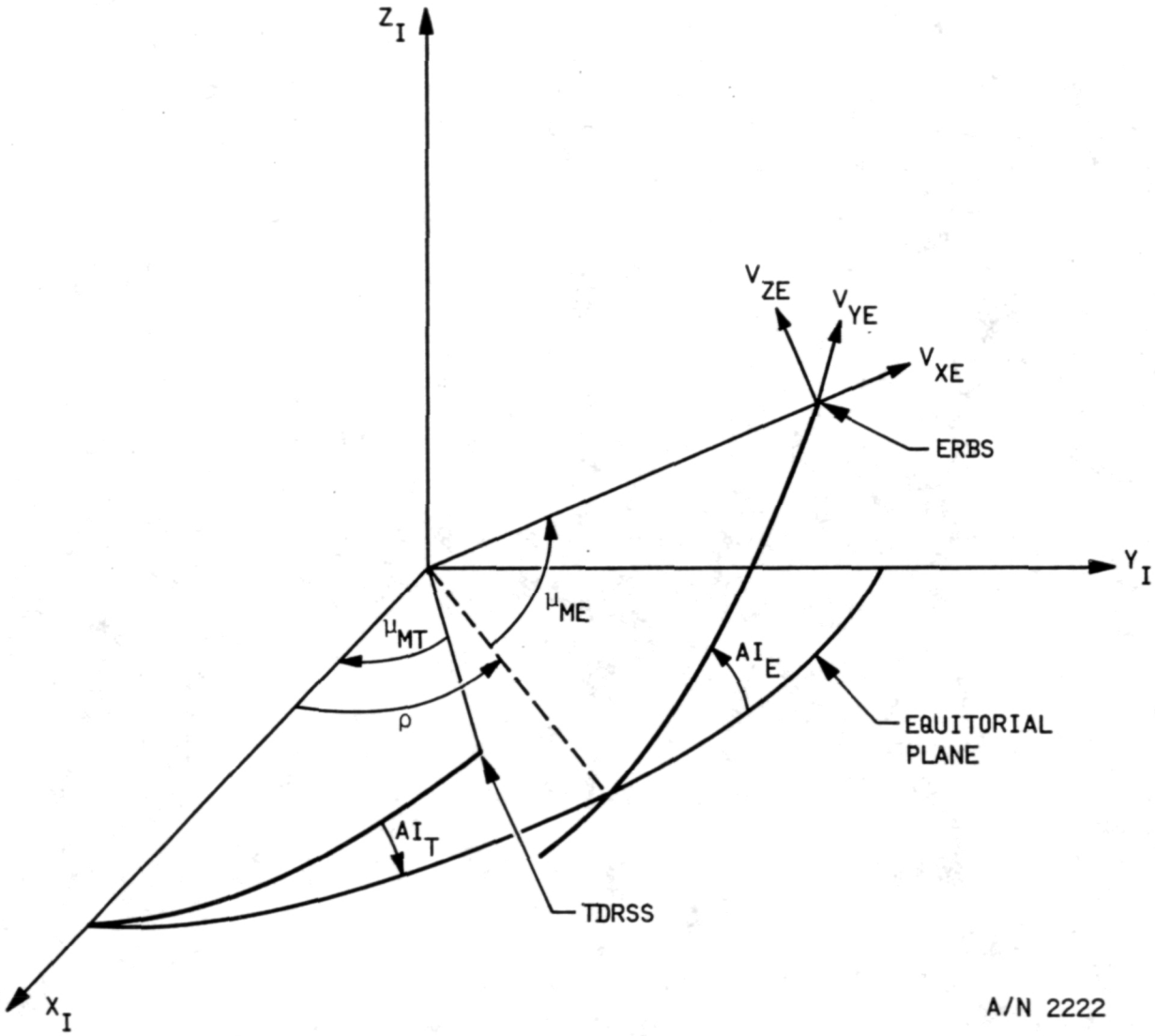
Bruce Thompson

Bruce Thompson
Senior Member of Technical Staff

Approved by:

John Bultena

John Bultena
ERBS, E&DH Subsystem Engineering
Manager


Z_I
V_{ZE}
V_{YE}
V_{XE}
ERBS
Y_I
μ_{ME}
μ_{MT}
ρ
AI_E
EQUITORIAL PLANE
AI_T
TDRSS
X_I

A/N 2222

TABLE OF CONTENTS

Section		Page
1	MICROPROCESSOR PROGRAM FOR STEERING THE ESSA/ERBS DIRECTIVE BEAM	1
	1.1 CALCULATING A TDRS BEAM STEERING VECTOR FOR THE ERBS SPACECRAFT	2
	1.2 COMMAND INPUT FOR THE ESSA/ERBS CONTROLLER	10
	1.3 REFERENCING TIME IN THE ESSA/ERBS CONTROLLER	15
	1.4 SOFTWARE VERIFICATION	16
2	MICROPROCESSOR SOFTWARE	17
	2.1 GENERAL TRACKING PROGRAM	18
	2.2 BEAM FORMING ROUTINE "BEAMS"	25
	2.3 ELEMENT ACTIVATION ROUTINE "FIRE"	25
	2.4 COMMAND ROUTINE	28

LIST OF FIGURES

Figure	Title	Page
i	Frontispiece	i
1-1	Coordinate Transformation #1	2
1-2	Coordinate Transformation #2	3
1-3	Coordinate Transformation #3	4
1-4	Coordinate Transformation #4	5
1-5	Coordinate Transformation #5	6
1-6	Coordinate Transformation #6	7
1-7	Coordinate System Translation	8
2.0-1	Counter Interrupt TASK	17
2.1-1	ERBS Tracking Program Initialization	19
2.1-2	ERBS/TDRS Tracking Program	20
2.1-3	ERBS/TDRS Tracking Program	22
2.1-4	ERBS/TDRS Tracking Program	23
2.2-1	BEAM ELEMENT Computation Routine	26
2.3-1	Element Activation Routine	27
2.4-1	Command Routine	29
2.4-2	Command Routine	30
2.4-3	Command Routine	31

SECTION 1 MICROPROCESSOR PROGRAM FOR STEERING THE ESSA/ERBS DIRECTIVE BEAM

The beam steering requirements for the ESSA/ERBS antenna are particularly severe. The antenna Z axis is constantly being reoriented to point along the nadir. This creates considerable relative motion between the vector from ERBS to TDRS and the antenna Z axis. This and other considerations led the ERBS project to forgo the automatic acquisition capability of the ESSA system and substitute a simplified "PROGRAMMED TRACK" program to determine where to point the ESSA directive beams.This program computes the ERBS orbit relative to the TDRSS orbits and translates the TDRSS position into the antenna coordinates. The beam steering angles are computed from these translated vectors.

The ERBS/ESSA "PROGRAMMED TRACK" microprocessor software evolved from the ESSA automatic acquisition software. To begin with. the program was exercised to see how well the automatic acquisition program subroutines would perform for the tracking calculations.We were concerned primarily with the trig functions. These were written as whole number entities supported by just the unsigned whole number multiply/divide feature of the TI-9900 microprocessor. These routines use table look-up and interpolation proceedures. They provide a good tradeoff of accuracy with speed and memory compactness for the acquisition program. The tracking program errors using these routines were well within the margin allowed by other expected system errors. The decision to adapt the ESSA software modules for the tracking program was based therefore on proven perforemance data.

Section 1.1 presents the geometric solution to the tracking problem and Section 1.2 discusses the command input data for the program. In section 1.3 ,the tracking program's method of relative time keeping is discussed. (It is necessary to understand the relative time keeping procedure to understand the command input and tracking features.) Some empirical results from the microprocessor program compared to a similiar program written in fortran for the VAX11/780 computer. are provided in Section 1.4 . Section 2 discussed the microprocessor program per se. Section 2.1 gives an overview of the program. Section 2.2 discusses the main beam forming routine "BEAMS" which determines a 12 element sub-set from the 145 element array. The 12 elements will be activated by the "FIRE" routine which is discussed in section 2.3. Paragraph 2.4 provides a flow chart for the command routine.

1.1 CALCULATING A TDRSS BEAM STEERING VECTOR FOR THE ERBS SPACECRAFT

One of the simplest solutions to a complex attitude determination problem is to bring the vector of interest step by step through successive coordinate rotations into a frame of reference pertinant to the desired solution. In this problem, the first frame of reference has the coordinate X-axis along the position vector to the TDRS satellite. The final frame of reference is the ESSA antenna coordinate system. The transformations are most easily understood if visualized one step at a time. Let us proceed step by step through the transformations.

o TRANSFORMATION 1: Visualize a coordinate system where the X-axis is pointing from the center of the earth to a TDRS satellite. We will let the Z-axis be normal to the TDRS orbit. (TDRS is considered to be in an orbit with an inertial period equal the inertial rotation period of the earth, which is slightly longer then 24 hours).Initially the TDRS orbit will have a zero inclination which will result in the TDRS satellite staying fixed over the same position on the earth. Gradually, the pull of the sun and moon will perturb the orbit to finite inclination**. This will cause the the orbit to trace a Lissajous pattern around the sub-satellite point on the equatorial crossing. The maximum latitude of the excursion will be equal to the inclination.

Grab the Z axis with your right hand. Your fingers will point in the direction of positive rotation. We now wish to move the X-axis from its current position to an X' position in the equatorial plane as shown in Figure 1-1. The angle from TDRS to the equatorial plane (measured in the TDRS orbit plane) is UMT. This is a negative rotation using the right hand rule.

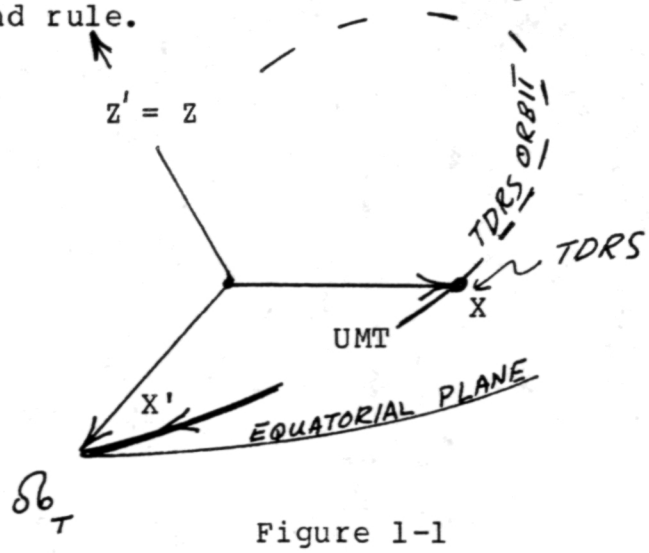


Figure 1-1

The new X' axis is also the ascending node of the TDRS orbit. The ascending node is the line formed by the intersection of the orbit plane and the equatorial plane as the satellite crosses from the southern to the northern hemisphere.

o TRANSFORMATION 2:This transformation consists of rotating the coordinate system around the new X'-axis through a negative TDRS orbit inclination angle. This rotation effectively places the new Y"axis in the equatorial plane as shown in Figure 1-2.

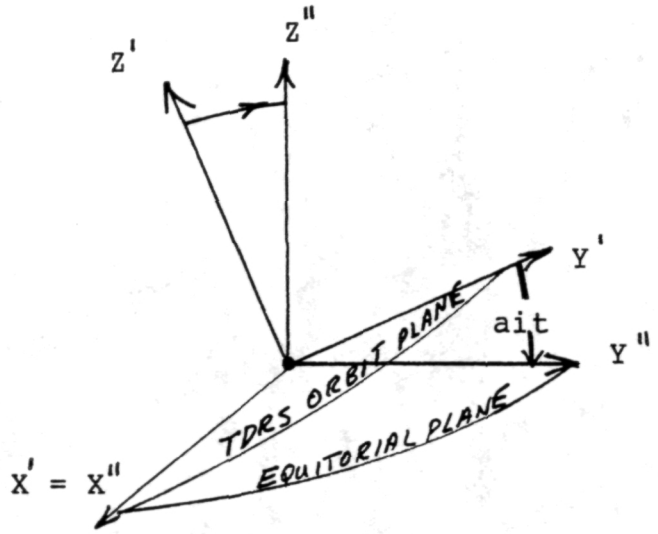


Figure 1-2

** The inclination of a typical TDRS orbit will increase from 0 to about 11 degrees in a nine year time span.

• TRANSFORMATION 3:To do this transformation, first define the parameter RHO(ρ). RHO is the difference in longitude between the TDRS orbit ascending node and the ascending node of the ERBS orbit at the moment of the next beam switch. The transformation consists of a rotation about the next Z axis through the the angle RHO. RHO is also the defference in the Right Ascension of the ERBS orbit node less the Right Ascension of the TDRS orbit node as shown in figure 1-3. The right ascension is the longitude of the node measured from an inertial reference(the Line of Aries Υ).

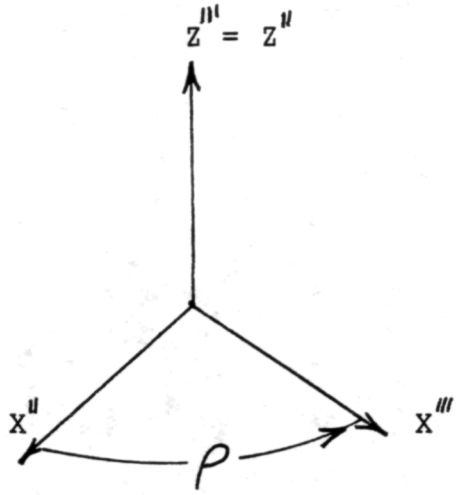


Figure 1-3

The ERBS orbit will be approximaty circular at an altitude of 600km inclined approximatly 50 degrees. This condition will cause the node to "regress" (move inertially counter clockwise) at a little more than five degrees per day. The TDRS orbit however will exhibit very little nodal motion. This is because the TDRS orbit initially has a very small inclination and a large semi-major axis. The parameters that are pertinant to the transformation are RHO and RHORATE. RHORATE is the angular change in RHO per one beam switching interval.

• TRANSFORMATION 4: The next transformation consists of a rotation about the ERBS orbit ascending node (X-axis) through the orbit inclination AI as shown in figure 1-4. This puts the Y^{IV}-Axis in the orbit plane along with the X^{IV}-axis . An approximate 50 degree orbit inclination is expected for the ERBS orbit.

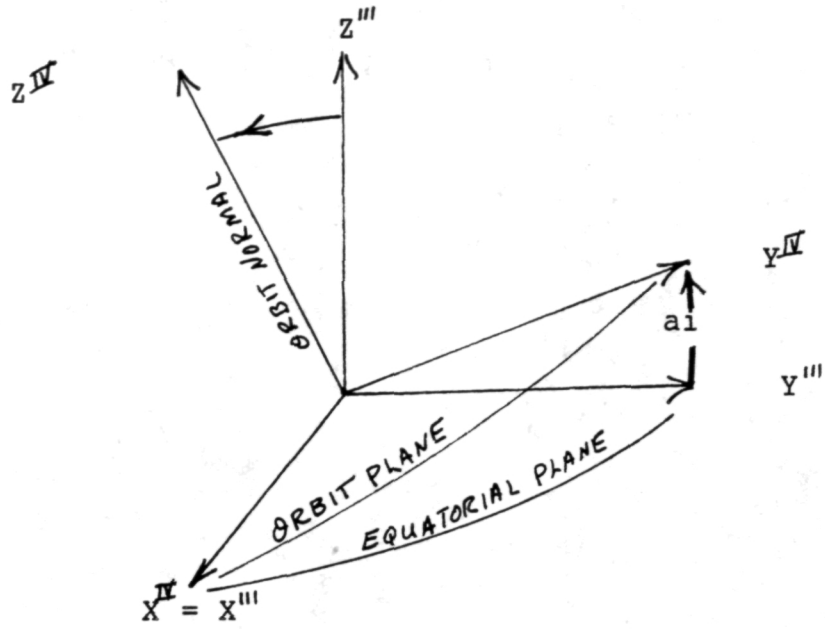
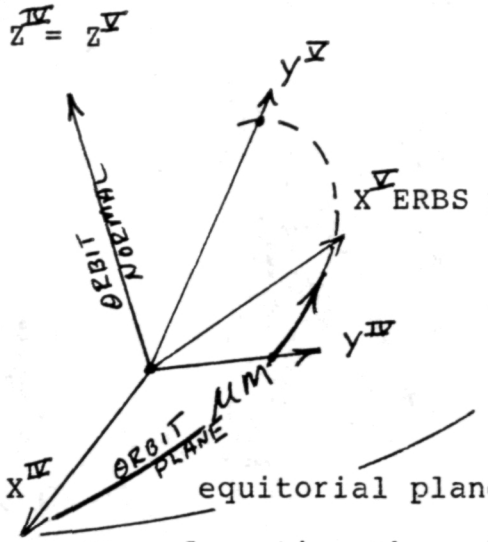


figure 1-4

• TRANSFORMATION 5: This transformation consists of a positive rotation around the orbit normal or Z^{IV} axis through the angle UM. UM is the angle from the ascending node of the orbit to the ERBS position vector at the moment of the next beam switch. UM is measured in the orbit plane as shown in Figure 1-5. UM is constantly being updated for the next beam switch. The parameter UMRATE is pertinent to updating UM. UMRATE is a function of the nodal period of the ERBS orbit.



The Y^{V} axis is now parallel to the velocity vector of the ERBS satellite.

Transformation Through Orbit Plane Angle UM

Figure 1-5

The X^{V} axis is now the local vertical, pointing from earth to the ERBS spacecraft.

• TRANSFORMATION 6: This is an optional transformation. The ERBS Spacecraft can be rotated around the vertical axis 180 degrees to fly backwards. This is a rotation around the X axis as shown in Figure 1-6. The program will examine a flag word in memory which can cause a branch around this transformation if the satellite is in its normal attitude.

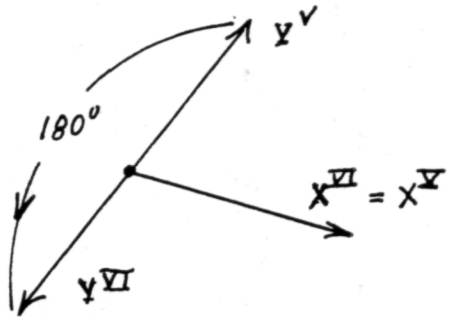


Figure 1-6

Final Rotation Around Local Vertical

• COORDINATE SYSTEM TRANSLATION: After the preceeding 5 rotations, we have 3 components (VTx, VTy, and VTz) of the cartesian vector VT that defines the direction to TDRS. VTx and VTy are in the orbit plane of ERBS. VTy is in the ERBS flight direction. VTz is normal to the ERBS orbit plane. Further VTx is co-linear with VE, the vector to erbs.

The vector of interest is between ERBS and TDRS, labled VL. It can be seen from Figure 1-7 that the 3 Cartesian coordinated describing VL are (VTx-|VE|) in the X direction , VTy in the Y direction and VTz in the Z direction or:

$$\overline{VL} = \begin{bmatrix} (VT_x - |\overrightarrow{VE}|) \\ VT_y \\ VT_z \end{bmatrix}$$

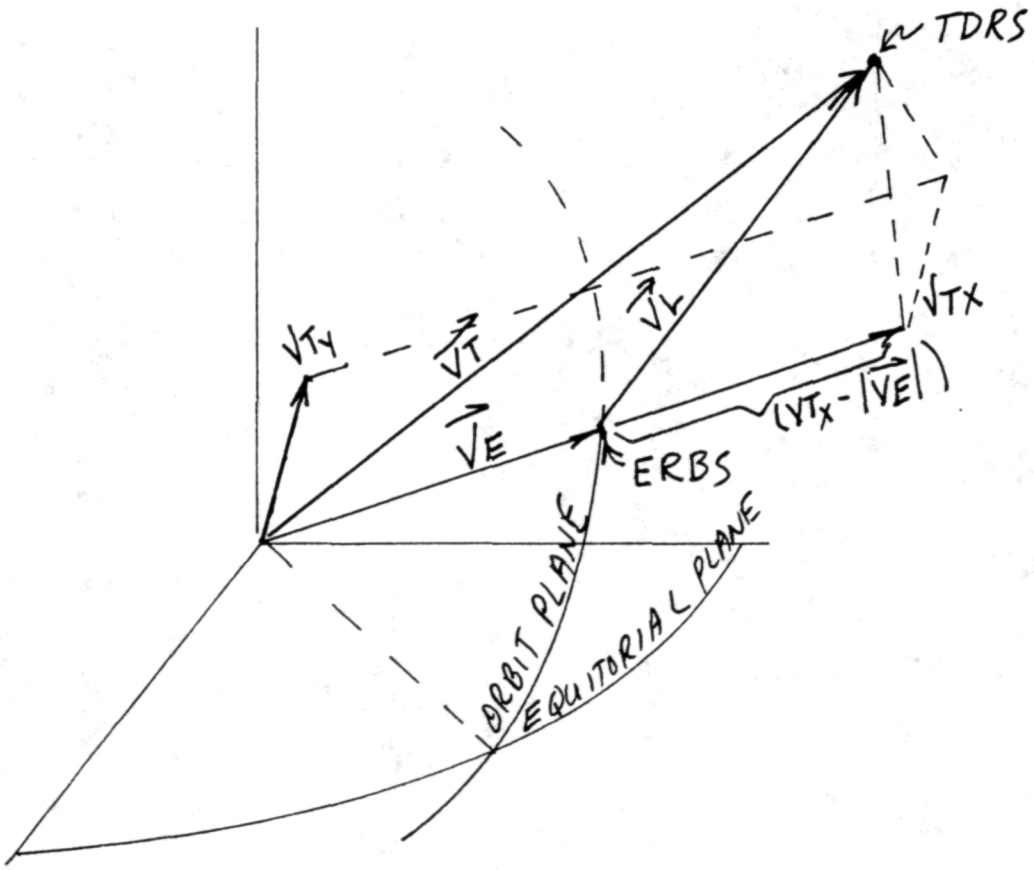


FIGURE 1-7

- COMPUTING THE BEAM STEERING ANGLES PHI AND THETA.

In the current system the translated X-axis is the Z-axis of the ESSA antenna. For the moment we will ignore this discrepancy, delete the prime notations, and compute phi and theta in the context of the current system.

Theta is the angle from the pole of the antenna to the pointing direction . In our current system:

$$THETA = \text{ARC COS}\left(X \Big/ \sqrt{(X^2 + Y^2 + Z^2)}\right)$$

where: X= VTx, Y= VTy, Z= VTz

Phi is measured counter-clockwise in the equitorial plane of the antenna. If we use the mathematical description shown below ,phi will be measured from the velocity vector to the pointing directions' projection onto the antenna equatorial plane.

$$PHI = \text{ARC TAN}\ (Z/Y)$$

The X,Y,Z components used above refer to the final coordinate system in which the prime notations have been deleted. The pointing vector to TDRS is now defined in antenna coordinates .

1.2 COMMAND INPUT DATA FOR THE ESSA/ERBS CONTROLLER

TABLE 1-1 shows the "TDRSS TRACKING REFERENCE TABLE" from the flight microprocessor program which references the parameter memory locations. The first twelve parameters are the data required as input for the calculations outlined in section 1.1. UM is the ERBS orbit plane angle measured from the ERBS orbit ascending node to the ERBS at the look ahead time (TUPD) which is always 0 to 15 seconds in advance of the current time. The program will perform the transformations shown in section 1.1 for just the designated West TDRS or just the East designated TDRS or optionally for both depending on the current setting of the flag SELTDR (see Table 1-1). Therefore 2 TDRS orbit plane angles ,UMTW and UMTE are registered for the designated West and East TDRS respectively. Similiarly RHOW and RHOE define the rotation angle from the respective West and East TDRS ascending node to the ERBS orbit ascending node.These parameters are true to the look ahead time which is always 0 to 15 seconds in advance of the current time. We will discuss the parameter time relationships in section 1.3 When the new values for the above are received via command update, they are moved into the ephemeris table in the microprocessor ram and their corresponding residual values (UMRES, UMTRW,UMTRE,RHOWR,RHOER) are set to zero. This clears the fractional value(portion less than .1 deg) which is constantly being updated using the rate algorithms described later in this paragraph.

We also need to know the orbit inclination of the ERBS orbit (AI), the orbit inclination of the designated West TDRS (AITW), and the orbit inclination of the designated East TDRS (AITE). These parameters are not time dependent.

All angles are input as degrees times 10. This gives us the accuracy required in a 16 bit whole number quantity.

The flag SELTDR is the key to how the program preforms the transformations. If SELTDR is set to 1 the program preforms the first coordinate rotation using just the values UMTW,AITW,RHOW. If SELTDR is set to 2, the rotation is done using the values UMTE,AITE,RHOE. If SELTDR is set to 0 the program loops through the set of transformations twice, using alternatly the first and second set of values. The program then selects the TDRS having the smallest theta. Thus the program will automatically select the TDRS whose direction is closest to the pole of the antenna.

The rate parameters RORATE and UMRATE reflect the rate that RHO and UM advance during the 15 second update period. They are provided to the program in an unconventional format. We know that for a nominal 600 km. orbit , UM will advance .9 and some fraction degrees in 15 sec.The altitude will of course vary from 600 km. but even a gross variation will not change the .9 deg part of the number.Therefore that part of the rate change is assumed by the program. The rate value provided to the spacecraft will be that part of the rate number to the right of the 9 digit or the significient digits beginning with the 1/100 digit. This residual is multiplied by 10 and then multiplied by 2 to the 16 power to create a binary number between 0 and 65535. The 16 bit whole number is then sent to the spacecraft via telemetered command. For each UM update calculation the program will add the whole number 9 to UM (All angles are retained in whole numbers of degrees x 10). The value of UMRATE is then added to a memory cell holding the UM residual value(UMRES). Whenever this summation overflows a 16 bit entity(65535) the program will increment UM. This effects a carry over of a 1/10 degree significient digit. This method provides the precision required to track UM to an accuracy of a fraction of a degree over several days of uninterrupted position extrapolation.The UMTW and UMTE calculations are preformed in the same fashion with the exception that the rates for both of these parameters are an assumed constant in the program as indeed they must be if the TDRS satellites are to remain in geo-synchronous orbits.

The parameter RORATE is the rate at which the ERBS orbit ascending node is closing on the TDRS ascending node. The ERBS orbit with its relatively low inclination and altitude will regress (move inertially westward) at a rate of 5 to 6 degrees per day. The ascending nodes of the TDRS satellites will move very slowly at very similiar rates. We are assuming that one average value for RORATE will suffice for both TDRS .***

The command input AI need probably be input only once during the life of the spacecraft. AITW and AITE will probably need to be updated every three to four months due to the suceptibility of the higher TDRS orbits to change inclination. IPH and ITH are input only if SELTRD is set to 3 which also causes the program to branch around the algorithm that updates phi and theta from the transformed TDRS vectors. (The program continues with the orbit parameter timeout updating while in the "FIXED POINT" mode to facilitate switching back to "PROGRAMMED TRACK").

The flags SELTDR and FLYBK are also set by ground command.FLYBK is set to 1 if the spacecraft is rotated around its vertical by 180 deg.

*** The recession rate of the orbit node varies proportionally to the cosine of the orbit inclination and inversly proportionally to the orbit semi-major axis raised to the 3.5 power.

```
*** *** *** *** *** *** *** *** *** *** *** *** *** *** *** ***
*** TDRSS EPHEMERIS TRACKING REFERENCE TABLE
UM        EQU       >CC00    ORBIT PLANE ANGLE ERBS @ TUPD
UMTW      EQU       >CC02    ORBIT PLANE ANGLE FOR WEST TDRS
UMTE      EQU       >CC04    ORBIT PLANE ANGLE FOR EAST TDRS
RHOW      EQU       >CC06    RHO ANGLE FOR WEST TDRS ORBIT
RHOE      EQU       >CC08    RHO ANGLE FOR EAST TDRS ORBIT
RORATE    EQU       >CC0A    RHO RATE OF CHANGE
UMRATE    EQU       >CC0C    UM RATE OF CHANGE
AI        EQU       >CC0E    ORBIT INCLINATION OF ERBS ORBIT
AITW      EQU       >CC10    ORBIT INCLINATION FOR TDRS WEST ORBIT
AITE      EQU       >CC12    ORBIT INCLINATION FOR TDRS EAST ORBIT
SELTDR    EQU       >CC14    FLAG FOR SELECTING EAST/WEST TDRS
FLYBK     EQU       >CC16    YAW AROUND FLAG (1) FLYING BACKWARDS
*
***       GSFC TEST CASE INPUT ***
*** MNEMONIC     HEX VALUE      DECIMAL VALUE
*         MU     => 517           130.3    DEG.
*         RHOW   => 5FC           153.2    DEG.
*         RORATE=> A06B          .062663   DEG./15 SEC.
*         UMRATE=> 4EF2          .930837   DEG./15 SEC.
*         AI     => 226            55.0    DEG.
*         AITW   => 64             10.0    DEG.
*
IPH       EQU       >CC18    BEAM STEERING PHI VALUE
ITH       EQU       >CC1A    BEAM STEERING THETA VALUE
*
TUPD      EQU       >CC1C    BEAM UP DATE TIME
***
*    THE BEAM UP DATE TIME ARE ADVANCED EVERY 1875 COUNTS ON
*    THE HIGH ORDER COUNTER. THIS CORRESPONDS IN TIME TO
*    1875 * 8 MILISECONDS WHICH IS EQUAL TO 15 SECONDS.
*    IN 15 SECONDS , THE SATELLITE WILL HAVE MOVED ABOUT
*    .93 DEGREES IN THE ORBIT PLANE AND THE LONGITUDE OF
*    TDRS WILL HAVE CLOSED ON THE ORBIT NODE BY ABOUT .63 DEG.
*
*    ALL ANGLES ARE IN DEGREES X10.
*
*    THE RATE PARAMETERS ARE :
*      (DEGREES*10/UPDATE PERIOD - LESS THE WHOLE NUMBER
*       - LEFT OF DECIMAL POINT) *2**16
*
*    SELTRD :0 SELECTS THE TDRS WITH THE LOWEST THETA
*           :1 SELECTS THE WEST TRDS
*           :2 SELECTS THE EAST TRDR
*           :3 SELECT THE COMMAND INPUT PHI AND THETA
*              WHILE STILL UPDATING ORBIT STEERING DATA
*
*                      TABLE 1-1
*** *** *** *** *** *** *** *** *** *** *** *** *** *** *** ***
```

1.3 REFERENCING TIME IN THE ESSA/ERBS CONTROLLER Event time is registered using an external counter which is counting a constant square wave clock signal. When the counter fills up and recycles to zero, it sends a pulse to an interrupt circuit in the microprocessor. This is the only interaction between the microprocessor and the counter.This means the counter is free running. The free running counter circumvents the problem many computer systems have with internal interrupt timers ,namely the gradual buildup of time errors from the time slice lost in resetting internal processor clocks.

The counter pulses arrive at the microprocessor every 8 milliseconds. The ESSA microprocessor simply counts these pulses. This is done as an independent task. The time pulse triggers interrupt 1. This jumps the processor from its current task to the counter program which simply increments a 16 bit register and then returns control back to the interrupted task. This counter register can also be addressed with the label "CLOCK2".

All the orbit calculation parameters are registered to a look-ahead time "TUPD". This in turn corresponds to a binary value of the counter register or "CLOCK2". When the commands arrive from the ground containing the orbit up date value UM , the processor loads the number 1875 in a register and adds the current value of CLOCK2 to it. The result is stored in the beam activation look-ahead time" , "TUPD". This means that the value transmitted via command for UM should be true for 15 seconds in advance of the instant of time that the command reaches the microprocessor.(The value 1875 x 8 millisecond/counter increment is equal to 15 seconds.) When the "UM" command data word is received, the processor will be directed back to the beginning of the orbit calculations loop which computes the look-ahead TDRS vector and the active beam elements to form a beam around that vector. Meanwhile the counter (CLOCK2) is advancing independently. After the beam elements have been computed, the main program executes a tight loop waiting for for "CLOCK2" to advance and equal "TUPD". When this occurs the processor fires out the beam and then computes new look-ahead values for UM,UMTW,UMTE,RHOW,and RHOE registered to a new look ahead time "TUPD" which is also advanced 15 seconds. The Processor then performs the new set of transformations, computes the new beam elements and then spends the better part of 15 seconds waiting for CLOCK2 to advance to equal TUPD. Ideally the new command data containing "UMTW", "UMTE","RHOW",AND "RHOE" would be transmitted just prior to the command containing "UM". This would effectivly register all the time dependent parameters to the same beam activation time "TUPD". If these update commands are not transmitted, with the "UM" command data word, a 0 to 15 second error in time correlation will occur. The next fastest changing parameters are "UMTW" and "UMTE". In 15 seconds these parameters change about .0625 degrees. Therefore not

updating these quantities would introduce nominal errors of about three hundredths of a degree. A singular omission of these command data would not produce a substantial error in the tracking results . The omission of these data for a number of sequential command updates would however.

One advantage of the time registration method described above is that there is no book keeping involved when the counter overflows. At some point in time we will add 1875 (1875 x 8msec.=15 sec.) to an almost full "TUPD" register and it will change from a very large number to a very small number. Similarily CLOCK2 will overflow and recycle to zero. The beam activation will occur when CLOCK2 counts up to the new small value of TUPD. other parameters.

1.4 SOFTWARE VERIFICATION

As mentioned earlier on of the initial concerns was whether or not the existing ESSA software trigonmetric functions were accurate enough to support the critical tracking routines. This question was answered by actual software verification tests in which all the mathematics and logic described in 1.1 through 1.3 were programmed in the ESSA EMU controller and compared to exact calculations done in Fortran on a VAX11/780 computer.

The Phi and Theta pointing directions are presented in one minute intervals in Table 1-2. For convenience exerpts of the results are compared after 6,12,18 and 24 hours. The data assumes a TDRS orbit at 0 degrees inclination.

In comparing the results in Table 1-2, the maximum observed error is on the order of a few tenths degrees. Since the beamwidth of the ESSA/ERBS antenna will be nominally 26 deg with 6 deg steering increments coordinate variations on the order of tenths of degrees will have no effect on the pointing accuracy or coverage gain.

The conclusion then is that the present ESSA EMU controller with its attendant software library functions will support a simplified orbital mechanics solution necessary to implement a programmed track function. In addition this capability has been implemented,debugged and demonstrated for the ERBS mission scenario.

ELAPSED TIME (hr)	ESSA RESULTS		EXACT RESULTS	
6	61.3	71.8	61.4	71.9
12	37.7	251.0	37.7	251.2
18	71.0	301.7	71.0	301.5
24	34.5	74.1	34.6	74.0

Table 2-1

SECTION 2 MICROPROCESSOR SOFTWARE

This section contains some overview flow charts of the ESSA/TDRS tracking software. No attempt has been made to make these flow charts rigerous. they are simply road maps to guide the reader through the source listing. The source listing has been carefully anotated to document each and every operation.

The tracking program is organized as three seperate program tasks operating asynchronously and independently. There is some subtle interaction between the Command routine and the general tracking program which will be explained in section 2.1 and 2.4. For the most the two highest priority tasks ,the Counter Interrupt routine and the Command routine simply modify or input values to the ram memory tables that the general tracking program will access during the course of its computations.The Counter Interrupt task and the Command Input routine are driven from external stimuli to the SBP-9900 internal interrupts 1 and 3. Interrupt 2 is not used. The main program is activated by the power on restart interrupt and the processor returns to this task after completing the Interrupt 1 and 3 tasks.

Figure 2.0-1 shows the function of the highest priority Counter interrupt task

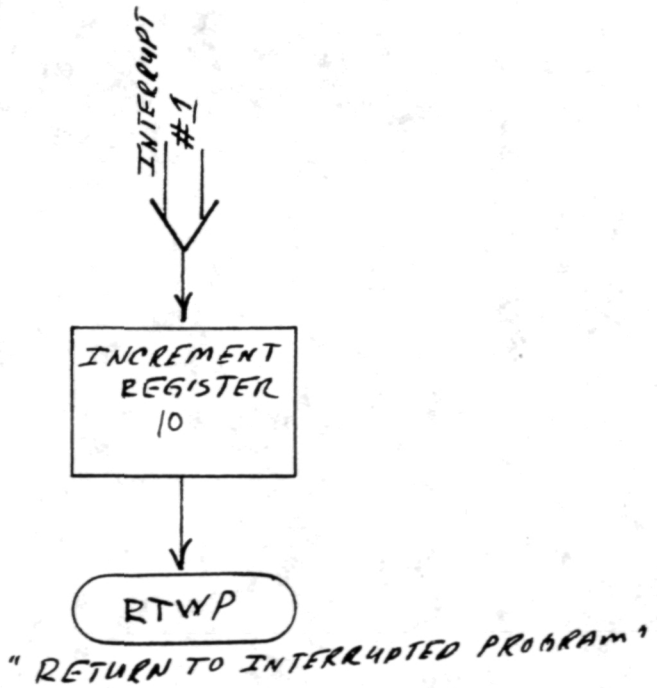


Figure 2.0-1
"Counter Interrupt Task"

2.1 GENERAL TRACKING PROGRAM

Figure 2.1-1 shows the initialization portion of the tracking program. Program location lables are shown in quotation marks. In a number of instances there is a memory location will be referred to in a dual fashion. For example the parameter "CLOCK2" and register 0 of the Timer Interrupt routine are the same cell of memory. In the equate statements at the beginning of the program the label "CLOCK2" has been equated to the first register location of the Counter Interrupt routine workspace. The reason for doing this is that a subprogram can address one of its designated registers in one half the machine cycles as it can a general label. Locations that are adressed frequently in tasks or subroutines have this duel referencing scheme. To make the flow charts easier to we have provided a table showing these duel locations.

label	register;subroutine/task	function
CLOCK2	0 ; TIMER INTERRUPT ROU.	FREE RUNNING TIMER
CLOCK3	3 ; TIMER INTERRUPT ROU.	CLOCK2 OVERFLOW
GSEOF	9 ; TIMER INTERRUPT ROU.	GSE OUTPUT FLAG
RNOTM	8 ; COMMAND ROUTINE	CMD. RUNOUT TIME
CMFPF	9 ; COMMAND ROUTINE	FIXED POINT FLAG
SETCMZ	10; COMMAND ROUTINE	COMMAND SEQUENCE FLAG
CMFPHI	11; COMMAND ROUTINE	FIXED POINT PHI VALUE
CMFTHE	12; COMMAND ROUTINE	FIXED POINT THETA VAL.

An example of this duel address scheme is illustrated in figure 2.1-1. Right after the Power on Interrupt is activated at turn on, processor sets the memory location "SETZM" to 0. This means that when the command routine is entered the first time, it will test its register 10(for 0) and conclude that the command input is a Command Identifier word. Further on in figure 2.1-3, we see the General Tracking Tracking program resetting "SETZM" if the look-ahead beam up date time has exceeded the command runout time "RNOTM". This provides us a convienient time limit to wait for a command data word. If is does not come in 15 to 30 seconds, the processor assumes it is not comming at all and resets "SETZM" so that it will start looking for command identifier words.

Right after the microprocessor is powered up,the steering mode select flag in memory location "SELTDR" is set to 3. This puts the

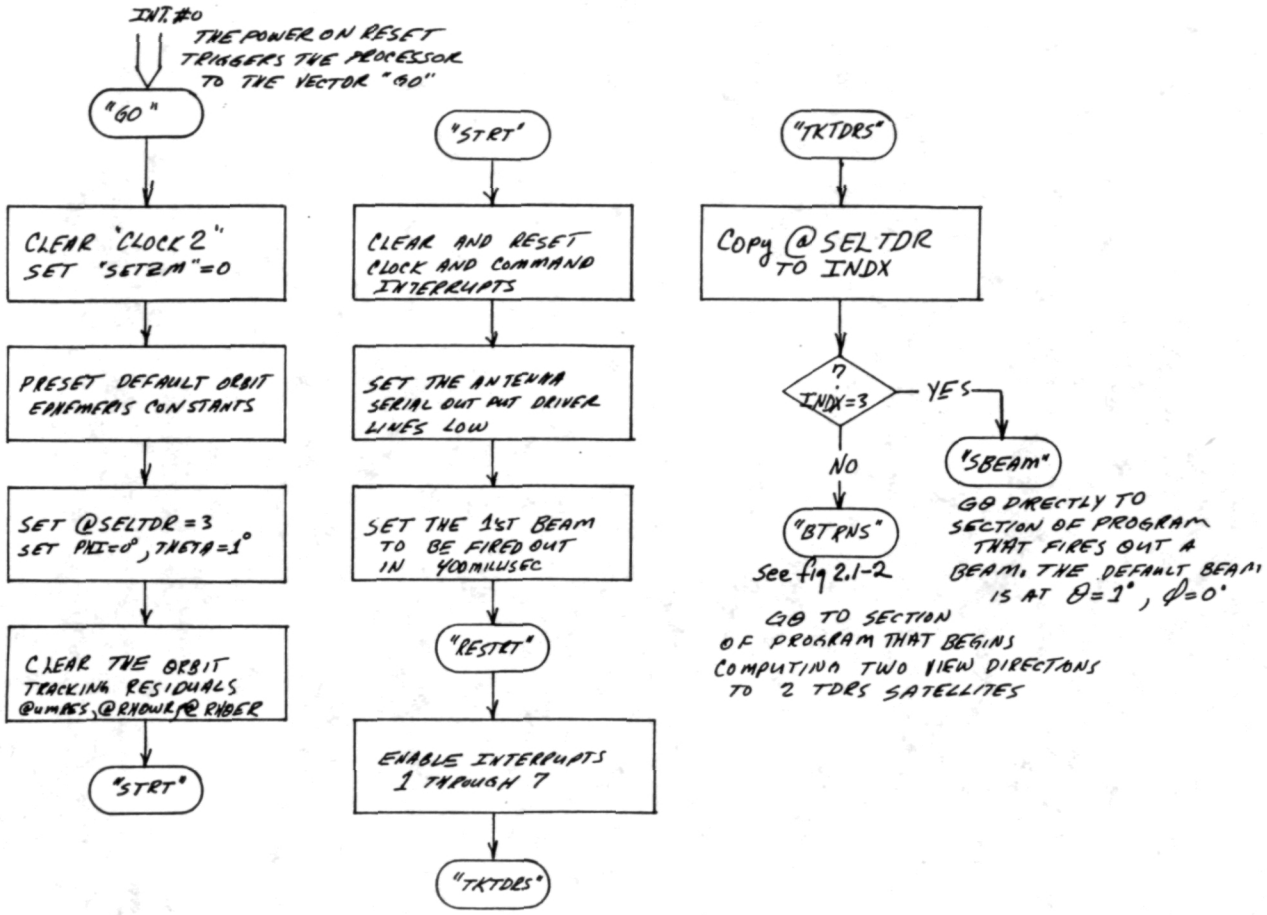


FIGURE 2.1-1 ERBS TRACKING INITIALIZATION

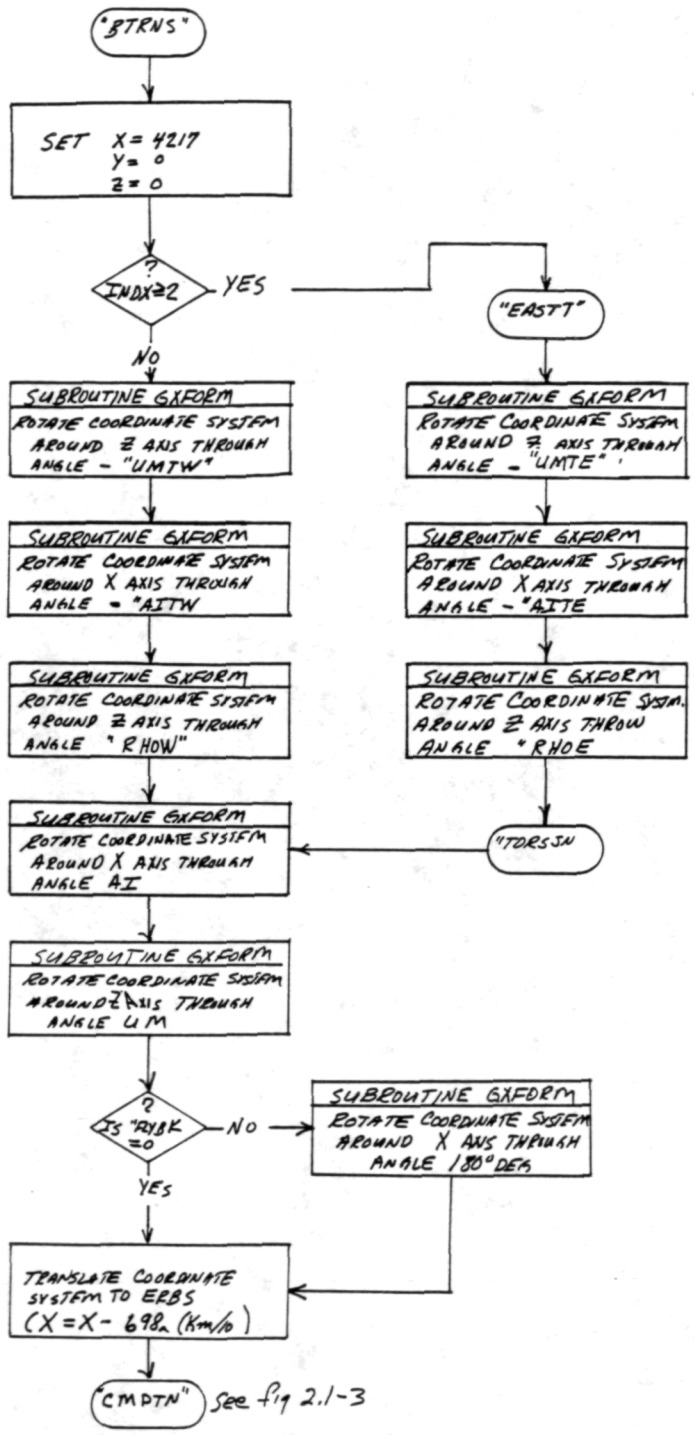


figure 2.1-2 ERBS/TDRS TRACKING PROGRAM

microprocessor in the "Fixed Point" steering mode . Since phi and theta are set to or near zero, the beam will be directed along the ERBS nadir. This condition will exist until "SELTDR" is set to 0,1,or 2 by ground command (see section 2.4). The reset portion of the program can also be re-executed by a ground command which branches the program back to the label "GO". The normal recycle location is at the label "TKTDRS" also shown on figure 2.1-1.

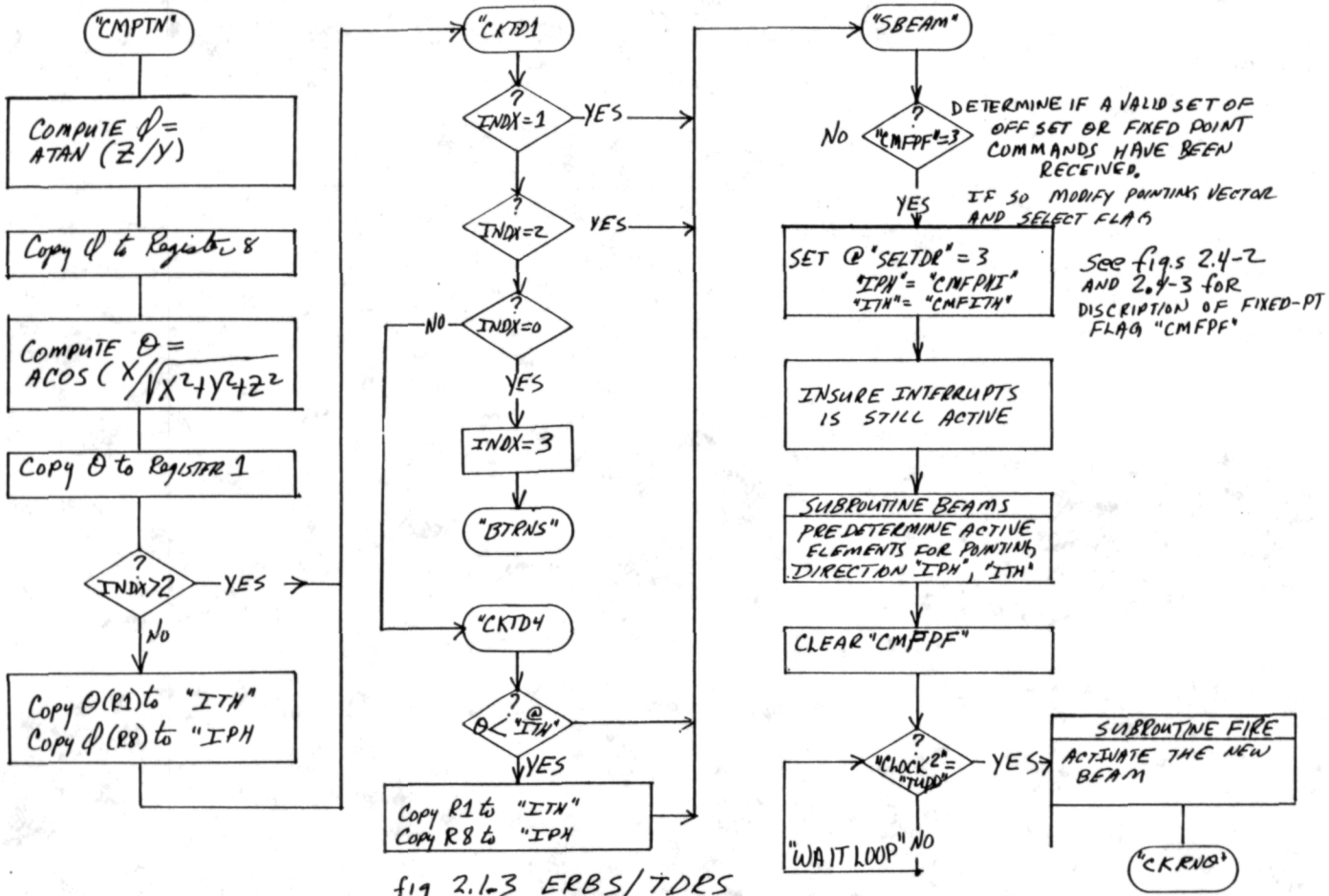
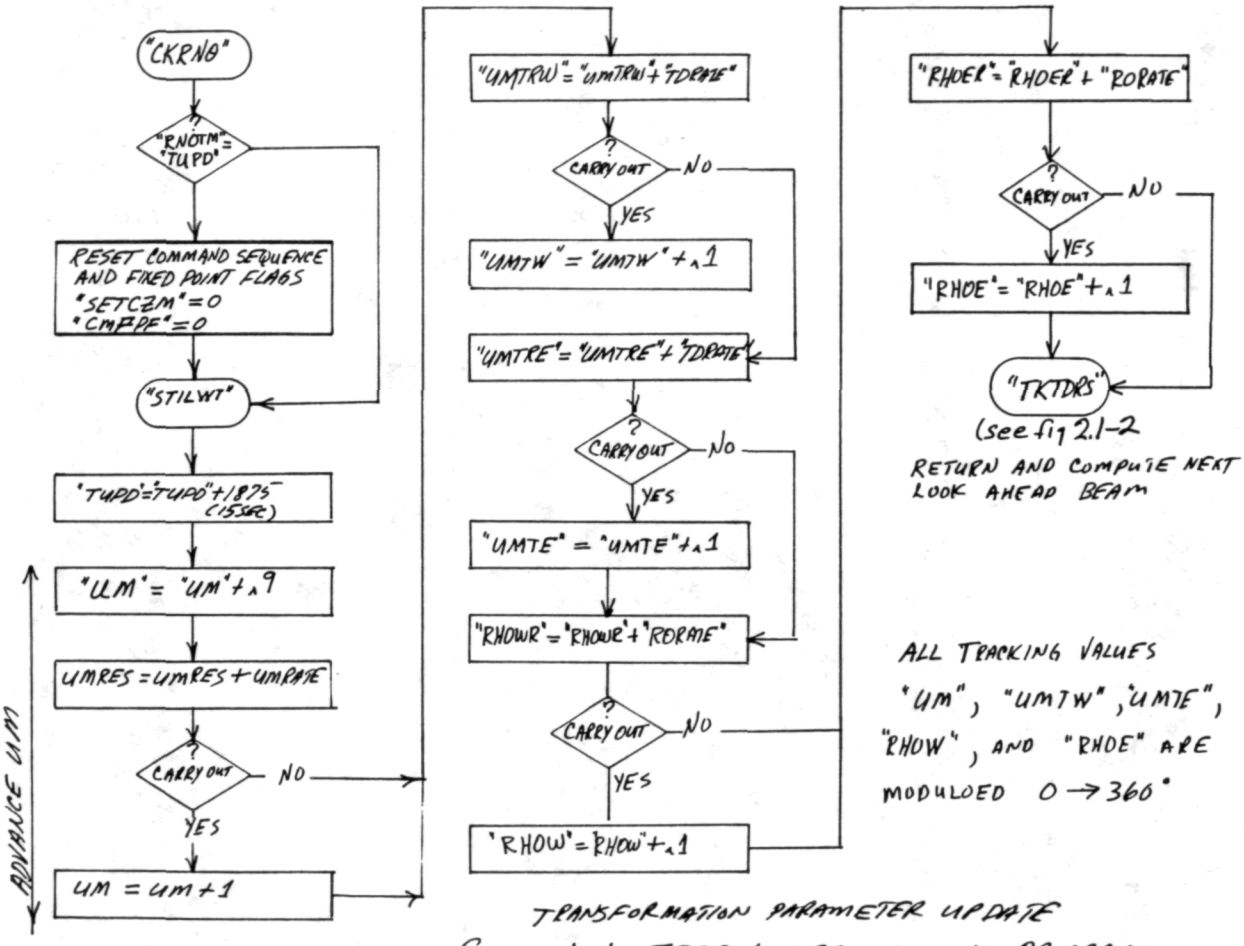


fig 2.1-3 ERBS/TDRS TRACKING PROGRAM



TRANSFORMATION PARAMETER UPDATE

fig 2.1-4 ERBS/TDRS TRACKING PROGRAM

Figure 2.1-2 shows the coordinate transformation section of the program. This section takes a TDRS vector initially defined in a TDRS coordinate system into antenna coordinates. The program takes only the left branch if "SELTDR" holds the value 1. It takes just the right branch if "SELTDR" is set to 2. If "SELTDR" holds the value 0, the program executes both branches and selects the optimum pointing vector as illustrated in figure 2.1-3. Figure 2.1-3 also shows the labled juncture "SBEAMS" which is the location the program branches to if it is in the Fixed Point mode, ("SELTDR"=3). Figure 2.1-3 also illustrates one more interaction between the Command Routine and the general tracking program. After finishing the transformations, the program examines the flag in "CMFPF" . If all proceedures were followed correctly for for inputing a fixed point command, this flag will be set to 3. the program then will set the flag "SELTDR" to 3 copy the Fixed Point pointing vector from the Command routine holding registers to the pointing vector input locations for subroutine "BEAMS" ,("IPH and "ITH"). Figure 2.1.3 also shows the wait loop where the program waits until the "CLOCK2" counter advances to equal the look-ahead up date time "TUPD".

Figure 2.1-4 show the section of the program that advances the tracking parameters held in locations "UM","UMTW","UMTE", "RHOW","RHOE" for the next look ahead time. An interaction proceedure with the Command routine also shown. If the main program determines that the update time has equaled the counter value held in "RNOTM" , the two key parameters in "SETCZM" and "CMFPF" are cleared. This forces all command data to be received at least 15 to 30 seconds after having sent the Command Identifier word and the entire Fixed Point command sequence to be completed in 15 to 30 seconds.

2.2 BEAM FORMING ROUTINE

Figure 2.2-1 shows the beam forming routine. This routine operates on the input pointing vector held in locations "ITH", and "IPH". The output from the program is a list of 12 elements to be activated in the 12 element table labled "TAB2".

2.3 ELEMENT ACTIVATION ROUTINE "FIRE"

Figure 2.3-1 illustrates the function preformed in subroutine "FIRE". This subroutine begins by setting a 10 word array called "BITS" to zero. This is the array which holds the the antenna serial output pattern. The routine then sets the status telemetry status bits which are included at the end of the 145 active element bits. The program then sets selected bits on according to the elements that are identified in the active element list labled "TAB2". The routine disables the interrupts before shifting out the bits serially to the flight electronics memory mapped I/O adresses and the CRU adresses that support the antenna test console. By supporting both functions in the same routine we provide wider data and clock pulses to both sets of control electronics without the need for unnecessary padding statements. The serial bit stream is output in less than 150 milliseconds after which the interrupts are re-enabled. The program than shifts out a byte of phi data and a byte of theta data to the flight control electronics. The value in "IPH" is devided by 20 which makes one significient count equal to 2 degrees. The value in "ITH" is divided by ten to make one count equal to 1 degrees.

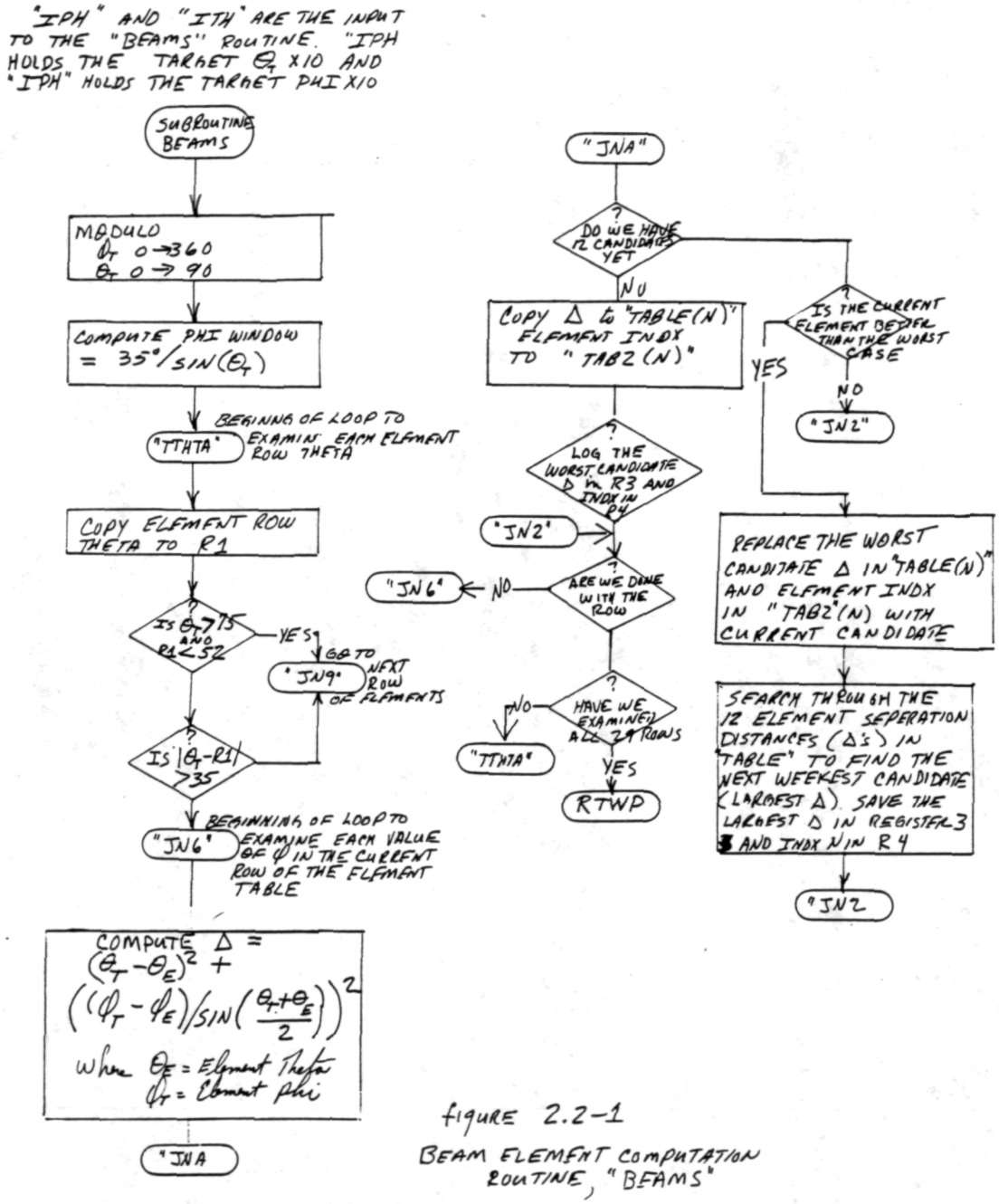


figure 2.2-1

BEAM ELEMENT COMPUTATION ROUTINE, "BEAMS"

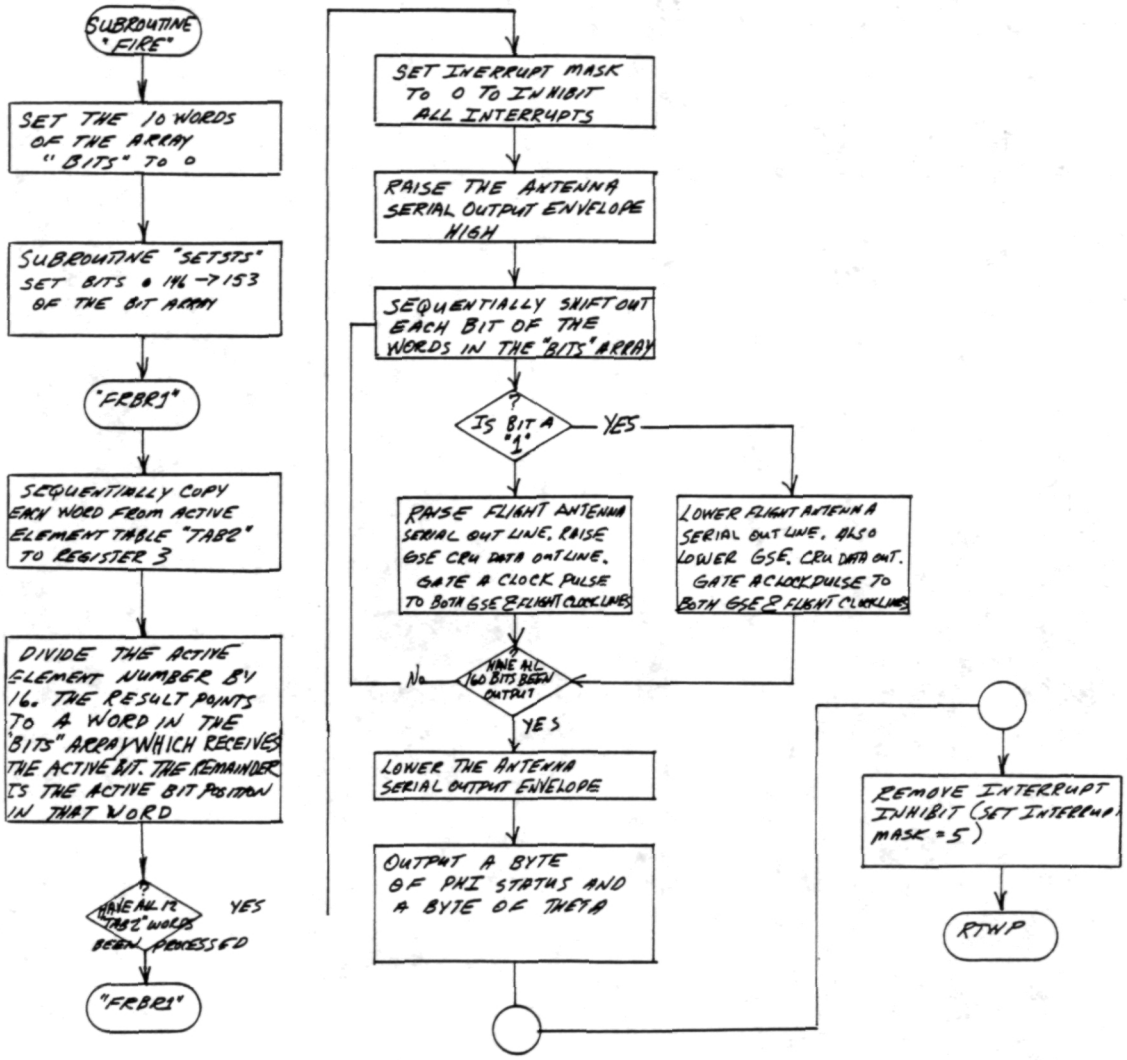


figure 2.3-1

ELEMENT ACTIVATION ROUTINE
(FIRE)

2.4 COMMAND ROUTINE

Figure 2.4-1 shows the portion of the program executed when the program is anticipating a Command Identifier word. The Command Routine uses it own work space register 10 to hold the flag that indicats which type of command is anticipated. The general program would adress this location using the label "SETZM". If anything goes wrong with a command sequence, this location is reset zero by the general program or the command routine itself. The value 0 keys the program to look for a command identifier word. Four of the command identifier words simply set flags in the general program data area and then returns to the calling program. Command identifier 2 sends the program back to the very beginning of the program. Commands 1, 7 and 8 key the program to expect a following command data word. Command 8 also initiates a progression for the parameter held in register 9 . If this parameter is sequenced properly the general program will put itself in the Fixed Point mode.

Figure 2.4-2 shows what the program does when it receives command that it preceives to be a command data word. For the most part this section simply moves the command data word to memory and returns to the interrupted program. The special action taken to handle the ephemeris input UM and the Fixed Point commands are shown in figure 2.4-3

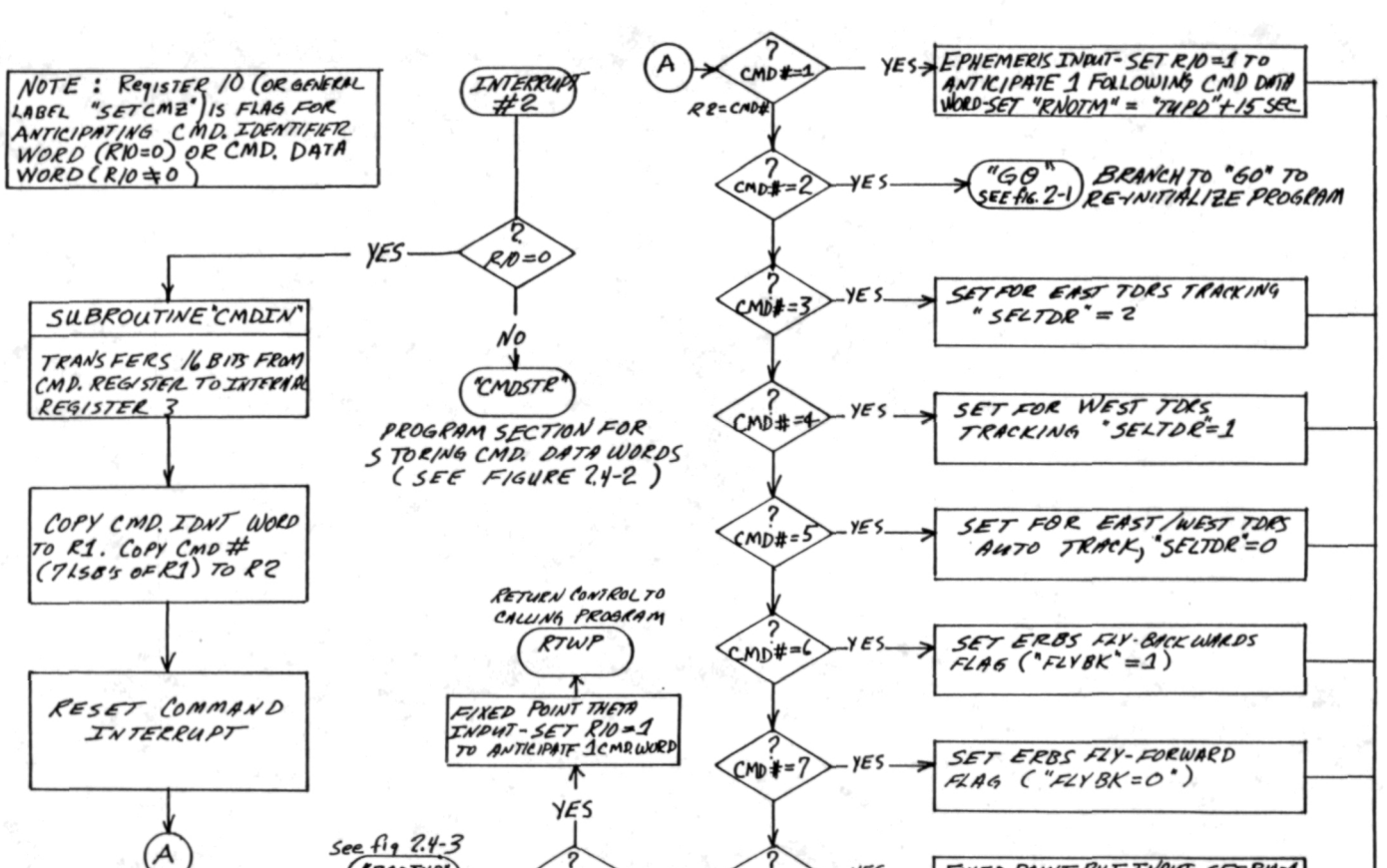


FIGURE 2.4-1 COMMAND IDENTIFIER INTERPERT ROUTINE

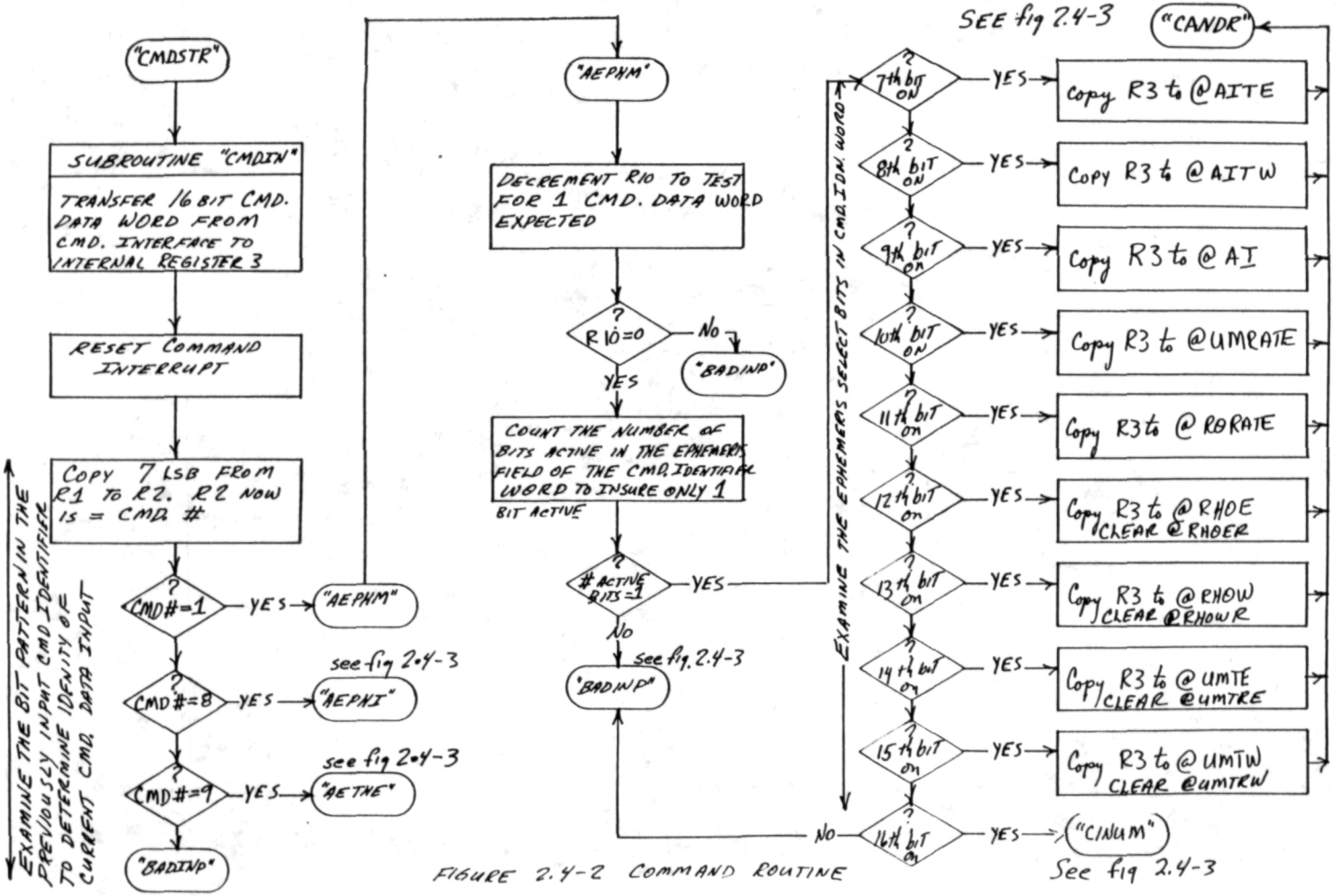


FIGURE 2.4-2 COMMAND ROUTINE

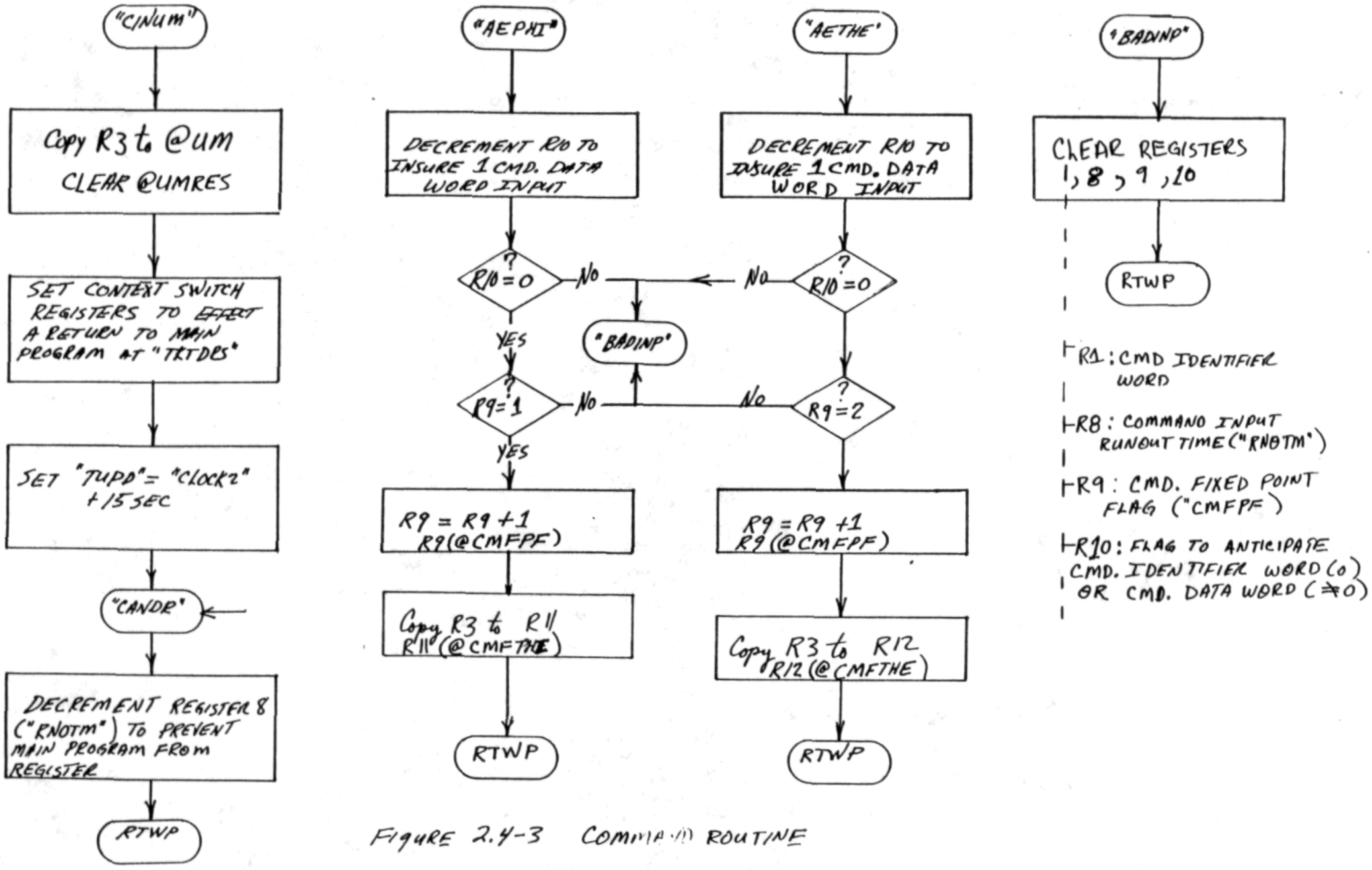


Figure 2.4-3 COMMAND ROUTINE



APPENDIX B

MOTOROLA REPORT:
SLE MODULE/TDRSS ENGINEERING
MODEL TRANSPONDER INTEGRATION AND
TEST WITH THE AUTONOMOUS OMNI
ANTENNA/MICROPROCESSOR

Prepared for
NASA/GODDARD SPACE FLIGHT CENTER
Greenbelt MD 20771

FINAL REPORT

SLE Module/TDRSS Engineering Model Transponder Integration and Test with the Autonomous Omni Antenna/Microprocessor

Contract NAS5-20827
Date: 11/15/82

Prepared by: Jim Dalton
Senior Engineer

Duane Forbes
Project Leader
Aerospace RF Section

John Almeida
Program Manager
Aerospace Electronics Office

MOTOROLA • Government Electronics Division • 8201 E McDOWELL ROAD SCOTTSDALE, ARIZ 85252

INTRODUCTION

The interface tests between the NASA Standard TDRSS Transponder and the Autonomous Omni Antenna were successfully completed during the period from October 25, 1982 to November 1, 1982. The transponder was the NST TDRSS Prototype with the SLE module installed which provides the signal level estimate voltage and transponder lock status for the antenna controller. In addition, the transponder's AGC voltage is brought out to a sample and hold circuit controlled by the antenna system. The block diagram of the set up for the test is shown in Figure 1.

List of Equipment

Transponder - 01-P02700L002 - Prototype

System Support Unit (ISEE) - 01-P04834J001 - S/N 2

TEST DESCRIPTION

The test was divided into four (4) major parts. These parts are listed below:

1.) Calibrate Transponder AGC TLM Voltage Versus Generator Output Level using a Standard Gain Horn Antenna. (Table 1, Figure 3.)

2.) Verify Antenna Gain in Omni Mode at 50 positions using Transponder AGC TLM Voltage. (Table 2.)

3.) Verify Correct Antenna Pointing Direction and Antenna Gain at Low Signal Level for 61 points. (Table 3.)

4.) Verify correct Antenna Pointing Direction and Antenna Gain at High Signal Level for 12 points. (Table 4.)

TEST RESULTS

Data taken during the test is included as Tables 1, 2, 3 and 4. Tables 2, 3 and 4 indicate the beam direction, AGC TLM voltage of the transponder and calculated gain using the AGC TLM voltage for the antenna.

A number of software programs for the antenna controller were tested during the time period of the interface test. The software program dated 10-30-82 was used to give the test results of Tables 2, 3 and 4. The revision of software contained data print statements, which increased the antenna final phase acquisition time to about 15 seconds (nominal ≈ 1.2 seconds).

A problem was noted during the test which related to the way the transponder's AGC is being held and to the length of time that the antenna controller holds the AGC. The problem is that when the AGC is being held, the output of the integrator in the AGC loop is open circuited (see Figure 2). When the antenna controller is holding the AGC, the AGC integrator will continue to integrate. Normally it will integrate in a direction to lower the signal gain because the controller is finding stronger beams. Also, the short delay between the Omni Mode and the first pointed beam (about 1 second) at which point the AGC is held, is not enough time for the AGC loop to recover from the increased signal. The result of this is that the AGC integrator output is at a level which turns the signal gain down, and sometimes squelches the signal all the way off. This causes the transponder to lose lock when the antenna controller releases the AGC. If the print statements were removed from the antenna controller's software, the time the AGC was to be held would be greatly reduced. But even with the reduced time, a large AGC error could be developed.

SUMMARY

The overall results of the interface test were successful as indicated by the data. However, two areas of the transponder interface design should be reviewed before a flight unit is built. These areas are:

1. The operation of the AGC integrator during the AGC held time.

2. The buffering of the interface circuits for the AGC hold circuit.

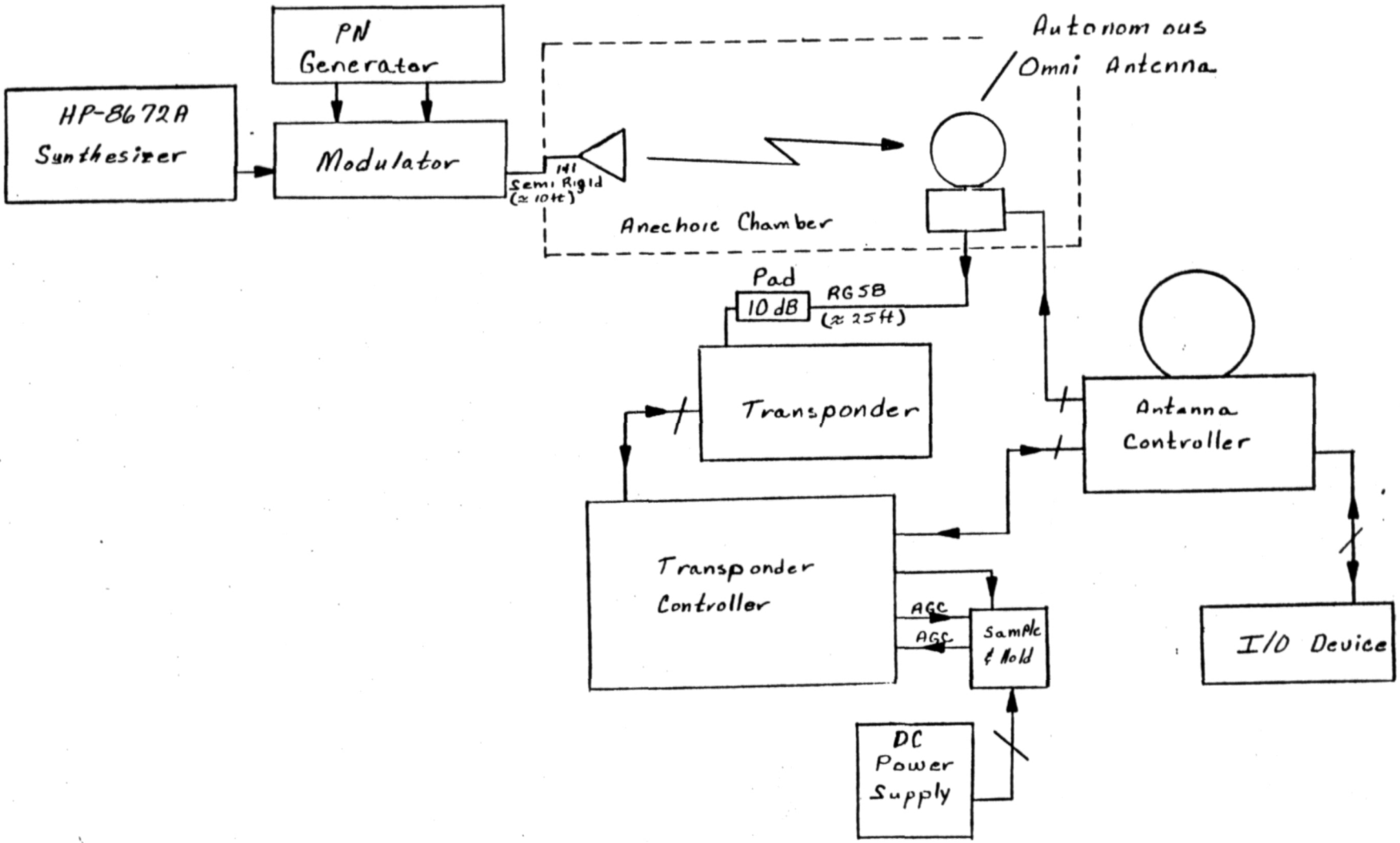


Figure 1.
Block Diagram of Test Set Up.

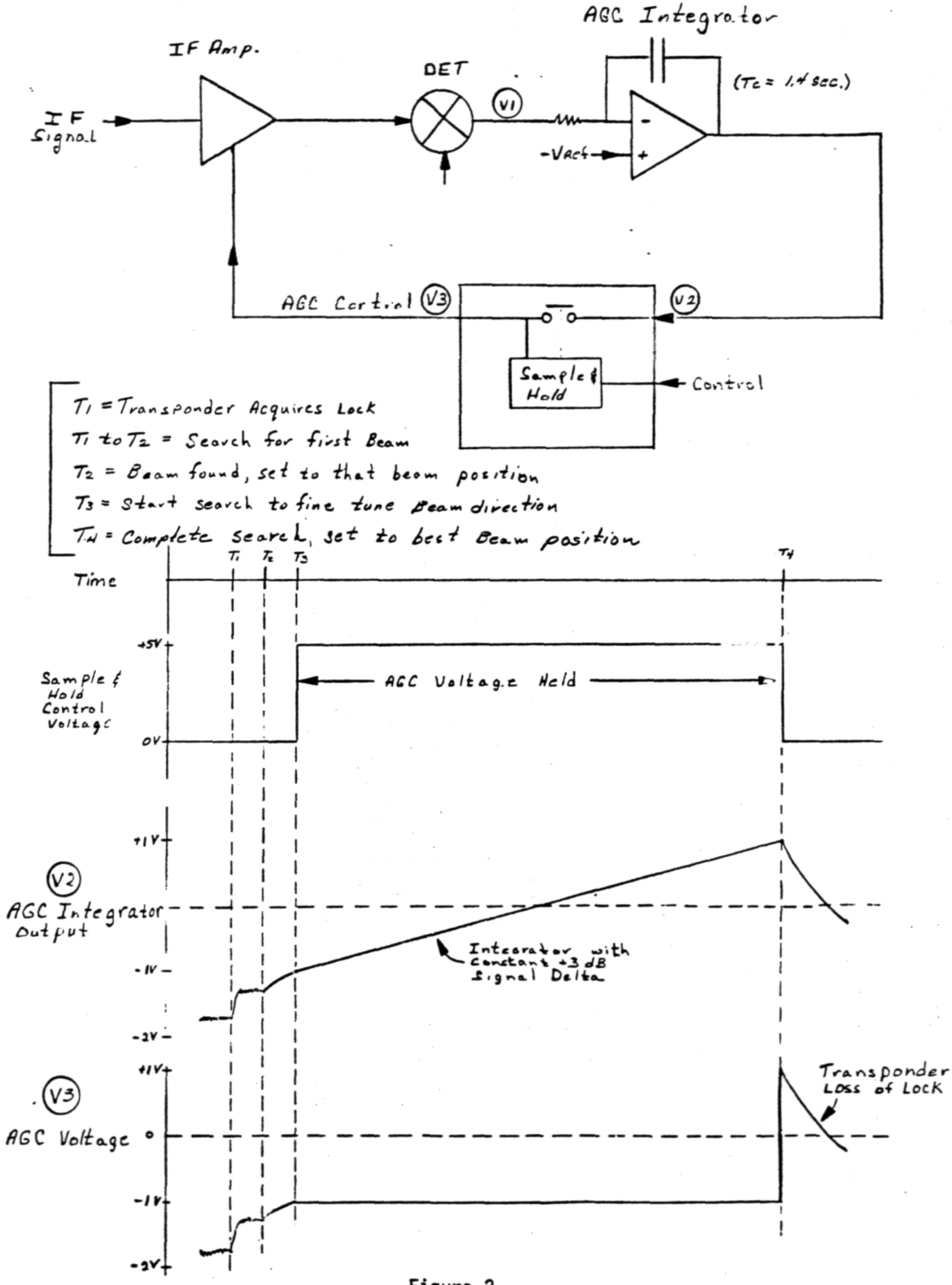


Figure 2.

Transponder AGC Integrator Output Versus Antenna Acquisition Time.

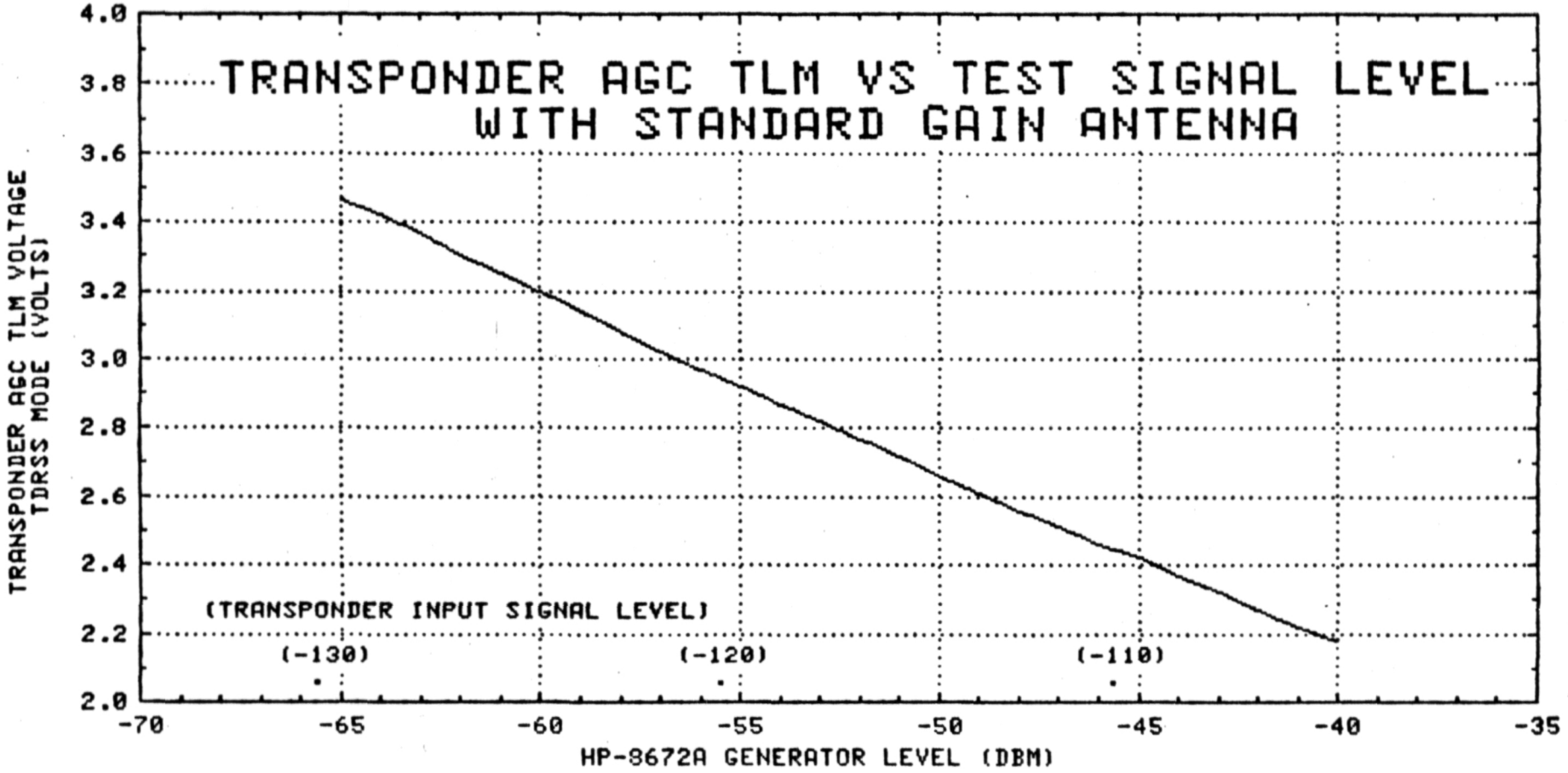

TRANSPONDER AGC TLM VS TEST SIGNAL LEVEL
WITH STANDARD GAIN ANTENNA
TRANSPONDER AGC TLM VOLTAGE
TDRSS MODE (VOLTS)
4.0
3.8
3.6
3.4
3.2
3.0
2.8
2.6
2.4
2.2
2.0
(TRANSPONDER INPUT SIGNAL LEVEL)
(-130)
(-120)
(-110)
-70
-65
-60
-55
-50
-45
-40
-35
HP-8672A GENERATOR LEVEL (DBM)

Figure 3.

HP 8672A GENERATOR LEVEL (DBM)	TRANSPONDER AGC TLM VOLTAGE (VOLTS)
-40	2.18
-41	2.22
-42	2.27
-43	2.32
-44	2.37
-45	2.42
-46	2.46
-47	2.51
-48	2.56
-49	2.61
-50	2.66
-51	2.72
-52	2.77
-53	2.82
-54	2.87
-55	2.92
-56	2.97
-57	3.02
-58	3.08
-59	3.14
-60	3.20
-61	3.25
-62	3.30
-63	3.37
-64	3.42
-65	3.47

Table 1.

Transponder AGC TLM Voltage Versus Generator Output Level
With Standard Gain Horn Antenna.

BEAM NO.	TRUE SIGNAL DIRECTION (DEG)		TRANSPONDER AGC TLM VOLTAGE (VOLTS)	ANTENNA GAIN *
	Θ	Θ		(DB)
1	0.1	0.1	2.88	4.4
2	1.5	45.0	2.88	4.4
3	3.0	90.0	2.87	4.6
4	4.5	135.0	2.86	4.8
5	6.0	180.0	2.87	4.6
6	7.5	225.0	2.91	3.8
7	9.0	270.0	2.98	2.5
8	10.5	315.0	3.09	0.5
9	12.0	5.0	3.13	-0.2
10	13.5	50.0	3.04	1.4
11	15.0	95.0	2.96	2.9
12	16.5	140.0	2.98	2.5
13	18.0	185.0	3.06	1.1
14	19.5	230.0	3.15	-0.6
15	21.0	275.0	3.37	-4.7
16	22.5	320.0	3.49	-6.9
17	24.0	10.0	3.41	-5.4
18	25.5	55.0	3.31	-3.6
19	27.0	100.0	3.16	-0.8
20	28.5	145.0	3.43	-5.8
21	30.0	190.0	3.39	-5.0
22	31.5	235.0	3.16	-0.8
23	33.0	280.0	3.30	-3.4
24	34.5	355.0	3.08	0.7
25	36.0	15.0	3.34	-4.1
26	37.5	60.0	3.35	-4.3
27	39.0	105.0	3.24	-2.3
28	40.5	150.0	3.16	-0.8
29	42.0	195.0	3.23	-2.1
30	43.5	240.0	3.07	0.9
31	45.0	285.0	3.19	-1.3
32	46.5	330.0	3.05	1.3
33	48.0	20.0	3.35	-4.3
34	49.5	65.0	3.19	-1.3
35	51.0	110.0	3.14	-0.4
36	52.5	155.0	3.18	-1.2
37	54.0	200.0	3.30	-3.4
38	55.5	245.0	3.32	-3.7
39	57.0	290.0	3.19	-1.3
40	58.5	335.0	3.16	-0.8
41	60.0	25.0	3.41	-5.4
42	61.5	70.0	3.23	-2.1
43	63.0	115.0	3.17	-1.0
44	64.5	160.0	3.36	-4.5
45	66.0	205.0	3.41	-5.4
46	67.5	250.0	3.50	-7.1
47	69.0	295.0	3.51	-7.3
48	70.5	340.0	3.26	-2.6
49	72.0	30.0	3.54	-7.8
50	73.5	75.0	3.35	-4.3

* ANT. GAIN CALCULATED FROM AGC TLM VOLTAGES AND USING BEAM POSITION 1 OMNI MODE (2.88 VOLTS) AS 4.4 DB

NOTE: HP-8672A GENERATOR SET TO -50DBM

Table 2.

Antenna Gain in Omni Mode Using Transponder AGC TLM Voltage.

BEAM NO.	TRUE DIRECTION (DEG)		TRANSPONDER AGC TLM VOLTAGE (VOLTS)	CALCULATED ANT. GAIN (DB)
	O	O		
1	0.1	0.1	2.73	5.5
2	1.5	45.0	2.75	5.1
3	3.0	90.0	2.67	6.6
4	4.5	135.0	2.69	6.3
5	6.0	180.0	2.67	6.6
6	7.5	225.0	2.73	5.5
7	9.0	270.0	2.70	6.1
8	10.5	315.0	2.65	7.0
9	12.0	5.0	2.62	7.5
10	13.5	50.0	2.67	6.6
11	15.0	95.0	2.77	4.8
12	16.5	140.0	2.76	5.0
13	18.0	185.0	2.65	7.0
14	19.5	230.0	2.66	6.8
15	21.0	275.0	2.67	6.6
16	22.5	320.0	2.62	7.5
17	24.0	10.0	2.77	4.8
18	25.5	55.0	2.68	6.4
19	27.0	100.0	2.68	6.4
20	28.5	145.0	2.62	7.5
21	30.0	190.0	2.62	7.5
22	31.5	235.0	2.75	5.1
23	33.0	280.0	2.73	5.5
24	34.5	355.0	2.62	7.5
25	36.0	15.0	2.74	5.3
26	37.5	60.0	2.65	7.0
27	39.0	105.0	2.60	7.9
28	40.5	150.0	2.73	5.5
29	42.0	195.0	2.60	7.9
30	43.5	240.0	2.74	5.3
31	45.0	285.0	2.60	7.9
32	46.5	330.0	2.60	7.9
33	48.0	20.0	2.74	5.3
34	49.5	65.0	2.57	8.5
35	51.0	110.0	2.67	6.6
36	52.5	155.0	2.72	5.7
37	54.0	200.0	2.65	7.0
38	55.5	245.0	2.69	6.3
39	57.0	290.0	2.63	7.4
40	58.5	335.0	2.63	7.4
41	60.0	25.0	2.60	7.9
42	61.5	70.0	2.56	8.7
43	63.0	115.0	2.55	8.8
44	64.5	160.0	2.60	7.9
45	66.0	205.0	2.69	6.3
46	67.5	250.0	2.65	7.0
47	69.0	295.0	2.64	7.2
48	70.5	340.0	2.61	7.7
49	72.0	30.0	2.57	8.5
50	73.5	75.0	2.70	6.1
51	75.0	120.0	2.58	8.3
52	76.5	165.0	2.62	7.5
53	78.0	210.0	2.77	4.8
54	79.0	255.0	2.62	7.5
55	80.5	300.0	2.67	6.6
56	82.0	345.0	2.59	8.1
57	83.5	30.0	2.57	8.5
58	85.0	75.0	2.57	8.5
59	86.5	120.0	2.65	7.0
60	88.0	165.0	2.60	7.9
61	89.5	210.0	2.72	5.7

* ANT. GAIN CALCULATED FROM AGC TLM VOLTAGES AND USING BEAM POSITION 1 OMNI MODE (2.79 VOLTS) AS 4.4 DB.

NOTE: HP-8672A GENERATOR SET TO -50 DBM

Table 3.

Antenna Gain in Pointed Mode at Low Signal Level.

BEAM NO.	TRUE SIGNAL DIRECTION (DEG)		TRANSPONDER AGC TLM VOLTAGE (VOLTS)	ANTENNA GAIN * (DB)
	Θ	Θ		
1	0.1	0.1	1.93	6.8
6	7.5	225.0	2.00	5.5
11	15.0	95.0	2.05	4.6
16	22.5	320.0	1.89	7.5
21	30.0	190.0	1.90	7.4
26	37.5	60.0	1.92	7.0
31	45.0	285.0	1.89	7.5
36	52.5	155.0	2.17	2.4
41	60.0	25.0	1.88	7.7
46	67.5	250.0	1.93	6.8
51	75.0	120.0	1.87	7.9
57	83.5	30.0	1.85	8.3

* ANT. GAIN CALCULATED FROM AGC TLM VOLTAGES AND USING BEAM POSITION 1 OMNI MODE (2.06 VOLTS) AS 4.4 DB.

NOTE: HP-8672A GENERATOR SET TO -35 DBM

Table 4.

Antenna Gain in Pointed Mode at High Signal Level.

TECHNICAL REPORT STANDARD TITLE PAGE

1. Report No.	2. Government Accession No.	3. Recipient's Catalog No.
F83-02		

4. Title and Subtitle	5. Report Date
Autonomous Omnidirectional Spacecraft Antenna System	February 1983
	6. Performing Organization Code
7. Author(s)	8. Performing Organization Report No.
Taliaferro H. Taylor	F83-02
9. Performing Organization Name and Address	10. Work Unit No.
Ball Aerospace Systems Division P.O. Box 1062 Boulder, CO 80306	11. Contract or Grant No. NAS5-26240
12. Sponsoring Agency Name and Address	13. Type of Report and Period Covered
Goodard Space Flight Center Greenbelt, MD 20771 Technical Monitor: Robert Jackson	Final July 1980 - Dec. 1982
	14. Sponsoring Agency Code

15. Supplementary Notes

16. Abstract

This report describes the development of a low gain Electronically Switchable Spherical Array Antenna. This antenna provides roughly 7 dBic gain for receive/transmit operation between user satellites and TDRSS. When used as a pair, the antenna provides spherical coverage. The antenna has been tested in its primary operating modes:

- Directed Beam
- Retrodirective
- Omnidirectional

This report concentrates on the tested performance of the antenna.

17. Key Words (Selected by Author(s))	18. Distribution Statement
Electronic Switching Spherical Array, TDRSS User Antenna	

19. Security Classif. (of this report)	20. Security Classif. (of this page)	21. No. of Pages	22. Price*
Unclassified	Unclassified	~ 200	unknown

*For sale by the Clearinghouse for Federal Scientific and Technical Information, Springfield, Virginia 22151.